

NOTE TO USERS

This reproduction is the best copy available.

UMI[®]



Université d'Ottawa • University of Ottawa



Université d'Ottawa - University of Ottawa

FACULTÉ DE ÉTUDES SUPÉRIEURES
ET POSTDOCTORALES

FACULTY OF GRADUATE AND
POSTDOCTORAL STUDIES

Matthew HEUFT

AUTEUR DE LA THÈSE - AUTHOR OF THESIS

Ph. D (Chemistry)

GRADE - DEGREE

Department of Chemistry

FACULTÉ, ÉCOLE, DÉPARTEMENT - FACULTY, SCHOOL, DEPARTMENT

TITRE DE LA THÈSE - TITLE OF THE THESIS

Design and Synthesis of Helical Acetylenic Carbo-and Heterocyclic
Cyclophanes

Alex Fallis

DIRECTEUR DE LA THÈSE - THESIS SUPERVISOR

CO-DIRECTEUR DE LA THÈSE - THESIS CO-SUPERVISOR

EXAMINATEURS DE LA THÈSE - THESIS EXAMINERS

L. Barriault

K. Fagnou

M. Haley

W. Wang

J.-M. De Koninck, Ph.D.

LE DOYEN DE LA FACULTÉ DES ÉTUDES
SUPÉRIEURES ET POSTDOCTORALES

DEAN OF THE FACULTY OF GRADUATE
AND POSTDOCTORAL STUDIES

Design and Synthesis of Helical Acetylenic Carbo- and Heterocyclic Cyclophanes

by

MATTHEW A. HEUFT

B.Sc. (Honours Chemistry, Co-op), University of Waterloo, 1999

A Thesis Submitted to the School of Graduate Studies and Research
in Partial Fulfillment of the Requirements for the Degree of Doctor of Philosophy

Ottawa-Carleton Chemistry Institute

Department of Chemistry
University of Ottawa
Ottawa, Ontario

Candidate

Supervisor

Matthew A. Heuft

Professor Alex G. Fallis

© Matthew A. Heuft, Ottawa, Canada, 2004



Library and
Archives Canada

Bibliothèque et
Archives Canada

Published Heritage
Branch

Direction du
Patrimoine de l'édition

395 Wellington Street
Ottawa ON K1A 0N4
Canada

395, rue Wellington
Ottawa ON K1A 0N4
Canada

Your file *Votre référence*
ISBN: 0-494-01709-0
Our file *Notre référence*
ISBN: 0-494-01709-0

NOTICE:

The author has granted a non-exclusive license allowing Library and Archives Canada to reproduce, publish, archive, preserve, conserve, communicate to the public by telecommunication or on the Internet, loan, distribute and sell theses worldwide, for commercial or non-commercial purposes, in microform, paper, electronic and/or any other formats.

The author retains copyright ownership and moral rights in this thesis. Neither the thesis nor substantial extracts from it may be printed or otherwise reproduced without the author's permission.

AVIS:

L'auteur a accordé une licence non exclusive permettant à la Bibliothèque et Archives Canada de reproduire, publier, archiver, sauvegarder, conserver, transmettre au public par télécommunication ou par l'Internet, prêter, distribuer et vendre des thèses partout dans le monde, à des fins commerciales ou autres, sur support microforme, papier, électronique et/ou autres formats.

L'auteur conserve la propriété du droit d'auteur et des droits moraux qui protègent cette thèse. Ni la thèse ni des extraits substantiels de celle-ci ne doivent être imprimés ou autrement reproduits sans son autorisation.

In compliance with the Canadian Privacy Act some supporting forms may have been removed from this thesis.

Conformément à la loi canadienne sur la protection de la vie privée, quelques formulaires secondaires ont été enlevés de cette thèse.

While these forms may be included in the document page count, their removal does not represent any loss of content from the thesis.

Bien que ces formulaires aient inclus dans la pagination, il n'y aura aucun contenu manquant.


Canada

Abstract

The purpose of this research project was to synthesize new acetylenic cyclophanes. These cyclophanes have unusual and aesthetically pleasing structures, pose synthetic challenges, have peculiar reactivity, and often exhibit interesting spectroscopic and physical properties. In addition to the successful synthesis of a number of new cyclophanes, several new synthetic strategies and methods were developed.

A one-pot preparation of arylbutadiynes **95** from chloroenyne **83** and arylhalides was accomplished. This method was used to prepare a variety of arylbutadiynes in 80-95% yields. A procedure was also developed for the *in situ* desilylation/dimerization of bulky silylalkynes.

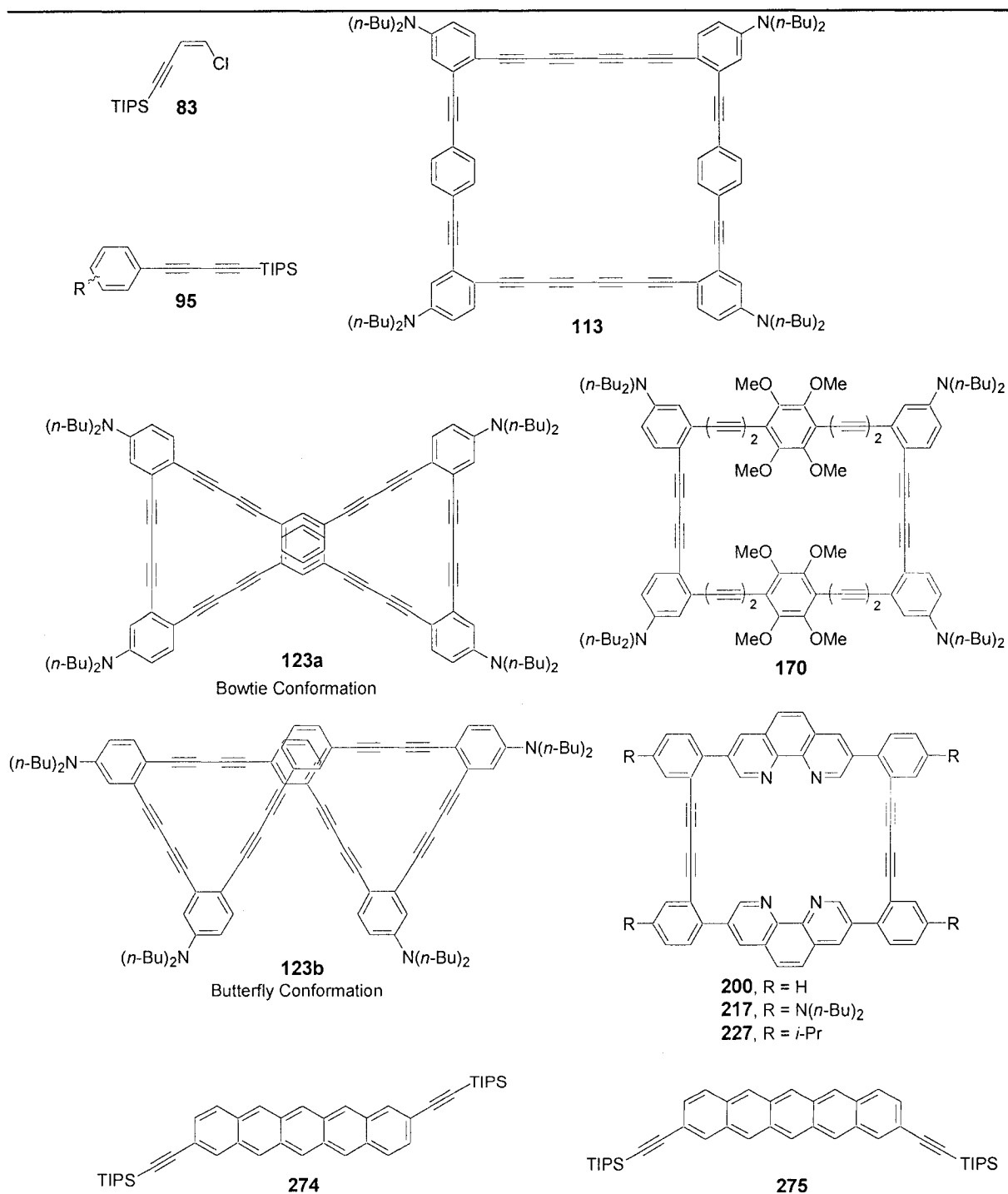
A molecular modeling study provided insight into the observed dimerization reaction products of α,ω -dialkyne precursors. Termini separation distances (r) less than 7 Å gave intramolecular coupling, while distances greater than 10 Å gave intermolecular reactions. Mixtures of intra- and intermolecular reaction products were obtained when $7 < r < 10$ Å.

The synthesis of two new C60 acetylenic cyclophanes revealed that the substitution pattern of the capping group controlled the conformation of the molecule. Cyclophane **113** with *para*-substituted capping groups adopted a helical (chiral) conformation and the isomeric *meta*-capped cyclophane **123** had a different molecular folding pattern with the potential to be planar.

Two classes of unsaturated cyclophanes were synthesized as ligands for the preparation of chiral, non-racemic helical complexes: A tetramethoxybenzene-capped, C60 acetylenic cyclophane as a potential η^{12} -bis(arene) ligand, and phenanthrolineophanes as tetradentate π -coordination ligands. Cyclophane **170** was successfully prepared, but metal complexes of **170** could not be prepared. Phenanthrolineophanes **200**, **217**, and **227** and their corresponding copper complexes were synthesized by a new, metal-templated procedure. Copper coordination was found to raise the helical isomerization barrier height by over 7 kcal/mol; however, isomerization still occurred at room temperature so enantiopure phenanthrolineophanes could not be isolated.

The first pentacenes with functional groups on the A and E rings have also been synthesized. A highlight of the rapid, four-step synthesis of pentacenes **274** and **275** was the absence of any chromatographic purification. The commercial potential of these new

pentacene compounds as organic semiconductors is being investigated in collaboration with the National Research Council of Canada.



Acknowledgements

There are a number of people who I would like to thank for their guidance, support, and friendship leading up to and during my graduate studies. Without these people I would not have become the person or scientist that I am today.

A few people really made chemistry come alive for me: Richard Keen (KCVI), Dr. Markus Wicki (3M), and Professor Mike Chong (University of Waterloo), and my Ph.D. supervisor, Professor Alex Fallis - Thanks!

Alex, I joined your group for the diverse projects that you tackle and your contagious enthusiasm for chemistry. Your lab was an excellent atmosphere in which to learn and grow as a chemist. I have valued the freedom that you gave me to pursue my interests in the lab and the advice that you have passed on along the way. The dramatic improvement in my squash game can also be attributed to you!

I also want to thank all of my co-workers in the Fallis group. There is not enough space to thank each of you individually, but each of you have touched my life in different ways. In particular, I want to thank Dr. Shawn Collins (You showed me the ropes when I joined the lab and were an excellent mentor on the cyclophane project. Your Canada Day parties are also not to be forgotten.), Dr. Pat Forgione, Jenny Tiffin (my coffee buddy), Matt Clay (You are a worthy recipient of the cyclophane project. Keep up the great work!), and Megan ApSimon (Thanks for all of your hard work as you toiled over starting materials for two summers with me - you are developing into a great scientist!).

Thanks Pat Bazinet, Michelle Chretien, Jay Conrad, and Pat Crewdson who helped me during my graduate work by running samples, interpreting data, and letting me work in their gloveboxes.

I am fortunate to be surrounded by many friends from both Ottawa U and Waterloo who have been very encouraging over the years: Julie Porter, Bryan "Tiny" Koivisto, Kelly Dyer, Dean Sas, Dr. Chris Coenjarts, Suvi Mohanty, and Jenn Snelgrove. A special thanks is reserved for Dr. Lisa Croll and Dr. Adrien Côté. You guys have been great friends for a number of years and we have shared many conferences, cottage weekends, and countless beers together. I am looking forward to many more.

Thank you Mom, Dad, Jeff, and Eric. You guys have supported me from my early undergrad days by sending timely care packages all the way through to the writing of my dissertation. Thank you all for your love and encouragement.

Finally, Jenn, your love, support, and understanding during my undergraduate and graduate studies has not gone unnoticed or unappreciated. I know that chemistry has captured a great deal of my time and attention, but it has not captured my heart. Don't worry, I will begin to earn my keep soon!

To my family

Table of Contents

ABSTRACT.....	ii
ACKNOWLEDGEMENTS	iv
TABLE OF CONTENTS	vii
LIST OF FIGURES	x
LIST OF SCHEMES	xiii
LIST OF SCHEMES	xiii
LIST OF TABLES	xvi
LIST OF TABLES	xvi
LIST OF ABBREVIATIONS	xvii
LIST OF ABBREVIATIONS	xvii
1. INTRODUCTION.....	2
1.1 CYCLOPHANES	2
1.2 PALLADIUM-CATALYZED COUPLING REACTIONS	4
1.3 ACETYLENE DIMERIZATION REACTIONS.....	7
1.3.1. <i>Symmetrical Di- and Oligoalkynes</i>	8
1.3.2. <i>Unsymmetrical Di- and Oligoalkynes</i>	10
1.4 PREVIOUS FALLIS LAB CYCLOPHANE CHEMISTRY	11
2. C60 ACETYLENIC CYCLOPHANES	16
2.1 RATIONAL SYNTHESIS OF C60 FROM ACETYLENIC CYCLOPHANE PRECURSORS.....	16
2.2 SYNTHESIS OF C ₆₀ H ₂₄ <i>PARA</i> -CYCLOPHANE 75	20
2.3 <i>IN SITU</i> DESILYLATION/DIMERIZATION OF SILYLALKYNES.....	23
2.4 SYNTHESIS OF <i>PARA</i> -CYCLOPHANE 104	27
2.5 STEPWISE SYNTHESIS OF <i>PARA</i> -CYCLOPHANE 113	33
2.6 INTER- VS. INTRAMOLECULAR DIMERIZATION OF α,ω -DIYNES	37
2.7 SYNTHESIS OF <i>META</i> -CYCLOPHANE 123	41
2.8 SUMMARY	48

3.	HELICAL ACETYLENIC CYCLOPHANES AND PHENANTHROLINOPHANES	50
3.1	UNSATURATED COMPOUNDS WITH HELICAL CHIRALITY	51
3.2	SYNTHESIS OF CYCLOPHANE 157 AS A η^{12} -BIS(ARENE) LIGAND	53
3.3	SYNTHESIS OF CYCLOPHANE 170 AS AN η^{12} -BIS(ARENE) LIGAND	58
3.4	BIS(ARENE) COMPLEXES	61
3.5	SYNTHESIS OF (η^{12} -CYCLOPHANE) COMPLEXES	63
3.6	1,10-PHENANTHROLINE-BASED COMPOUNDS.....	66
3.7	SYNTHESIS OF PHENANTHROLINOPHANES 200 AND 217	68
3.8	PROPERTIES OF PHENANTHROLINOPHANES 200 AND 217	76
3.9	PREPARATION OF PHENANTHROLINOPHANE 227	79
3.10	SUMMARY	84
4.	2,9- AND 2,10-DISUBSTITUTED PENTACENE-BASED MOLECULES.....	87
4.1	ORGANIC SEMICONDUCTORS	87
4.2	DISUBSTITUTED PENTACENE RETROSYNTHETIC PLAN.....	93
4.3	SYNTHESIS OF 1,4,5,8-ANTHRADIQUINONE (249)	94
4.4	SYNTHESIS OF SILYL ETHERS 247 AND 268	97
4.5	PREPARATION OF DITRIFLATES 246 AND 271	102
4.6	2,9- AND 2,10-DISUBSTITUTED PENTACENES	104
4.7	SUMMARY	106
5.	CONCLUSIONS	109
5.1	NEW METHODS	110
5.2	SYNTHESIS OF NEW COMPOUNDS	113
5.3	FUTURE WORK	119
5.3.1.	<i>Chiral, Non-Racemic Cyclophanes.....</i>	<i>119</i>
5.3.2.	<i>Substituted Pentacene Compounds for use as Organic Semiconductors.....</i>	<i>120</i>
5.4	CLAIMS TO ORIGINAL RESEARCH	123
6.	EXPERIMENTAL SECTION.....	125
6.1	GENERAL EXPERIMENTAL.....	125

6.2	DETAILED EXPERIMENTAL PROCEDURES.....	126
7.	REFERENCES.....	176
	APPENDIX.....	188
A.1	CYCLOPHANE NOMENCLATURE.....	188
A.2	PHENANTHROLINOPHANE HELICAL INTERCONVERSION BARRIER HEIGHT DETERMINATION.....	190
A.3	SELECTED ^1H , ^{13}C , AND MASS SPECTRA.....	192
A.4	X-RAY CRYSTALLOGRAPHIC DATA.....	220

List of Figures

Figure 1: [2.2]Metacyclophane (1) and [2.2]paracyclophane (2).....	3
Figure 2: Examples of current cyclophane research.....	3
Figure 3: Catalytic cycle for the Negishi reaction.	5
Figure 4: Catalytic cycle for the Sonogashira reaction.	7
Figure 5: Catalytic cycle for the palladium-catalyzed dimerization of alkynes.	10
Figure 6: Proposed eneynecyclophane 43 as a C ₆₀ synthetic precursor.....	12
Figure 7: Potential liquid crystal cyclophane 54 and strained cyclophanes 55, 56, and 57.	14
Figure 8: Cubane (58), dodecahedron (59), and buckminsterfullerene (41).	16
Figure 9: Retrosynthetic analysis of cyclophane 75.....	21
Figure 10: Rational functionalization of cyclophane 104 with solubilizing n-Bu ₂ N groups.	28
Figure 11: Retrosynthetic analysis of cyclophane 104.....	29
Figure 12: X-ray structure of cyclophane 112 (a) top view; (b) side view; (c) crystal packing.....	32
Figure 13: Retrosynthetic analysis of cyclophane 113.....	33
Figure 14: Molecular model of cyclophane 113 illustrating its twisted, C ₂ -symmetric conformation.	36
Figure 15: Isomerization pathway of cyclophane 113.	37
Figure 16: Dimerization reactions leading to (a) an intramolecular product,	38
Figure 17: Manipulation of molecular modeling structures to obtain a “reactive” conformation.	39
Figure 18: Tobe's meta-diethynylbenzene macrocycle 122 and a proposed C ₆₀ meta-cyclophane, 123.	41
Figure 19: Retrosynthetic analysis of meta-cyclophane 123.....	42
Figure 20: Possible conformations of cyclophane 123.	46
Figure 21: Molecular modeling of the bowtie conformation of cyclophane 123a.	47
Figure 22: Molecular modeling of the butterfly conformation of cyclophane 123b.	47
Figure 23: Modification of cyclophane 123 to favor planar cyclophane conformations.....	48
Figure 24: X-ray crystal structure of cyclophane 52 illustrating the overlapping capping aryl rings.....	50
Figure 25: Tor's tunable fluorophores 136 ^{84a} and a conceptual phenanthrolinephane 137.	51

Figure 26: Design criteria for η^{12} -(cyclophane) complex 156	54
Figure 27: Retrosynthetic analysis of η^{12} -(cyclophane) complex 156	55
Figure 28: Cyclophane 170 and a molecular model of η^{12} -bis(cyclophane) chromium complex 171	58
Figure 29: Retrosynthetic analysis of cyclophane 170	59
Figure 30: Low resolution X-ray crystal structure of cyclophane 170	61
Figure 31: Sandwich structures of bis(arene) (179) and metallocene (180) complexes.....	61
Figure 32: Phenanthroline based copper(I) compounds.....	66
Figure 33: A luminescent Cu(I)-phenanthroline complex. ^{113b}	67
Figure 34: Molecular model of phenanthrolinophane 200	68
Figure 35: Retrosynthetic analysis of copper(phenanthrolinophane) complex 201	69
Figure 36: UV-VIS spectra of the phenanthrolinophanes in methylene chloride.	76
Figure 37: Normalized emission spectra of 200 , 216 , and 217 in methylene chloride.	77
Figure 38: Stacked variable temperature ¹³ C NMR spectra of copper(phenanthrolinophane) complex 218	79
Figure 39: Stacked variable temperature ¹³ C NMR spectra of copper(phenanthrolinophane) complex 228	82
Figure 40: A potential energy diagram illustrating the difference in isomerization barrier heights ($\Delta\Delta G^\ddagger$) of phenanthrolinophane 227 and its copper(I) complex, 228 . .	83
Figure 41: Proposed mechanisms for phenanthrolinophane helical inversion.....	84
Figure 42: Pentacenophane 229 and a 2,10-disubstituted pentacene building block (230). .	87
Figure 43: Energy band diagram illustrating insulators, metals, and semiconductors.	88
Figure 44: Diagram of a typical FET device.....	89
Figure 45: Molecular organic semiconductors:	90
Figure 46: Packing diagram of 6,13-disubstituted pentacene (243).	92
Figure 47: Proposed packing diagram of 2,9-disubstituted pentacene derivatives. ¹⁴¹	93
Figure 48: Retrosynthetic plan for the preparation of 2,9-disubstituted pentacenes (244). .	94
Figure 49: Preparative HPLC chromatogram illustrating the separation of silyl ethers 247 and 268	100
Figure 50: Single crystal X-ray structure of silyl ether 247	101

<i>Figure 51: Molecular modeling study used to predict dimerization reaction products</i> <i>(Section 2.6).</i>	111
<i>Figure 52: Second generation phenanthrolinephanes.</i>	119
<i>Figure 53: An allene cyclophane synthetic target.</i>	120
<i>Figure 54: A new synthetic route to 2,9- and 2,10-disubstituted pentacenes.</i>	120
<i>Figure 55: Unsymmetrically disubstituted pentacenes with electron-donating (ED)</i>	121
<i>Figure 56: Oligopentacenes as organic semiconductors.</i>	121
<i>Figure 57: Pseudo meta-capped, planar pentacenophane</i> 229	122

List of Schemes

<i>Scheme 1: Transmetallation step of the Negishi reaction.</i>	5
<i>Scheme 2: Glaser alkyne dimerization reaction.</i>	8
<i>Scheme 3: Eglinton and Hay alkyne dimerization reactions.</i>	8
<i>Scheme 4: A proposed radical mechanism for the copper-mediated alkyne dimerization reaction.</i>	9
<i>Scheme 5: Ionic copper-mediated alkyne dimerization reaction mechanism.</i>	9
<i>Scheme 6: Chodkiewicz-Cadiot reaction to yield unsymmetrical diynes.</i>	10
<i>Scheme 7: Palladium-catalyzed preparation of unsymmetrical diynes.</i>	11
<i>Scheme 8: Synthesis of eneynecyclophanes 39 and 40.</i>	11
<i>Scheme 9: Attempted synthesis of 1,3,5-eneynecyclophane 49.</i>	13
<i>Scheme 10: Synthesis of cyclophanes 52 and 53.</i>	13
<i>Scheme 11: Pyrolysis of Vollhardt's dehydroannulene 60 to give carbon-rich compounds.</i>	17
<i>Scheme 12: Rubin's C₆₀H₁₈ cyclophane precursor to C₆₀.</i>	17
<i>Scheme 13: Rubin's C₆₀H₆(CO)₁₂ cyclophane 69 as a C₆₀ precursor.</i>	18
<i>Scheme 14: Laser desorption mass spectrometry of cyclophanes 69 and 70 to give C₆₀H₆ and C₆₀.</i>	19
<i>Scheme 15: Scott's rational C₆₀ synthesis.</i>	20
<i>Scheme 16: Preparation of 1,4-diethynylbenzene (77).</i>	21
<i>Scheme 17: Preparation of bromide 78 and iodide 86.</i>	22
<i>Scheme 18: Synthesis of dimerization precursor 76.</i>	22
<i>Scheme 19: Attempted formation of cyclophane 75 by the dimerization of 76.</i>	23
<i>Scheme 20: Mori's dimerization of TMS-alkynes.</i>	24
<i>Scheme 21: Haley's desilylation/dimerization of butadiynes.</i>	24
<i>Scheme 22: Synthesis of cyclophane 104 precursor 106.</i>	30
<i>Scheme 23: In situ generation of organozincate 111 and Sonogashira coupling to give diyne 95.</i>	30
<i>Scheme 24: Dimerization of 106 to give cyclophanes 104 (dimer) and 112 (monomer).</i>	31
<i>Scheme 25: Synthesis of cyclophane 113.</i>	35
<i>Scheme 26: Synthesis of dibromide 126.</i>	42
<i>Scheme 27: Preparation of alkyne 125.</i>	44

Scheme 28: Synthesis of meta-cyclophane 123	45
Scheme 29: Katz's helicene synthesis.	52
Scheme 30: Fox's helical cyclophane 147 based on helicene bridges.....	52
Scheme 31: Marsella's cyclooctatetrathiophene-based cyclophane 152	53
Scheme 32: Otera's 1,1'-binaphthyl-based cyclophane 155	53
Scheme 33: Preparation of diiodide 162	56
Scheme 34: Attempted synthesis of dimerization precursor 158	56
Scheme 35: Preparation of dibromide 174	59
Scheme 36: Synthesis of cyclophane 170	60
Scheme 37: Hein Grignard synthesis of bis(arene) complexes.	62
Scheme 38: Fischer-Hafner synthesis of bis(arene) complexes.	62
Scheme 39: [2,2]paracyclophane (2) as a η^{12} -bis(arene) ligand.....	63
Scheme 40: Potential preparation of bis(arene) chromium complexes by photolysis.....	65
Scheme 41: Arene metathesis of bis(arene) molybdenum complexes.....	65
Scheme 42: Preparation of Cu(I)(phen) ₂ complexes.	67
Scheme 43: Proposed mechanism for the bromination of pyridine in the 3 position. ¹²⁰	70
Scheme 44: Synthesis of copper(phenanthroline) complex 213	72
Scheme 45: Proposed formation of complex 214 during the dimerization of 212	72
Scheme 46: Copper-template synthesis of phenanthroline 200	73
Scheme 47: Synthesis of phenanthroline 217 and its copper(I) complex 218	75
Scheme 48: Preparation of iodide 225	80
Scheme 49: Synthesis of phenanthroline 227	81
Scheme 50: Synthesis of pentacene (232).	90
Scheme 51: Retro Diels-Alder approach to pentacene thin films. ¹³⁹	91
Scheme 52: Synthesis of pentacene thin films by a Diels-Alder/retro Diels-Alder approach. ¹⁴⁰	91
Scheme 53: Synthesis of 6,13-disubstituted pentacene derivatives.	92
Scheme 54: Cory's preparation of 1,4,5,8-anthradiquinone (249).....	95
Scheme 55: Proposed mechanism for the preparation of 251 via a benzyne intermediate. ¹⁴⁷	96
Scheme 56: [4+2] Cycloaddition/aromatization strategy to naphthaquinones.	97

<i>Scheme 57: Double Diels-Alder reaction of anthraquinone 249 and diene 261</i>	98
<i>Scheme 58: Double Diels-Alder reaction of diene 248 and anthraquinone 249</i>	99
<i>Scheme 59: Preparation of diol 270</i>	102
<i>Scheme 60: Desilylation/triflation of silyl ethers 247 and 268 to afford ditriflates 246 and 271</i>	104
<i>Scheme 61: Preparation of diquinones 272 and 273</i>	105
<i>Scheme 62: Reaction of pentacene 274 with O₂ to give endoperoxide 276</i>	106
<i>Scheme 63: Preparation of arylbutadiynes from chloroenyne 83 (Section 2.4)</i>	110
<i>Scheme 64: In situ desilylation/dimerization of bulky, silyl-protected arylbutadiynes (Section 3.7)</i>	110
<i>Scheme 65: Copper-templated dimerization reaction (Section 3.7)</i>	112
<i>Scheme 66: In situ desilylation/triflation route to ditriflates 246 and 271 (Section 4.5)</i>	112
<i>Scheme 67: Synthesis of cyclophane 112 (Section 2.4)</i>	113
<i>Scheme 68: Synthesis of C₆₀ para-cyclophane 113 (Section 2.5)</i>	114
<i>Scheme 69: Synthesis of C₆₀ meta-cyclophanes 123a and 123b (Section 2.7)</i>	115
<i>Scheme 70: Synthesis of cyclophane 170 as a potential η^{12}-bis(arene) ligand (Section 3.3)</i>	116
<i>Scheme 71: Synthesis of phenanthrolinephanes (Sections 3.7 and 3.9)</i>	117
<i>Scheme 72: Synthesis of disubstituted pentacenes 274 and 275 (Section 4.6)</i>	118

List of Tables

<i>Table 1: Optimization of the in situ desilylation/dimerization protocol</i>	25
<i>Table 2: Examples of the in situ desilylation/dimerization reaction</i>	26
<i>Table 3: Molecular modeling calculations of α,ω-diyne termini separation distances (r) and the product(s) observed from their dimerization</i>	40
<i>Table 4: Sonogashira reaction conditions for the preparation of silylalkyne 129</i>	43
<i>Table 5: Reaction conditions for the conversion of diiodide 160 to dimerization precursor 166 or 167</i>	57
<i>Table 6: Attempted metallation reactions of cyclophane 170</i>	64
<i>Table 7: Bromination of 1,10-phenanthroline reaction conditions</i>	70
<i>Table 8: UV-VIS and fluorescent spectra maxima of the phenanthrolineophanes and selected reference spectra</i>	78
<i>Table 9: Electron (μ_e) and hole (μ_h) mobilities of organic semiconductors.¹³³</i>	89
<i>Table 10: Reaction conditions for the preparation of 1,4,5,8-tetramethoxyanthracene (251)</i>	95
<i>Table 11: Attempted conversion of diol 270 to ditriflate 246</i>	103
<i>Table 12: Reaction conditions for the reduction of diquinone 272 to pentacene 274</i>	106

List of Abbreviations

Ac	acetyl
aq	aqueous
calcd	calculated
cat.	catalytic
d	doublet
DBA	dehydrobenzoannulene
dd	doublet of doublets
dt	doublet of triplets
DMAP	<i>N,N</i> -dimethyl-4-aminopyridine
DMF	<i>N,N</i> -dimethylformamide
ED	electron-donating group
eq	equivalents
EW	electron-withdrawing group
HOMO	highest occupied molecular orbital
HPLC	high-performance liquid chromatography
HRMS	high resolution mass spectroscopy
IR	infrared spectroscopy
<i>J</i>	coupling constant
LDA	lithium diisopropylamide
LTMP	lithium 2,2,6,6-tetramethylpiperidine
LUMO	lowest unoccupied molecular orbital
M ⁺	molecular ion
mp	melting point
MS(CI)	mass spectrum by chemical ionization
MS(EI)	mass spectrum by electron impact ionization
MS(ES)	mass spectrum by electrospray ionization
MS(FAB)	mass spectrum by fast atom bombardment ionization
NBS	<i>N</i> -bromosuccinimide
NIS	<i>N</i> -iodosuccinimide

NMR	nuclear magnetic resonance
ODCB	<i>ortho</i> -dichlorobenzene
ppm	parts per million
py	pyridine
q	quartet
R	alkyl
rt	room temperature
s	singlet
t	triplet
TBAF	tetrabutylammonium fluoride
TBS	<i>tert</i> -butyldimethylsilyl
TES	triethylsilyl
Tf	trifluoromethylsulfonyl (triflate)
THF	tetrahydrofuran
TIPS	triisopropylsilyl
TLC	thin layer chromatography
TMEDA	<i>N,N,N',N'</i> -tetramethylethylenediamine
TMS	trimethylsilyl
TPS	triphenylsilyl

Chapter

INTRODUCTION

- 1.1 Cyclophanes
 - 1.2 Palladium-Catalyzed Coupling Reactions
 - 1.3 Acetylene Dimerization Reactions
 - 1.3.1 *Symmetrical Di- and Oligoalkynes*
 - 1.3.2 *Unsymmetrical Di- and Oligoalkynes*
 - 1.4 Previous Fallis Lab Cyclophane Chemistry
-

1. Introduction

Synthetic organic chemistry encompasses the synthesis of target molecules and the development of new methods to be used in the preparation of these targets.¹ The focus of the research presented in this dissertation is on the synthesis of new unsaturated cyclophanes and related compounds and highlighted by the development of new methods and strategies to achieve the synthetic goals.

The first synthetic targets were a series of C₆₀-acetylenic cyclophanes (Chapter 2). This project was an extension of previous research in the Fallis lab on the synthesis of large macrocycles to examine their spectroscopic and physical properties. The C₆₀ cyclophanes were of initial interest as potential precursors to fullerenes.

Related research involved the preparation of enantiopure, helical acetylenic cyclophanes by using metals to inhibit helical interconversion (Chapter 3). Two classes of cyclophanes were synthesized. The first class was a tetramethoxybenzene-capped cyclophane as a potential η^{12} -bis(arene) ligand, while the second class was phenanthroline-capped cyclophanes capable of making π -complexes with metals.

The last project involved the synthesis of new pentacene derivatives with substituents on the A and E rings (Chapter 4). Introduction of substituents on the α and ω rings of acenes remains a synthetic challenge and there have been no reported preparations of pentacene derivatives with these substitution patterns. Pentacene and related compounds have been shown to be organic semiconductors. The semiconducting properties of these new pentacenes will be studied as well as their potential as model compounds for crystal engineering research.

The remainder of this chapter will provide a brief history of cyclophanes, discuss palladium-catalyzed and copper-mediated reactions that were used in the synthesis of various acetylenic cyclophanes, and present the previous cyclophane work from the Fallis lab that formed a foundation for the research described within this dissertation.

1.1 Cyclophanes

Cyclophanes are defined as "*molecules with at least one aromatic ring bridged by at least one aliphatic n-membered bridge*".² Cyclophanes first appeared in the literature in 1899 when Pellegrin reported the synthesis of "di-*m*-xylylene" (**1**).³ No further work was

conducted on these compounds for 50 years until Brown reported the synthesis and X-ray crystal structure of "di-*p*-xylylene" (**2**).⁴ Despite these earlier reports, Cram is considered the father of cyclophane chemistry after he reported the synthesis of a series of new compounds and introduced the term "cyclophane" that was a contraction of the words *cyclo*, *phenyl*, and *alkane*.⁵ A systematic nomenclature system was later proposed by Vögtle and is still used today.⁶

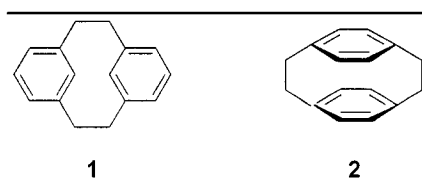


Figure 1: [2.2]*Metacyclophane* (**1**) and [2.2]*paracyclophane* (**2**).

Cyclophanes have unusual and aesthetically pleasing structures, pose synthetic challenges, have peculiar reactivity, and often exhibit interesting spectroscopic and physical properties.⁷ Current cyclophane research reflects all of these interests. Photolysis of [3₃](1,3,5)cyclophane (**3**) led to new complex carbon-caged compounds (Figure 2).⁸ New phenanthrenoparacyclophanes (**4**) were prepared in order to study their NMR properties.⁹ A number of chiral cyclophanes have recently been prepared. These non-racemic cyclophanes have been used as asymmetric catalysts (**5**)¹⁰ and have the ability to bind metal ions (**6**).¹¹ New cyclophane-based materials have also emerged, such as the optically active [2.2]*paracyclophane* derivative **7**, which exhibits mesogenic properties (liquid crystal),¹² and various polyunsaturated cyclophanes.¹³

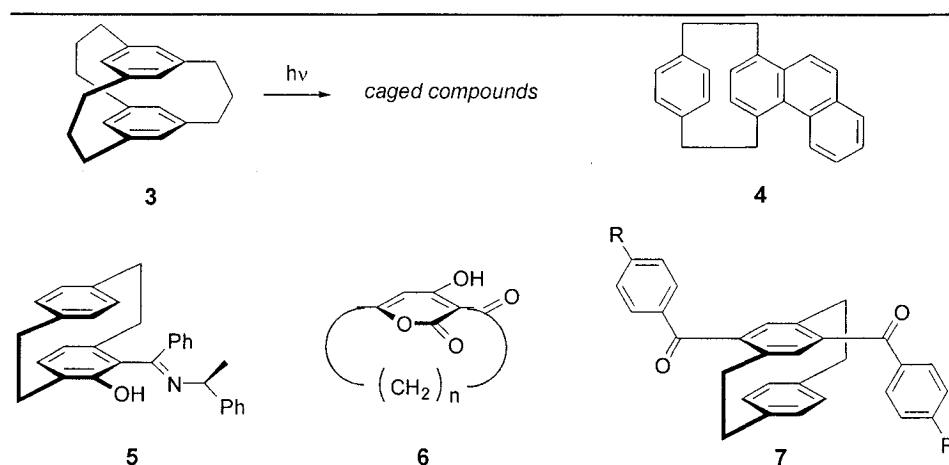


Figure 2: Examples of current cyclophane research.

1.2 Palladium-Catalyzed Coupling Reactions

Two palladium-catalyzed coupling reactions were used extensively during the synthesis of the acetylenic cyclophanes reported in this thesis: The Negishi and Sonogashira coupling reactions. An introduction to palladium-catalyzed coupling reactions is presented in this section with an emphasis on these two reactions.

Over the last twenty years the development of palladium catalysts for the formation of new carbon-carbon bonds has revolutionized synthetic organic chemistry. The high cost of palladium is far out-weighed by the versatility and functional group tolerance of its catalysts. Furthermore, palladium has not posed the toxicity problems that have plagued other metals.

Palladium is a noble metal (d^{10}), forms square-planar complexes, and exists in two oxidation states, Pd(0) and Pd(II). As a result, the mechanisms of palladium-catalyzed coupling reactions are well understood. The Stille coupling reaction, a palladium-catalyzed coupling reaction of an organic halide with an organostannane, has been most widely studied.¹⁴ However, the mechanism for the Stille reaction is the same for a variety of organometallic coupling partners, such as organo-Zn (Negishi reaction), B (Suzuki reaction), Mg (Kumada-Tamao), Al (Nozaki-Oshima), Cu (Normant), and Zr (Negishi) compounds.^{15,16}

The catalytic cycle for the Negishi reaction is shown in Figure 3.¹⁷ Each step of the catalytic cycle has been extensively studied¹⁸ and recently an anionic catalytic cycle has been accepted.¹⁷ A number of commercially available palladium(0) and palladium(II) complexes can be used to generate active catalyst **9**.

The first step of the catalytic cycle is the oxidative addition of an organic halide **10**,¹⁹ leading to anionic Pd(II) complex **11**. The order of organohalide reactivity is vinyl iodide \cong vinyl bromide > aryl iodide > vinyl chloride \gg aryl bromide \gg aryl chloride. Vinyl halides and aryl iodides are all reactive enough to undergo oxidative insertion at room temperature. Higher reaction temperatures are often required for aryl bromides and chlorides, although the use of electron-donating phosphine ligands have been shown to overcome this synthetic difficulty.^{20,21}

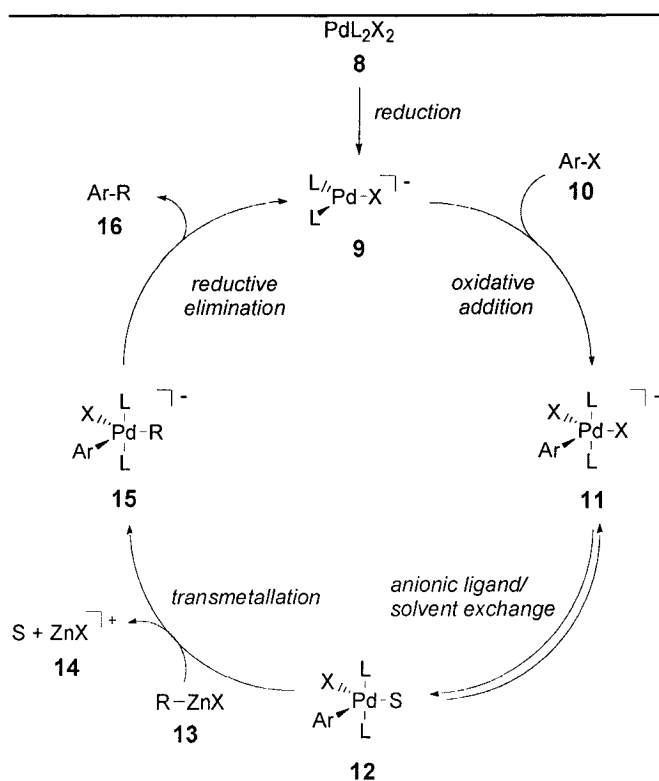
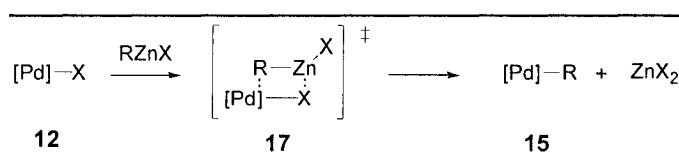


Figure 3: Catalytic cycle for the Negishi reaction.

Trigonal bipyramidal palladium(II) complex **11** is in equilibrium with neutral palladium(II) complex, **12** (S = solvent). Complex **12** then undergoes transmetalation with organometallic **13**. A number of organometallic coupling partners are known to participate in the transmetalation step (*vide supra*). Mechanistic studies suggest that the transmetalation step occurs with the organic portion of the organometallic being exchanged for the solvent on the palladium complex to give **15** (Scheme 1).²² The resulting palladium(II) complex **15** then reductively eliminates the coupled product (**16**) and regenerates the active palladium catalyst, **9**.



Scheme 1: Transmetalation step of the Negishi reaction.

The Sonogashira reaction is a palladium-catalyzed cross-coupling of organic halides with terminal alkynes in the presence of a co-catalyst, such as copper iodide, and an amine base.^{23,24} The active Pd(0) catalyst **9** is generated from successive transmetalation reactions

with copper acetylide **19** to give the Pd(II) complex **22** followed by reductive elimination (Figure 4). An excess of the terminal alkyne **20** is required in the reaction as two equivalents of the alkyne are consumed to generate every equivalent of active catalyst.

The Sonogashira palladium catalytic cycle operates in the same manner as the Negishi reaction – oxidative insertion of an organic halide, transmetallation, and reductive elimination – except that the copper acetylide used in the transmetallation step is generated catalytically from copper(I) iodide and a terminal alkyne in the presence of an amine base. The use of an amine base is important and diethylamine or triethylamine are often used as co-solvents with THF. Various other amine bases have been used, particularly when organic triflates are used in place of organic halides.

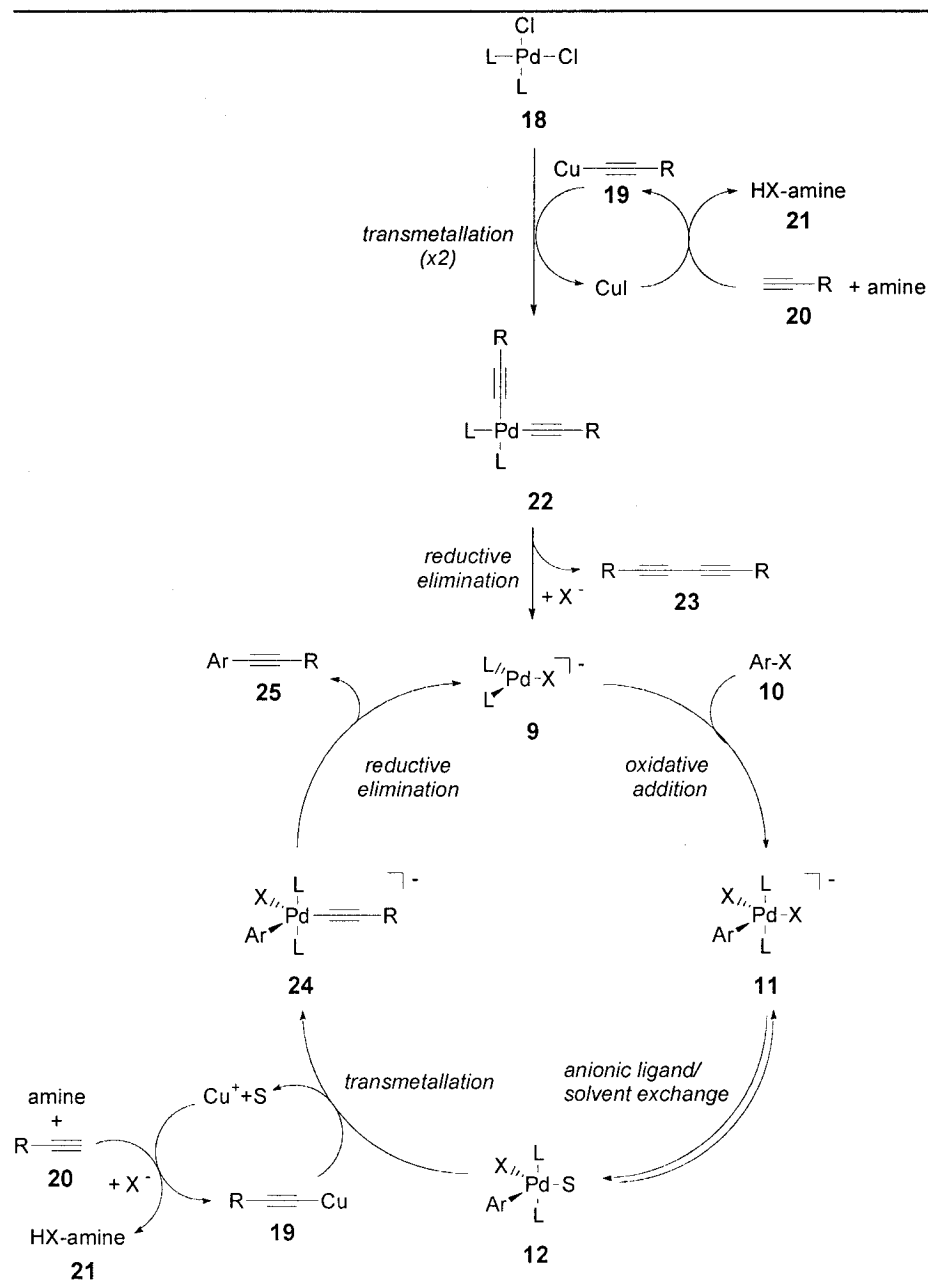


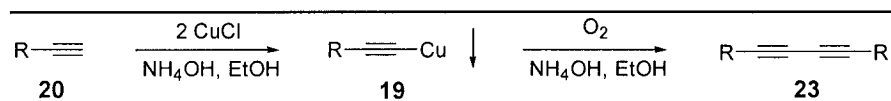
Figure 4: Catalytic cycle for the Sonogashira reaction.

1.3 Acetylene Dimerization Reactions

Di- and oligoalkynes are structural features found in many natural products. More recently, new alkyne-based materials have been synthesized to study their interesting electronic and optical properties. These synthetic targets have prompted the development of numerous methods for the preparation of symmetrical and unsymmetrical dialkynes.

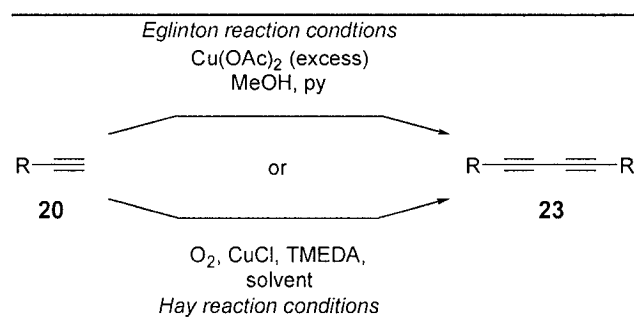
1.3.1. Symmetrical Di- and Oligoalkynes

The dimerization of symmetrical dialkynes was first reported by Glaser.²⁵ In the Glaser dimerization reaction a terminal alkyne (**20**) is converted to copper acetylide **19**, which is then dimerized to dialkyne **23** in the presence of oxygen or other oxidants (Scheme 2). Isolation of copper acetylide **19** limited the use of this procedure and led to the development of new one-pot dimerization procedures by Eglinton and Hay.



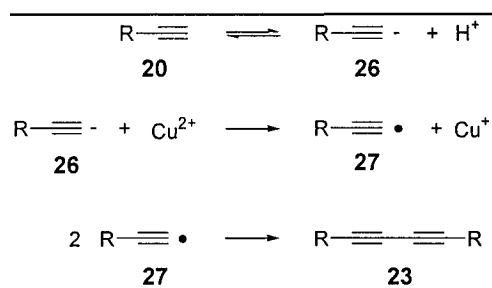
Scheme 2: Glaser alkyne dimerization reaction.

Eglinton showed that terminal alkynes could be dimerized using an excess of a copper (II) salt, often $\text{Cu}(\text{OAc})_2$, in a mixture of methanol and pyridine (Scheme 3).²⁶ Hay's alkyne dimerization used a copper(I) salt (CuCl) in the presence of *N,N,N',N'*-tetramethylethylenediamine (TMEDA).²⁷



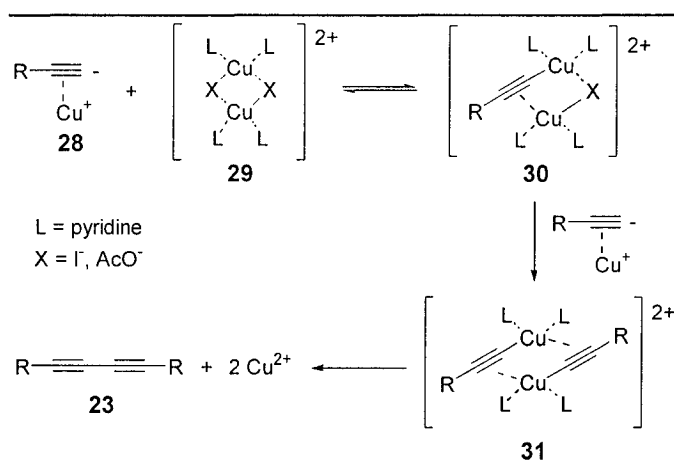
Scheme 3: Eglinton and Hay alkyne dimerization reactions.

The mechanism of the copper-mediated alkyne dimerization reaction remains poorly understood.²⁸ A radical mechanism was initially proposed (Scheme 4),²⁹ but mixtures of electronically different alkynes gave predominantly homocoupled products, which would not be observed under free radical reaction conditions.



Scheme 4: A proposed radical mechanism for the copper-mediated alkyne dimerization reaction.

Later research showed that the rate of dimerization was faster for acidic alkynes under basic conditions. Furthermore, Cu(I) was required for the reaction to occur under acidic conditions, which suggested that copper may complex to the triple bond, thereby increasing the acidity of the terminal proton.³⁰ This observation explained why conjugated substrates reacted slower than unconjugated ones as conjugated alkynes would have less localized electron density and disfavor copper coordination. These findings, coupled with the fact that the rate of the dimerization reaction was found to be second order with respect to the alkyne, led to the development of a new ionic mechanism based on dimeric copper(II) acetylide complex **31**, which would collapse to give symmetrical alkyne product **23** (Scheme 5).³⁰ This mechanism, or variants of it, are generally accepted today.



Scheme 5: Ionic copper-mediated alkyne dimerization reaction mechanism.

Symmetrical di- and oligoalkynes have also been prepared using palladium-catalyzed alkyne dimerization reactions. These reactions follow a catalytic cycle similar to the Sonogashira reaction described above; however, oxidants such as chloroacetone,³¹ I₂,³² or ethyl bromoacetate³³ are required to regenerate the active palladium(II) catalyst, **32**, which

then undergoes successive transmetallations to give **22** followed by reductive elimination of symmetrical dialkyne product **23** (Figure 5).

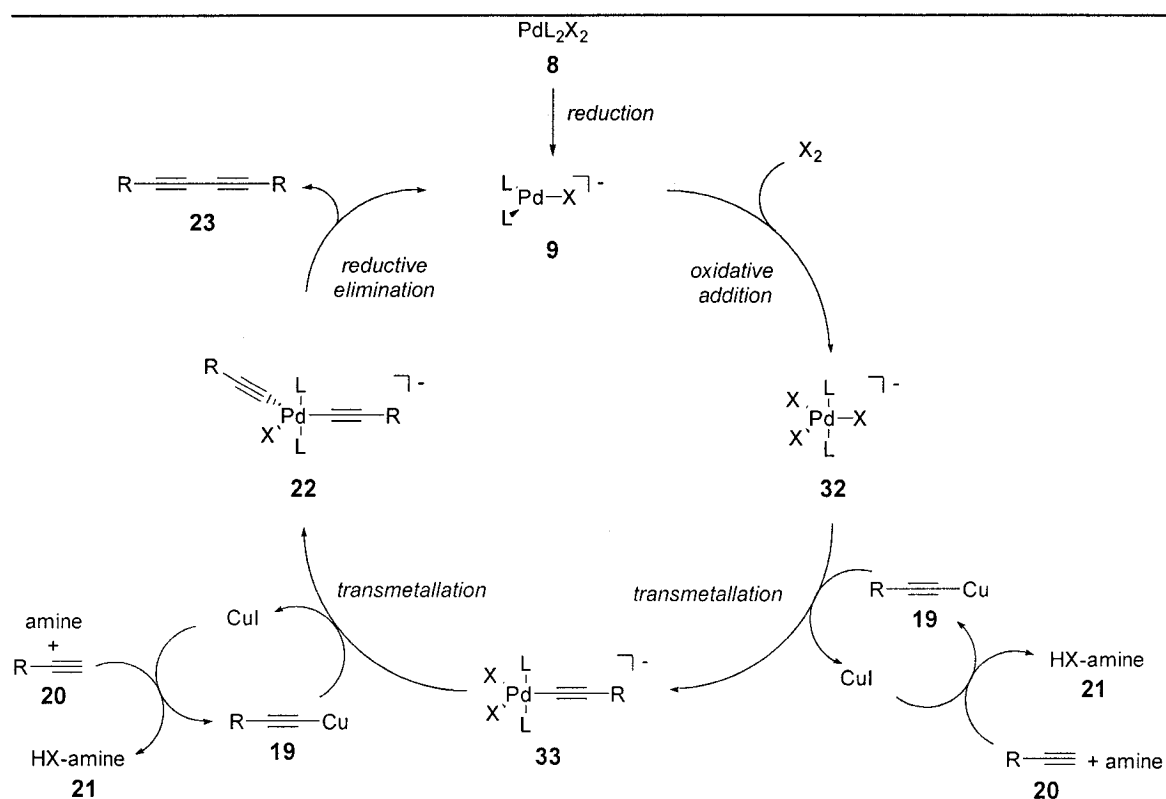
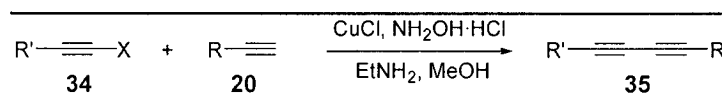


Figure 5: Catalytic cycle for the palladium-catalyzed dimerization of alkynes.

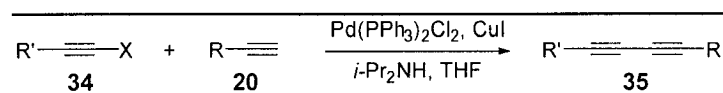
1.3.2. Unsymmetrical Di- and Oligoalkynes

Methods have also been developed for the preparation of unsymmetrical alkynes. Chodkiewicz and Cadot developed a copper(I)-mediated reaction of a haloalkyne **34** ($\text{X} = \text{Br}, \text{I}$) and a terminal alkyne **20** to yield unsymmetrical diynes **35** (Scheme 6).³⁴



Scheme 6: Chodkiewicz-Cadot reaction to yield unsymmetrical diynes.

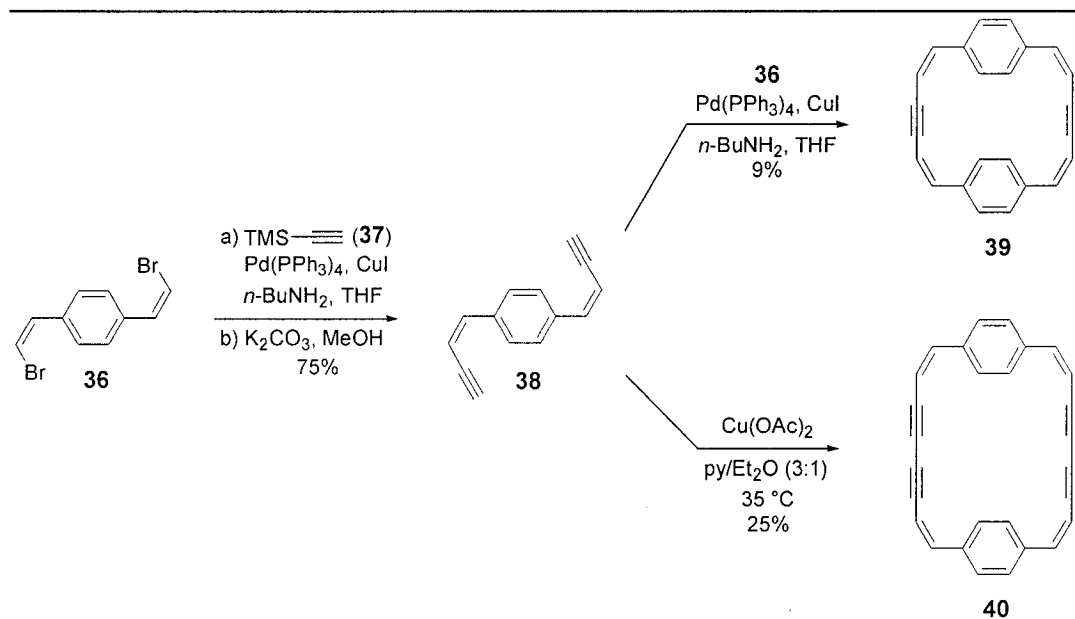
Palladium-catalyzed coupling reactions have also been used to prepare unsymmetrical diynes. Haloalkynes **34** are reacted with terminal alkynes **20** under Sonogashira reaction conditions to yield unsymmetrical diynes **35** (Scheme 7).³⁵



Scheme 7: Palladium-catalyzed preparation of unsymmetrical diynes.

1.4 Previous Fallis Lab Cyclophane Chemistry

The Fallis group has studied the synthesis of unsaturated cyclophanes for the past ten years. The first compounds that were prepared were eneyncyclophanes **39** and **40**.³⁶ Both cyclophanes were prepared from dibromide **36** in two steps using either palladium or copper coupling reactions (Scheme 8). The capping aryl rings were found to freely rotate through the cavity of the molecules, which is not observed for [2.2]*paracyclophanes*. Furthermore, these cyclophanes were not flat as illustrated, but adopted helical conformations and were thus chiral.



Scheme 8: Synthesis of eneyncyclophanes **39** and **40**.

Encouraged by these preliminary results, a highly convergent route to cyclophane **43** was envisioned, which could be a synthetic precursor to buckminsterfullerene **41** (Figure 6). Cyclotrimerization of enediyne **45** would rapidly lead to dimerization precursor **44**. Dimerization of **44** would give cyclophane **43**, which could then be oxidized to highly strained C₆₀ cyclophane **42**, which should isomerize to buckminsterfullerene **41**.

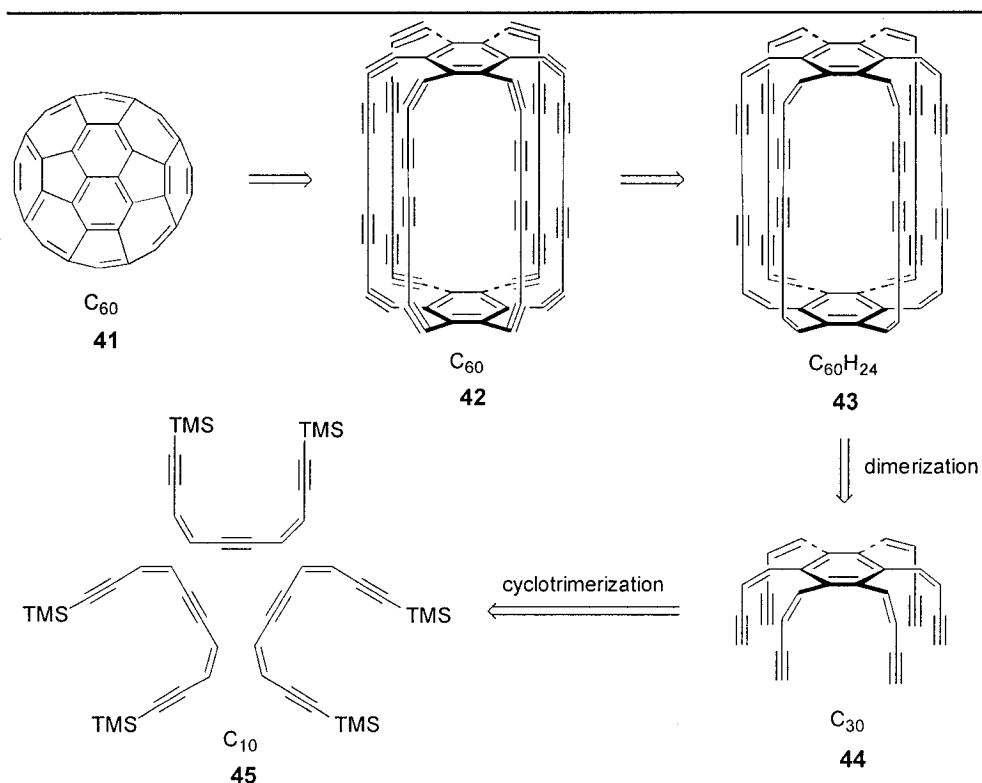
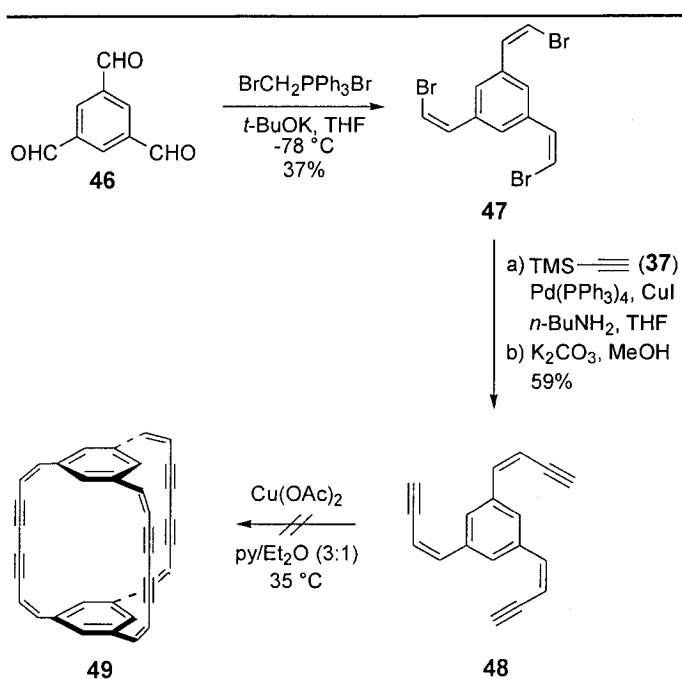


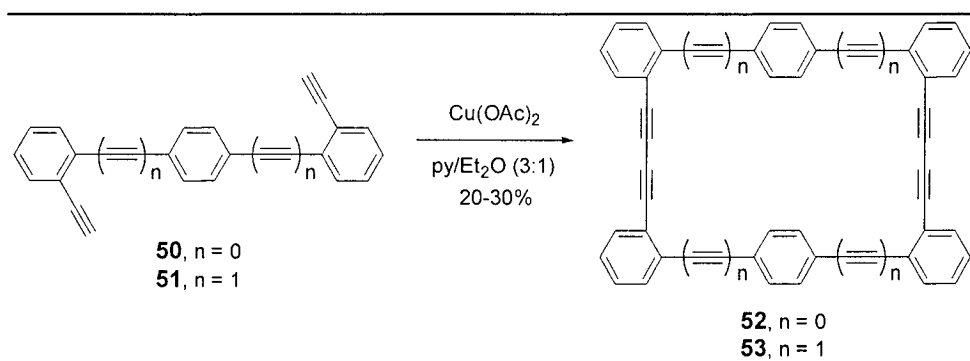
Figure 6: Proposed eneyncyclophane 43 as a C₆₀ synthetic precursor.

However, extension of the eneyncyclophane chemistry to the synthesis of 1,3,5-cyclophanes, such as 49, proved to be difficult. The Wittig reaction used to synthesize tribromide 47 gave mixtures of *cis* and *trans* isomers, although dimerization precursor 48 could be isolated (Scheme 9).³⁷ Unfortunately, cyclophane 49 was not obtained from the copper-mediated dimerization reaction.



Scheme 9: Attempted synthesis of 1,3,5-eneynecyclophane 49.

The next generation of cyclophanes had aryl rings in place of the olefins in order to simplify the cyclophane synthesis by eliminating the olefin stereochemistry problems. Cyclophanes **52** and **53** were prepared and found to adopt helical conformations (Scheme 10).³⁸ The synthesis of these cyclophanes followed the same strategy that was used to prepare the eneyne cyclophanes as a copper-mediated dimerization reaction was used to form the macrocycle in the final step.



Scheme 10: Synthesis of cyclophanes **52** and **53**.

Cyclophane **54** with substituents on the capping aryl rings was prepared as a potential liquid crystal (Figure 7).³⁹ Also, strained cyclophanes **55**, **56**, and **57** were prepared.

Cyclophane **57** had the greatest strain with alkyne bond angles as low as 153.4° , considerably distorted from the preferred 180° bond angle for *sp*-hybridized carbon atoms.⁴⁰

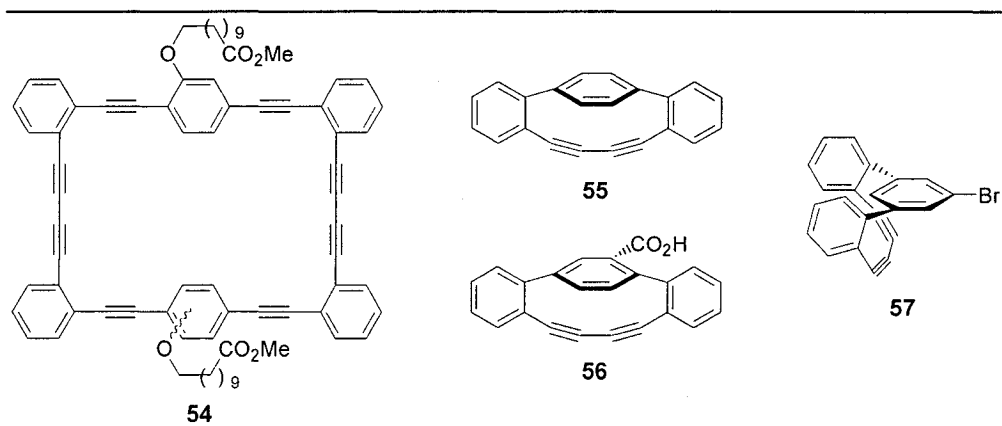


Figure 7: Potential liquid crystal cyclophane **54** and strained cyclophanes **55**, **56**, and **57**.

Chapter

C60 ACETYLENIC CYCLOPHANES

- 2.1 Rational Synthesis of C₆₀ from Acetylenic Cyclophane Precursors
 - 2.2 Synthesis of C₆₀H₂₄ *para*-Cyclophane **75**
 - 2.3 *In Situ* Desilylation/Dimerization of Silylalkynes
 - 2.4 Synthesis of *para*-Cyclophane **104**
 - 2.5 Stepwise Synthesis of *para*-Cyclophane **113**
 - 2.6 Inter- vs. Intramolecular Dimerization of α,ω -Diyne
 - 2.7 Synthesis of *meta*-Cyclophane **123**
 - 2.8 Summary
-

2. C₆₀ Acetylenic Cyclophanes

This chapter contains the work related to the synthesis of C₆₀ acetylenic cyclophanes; *i.e.* acetylenic cyclophanes that contain sixty carbon atoms within the macrocycle. These unsaturated molecules were initially of interest as synthetic precursors to buckminsterfullerene (C₆₀). Synthetic strategies and chemistry that were developed from previous cyclophane work in the Fallis group was applied to the synthesis of these larger molecules.

2.1 Rational Synthesis of C₆₀ from Acetylenic Cyclophane Precursors

The synthesis of polyhedra such as cubane (**58**)⁴¹ and dodecahedron (**59**)⁴² were synthetic landmarks and proved to require a great deal of creativity to complete. Thus, when buckminsterfullerene (C₆₀, **41**), a new allotrope of carbon, was reported in 1985⁴³ a number of synthetic groups were interested in tackling this new, complex target.

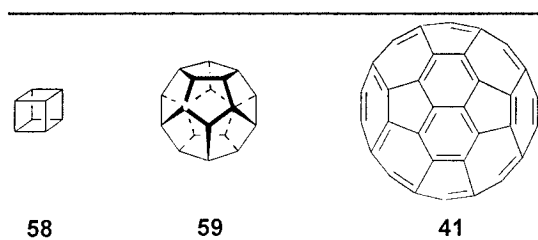
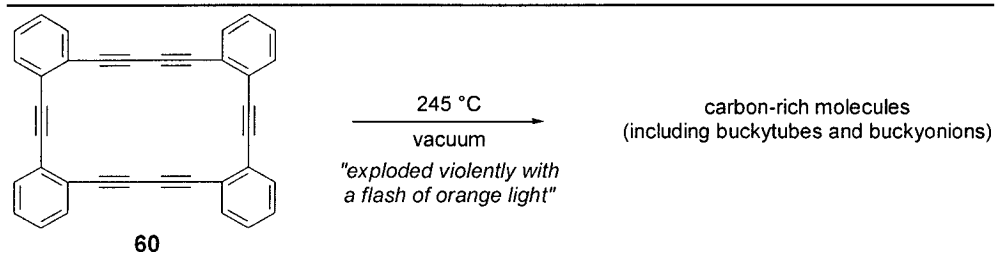


Figure 8: Cubane (**58**), dodecahedron (**59**), and buckminsterfullerene (**41**).

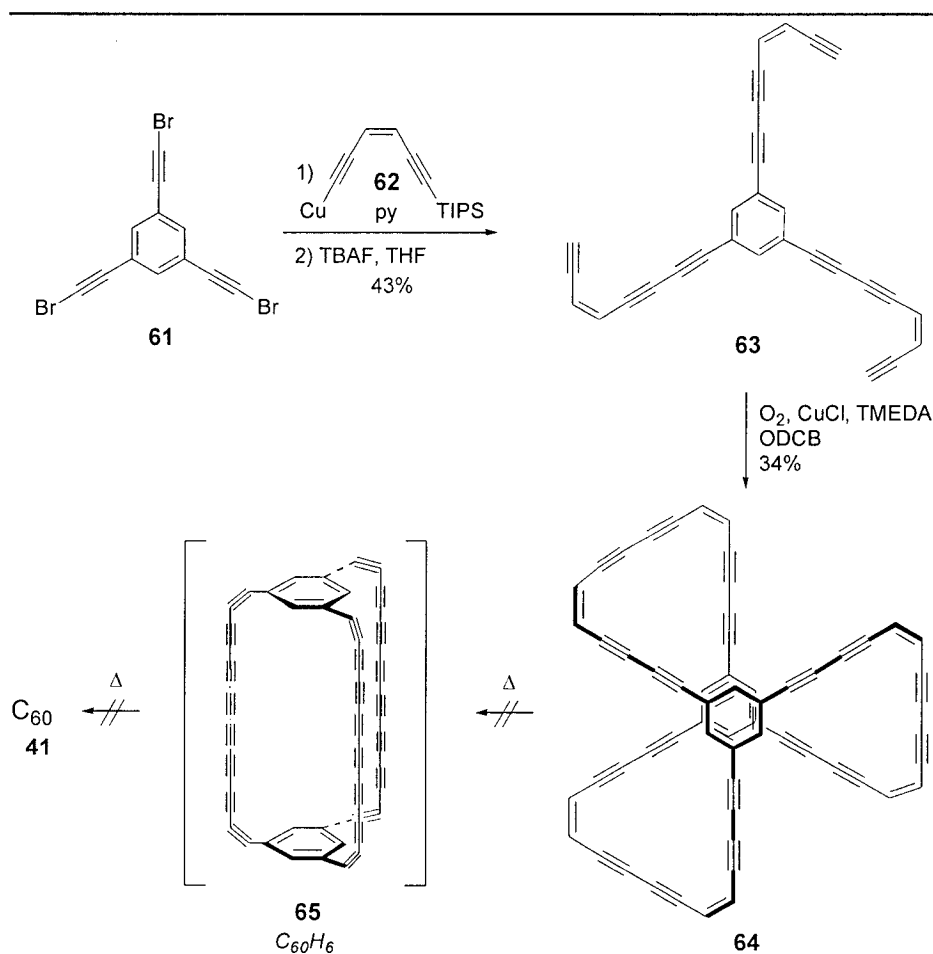
The preparation of C₆₀ is currently achieved from carbon-rich vapours, which can be formed in several ways including passing an electric arc between two graphite rods in an evacuated chamber.⁴⁴ Several fullerene products are produced by this evaporation method (C₆₀, C₇₀, and small amounts of higher fullerenes), and the separation and purification of these compounds is difficult.⁴⁴ High purity C₆₀ is of particular interest as a *n*-doped semiconducting material as impurities greatly attenuate its performance. Thus, an efficient, rational synthesis of C₆₀ is more than just an academic interest.

A landmark paper by Vollhardt's group in 1997 reported the thermal rearrangement of dehydroannulene **60** to carbon-rich compounds including buckytubes and buckyonions (Scheme 11).⁴⁵ Calculations predict that C₆₀ is thermodynamically stable suggesting that strained, unsaturated macrocycles could be used as suitable synthetic precursors.⁴⁶



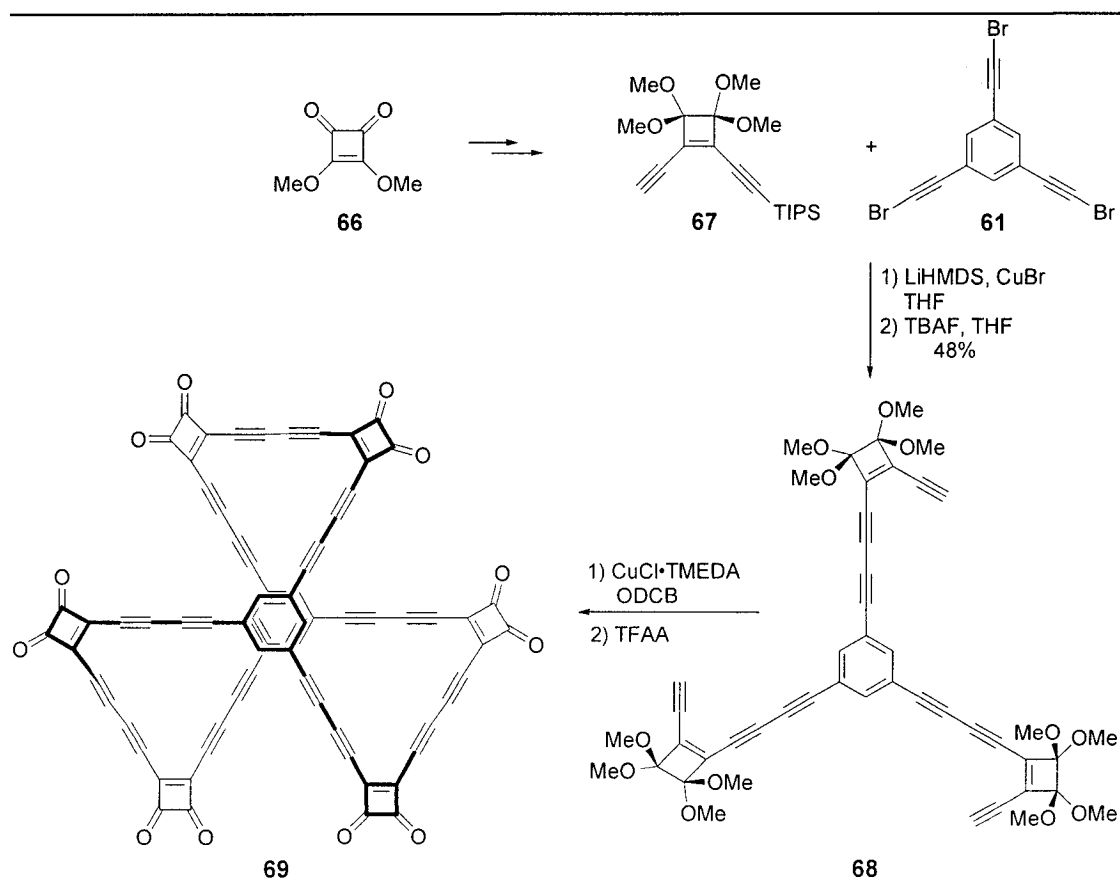
Scheme 11: Pyrolysis of Vollhardt's dehydroannulene **60 to give carbon-rich compounds.**

Several groups have explored the possibility of using unsaturated precursors to fullerene materials⁴⁶ including cyclic alkynes⁴⁷ and trindane building blocks,⁴⁸ but only unsaturated cyclophanes will be included in this discussion. The first acetylenic cyclophane that was designed and synthesized specifically as a C_{60} precursor was cyclophane **64** (Scheme 12).⁴⁹ Thermolysis of **64** favored Bergman cyclizations of the enediyne moieties and not dehydrogenation to form the desired $C_{60}H_6$ -cyclophane **65** intermediate.



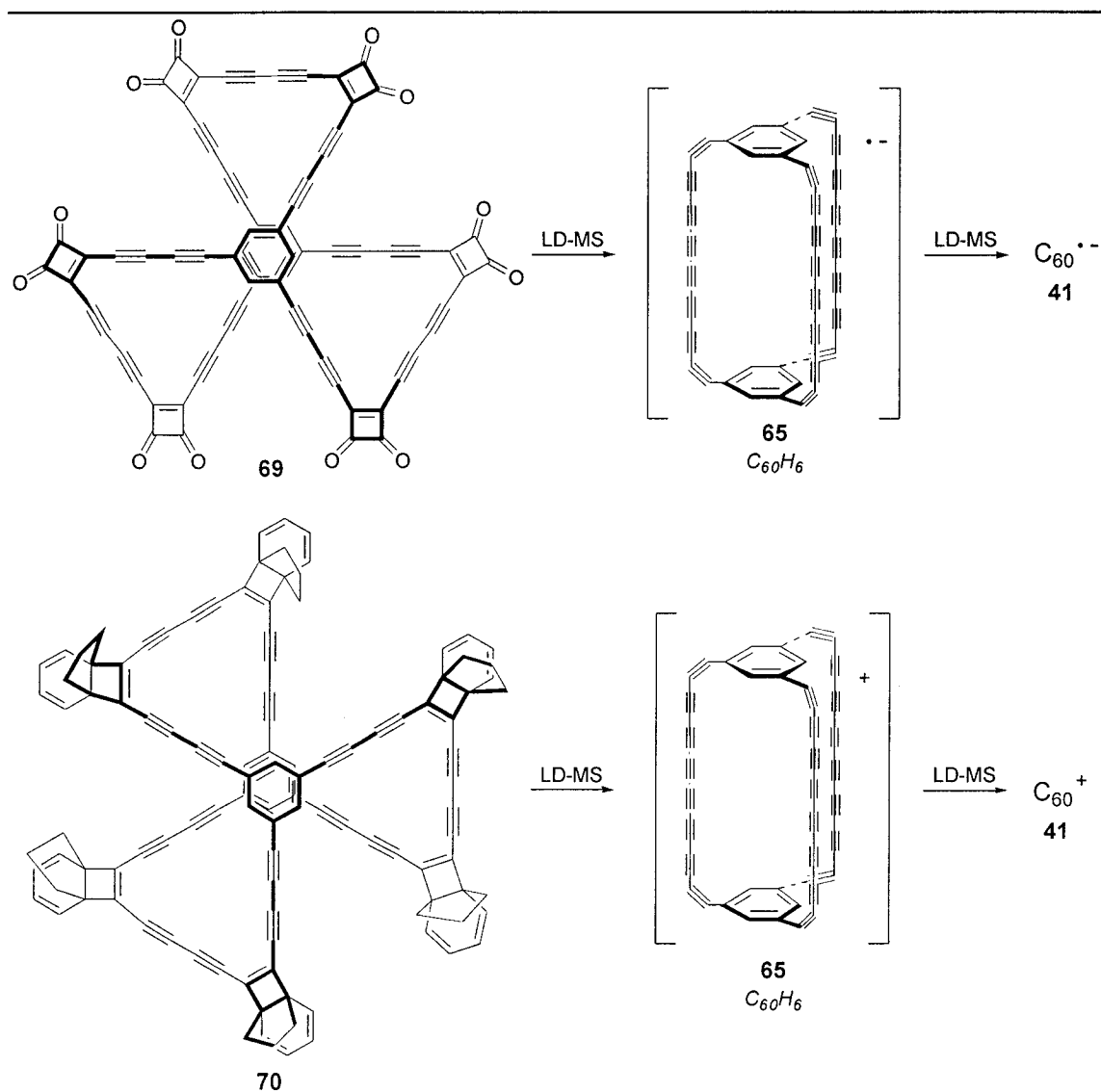
Scheme 12: Rubin's $C_{60}H_{18}$ cyclophane precursor to C_{60} .

In order to favor the formation of cyclophane **65** and prevent Bergman cyclizations observed during thermolysis of cyclophane **64**, Rubin's group prepared a new cyclophane, **69**, with cyclobutenedione in place of olefins (Scheme 13).⁵⁰



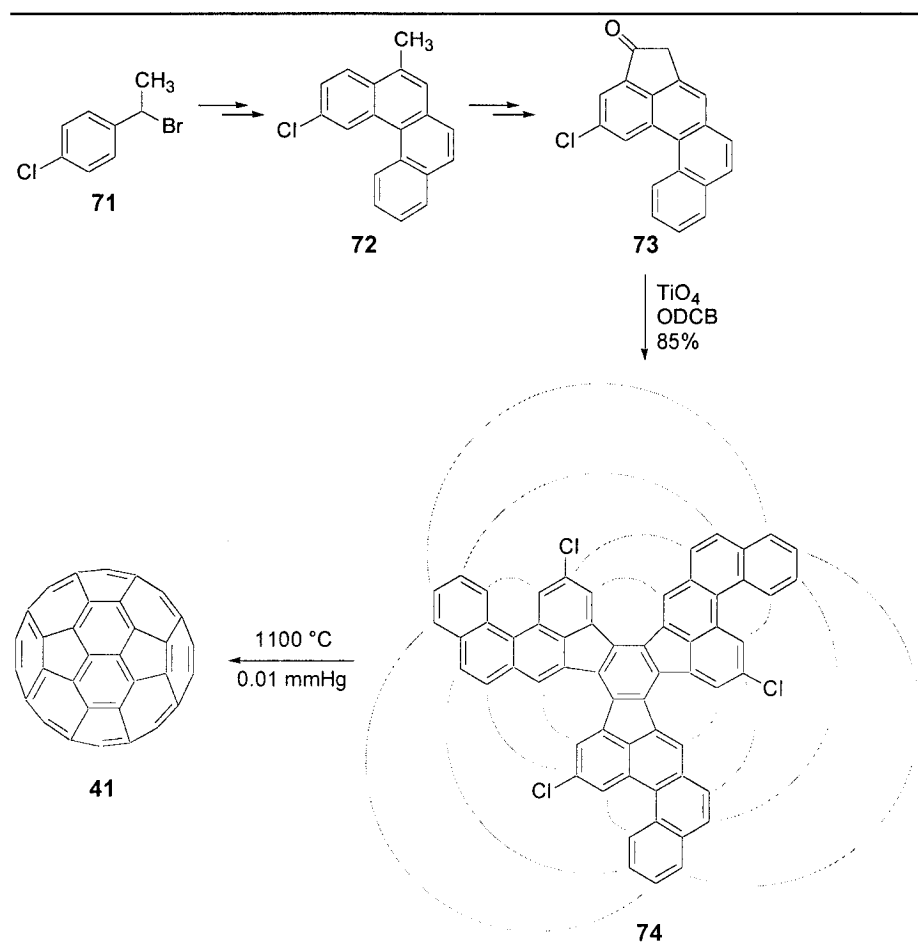
Scheme 13: Rubin's $C_{60}H_6(CO)_{12}$ cyclophane **69** as a C_{60} precursor.

Knowing cyclobutenedione releases acetylenes and carbon monoxide under vacuum in the gas phase, cyclophane **69** was expected to form cyclophane **65** *en route* to C_{60} under vacuum (Scheme 14). A similar approach was investigated by Tobe's group with cyclophane **70** expected to undergo a cycloreversion of the [4.3.2]propellatriene subunit to give cyclophane **65** and C_{60} (Scheme 14).⁵¹ In both cases, laser desorption mass spectrometry (LD MS) gave rise to the $C_{60}H_6$ cyclophane **65** and C_{60} . Although these species were detected, they could not be isolated.



Scheme 14: Laser desorption mass spectrometry of cyclophanes 69 and 70 to give $C_{60}H_6$ and C_{60} .

The first rational synthesis of C_{60} was reported in 2002 by Scott's group (Scheme 15).⁵² The synthesis was completed in 12 linear steps from commercially available starting materials to give milligram quantities of C_{60} in 1% yield in the last step. High purity C_{60} was obtained as no other fullerene products could be detected. This observation provided evidence that their pyrolysis precursor 74 underwent a zipper-type reaction as opposed to a fragmentation/recombination.



Scheme 15: Scott's rational C₆₀ synthesis.

2.2 Synthesis of C₆₀H₂₄ *para*-Cyclophane 75

Cyclophane **75** was chosen as our first synthetic target for a number of reasons. Not only would cyclophane **75** be the second molecule to contain an octatetrayne bridge,⁵³ but the high degree of symmetry present in the molecule should allow for its rapid synthesis. Furthermore, our group's synthetic strategy used to prepare previous cyclophanes could be applied to the synthesis of **75**.^{38,39} Retrosynthetic analysis suggests that a copper mediated Eglinton coupling of two C₃₀ precursors (**76**) would lead to cyclophane **75** (Figure 9). Precursor **76** could be rapidly assembled *via* a Sonogashira reaction of 1,4-diethynylbenzene (**77**) with two equivalents of bromide **78**, two substrates that have been previously prepared in our lab.⁵⁴

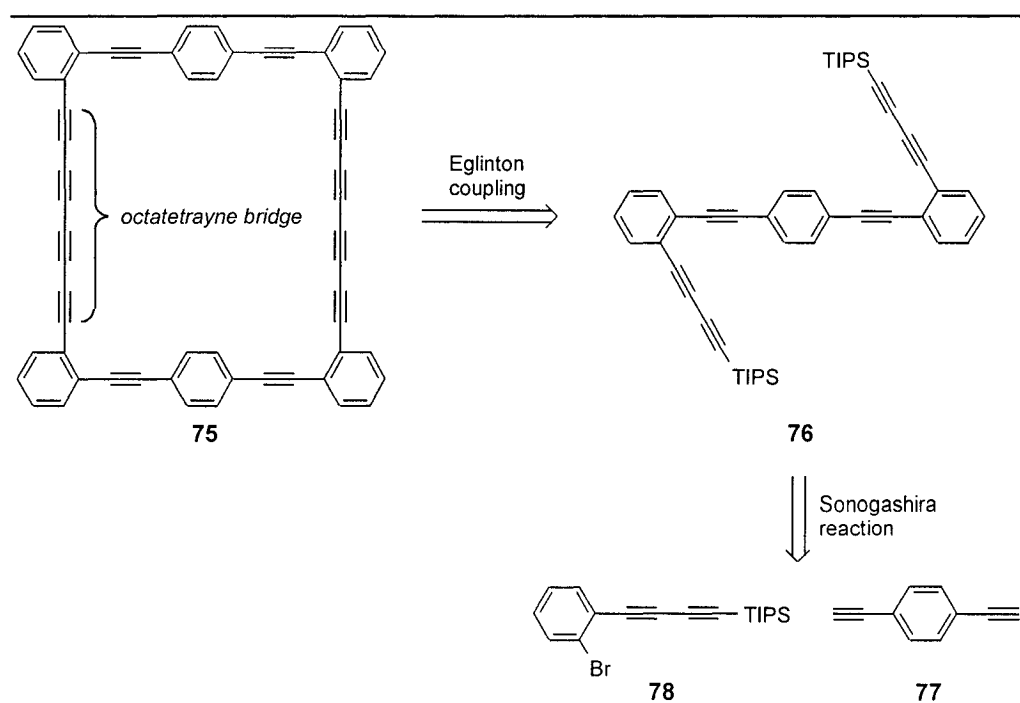
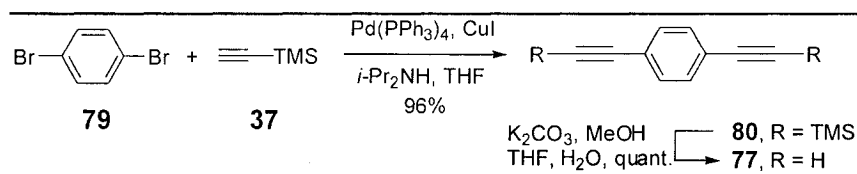


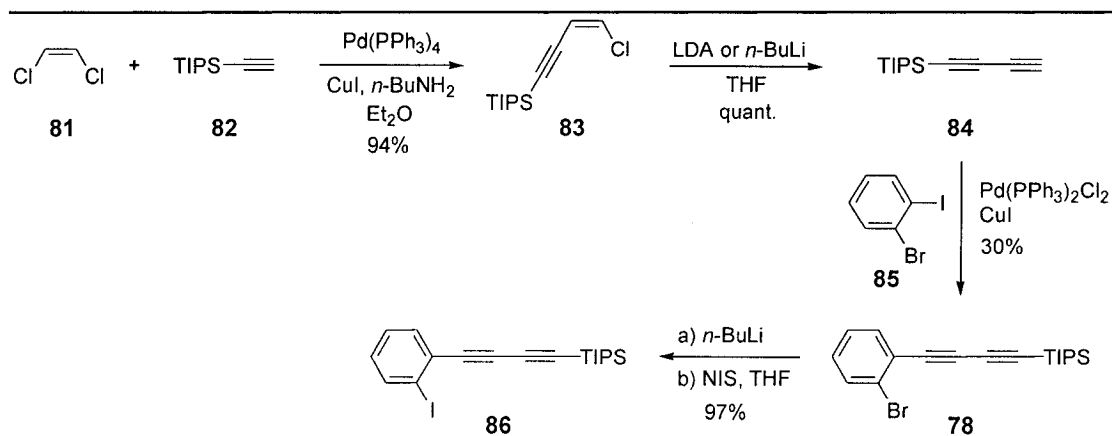
Figure 9: Retrosynthetic analysis of cyclophane 75.

The preparation of 1,4-diethynylbenzene (**77**) began with a Sonogashira reaction of 1,4-dibromobenzene (**79**) and trimethylsilylacetylene (TMS-acetylene, **37**) (Scheme 16). Protodesilylation with K_2CO_3 in wet methanol/THF gave **77** in 96% combined yield.



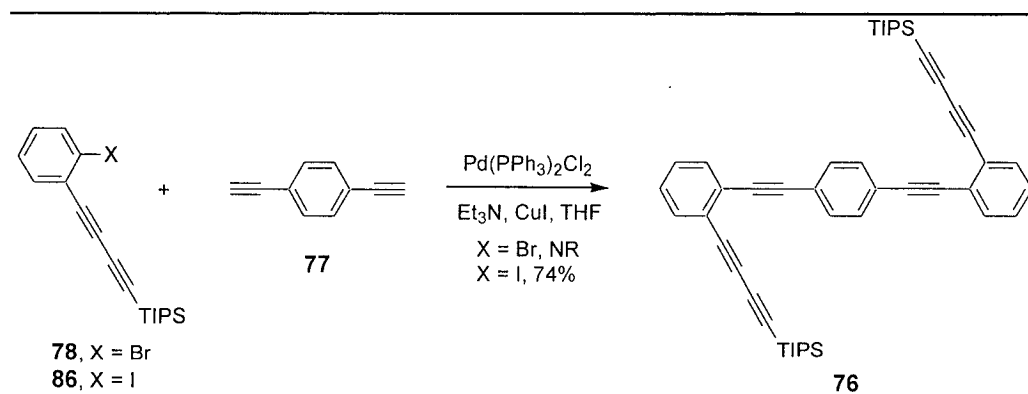
Scheme 16: Preparation of 1,4-diethynylbenzene (**77**).

Bromide **78** was also prepared using a Sonogashira reaction (Scheme 17). *cis*-1,2-Dichloroethane (**81**) underwent a Sonogashira reaction with triisopropylsilylacetylene (TIPS-acetylene, **82**) to afford enynechloride **83** in 94% yield.⁵⁵ Treatment of **83** with either *n*-BuLi or LDA gave silylbutadiyne **84** in quantitative yield, but **84** had to be used immediately as storage led to significant decomposition. Bromide **78** was prepared *via* a Sonogashira reaction of **84** with 1-bromo-2-iodobenzene (**85**). Chromatographic separation of bromide **78** from **85** was difficult, but purified bromide **78** could be obtained in 30% after repeated flash chromatography.



Scheme 17: Preparation of bromide **78** and iodide **86**.

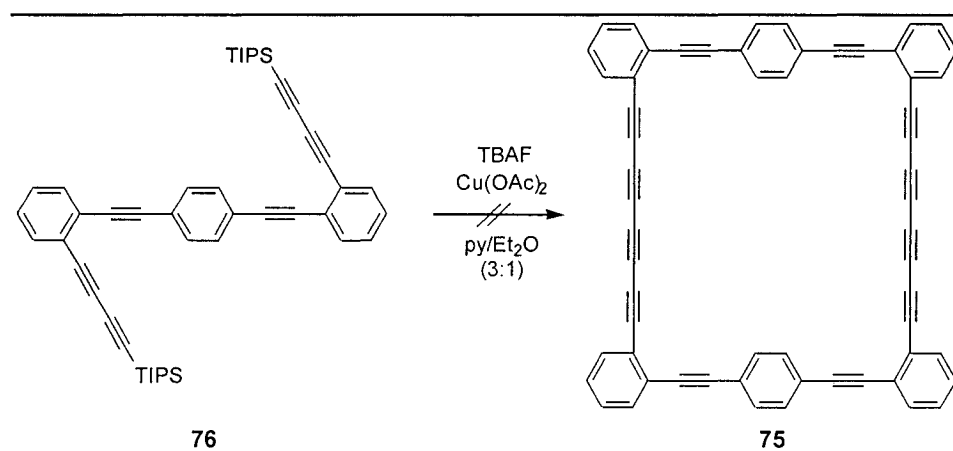
Construction of cyclophane **75** continued with the Sonogashira reaction of 1,4-diethynylbenzene (**77**) and an excess of bromide **78** (Scheme 18). Unfortunately, bromide **78** was the major compound isolated from the reaction. In addition, all of **77** was consumed, presumably to yield homocoupled products. The isolation of bromide **78** suggested that palladium was not oxidatively inserting into the aryl carbon-bromide bond, which is the first step of the Sonogashira reaction catalytic cycle. To overcome this difficulty, bromide **78** was converted to the corresponding iodide, **86**, by lithium-halogen exchange with *n*-BuLi, followed by quenching with *N*-iodosuccinimide (Scheme 17). As expected, the Sonogashira reaction of iodide **86** and **77** proceeded smoothly to afford **76** in 74% yield (Scheme 18).



Scheme 18: Synthesis of dimerization precursor **76**.

We were concerned with the potential instability of the deprotected arylbutadiyne moieties⁵⁶ so one-pot deprotection/dimerization procedures were considered (see Section 2.3). However, all known deprotection/dimerization methods used to dimerize

trimethylsilylalkynes (TMS-alkynes) could not be extended to bulkier silylalkynes. We were faced with the choice of either preparing the TMS-analogue of **76** or developing a more general desilylation/dimerization protocol. We decided that a desilylation/dimerization method that could be applied to a variety of silylalkynes was worth investigating and the results of this study are presented in the following section.



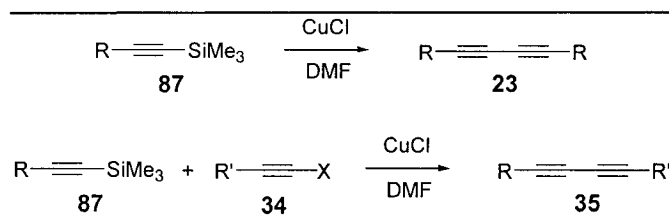
Scheme 19: Attempted formation of cyclophane **75** by the dimerization of **76**.

When our desilylation/dimerization method [TBAF, Cu(OAc₂), py/Et₂O (3:1)] (see Section 2.3) was used in the dimerization of **76**, no reaction products were isolated (Scheme 19). This result was not unexpected as other highly-unsaturated molecules with high molecular weights tend to suffer from poor solubility. Alkyl (*i*-Pr,⁴⁵ *t*-Bu,⁵⁷ and *n*-Dec⁵⁸), heteroatom (ethers⁵⁹ and tertiary amines⁶⁰), and ester⁶¹ substituents have been added to the aromatic rings to improve the solubility of these unsaturated macrocycles. For this reason, we decided to study functionalized cyclophanes despite the appeal of the parent, unsubstituted compound. The design and synthesis of a functionalized analogue of cyclophane **75** is found in Section 2.4.

2.3 *In situ* Desilylation/Dimerization of Silylalkynes

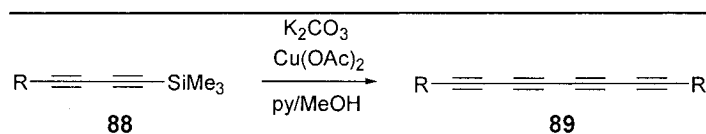
Most polyynes are prepared by the oxidative coupling of 1-alkynes as described in Section 1.3. However, the rapid decomposition of many 1-alkynes poses a challenge in preparing polyynes in this fashion.⁵⁶ One-pot desilylation/dimerization methods have been developed to eliminate the isolation, purification, and handling of unstable 1-alkynes in the preparation of polyynes. Mori's group reported high yields (80-100%) for the dimerization

of TMS-alkynes **87** using CuCl in DMF under an air or oxygen atmosphere (Scheme 20).⁶² This procedure has also been applied to the synthesis of asymmetrically substituted polyynes **35** when TMS-alkynes **87** are mixed with 1-chloroalkynes **34** (X = Cl).⁶³



Scheme 20: Mori's dimerization of TMS-alkynes.

Haley's group reported a different method that combines standard Eglinton coupling conditions with an excess of potassium carbonate to effect the desilylation/dimerization of TMS-ethynes and TMS-butadiynes **88** in good yields (Scheme 21).⁵³



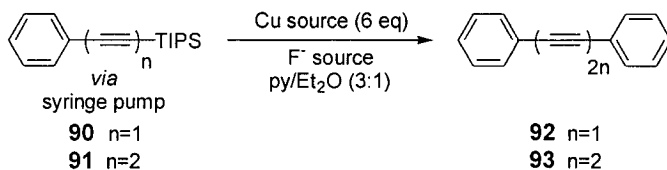
Scheme 21: Haley's desilylation/dimerization of butadiynes.

The limitation of both of these methods is that they are confined to TMS-alkynes, as bulkier triisopropylsilyl- (TIPS-) and *t*-butyldimethylsilyl- (TBS-) alkynes are unreactive under these reaction conditions. We decided to pursue an alternative desilylation/dimerization protocol using a fluoride source to effect the desilylation of triisopropylsilyl-protected alkynes in the presence of a copper source to carryout the dimerization reaction.⁶⁴

Two model compounds, **90** and **91**, were chosen to establish reaction conditions (Table 1). Compound **90** was stirred with a fluoride source, tetrabutylammonium fluoride (TBAF),⁶⁵ and a copper source, Cu(OAc)₂, in pyridine/ether (3:1) for four hours to give diyne **92** in 68% yield (entry 1). The yield decreased when the concentration of **90** was doubled (entry 2). This suggested that the deprotected ethynylbenzene intermediate was rapidly decomposing, so the addition of **90** was controlled by syringe pump (entry 3). Unfortunately, the yields were comparable to those without the controlled addition of **90**. Increasing the number of fluoride equivalents also had no effect on the yield of the reaction (entry 4). The use of CuF₂ as a combined fluoride and copper ion source was also

unsuccessful as only starting material was isolated, likely due to the insolubility of copper (II) fluoride in common organic solvents (entry 5).

Table 1: Optimization of the *in situ* desilylation/dimerization protocol.



entry	substrate	[] (mM)	Cu source	F ⁻ source	time (h)	yield (%)
1	90	2.0	Cu(OAc) ₂	TBAF	4	68 ^a
2	90	4.0	Cu(OAc) ₂	TBAF	4	45 ^a
3	90	4.0	Cu(OAc) ₂	TBAF	3	42
4	90	4.0	Cu(OAc) ₂	TBAF ^b	2	45
5	90	4.0	CuF ₂	-	2	NR
6	91	2.0	Cu(OAc) ₂	TBAF	2	15-40
7	91	2.0	Cu(OAc) ₂	CsF	3	6
8	91	2.0	CuCl/TMEDA	TBAF	2	< 5 ^c
9	91	2.0	Cu(OAc)₂	TBAF	3	100^d

^a substrate not added by syringe pump
^c benzene used as solvent

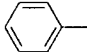
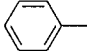
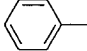
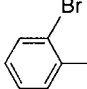
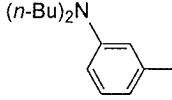
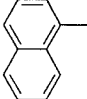

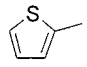
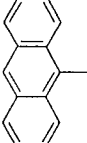
^b 2 eq of TBAF was used
^d TBAF added via syringe pump instead of substrate

Despite the modest yields, we attempted the dimerization of **91**, but the results were not reproducible, varying from 15 to 40% (entry 6). The tetrayne yield dropped to just 6% when cesium fluoride was used instead of TBAF (entry 7).⁶⁶ Hay reaction conditions replaced Eglinton reaction conditions (see Section 1.3), but **93** was isolated in only 5% yield (entry 8). Limitation of the large relative concentration of fluoride ion with respect to substrate in the reaction was accomplished by syringe pump addition of TBAF to a solution of **91** (entry 9). The result was the quantitative formation of tetrayne **93**.

Table 2: Examples of the *in situ* desilylation/dimerization reaction.

$$\text{R} \left(\text{C} \equiv \text{C} \right)_n \text{-TIPS} \xrightarrow[\text{py/Et}_2\text{O (3:1)}]{\text{Cu(OAc)}_2 \text{ (3 eq)}} \text{R} \left(\text{C} \equiv \text{C} \right)_{2n} \text{R}$$

[3.3 mM] TBAF (1 eq) *via* syringe pump
2-3 h

entry	R	n	substrate	product	yield (%)
1		1	90	92	100
2		2	91	93	73 ^a 100
3		2	91^b	93	93
4		2	78	94	98
5		2	95	96	82
6		2	97	98	96
7		2	99	100	92
8		2	101	102	82
9		3	103	-	-

^a substrate concentration was 1.7 mM ^b TMS group in place of a TIPS group

With an optimized desilylation/dimerization procedure in hand, the generality of the method was investigated by dimerizing the compounds listed in Table 2. Substrate concentration was found to be important as the more concentrated reaction gave better yields (entry 2). As expected, the procedure was shown to work well with TMS-diyne, as **90** was dimerized to **92** in 93% yield (entry 3). The procedure also tolerates a variety of substituents. 2-Bromo- and 3-amino-substituted TIPS-butadiynes, **78** and **95**, were dimerized in 98% and 82% yields respectively (entries 4 and 5). 1,8-Bis-(1-naphthyl)-octa-1,3,5,7-tetrayne (**98**), a compound that has been studied due to its interesting bathochromic shifts,⁶⁷ was prepared by the desilylation/dimerization of **97** in 96% yield (entry 6). Alkyl substituents were also compatible with this synthetic method as **99** was dimerized to tetrayne **100** in 98% yield

(entry 7). Heterocyclic polyynes can also be prepared easily with this procedure. For example, **101** was successfully dimerized to dithiophene-tetrayne **102** in 82% yield (entry 8). We also tried to dimerize hexatriyne **103** but the reaction gave products that could not be identified (entry 9).

We were successful in developing a new *in situ* desilylation/dimerization method for the preparation of symmetrical polyynes. The addition of TBAF as a fluoride ion source to a solution of silylalkyne and Cu(OAc)₂ in a mixture of pyridine/ether (3:1) gave the desired polyyne products in greater than 80% yields for a wide variety of substrates. In addition, the procedure can be applied to bulky silylalkynes such as TIPS-alkynes and is not limited to TMS-alkynes as in previously reported methods.

2.4 Synthesis of *para*-Cyclophane **104**

In order to circumvent the solubility problems that arose in the synthesis of cyclophane **75**, a new *para*-cyclophane, **104**, was envisioned (Figure 10). Dibutylamino groups⁶⁰ were chosen over other known solubilizing substituents (Section 2.2) as they have the additional benefit of allowing for modulation of the cyclophane's electronic properties. The location of the substituent was also carefully considered. Previous studies have shown that incorporation of substituents on the capping aryl rings led to inseparable mixtures of cyclophane regioisomers.³⁹ However, by functionalizing the aryl rings on the bridges, a single regioisomer would be formed and a high degree of molecular symmetry maintained, as illustrated by **104** (Figure 10).

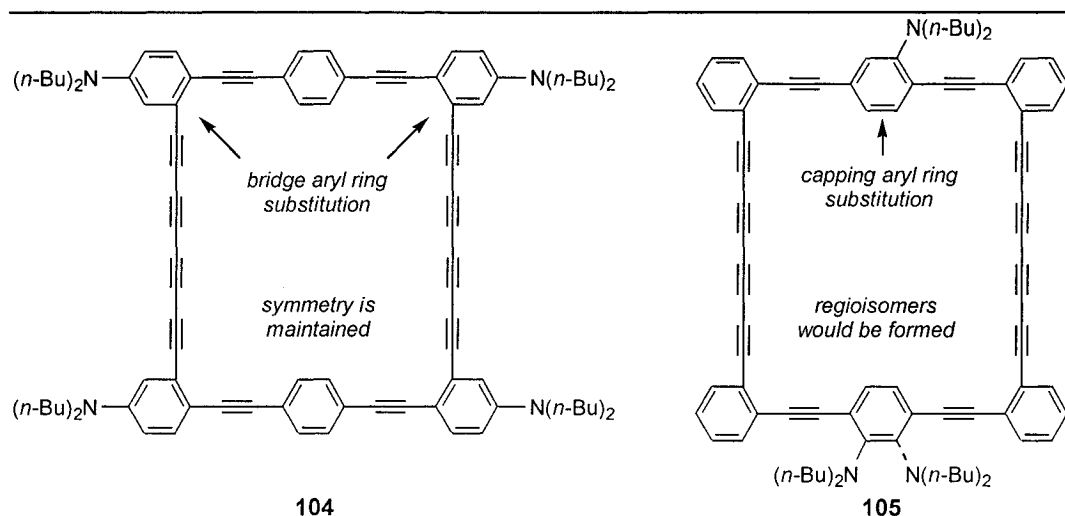
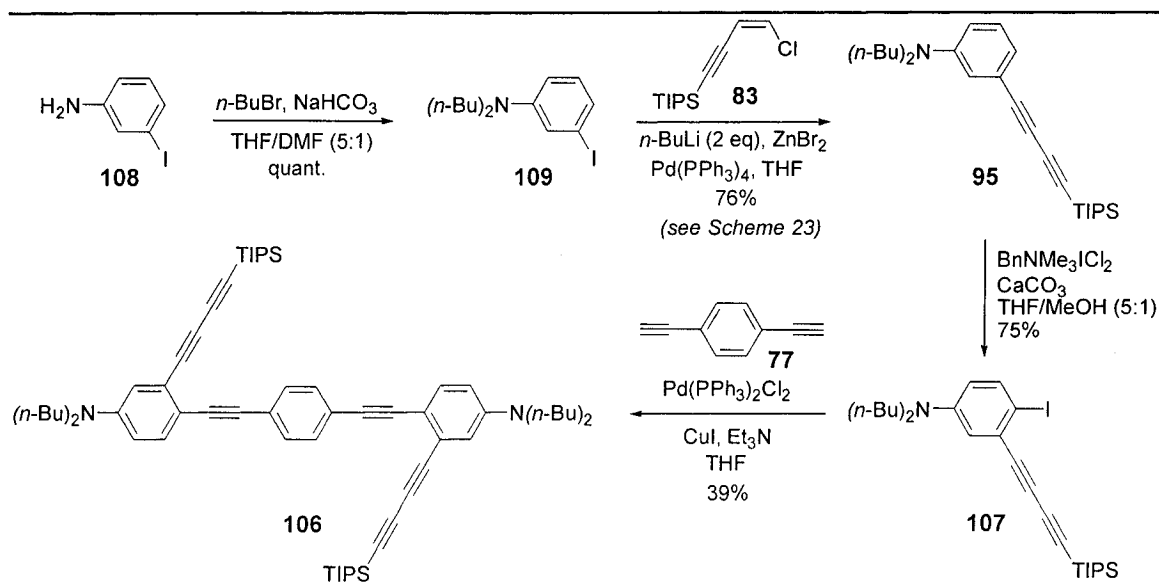


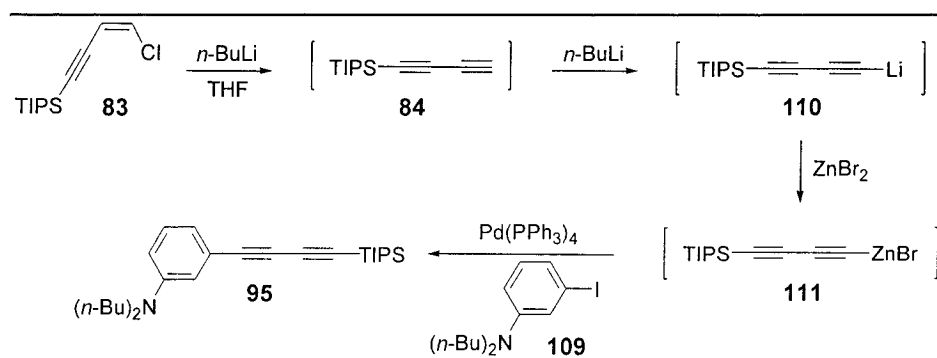
Figure 10: Rational functionalization of cyclophane **104 with solubilizing n -Bu₂N groups.**

The synthetic approach to cyclophane **104** was analogous to the one used in the preparation of cyclophane **75**, as the macrocycle would be formed by dimerizing two C₃₀ precursors **106** (Figure 11). In this case, iodide **107**, which contains the dibutylamino moiety, would be required for the reaction with 1,4-diethynylbenzene (**77**) instead of bromide **78**. Iodide **107** could be prepared in three steps from 3-iodoaniline (**108**) based on a sequence reported by Haley and coworkers used in their synthesis of dehydrobenzo[18]annulenes.⁶⁰



Scheme 22: Synthesis of cyclophane **104** precursor **106**.

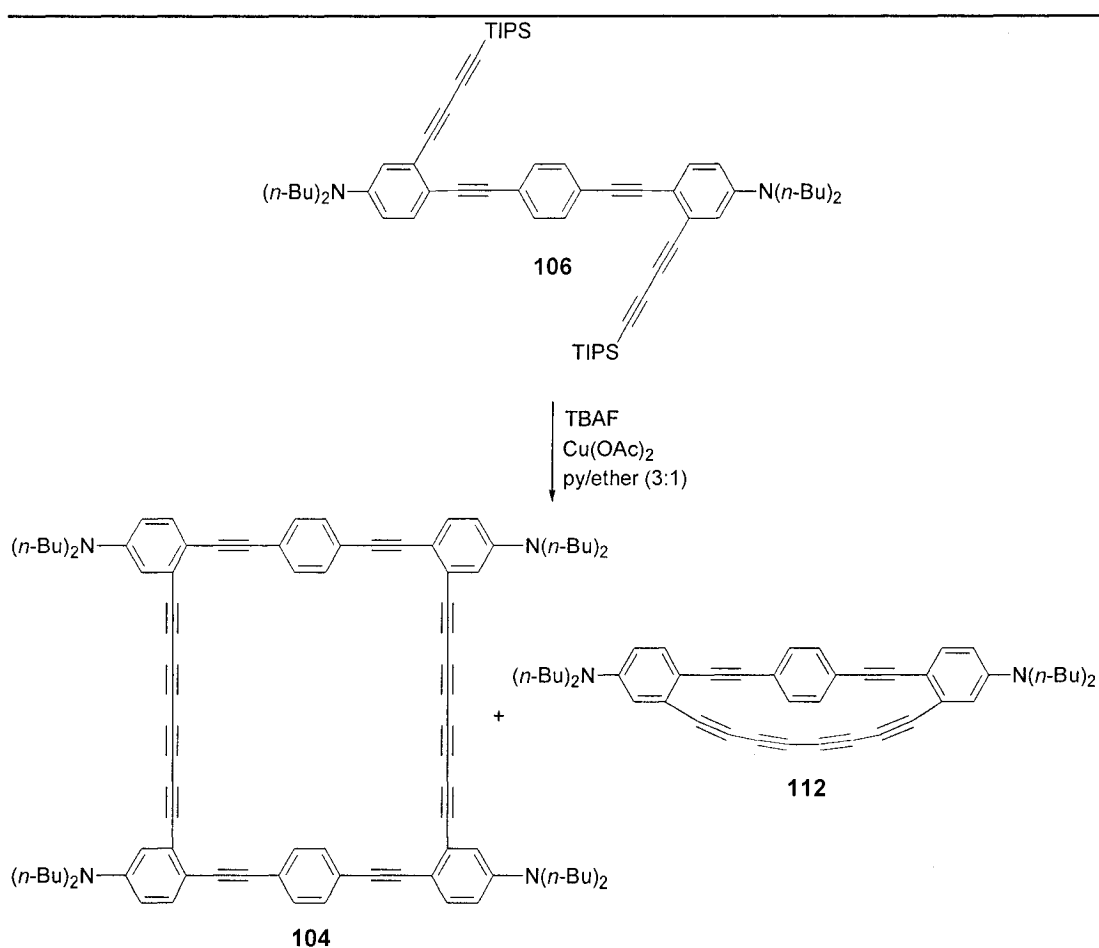
We developed a new method for the synthesis of arylbutadiynes by a Negishi coupling of the organozincate prepared from **83** with an arylhalide, **109** (Scheme 23). Chloroenyne **83** was treated with two equivalents of *n*-BuLi at $-78\text{ }^{\circ}\text{C}$. The first equivalent of base forms butadiyne **84** by deprotonation and elimination of chloride ion. The second equivalent of *n*-BuLi then forms organolithium **110**. Transmetalation of **110** with ZnBr_2 affords organozincate **111**, which readily undergoes a Negishi coupling reaction with arylhalides (such as **109**) using catalytic palladium(0) $[\text{Pd}(\text{PPh}_3)_4]$. This one-pot procedure is superior to the stepwise protocol that we traditionally used (Scheme 17, Section 2.2) as the isolation, purification, and storage of butadiyne **84** is avoided.



Scheme 23: *In situ* generation of organozincate **111** and Sonogashira coupling to give diyne **95**.

Our *in situ* desilylation/dimerization protocol was applied to the dimerization of **106** (Scheme 24). When the concentration of **106** was 2.1 mM, the only observed product was

monomer **112** in 46% yield. This cyclophane was formed from the intramolecular dimerization of the α,ω -butadiynes in **106**. When the concentration of **106** was raised to 5.3 mM monomer **112** was still the major product (26% yield); however, a small amount of a compound believed to be cyclophane **104** was also formed. The reaction was not repeated at higher concentrations as the amount of undesired oligomerization would increase. This was not the first time that an intramolecular coupling product was observed from the dimerization reaction.³⁸ A study on the effect of the intramolecular distance of reactive termini in the dimerization reaction is presented in Section 2.6.



Scheme 24: Dimerization of **106** to give cyclophanes **104** (dimer) and **112** (monomer).

A single crystal of cyclophane **112** suitable for X-ray analysis was grown by the slow evaporation of a methylene chloride solution (Figure 12).⁶⁹ The macrocycle of the cyclophane is planar and has C_{2v} symmetry. All of the sp -hybridized carbon atoms are bent

from their preferred 180° bond angle. The most distorted bonds are 167.9° and are found in the octatetrayne bridge.

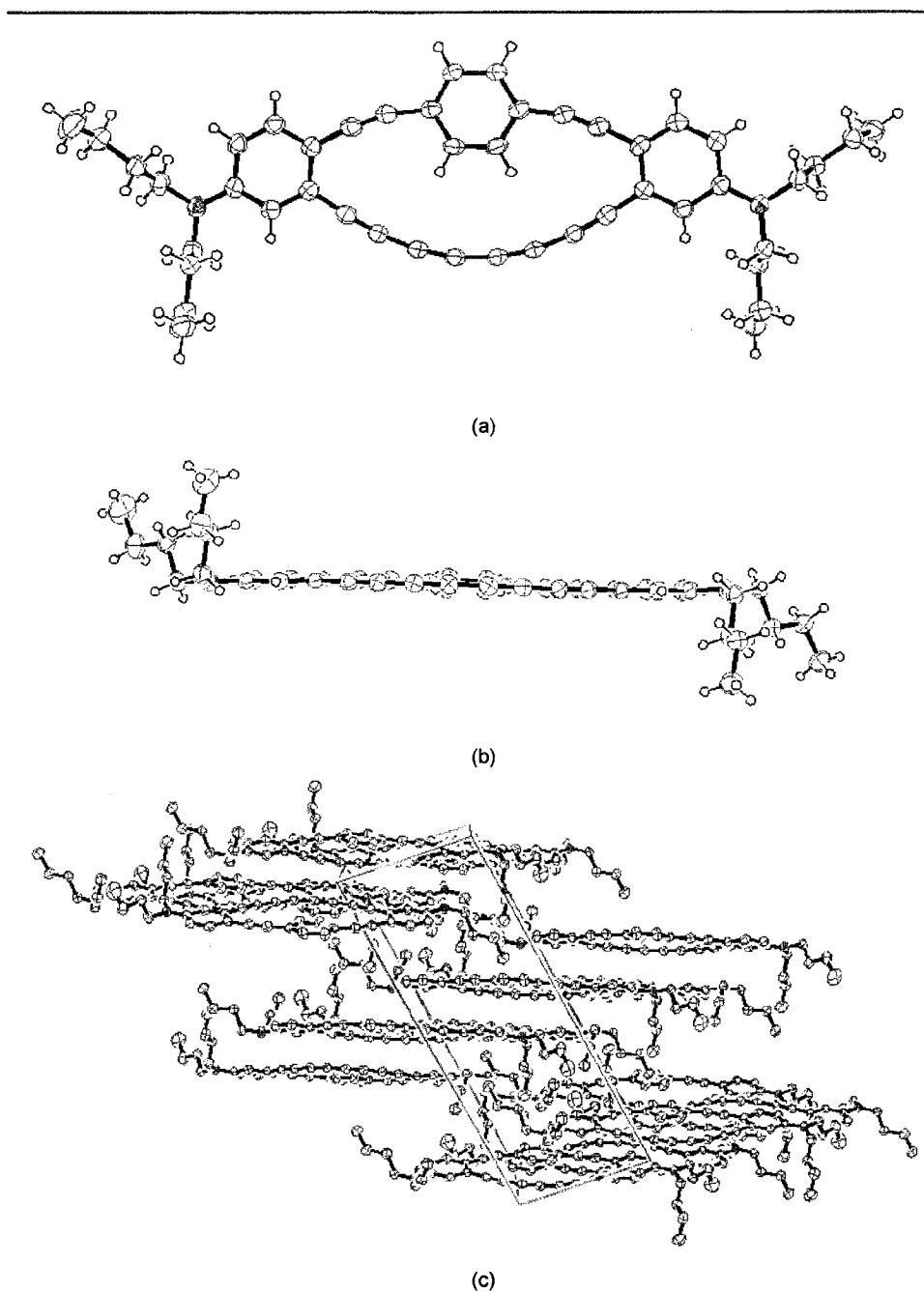


Figure 12: X-ray structure of cyclophane 112 (a) top view; (b) side view; (c) crystal packing.

The crystal packing diagram of cyclophane **112** was also examined since the organization of unsaturated molecules in the solid state is of interest from a crystal engineering and solid state polymerization⁷⁰ standpoint. Cyclophane **112** packed as dimers,

with the octatetrayne bridges adjacent to one another. These dimer units do not lie in a plane to form a sheet, but are instead arranged to form shallow steps. The close proximity of the tetraoctyne bridges predisposes them to solid state polymerization and may be a reason why growing crystals was difficult.⁷⁰

Unfortunately, X-ray quality crystals of cyclophane **104** were not obtained, in part due to the small amount of material that was prepared. In order to prepare more material, another synthetic route was investigated in which the undesired intramolecular coupling reaction would not compete with the desired intermolecular dimerization (Section 2.5).

2.5 Stepwise Synthesis of *para*-Cyclophane **113**

A synthetic route to cyclophane **113** was considered (Figure 13) since the dimerization strategy led to a mixture of compounds with the desired cyclophane **104** as the minor product.

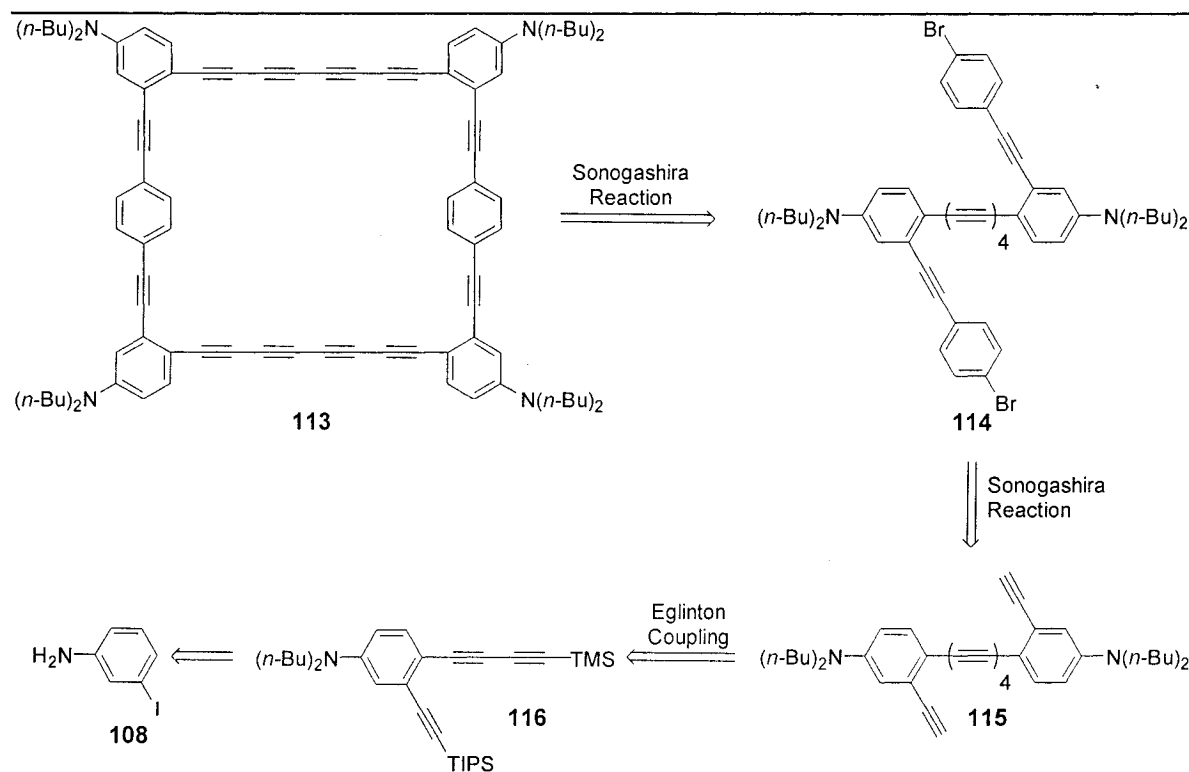


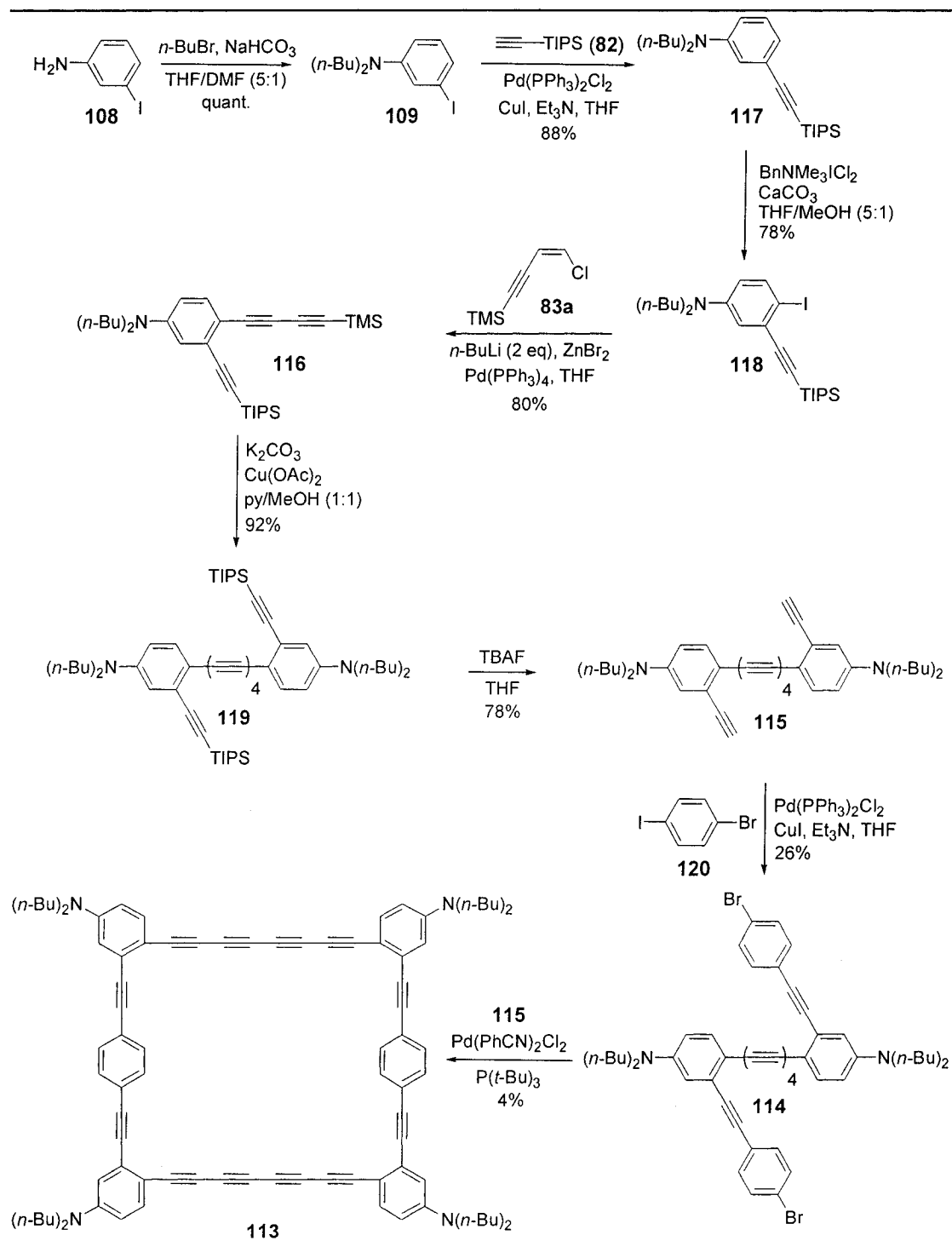
Figure 13: Retrosynthetic analysis of cyclophane **113**.

The advantage of this route is that the octatetrayne bridge would be formed earlier in the synthesis. *para*-Cyclophane **113** would be formed *via* a Sonogashira reaction between

dibromide **114** and hexyne **115**. Dibromide **114** would also be prepared by a Sonogashira reaction of hexyne **115** with two equivalents of 1-bromo-4-iodobenzene (**120**). Hexyne **115** would be prepared by the desilylation/dimerization of silylbutadiyne **116**, which in turn can be prepared from 3-iodoaniline (**108**) in four steps.⁶⁰

The synthesis of cyclophane **113** is shown in Scheme 25. The preparation of iodide **118** was previously reported by Haley's group.⁶⁰ 3-Iodoaniline (**108**) was alkylated with *n*-butylbromide in the presence of sodium bicarbonate to give **109**. A Sonogashira reaction of **109** with TIPS-acetylene (**82**) gave **117**, and iodination with BnNMe₃ICl₂ in the presence of calcium carbonate gave iodide **118** in 67% yield over three steps. The diyne moiety was installed using the one-pot Negishi coupling with **83** described in Scheme 23 to give butadiyne **116** in 80% yield. The tetrayne bridge was then successfully formed by the desilylation/dimerization of **116** with potassium carbonate and Cu(OAc)₂ in methanol/pyridine (1:1) to give **119** in 92% yield.⁶⁰ Removal of the two triisopropylsilyl-protecting groups with TBAF afforded hexyne **115** in 97% yield, but **115** had to be used without purification as it was found to decompose on silica gel.

Sonogashira reaction of hexyne **115** with two equivalents of 1-bromo-4-iodobenzene (**120**) gave dibromide **114** in 26% yield. The low yield resulted from the instability of **114** on silica gel. In order to avoid the loss material from the isolation and purification of dibromide **114** this late in the synthesis, the reaction of hexyne **115** with **120** was repeated, and the disappearance of **115** was monitored. Once all of **115** was consumed, Pd(PhCN)₂Cl₂ and P(*t*-Bu)₃²¹ were added and the reaction was heated to reflux. A second equivalent of hexyne **115** was then added dropwise over four hours to give cyclophane **113** in 4% yield (45% yield for each of the four new carbon-carbon bonds formed). The additional benefit of this stepwise synthetic approach is that unsymmetrical cyclophanes can be prepared.



Scheme 25: Synthesis of cyclophane **113**.

Numerous attempts to grow X-ray quality crystals of cyclophane **113** were unsuccessful. Calculations to determine the lowest energy conformation of cyclophane **113** were conducted and revealed that cyclophane **113** adopts a twisted, C_2 -symmetric

conformation (Figure 14). The twisted conformation of **113** was expected based on our previous work on cyclophanes.³⁸ Proton and carbon NMR spectra of cyclophane **113** were consistent with a C_2 -symmetric structure.

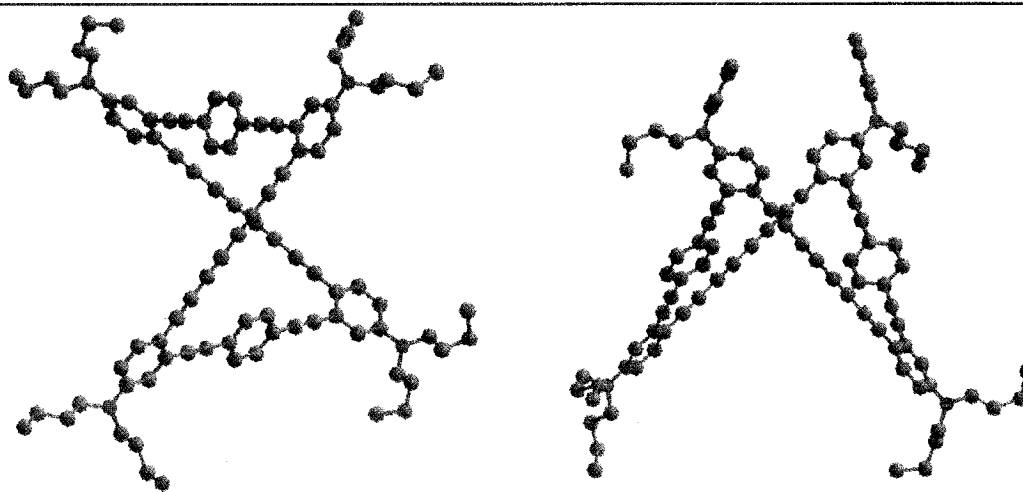


Figure 14: Molecular model of cyclophane 113 illustrating its twisted, C_2 -symmetric conformation.

Unlike our previous cyclophanes,³⁶⁻⁴⁰ cyclophane **113** was conformationally stable at room temperature. Isomerization of **113** from one helical conformer to the other would require passing through a strained, planar, rectangular-like intermediate that in this case was of sufficiently high energy to hinder isomerization (Figure 15). A large number of unsaturated macrocycles are shape-persistent and were the subject of a recent microreview.⁷¹

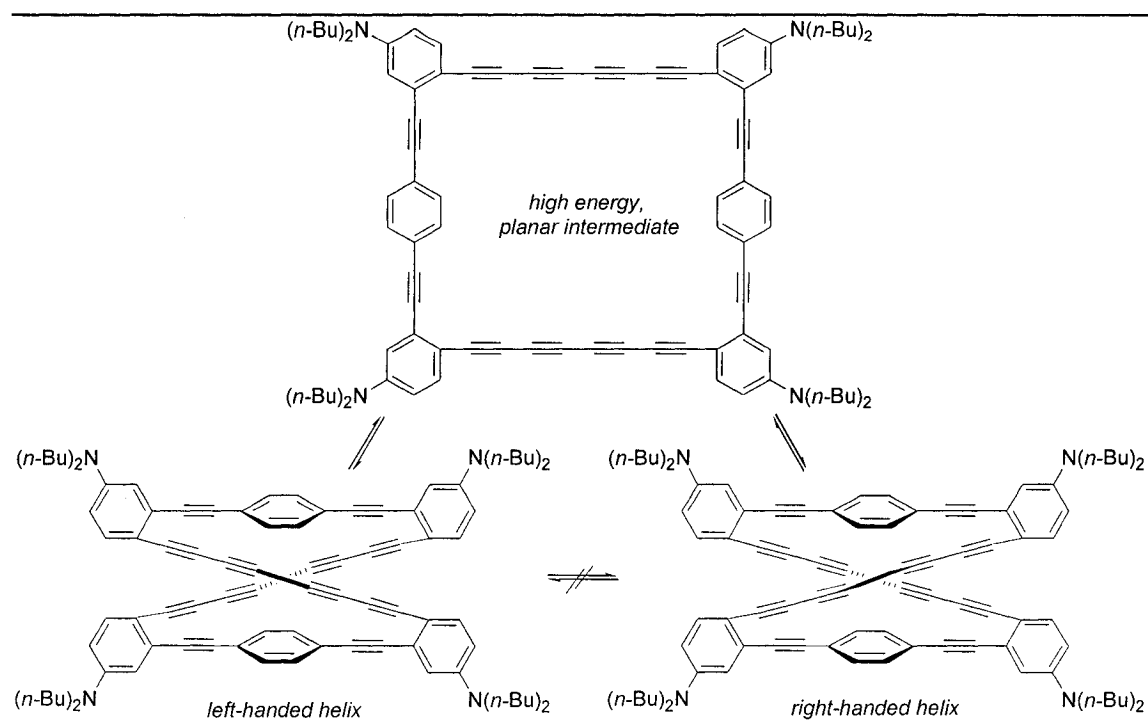


Figure 15: Isomerization pathway of cyclophane 113.

2.6 Inter- vs. Intramolecular Dimerization of α,ω -Diyne

In Section 2.4 the dimerization of **106** to form cyclophane **104** was described, but cyclophane **112** arising from an intramolecular dimerization was formed instead (Figure 16, a). However, in previous publications we described the successful application of this dimerization strategy for the preparation of cyclophanes **52** and **53** from substrates **50** and **51** respectively (Figure 16, b and c), although in the former case, a mixture of intra- and intermolecular products was obtained.³⁸ Other groups have also observed intramolecular coupling products in the dimerization of α,ω -diynes.^{70,72}

In order to effectively plan the synthesis of cyclophanes and related unsaturated macrocycles we decided to investigate the subtleties of the dimerization reaction. Intramolecular coupling would predominate when the terminal alkynes of the dimerization substrate can adopt a conformation in which they are close to one another in space. Although the choice of coupling reagents⁷¹ and reactions conditions⁷³ can also affect the dimerization reaction, the nature of the substrate should have the greatest influence on whether intra- or intermolecular reaction products would be formed.

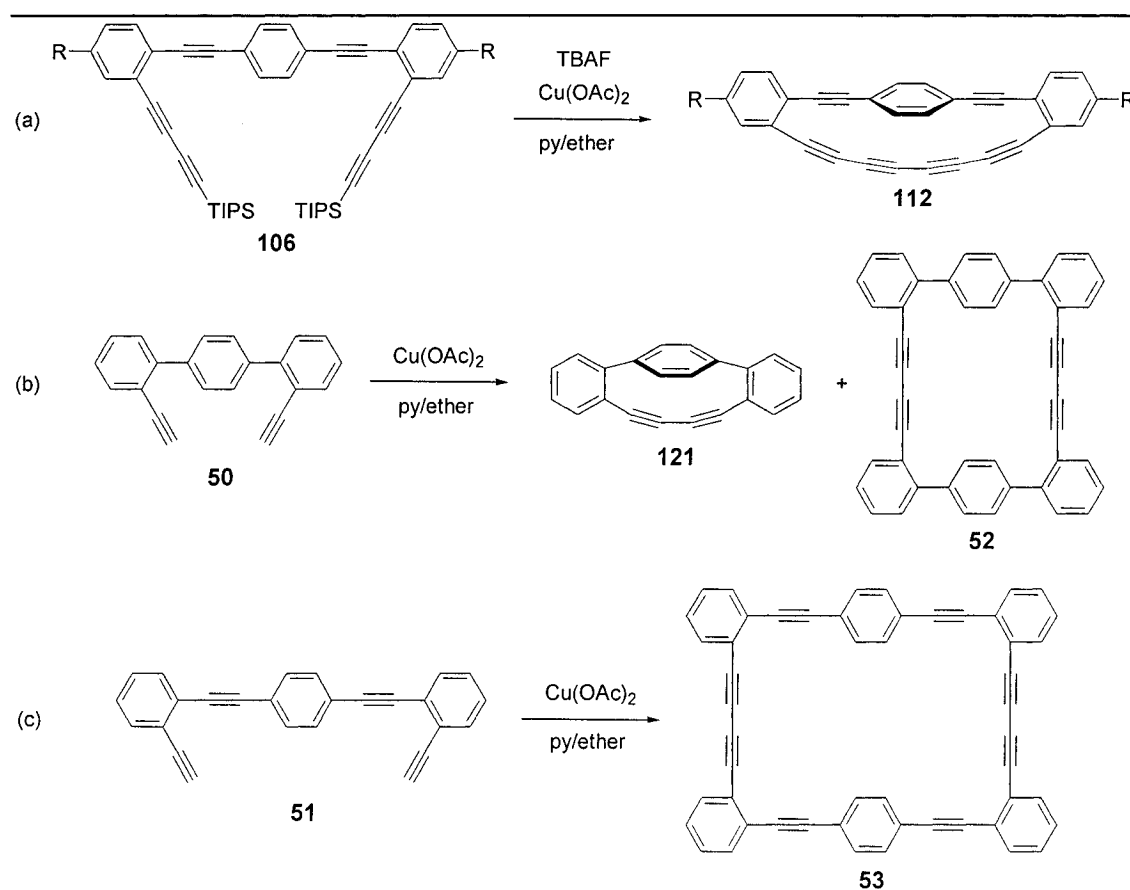


Figure 16: Dimerization reactions leading to (a) an intramolecular product, (b) inter- and intramolecular products, and (c) an intermolecular product.

Molecular modeling was conducted on substrates that were dimerized under copper coupling conditions, leading to both intra- and intermolecular products whose structures were proven by X-ray crystallography. Density functional theory (DFT) calculations were performed on substrates **50**, **51**, and **106**, in addition to relevant examples from the literature. A DN basis set was used to find the lowest energy conformation of the dimerization substrates.⁷⁴ In most cases, the lowest energy substrate conformation was not helpful as the acetylene moieties of interest were not oriented toward one another, resulting in large termini separations. Consequently, useful substrate conformations were selected in which the α,ω -diynes were in close proximity to one another (Figure 17). This conformation was energetically minimized and subsequently used to find the termini separation distance.

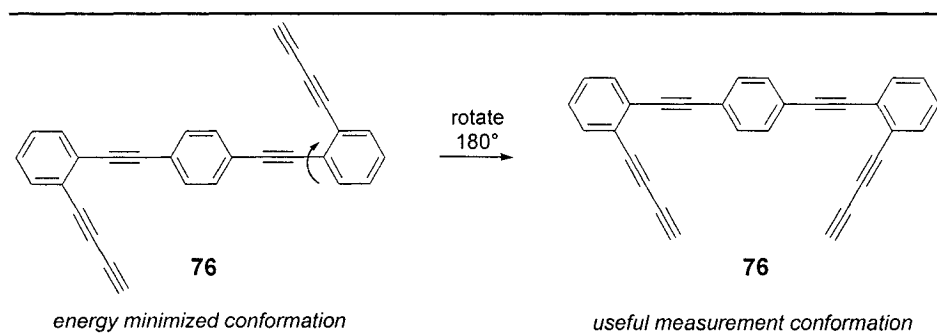
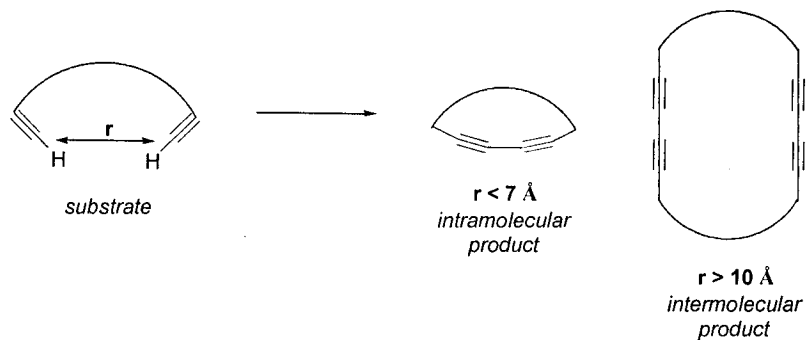


Figure 17: Manipulation of molecular modeling structures to obtain a “reactive” conformation.

The molecular modeling results are presented in Table 3. Intramolecular coupling products were obtained for each substrate with a terminal alkyne separation distance (r) of less than 7 Å (entries 1-3). When the value of r was between 7-10 Å, a mixture of intra- and intermolecular products resulted (entry 4). Separation distances greater than 10 Å led exclusively to intermolecularly coupled products (entries 5-7).

Although these results provided a straightforward method to predict whether inter- or intramolecular coupling would be favored for a given dialkyne substrate, the model does not take into account substrates with small termini separation distances ($r < 7$ Å) that cannot undergo an intramolecular dimerization reaction due to a highly-strained transition state. In these cases the intermolecular dimerization product would be observed. Recently, Tobe's group reported a qualitative summary of the dimerization reaction products arising from various α,ω -diynes^{70d} illustrating the usefulness of this study as a guide for the design and successful synthesis of complex unsaturated macrocycles.⁷⁵

Table 3: Molecular modeling calculations of α,ω -diyne termini separation distances (r) and the product(s) observed from their dimerization.



entry	substrate	r (Å)	coupling product	ref
1	<p style="text-align: center;">57a</p>	4.05	intra	72c
2	<p style="text-align: center;">76</p>	5.94	intra	64
3	<p style="text-align: center;">55a</p>	6.41	intra	40
4	<p style="text-align: center;">50</p>	7.49	intra and inter	38
5	<p style="text-align: center;">51</p>	12.12	inter	38
6	<p style="text-align: center;">124a</p>	12.81	inter	76
7	<p style="text-align: center;">124</p>	13.66	inter	77

2.7 Synthesis of *meta*-Cyclophane **123**

The twisted conformation of *para*-cyclophane **113** prompted us to consider how structural changes to the cyclophane macrocycle would effect the molecule's conformation. A report that a C₆₀ *meta*-diethynylbenzene macrocycle **122** comprised of *meta*-substituted benzene rings was planar⁶¹ increased our curiosity. In order to further explore the molecular folding of these unsaturated macrocycles, another cyclophane that contained 60 carbon atoms within the macrocyclic core was envisioned. *meta*-Cyclophane **123** was designed as a cross between *para*-cyclophane **113**, with *ortho*-substituted bridge benzene rings that contain dibutylamino groups for solubility, and *meta*-diethynylbenzene **122**, with *meta*-substituted capping benzene rings and each of the six benzene rings separated by butadiynyl groups (Figure 18).

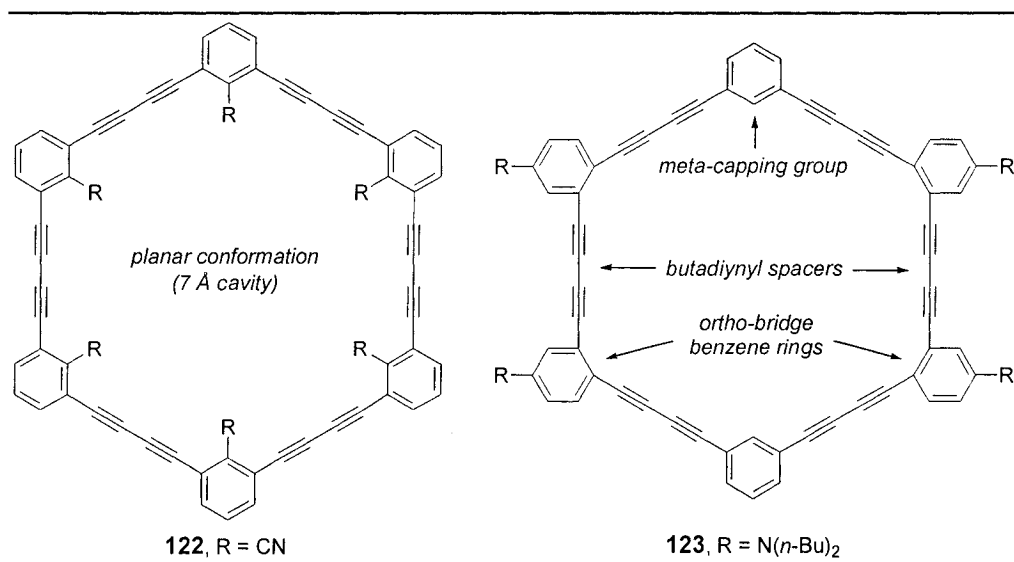


Figure 18: Tobe's *meta*-diethynylbenzene macrocycle **122** and a proposed C₆₀ *meta*-cyclophane, **123**.

The first synthetic route to cyclophane **123** that was considered was the dimerization of C₃₀-precursor **124** (Figure 19). Molecular modeling of **124** was conducted and the distance (r) between the α,ω -diynes was found to be 13.7 Å (Table 3, Section 2.6). The large distance between the reacting termini suggested that the intermolecular dimerization of **124** should be favored and lead to cyclophane **123**. Dimerization precursor **124** could be rapidly synthesized by a Cadiot-Chodkiewicz cross-coupling of alkyne **125** and dibromide **126**.⁵⁴ Alkyne **125** could in turn be prepared from iodide **118**.

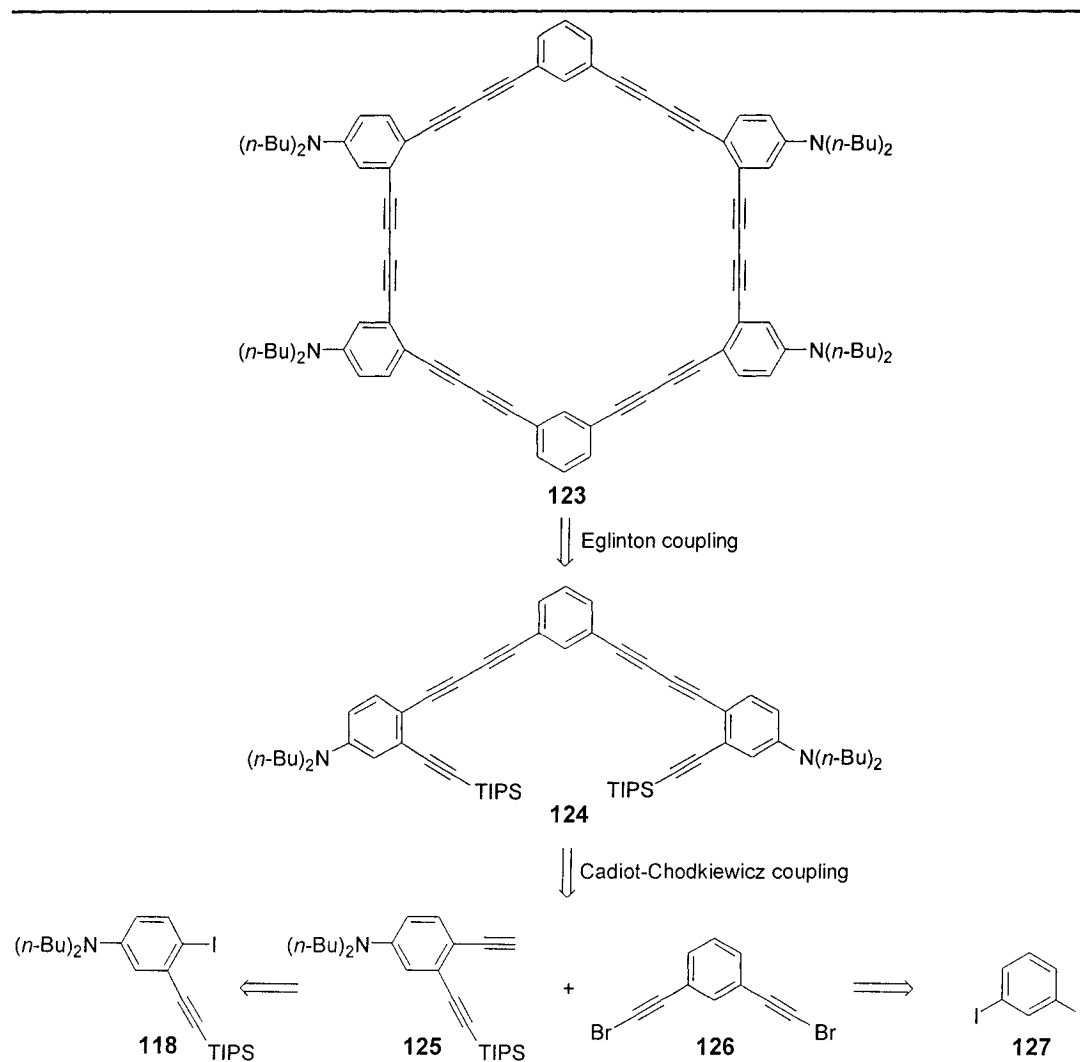
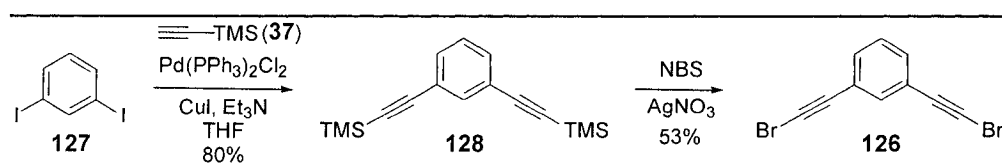


Figure 19: Retrosynthetic analysis of *meta*-cyclophane **123**.

The synthesis of dibromide **126** was conducted as shown in Scheme 26. A Sonogashira coupling of 1,3-diiodobenzene (**127**) with TMS-acetylene (**37**) afforded **128** in 80% yield. A bromodesilylation of **128** mediated by silver nitrate⁷⁸ gave dibromide **126** in 53% yield.

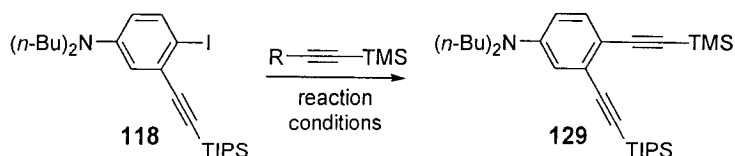


Scheme 26: Synthesis of dibromide **126**.

Unfortunately, the preparation of alkyne **125** was not as straightforward (Table 4). A Sonogashira reaction of iodide **118** and TMS-acetylene (**37**) did not lead to silylalkyne **129** as only **118** was recovered from the reaction (entry 1). Organozincate **130** was prepared *in situ*,

but a Negishi reaction with **118** did not lead to **129** (entry 2). Since the oxidative insertion of palladium into the aryl carbon-iodide bond of **118** was not facile, Fu's Sonogashira reaction conditions were used (entry 3).²¹ The reaction gave **129** as desired in 43% yield, but **118** was also recovered (10%). Unfortunately, when the reaction was scaled up, **118** was the major material isolated.

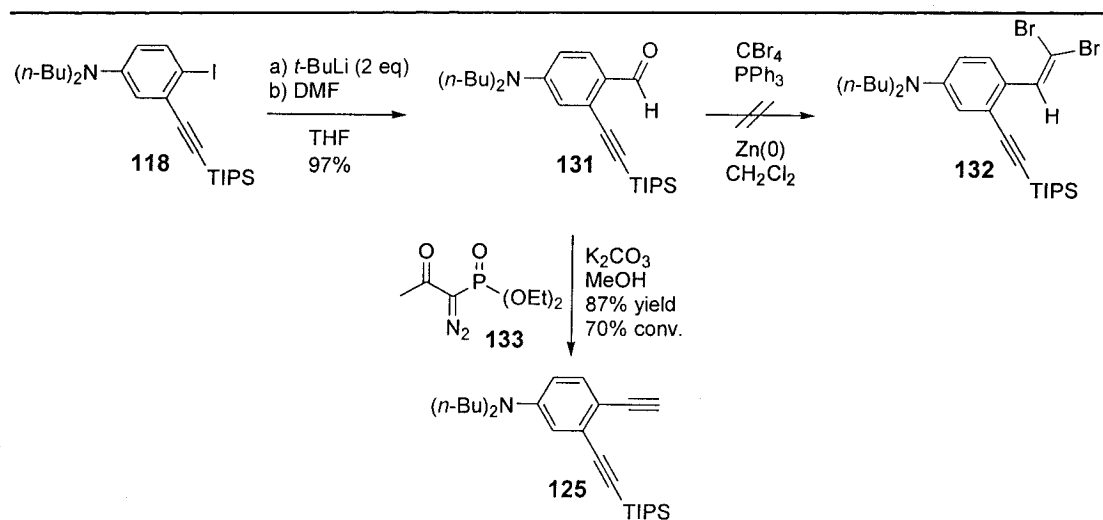
Table 4: Sonogashira reaction conditions for the preparation of silylalkyne **129.**



entry	substrate	reaction conditions	result
1	37 , R = H	Pd(PPh ₃) ₂ Cl ₂ , CuI Et ₃ N, THF	no product (118 recovered)
2	130 , R = ZnBr ^a	Pd(PPh ₃) ₄ THF	no product (118 recovered)
3	37 , R = H	Pd(PhCN) ₂ Cl ₂ , P(<i>t</i> -Bu) ₃ <i>i</i> -Pr ₂ NH, CuI, THF	43% yield (10% 118 recovered)

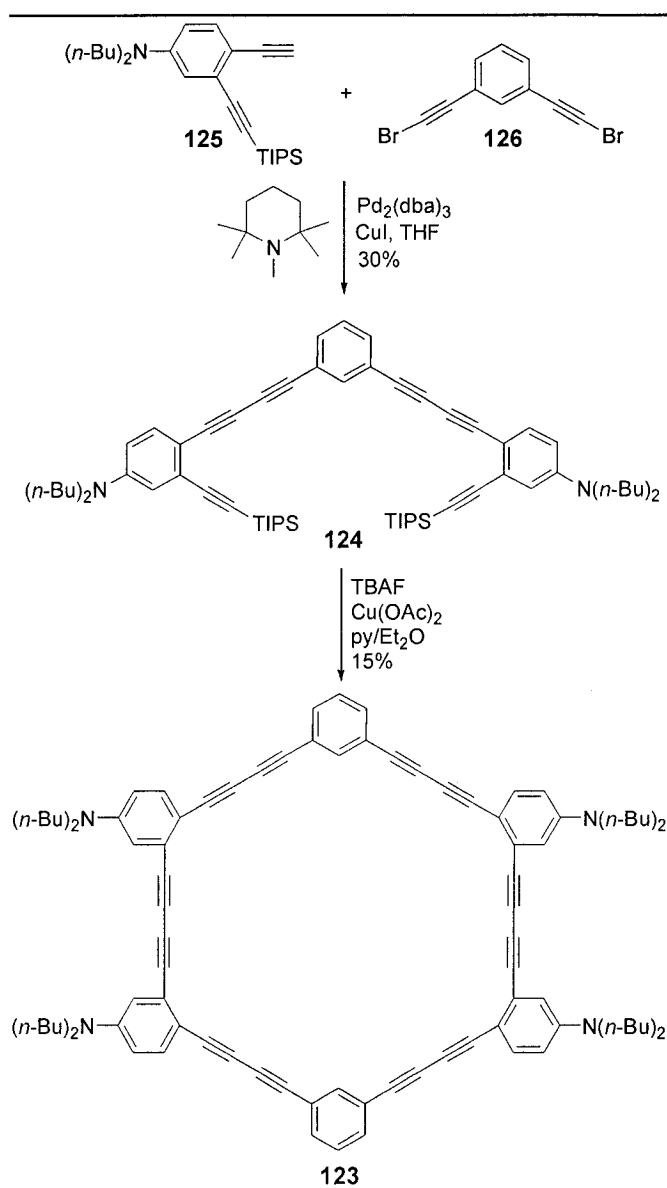
^a prepared *in situ*

An alternative approach to alkyne **125** *via* aldehyde **131** was investigated (Scheme 27). Iodide **118** was converted to the corresponding organolithium with two equivalents of *t*-BuLi at -78 °C and was quenched with *N,N*-dimethylformamide to give aldehyde **131**. A Corey-Fuchs transformation⁷⁹ of aldehyde **131** was unsuccessful as dibromide **132** could not be formed. The difficulty in performing both the Corey-Fuchs reaction on **131** and the Sonogashira reaction with **118** was attributed primarily to the steric bulk of the proximal triisopropylsilyl-protecting group. An alternative reagent, **133**, reported by Ohira was known to convert aldehydes to alkynes in one pot.⁸⁰ The advantages of this procedure over the Corey-Fuchs method are that the reaction did not proceed *via* a bulky, dibromide intermediate and the reaction conditions were much milder as K₂CO₃ was used instead of *n*-BuLi. When aldehyde **131** was reacted with **133** in K₂CO₃ over 48 h, alkyne **125** was formed in 87% yield with 70% conversion. A longer reaction time should lead to complete conversion of aldehyde **131** to alkyne **125**. The fact that the reaction of aldehydes with Ohira's reagent traditionally takes less than 2 h, confirmed that aldehyde **131** was sterically hindered.



Scheme 27: Preparation of alkyne **125**.

The synthesis of *meta*-cyclophane **123** continued with a Cadiot-Chodkiewicz coupling of alkyne **125** and dibromide **126** to give the dimerization precursor **124** in 30% (Scheme 28). A significant amount of **134** (13%),⁸¹ resulting from the homocoupling of **125**, was also isolated. Our *in situ* desilylation/dimerization method⁶⁴ was applied to **124** and two compounds were obtained in 15% combined yield that were consistent with the general structure of cyclophane **123**.



Scheme 28: Synthesis of *meta*-cyclophane **123**.

Size-exclusion semi-prep HPLC⁸² was used to separate the two compounds that were formed in the dimerization reaction. The major isomer (8% yield) displayed higher symmetry than the minor isomer (3% yield) in the ¹H and ¹³C NMR spectra. The major isomer had six signals for the sp-hybridized alkyne carbon atoms, whereas the minor isomer had 12 signals. The spectra of the major isomer did not change upon heating to 100 °C.

Two different conformations of **123** could result from the dimerization reaction depending on how the molecule twisted after the first octatetrayne bridge was formed (Figure 20). A "bowtie conformation" (**123a**) would possess C_{2h} symmetry and a "butterfly

conformation" (**123b**) would be in the lower C_2 -symmetric point group. Interconversion from one conformer to the other would require the capping group to pass through the central cavity of the molecule and would be very energetically demanding.

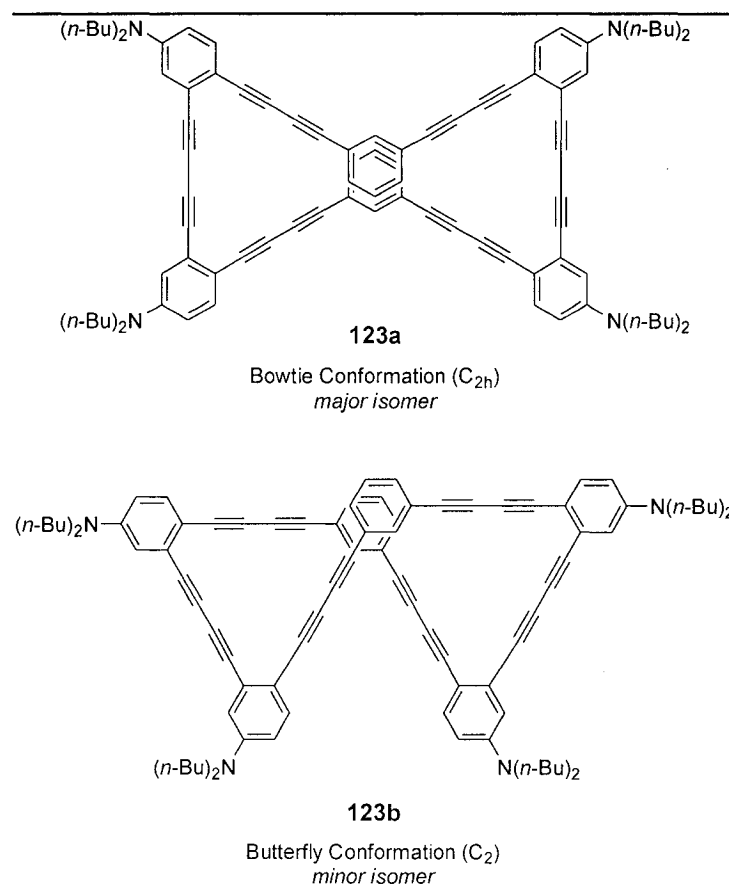


Figure 20: Possible conformations of cyclophane 123.

Unfortunately, the structures of **123a** and **123b** could not be unambiguously proven as X-ray quality crystals could not be obtained. However, molecular modeling calculations revealed that the bowtie and butterfly conformational isomers were the lowest energy conformers (Figure 21 and Figure 22).⁷⁴

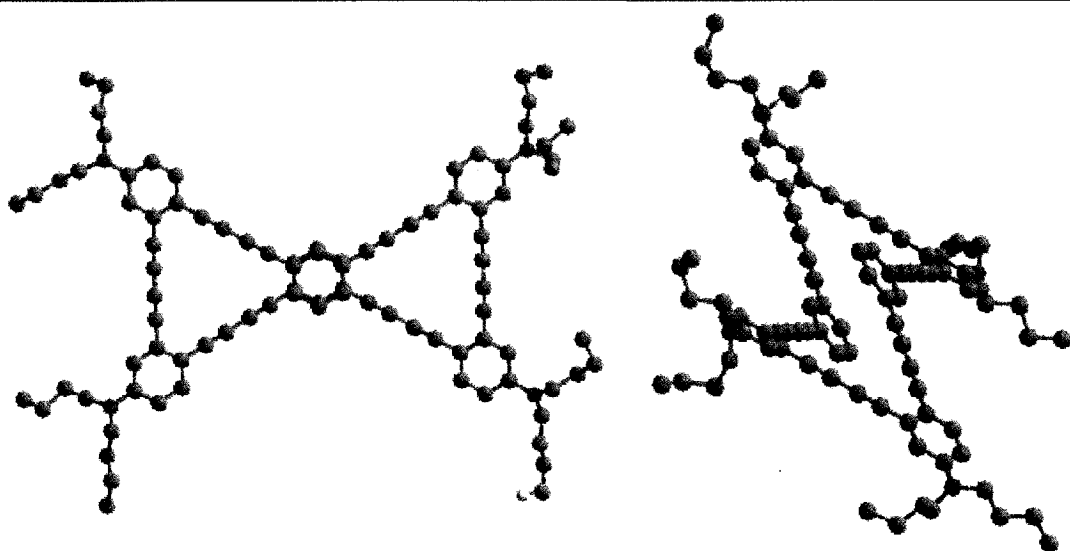


Figure 21: Molecular modeling of the bowtie conformation of cyclophane 123a.

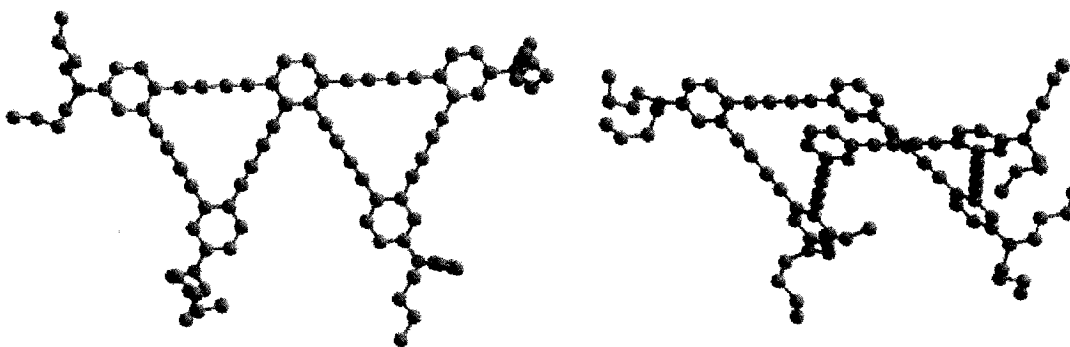


Figure 22: Molecular modeling of the butterfly conformation of cyclophane 123b.

The molecular models of cyclophane **123** provided some useful insight for future cyclophane design. First, atropisomers **123a** and **123b** have the capping rings face-to-face π -stacking with a separation distance of 3.55 and 3.52 Å between of aryl rings, which is close to 3.40 Å observed between the planes of graphite.⁸³ The close proximity of the capping aryl rings makes cyclophane **123** an attractive ligand for bis(arene) complexes when appropriately functionalized (Section 3.3).

Second, close inspection of the molecular model of **123b** indicates that the compound would be planar if the capping groups did not bump into one another. By modifying the alkyne spacers between the aryl rings, planar cyclophanes could be prepared (Figure 23). Planar, unsaturated compounds are of interest for a variety of molecular electronic applications.

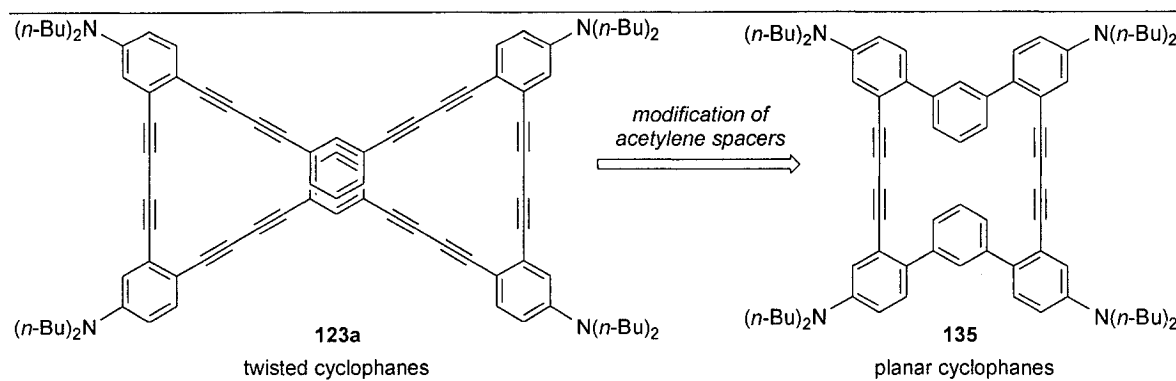


Figure 23: Modification of cyclophane 123 to favor planar cyclophane conformations.

2.8 Summary

In conclusion, a new *in situ* desilylation/dimerization protocol was developed to allow bulky silyl-protected acetylenes to participate in the dimerization reaction. In addition, a semi-empirical study of α,ω -alkyne dimerization precursors allowed for the prediction of dimerization reaction products based on the terminal alkyne separation distance. Armed with these developments, cyclophane **112** and two C₆₀ acetylenic cyclophanes **113** and **123** have been synthesized with **123** existing as two atropisomers, **123a** and **123b**.

Cyclophanes **113** and **123** were not exposed to laser desorption mass spectrometry (LD MS) or thermolysis. Although there is excellent precedence for the formation of carbon-rich molecules such as buckytubes and buckyonions,⁴⁵ there was only a small chance that C₆₀ would be formed. However, the molecular folding differences observed for *meta*- and *para*-capped cyclophanes formed the basis for further cyclophane targets as liquid crystal and semiconducting materials as described in Chapters 3 and 4.

Chapter

HELICAL ACETYLENIC CYCLOPHANES AND PHENANTHROLINOPHANES

- 3.1 Unsaturated Compounds with Helical Chirality
 - 3.2 Synthesis of Cyclophane **157** as an η^{12} -Bis(arene) Ligand
 - 3.3 Synthesis of Cyclophane **170** as an η^{12} -Bis(arene) Ligand
 - 3.4 Bis(arene) Complexes
 - 3.5 Synthesis of (η^{12} -Cyclophane) Complexes
 - 3.6 1,10-Phenanthroline-Based Compounds
 - 3.7 Synthesis of Phenanthrolinephanes **200** and **217**
 - 3.8 Properties of Phenanthrolinephanes **200** and **217**
 - 3.9 Preparation of Phenanthrolinephane **227**
 - 3.10 Summary
-

3. Helical Acetylenic Cyclophanes and Phenanthrolinophanes

Chiral cyclophane **52** could not be isolated as a pure enantiomer since it was prone to rapid isomerization from one helical isomer to the other (helical inversion). Preparation of chiral, non-racemic cyclophanes could be possible by building a locking mechanism into the cyclophane to inhibit helical isomerization. The resulting chiral cyclophanes could then be used as ligands for asymmetric catalysts, packing materials for asymmetric separations, or type III liquid crystalline materials when appropriately functionalized.

One possible locking mechanism could be the coordination of metals within the cyclophane's macrocyclic core. For example, the X-ray crystal structure of cyclophane **52** (Figure 24)³⁸ shows that the two capping aryl rings are π -stacked face-to-face, suggesting that **52** would be a good η^{12} -bis(arene) ligand.

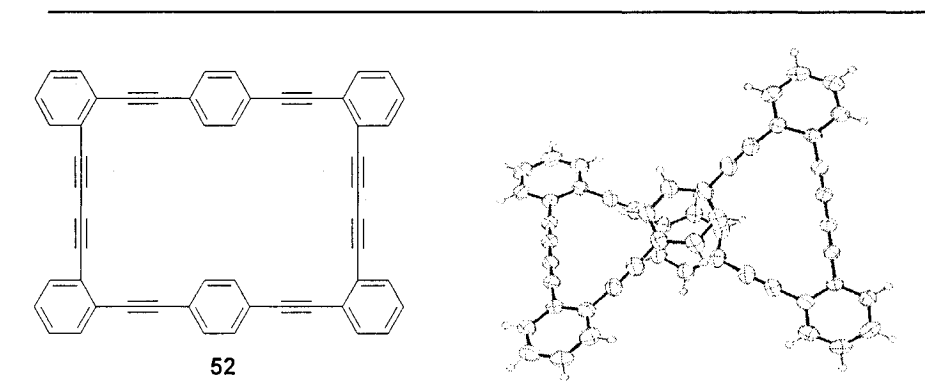


Figure 24: X-ray crystal structure of cyclophane **52** illustrating the overlapping capping aryl rings.

Other metal-based locking mechanisms can also be imagined. Incorporation of heterocycles into the cyclophane macrocycle, particularly as the capping groups, would enable metals to be bound within the cyclophane's core through π -coordination. 1,10-Phenanthroline and other bidentate-based unsaturated compounds have been prepared and shown to bind a variety of transition metals (Figure 25).⁸⁴ Thus, an appropriate combination of a heterocyclic cyclophane and metal should lead to a cyclophane complex in which helical inversion is stopped to give separate enantiomers. One conceivable target is phenanthrolinophane **137** (Figure 25).

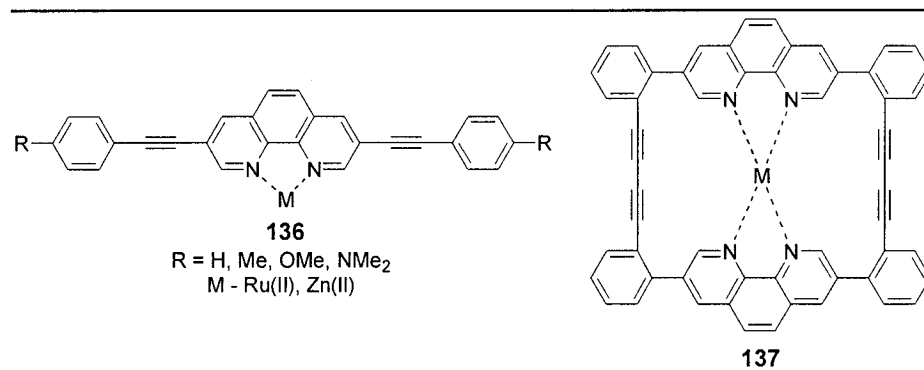
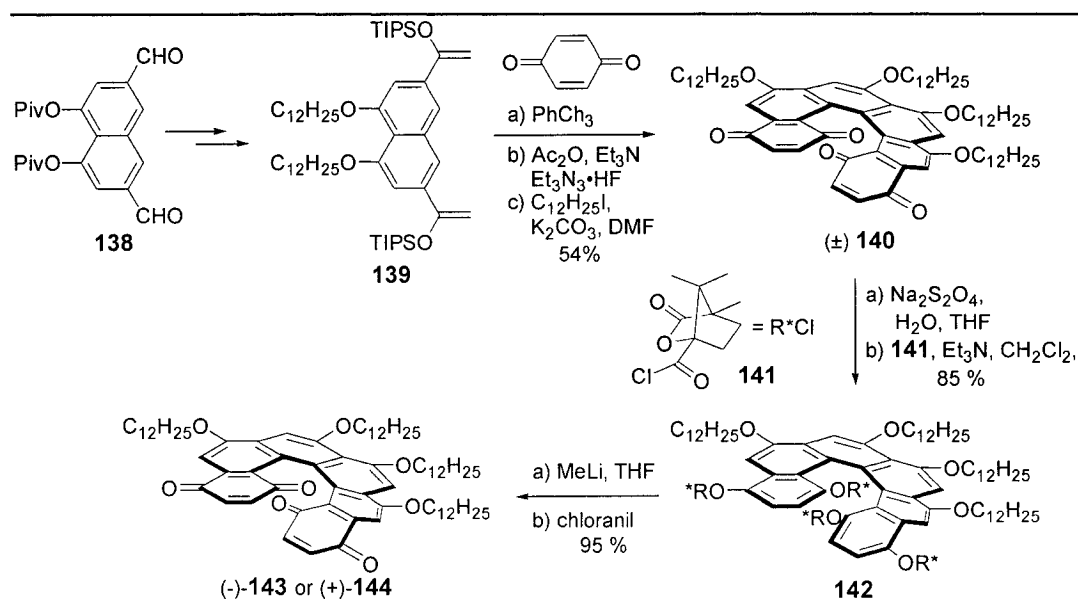


Figure 25: Tor's tunable fluorophores 136^{84a} and a conceptual phenanthroline 137.

The research presented in this chapter is related to the design and synthesis of helical cyclophanes and their corresponding metal complexes *en route* to helical, unsaturated compounds.

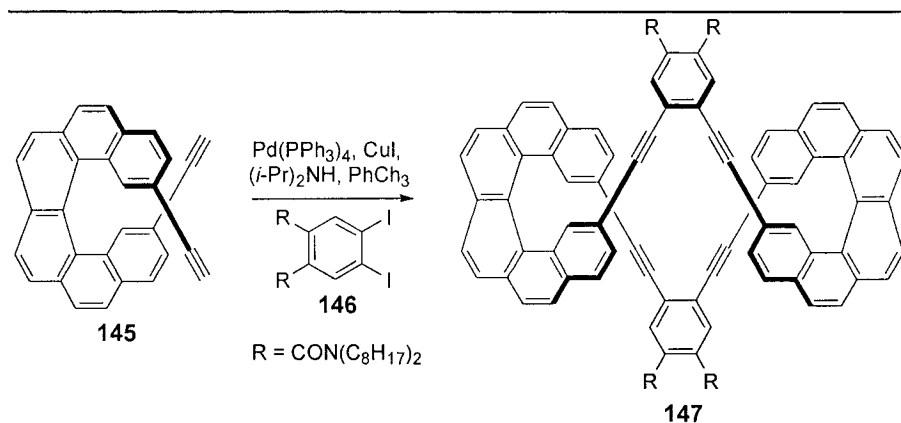
3.1 Unsaturated Compounds with Helical Chirality

The double helical structure of deoxyribose nucleic acid (DNA)⁸⁵ has inspired research of compounds that have double helices. Most of this research is focused on helical polymers;⁸⁶ however, recently a few unsaturated compounds have been prepared that possess helical chirality. The synthesis of a helicene by Katz's group was the first non-racemic, helical unsaturated compound reported.⁸⁷ An improved synthesis of helicenediquinone (\pm)-**140** functionalized for use as a liquid crystal is shown in Scheme 29.⁸⁸ Enantiopure helicene, (+)-**143** or (-)-**144**, could be obtained from the separation of diastomeric camphanoyl esters (**142**).



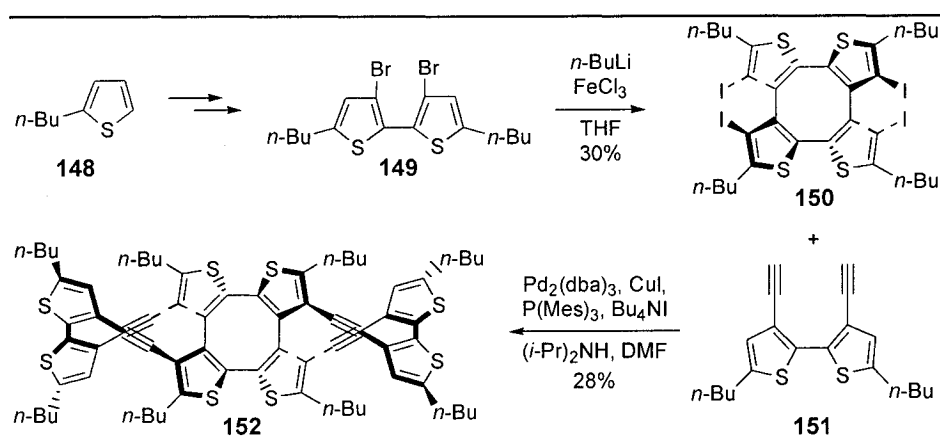
Scheme 29: Katz's helicene synthesis.

Helical cyclophane **147** was prepared by Fox's group with the helical nature of the compound arising from two helicene moieties incorporated within the bridge (Scheme 30).⁸⁹ Enantiopure cyclophane was obtained when chiral, non-racemic helicene **145** was used in the preparation.



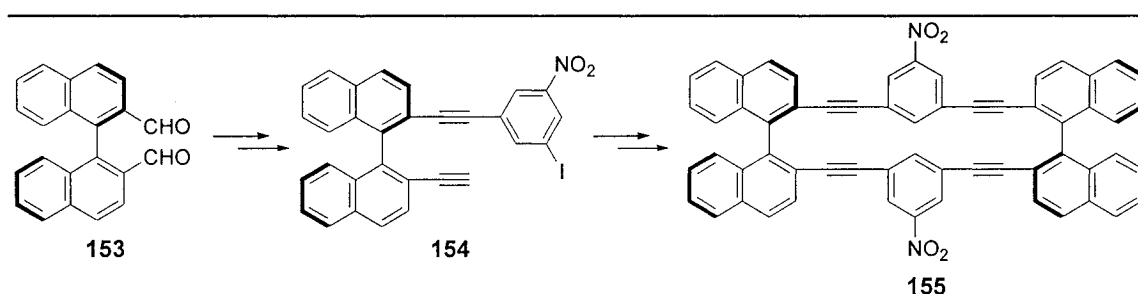
Scheme 30: Fox's helical cyclophane **147** based on helicene bridges.

Marsella's group investigated the use of cyclooctatetrathiene **150** as a helical scaffold on which to build a cyclophane **152** (Scheme 31).⁹⁰ To date, an enantiopure preparation of cyclooctatetrathiene **150** has not been reported and thus a chiral, non-racemic version of cyclophane **152** still remains to be synthesized.



Scheme 31: Marsella's cyclooctatetrathiophene-based cyclophane **152**.

Otera's group reported cyclophane **155** constructed from a 1,1'-binaphthyl helical scaffold (Scheme 32).⁹¹ Both enantiomers of 2,2'-biformyl-1,1'-binaphthyl (**153**) are easily obtained from BINOL and both enantiomers of cyclophane **155** were prepared. The Sonogashira dimerization of iodide **154** led to a trace amount of cyclophane **155**. A stepwise synthesis of cyclophane **155** from iodide **154** was found to be much more efficient despite the longer synthetic route.⁹¹



Scheme 32: Otera's 1,1'-binaphthyl-based cyclophane **155**.

In cyclophanes **147**, **152**, and **155** shown above, the compound's helical conformation resulted from a chiral directing group (*i.e.* helicene, cyclooctatetrathiophene, or 1,1'-binaphthyl). Our approach to helical, unsaturated cyclophane differs from the others in that there is no need for a helical scaffold as the helical nature of the compound would arise from the cyclophane's twisted conformation.

3.2 Synthesis of Cyclophane **157** as a η^{12} -Bis(arene) Ligand

The first η^{12} -bis(arene) complex that was envisioned is shown in Figure 26 and several design considerations are highlighted. Dibutylamino substituents on the bridging aryl rings

should aid solubility and ease synthetic manipulations as they did in the synthesis of cyclophanes **113** and **123**. Also, tetramethoxy-substituted capping aryl rings were chosen to favor metal complexation over the bridging aryl rings, as electron-rich aryl rings are known to be better η^6 -ligands. Finally, metals such as Cr(0), Mo(0), and Fe(II) could be used to make bis(arene) complexes that inhibit helical isomerization.

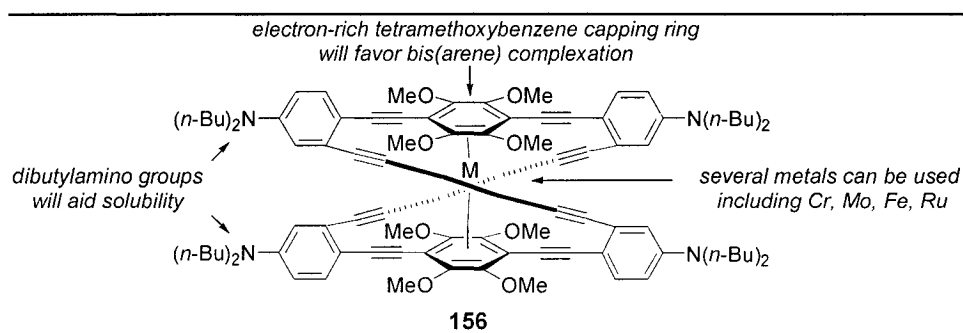


Figure 26: Design criteria for η^{12} -(cyclophane) complex **156.**

Retrosynthetic disconnections of complex **156** are shown in Figure 27. Coordination of various metals would occur once cyclophane **157** had been synthesized. This approach would allow for the preparation of several metal complexes and eliminate the need to carry organometallic intermediates through the synthesis. Cyclophane **157** could be synthesized by the desilylation/dimerization of **158**, analogous to the synthesis of parent cyclophane **52**. Based on the synthesis of cyclophane **123**, a Sonogashira reaction of iodide **118** and dialkyne **159** to form dimerization precursor **158** would be difficult. Thus, an alternate step-wise approach to **158** was devised from diiodide **160** and diamine **161**. A Sonogashira reaction of alkyne **163** and diiodide **162**⁹² would lead to diamine **161**.

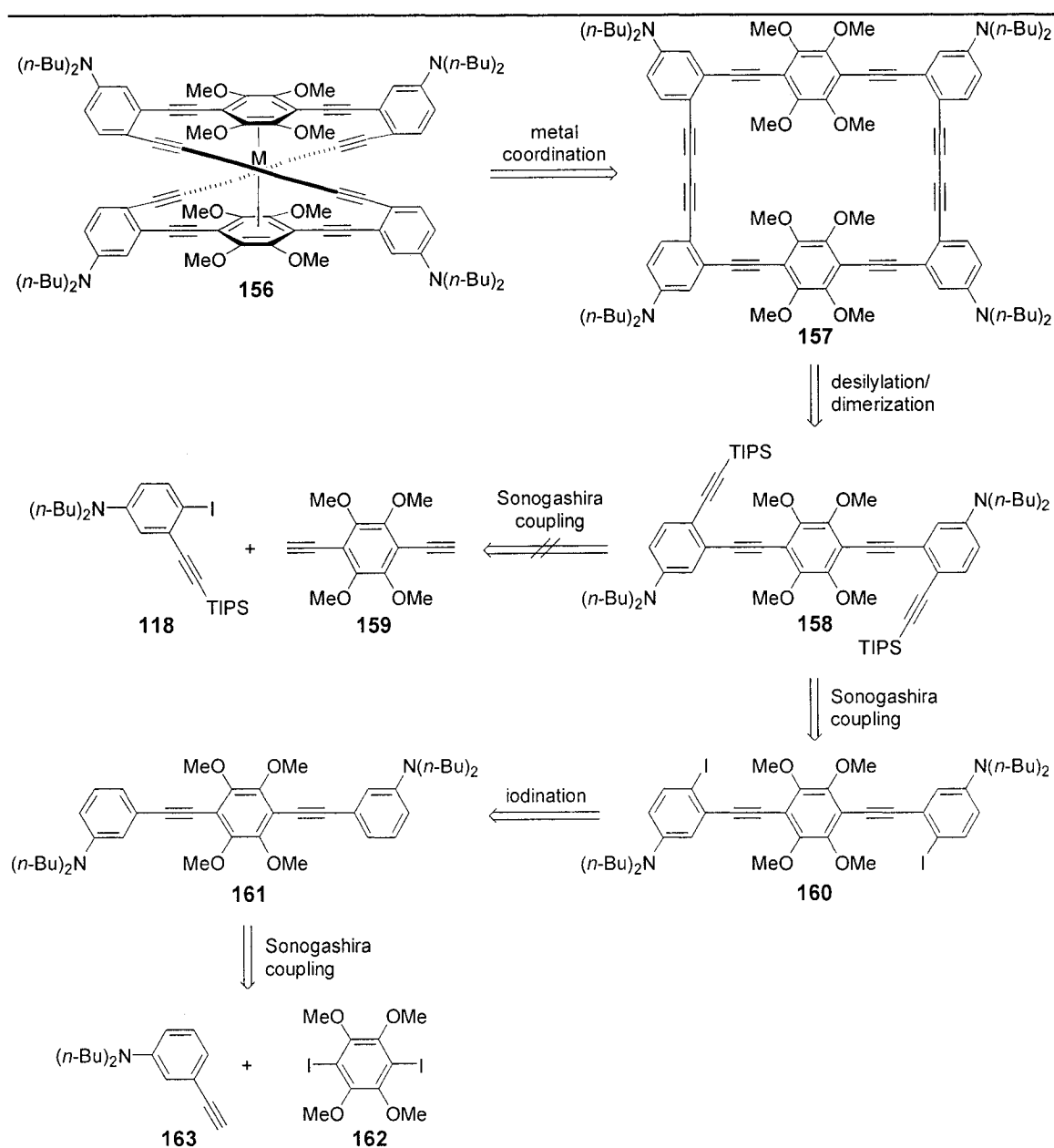
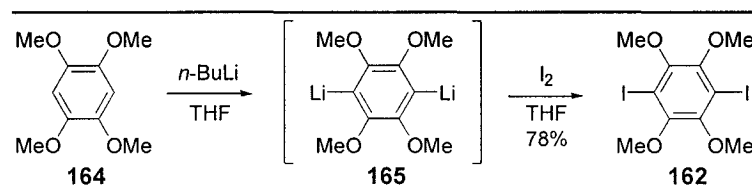


Figure 27: Retrosynthetic analysis of η^{12} -(cyclophane) complex **156**.

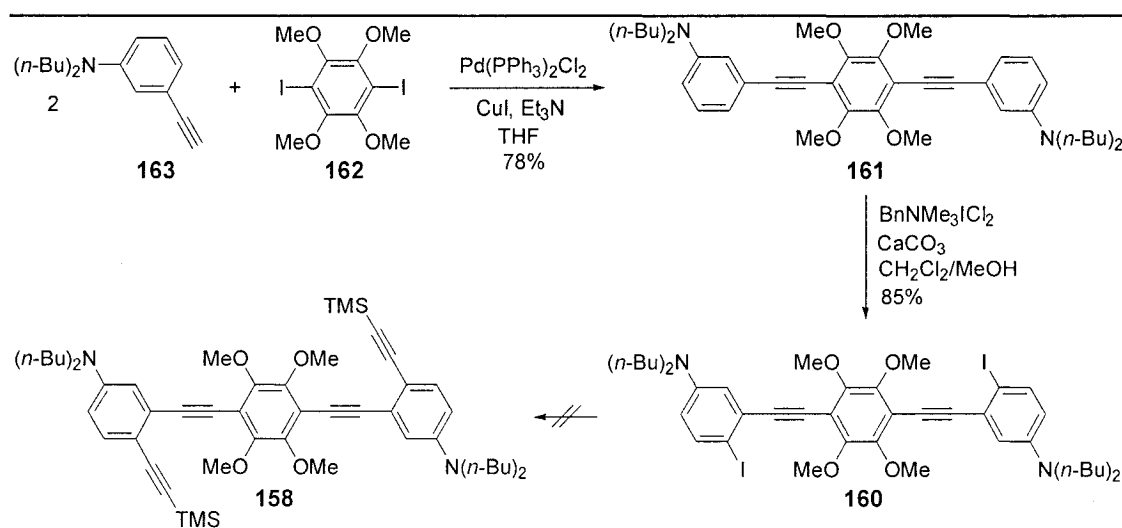
Diiodide **162**⁹³ was rapidly prepared from 1,2,4,5-tetramethoxybenzene (**164**) by improving the known syntheses (Scheme 33).⁹² Dilithium **165** was formed by the treatment of **164** with a solution of *n*-BuLi in hexane and was quenched with a solution of iodine in THF over 30 minutes at 0 °C to give diiodide **162** in 35% yield.^{92b} We suspected that the low yield of **162** could be attributed to the reduced reactivity of **165**, resulting from stabilization of the dilithium species by the neighboring oxygen atoms. By heating the

reaction to reflux for one hour after the addition of iodine, diiodide **162** was isolated in 78% yield, twice the reported yield for the reaction.⁹²



Scheme 33: Preparation of diiodide **162**.

A Sonogashira reaction between diiodide **162** and alkyne **163** using $\text{Pd}(\text{PPh}_3)_2\text{Cl}_2$, CuI , and Et_3N gave diamine **161** in 78% yield (Scheme 34). Treatment of **161** with two equivalents of Kajigaeshi's reagent ($\text{BnNMe}_3\text{ICl}_2$)⁶⁸ and calcium carbonate gave diiodide **160** in 85% yield. Unfortunately, Sonogashira reactions of diiodide **160** with various alkynes were all unsuccessful (Table 5).

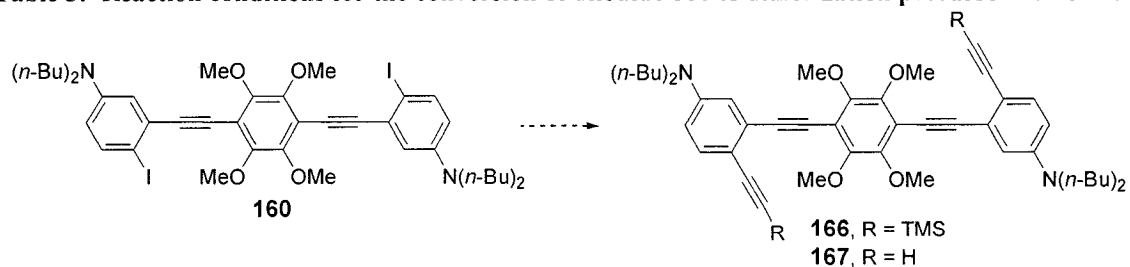


Scheme 34: Attempted synthesis of dimerization precursor **158**.

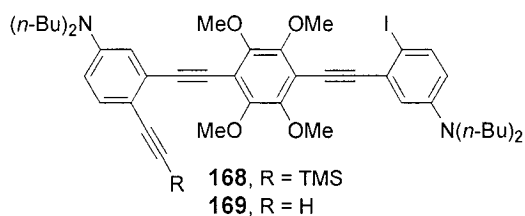
When traditional Sonogashira reaction conditions were used [$\text{Pd}(\text{PPh}_3)_2\text{Cl}_2$, CuI , Et_3N , THF, alkyne] with TMS-acetylene (**37**) at room temperature, only starting material was isolated (entry 1). To reduce steric congestion, a reaction of **160** with acetylene gas was conducted at 110 °C (entry 2). Unfortunately, significant decomposition occurred and neither starting material nor reaction products were isolated. Fu's Sonogashira reaction conditions were also used [$\text{Pd}(\text{BnCN})_2\text{Cl}_2$, CuI , Et_3N , THF, alkyne].²¹ When TMS-acetylene (**37**) was the alkyne source, some mono adduct, **168**, was isolated in addition to starting

material **160** (entry 3). A more promising result was obtained when the reaction was repeated with acetylene gas as a mixture of mono adduct **169** and the desired dimerization precursor **167** were obtained in < 10% and 27% yields respectively (entry 4). Unfortunately, further reaction optimization did not give better results.

Table 5: Reaction conditions for the conversion of diiodide **160 to dimerization precursor **166** or **167**.**



entry	alkyne	reaction conditions	result
1	TMS-acetylene (37)	Pd(PPh ₃) ₂ Cl ₂ , CuI Et ₃ N, THF, rt	recovery of 160
2	acetylene (15 psi)	Pd(PPh ₃) ₂ Cl ₂ , CuI Et ₃ N, THF, 110 °C	decomposition
3	TMS-acetylene (37)	Pd(BnCN) ₂ Cl ₂ , CuI Et ₃ N, THF, rt	168 (< 10%) and recovery of 160
4	acetylene (15 psi)	Pd(BnCN) ₂ Cl ₂ , CuI Et ₃ N, THF, rt	169 (< 10%) 167 (27%)



Based on these Sonogashira reaction results we concluded that the oxidative insertion of palladium into the aryl carbon-iodine bond was hindered by the steric bulk of the methoxy substituents on the capping aryl ring. The steric environment surrounding the iodine atom could be reduced by adding a second alkyne into the bridge between the capping and bridging aryl rings and allow the Sonogashira reaction to proceed. Thus, a new cyclophane target was designed that contained butadiyne spacers between capping and bridging aryl rings (Section 3.3, Figure 28).

3.3 Synthesis of Cyclophane **170** as an η^{12} -Bis(arene) Ligand

The difficulties in synthesizing cyclophane **157** were attributed to the steric bulk of the tetramethoxy substituents on the capping aryl ring. Cyclophane **170** was designed to relieve steric congestion near the iodine atoms by having additional alkynes between the capping and bridging aryl rings (Figure 28). Furthermore, cyclophane **170** would have sixty carbon atoms in its macrocyclic core and be a configurational isomer to *meta*-cyclophane **123** by having butadiyne spacers between each aryl ring.

Since small changes to the cyclophane's macrocycle have dramatic effects on the molecule's conformation, molecular modeling of cyclophane **170** was conducted. Fortunately, molecular modeling predicted that cyclophane **170** would adopt a twisted conformation with π -stacked capping aryl rings to allow for the preparation of bis(arene) metal complexes.

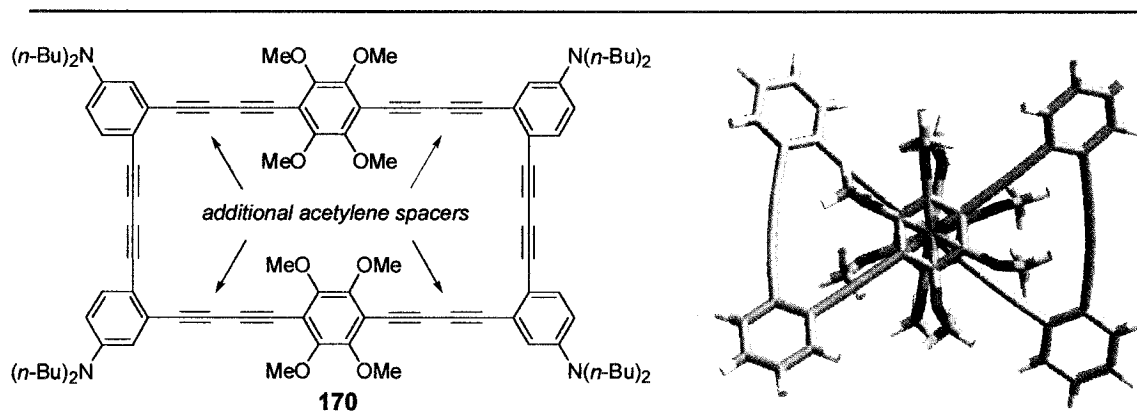


Figure 28: Cyclophane **170** and a molecular model of η^{12} -bis(cyclophane) chromium complex **171**.

The synthetic strategy for the synthesis of η^{12} -(cyclophane) chromium complex **171** was similar to the one used for complex **156** (Figure 29). Metallation would take place after the preparation of cyclophane **170**, which would come from the desilylation/dimerization of **172**. Dimerization precursor **172** would arise from a Sonogashira reaction of TMS-acetylene (**37**) and diiodide **173**. A Cadiot-Chodkiewicz cross-coupling reaction of dibromide **174** and alkyne **163** followed by iodination would give diiodide **173**.

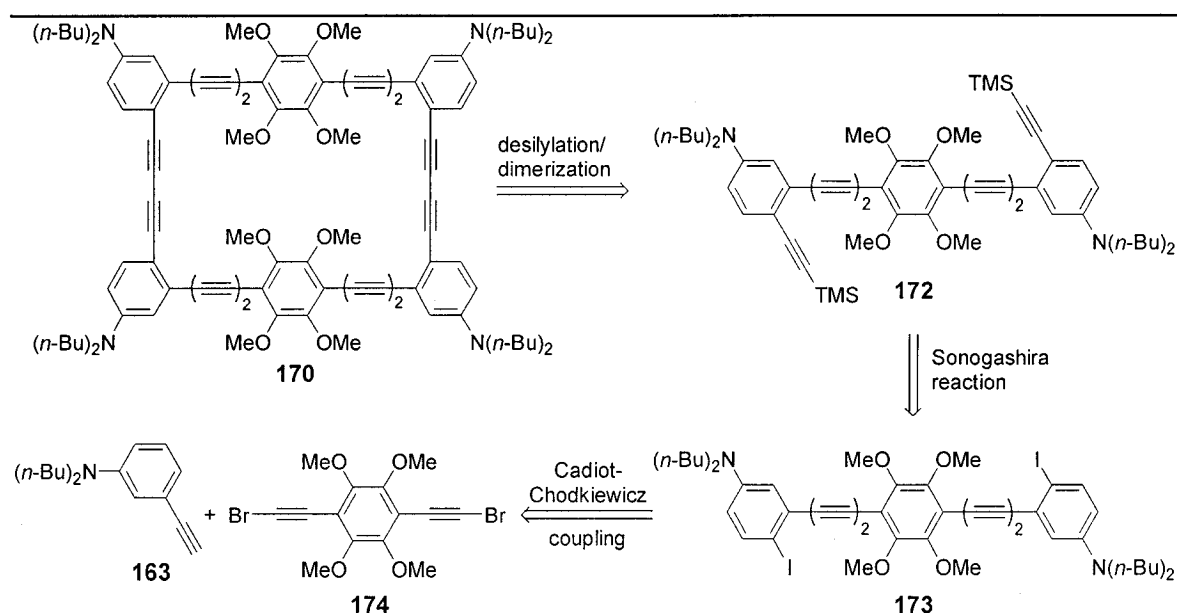
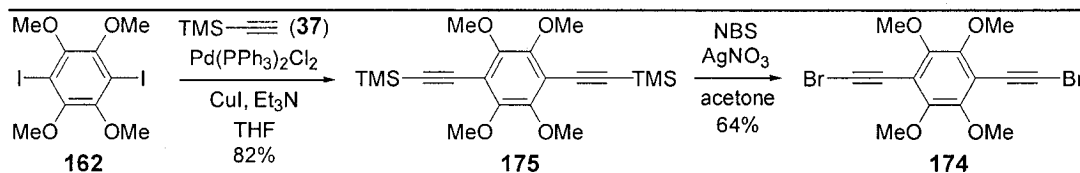


Figure 29: Retrosynthetic analysis of cyclophane **170**.

Dibromide **174** was rapidly synthesized from 1,4-diiodo-2,3,5,6-tetramethoxybenzene (**162**) in two steps (Scheme 35). A Sonogashira reaction of **162** and TMS-acetylene (**37**) using $\text{Pd}(\text{PPh}_3)_2\text{Cl}_2$, CuI , and Et_3N in THF gave silylalkyne **175**. Bromodesilylation of **175** with NBS and silver nitrate in acetone⁹⁴ gave dibromide **174** in 53% yield over both steps.

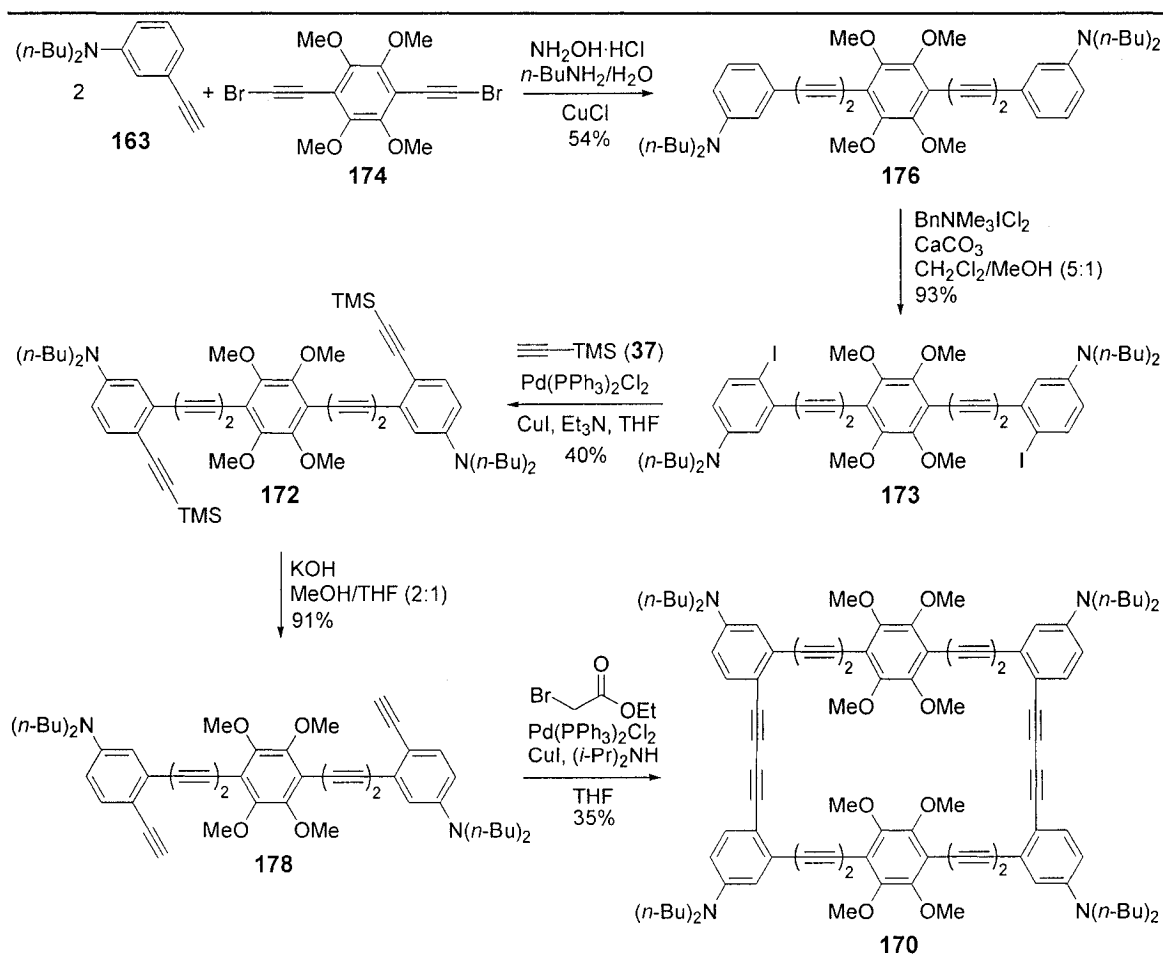


Scheme 35: Preparation of dibromide **174**.

The synthesis of cyclophane **170** continued with a Cadiot-Chodkiewicz cross-coupling reaction of dibromide **174** and alkyne **163** using CuCl and $\text{NH}_2\text{OH}\cdot\text{HCl}$ in a mixture of *n*-butylamine/water (3:7)⁹⁵ to give **176** in 58% yield. A homo-coupling side product, **177**,⁹⁶ was also isolated in 13% yield. Iodination of **176** using Kajigaeshi's reagent ($\text{BnNMe}_3\text{ICl}_2$)⁶⁸ with calcium carbonate in a mixture of methylene chloride/methanol (5:1) gave diiodide **173** in 93% yield. A Sonogashira reaction of diiodide **173** with $\text{Pd}(\text{PPh}_3)_2\text{Cl}_2$, CuI , Et_3N , and an excess of TMS-acetylene (**37**) in THF gave a mixture of the mono- and disilylalkyne **172**. Longer reaction times and addition of more $\text{Pd}(\text{PPh}_3)_2\text{Cl}_2$ and CuI catalysts did not lead to complete conversion. Separation of the two reaction products by flash chromatography was

difficult, but purified disilylalkyne **172** was obtained in 40% yield with another ~30% present as a mixture.

Dimerization of disilylalkyne **172** was attempted using our desilylation/dimerization method.⁹⁷ However, when disilylalkyne **172** was treated with TBAF and Cu(OAc)₂ in a mixture of pyridine/ether (3:1), desilylated product **178** was obtained as the major product. Since arylethyne are not as prone to decomposition as arylbutadiynes, dimerization of dialkyne **178** was investigated. Desilylation of **172** with potassium carbonate in acetone was unsuccessful, resulting in quantitative recovery of starting material. However, by stirring **172** with potassium hydroxide in a mixture of wet methanol/THF (2:1) for 12 hours, dialkyne **178** was obtained in 91% yield. Dimerization of **178** using a new palladium-catalyzed dimerization procedure (ethyl bromoacetate, Pd(PPh₃)₂Cl₂, CuI, (*i*-Pr)₂NH)³³ gave cyclophane **170** in 35% yield.



Scheme 36: Synthesis of cyclophane **170**.

X-ray quality crystals of cyclophane **170** were obtained by the slow evaporation of a chloroform solution. A low resolution crystal structure of cyclophane **170** illustrates the twisted conformation of the molecule and predicted π -stacked capping aryl rings, but other physical data such as bond lengths and angles could not be determined (Figure 30).

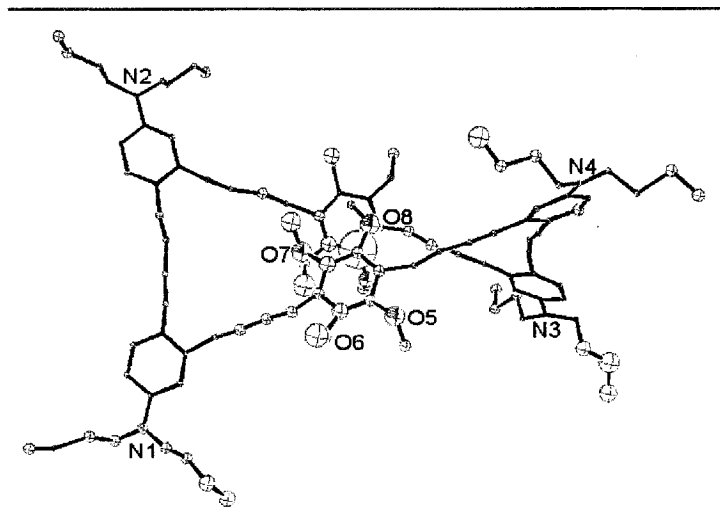


Figure 30: Low resolution X-ray crystal structure of cyclophane **170**.

3.4 Bis(arene) complexes

The first bis(arene) complexes were made by Franz Hein in 1918, but the structure of these compounds was not determined until 1957 by Harold Zeiss.⁹⁸ Bis(arene) complexes **179** were found to be sandwich compounds and are structurally related to metallocenes, **180**. Metallocenes have two six-electron donating cyclopentadienyl anions that bind in an η^5 -manner (Figure 31). Bis(arene) complexes differ in that they have two neutral aryl rings that donate six π -electrons to a metal in an η^6 -fashion. Electron-rich aryl rings form bis(arene) complexes with greater air stability.

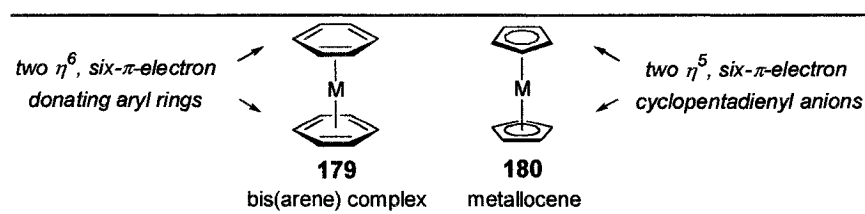
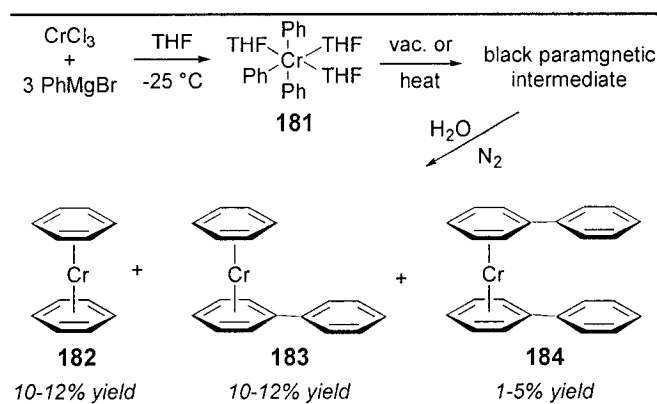


Figure 31: Sandwich structures of bis(arene) (**179**) and metallocene (**180**) complexes.

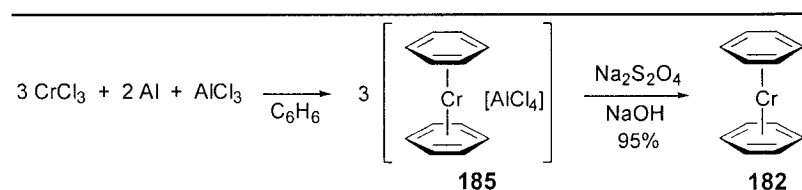
Bis(arene) complexes have traditionally been prepared with neutral group VI and divalent group VIII metals, with bis(arene) chromium(0) complexes being the most prevalent. The most common methods used to prepare bis(arene) complexes are the Hein Grignard, Fischer-Hafner aluminum, and metal vapour syntheses.⁹⁹

The Hein Grignard synthesis involves treating CrCl_3 with three equivalents of an aryl Grignard reagent (Scheme 37). The resulting solution of organochromium complex **181** is either heated or concentrated to give a black paramagnetic intermediate that is hydrolyzed to give bis(arene) complex **182** as a mixture of metallated compounds.¹⁰⁰



Scheme 37: Hein Grignard synthesis of bis(arene) complexes.

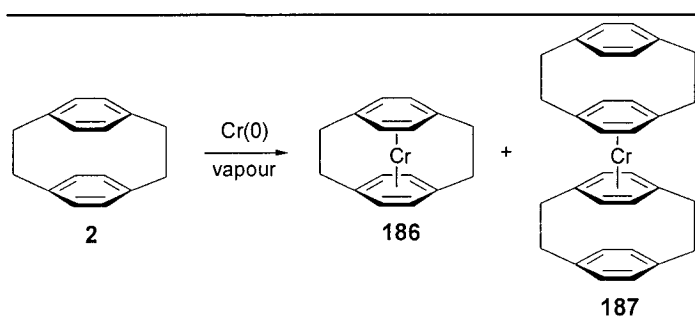
A more efficient route to bis(arene) complexes is the Fischer-Hafner aluminum synthesis (Scheme 38).¹⁰¹ In this method, CrCl_3 is treated with aluminum metal and AlCl_3 in the presence of the arene, which in many cases is the solvent. Chromium(III) is reduced by aluminum to give a paramagnetic, chromium(I) sandwich complex **185** that is further reduced by sodium dithionite ($\text{Na}_2\text{S}_2\text{O}_4$) to afford the desired bis(arene) chromium compound, **182**.



Scheme 38: Fischer-Hafner synthesis of bis(arene) complexes.

Bis(arene) complexes can also be synthesized by condensing metal vapours in the presence of aryl ligands.¹⁰² Metals are vapourized by resistive heating under high vacuum (10^{-3} Torr) and condensed in the presence of the arene, which is either gaseous or in an inert

solvent. Metal vapour synthesis was used to prepare a bis(arene) complex of [2,2]*paracyclophane* (**2**) as an η^{12} -bis(arene) ligand (Scheme 39).¹⁰³ Two complexes were isolated from the reaction, the desired (η^{12} -[2,2]*paracyclophane*)Cr(0) complex (**186**) and bis(η^6 -[2,2]*paracyclophane*)Cr(0) complex (**187**) in a combined 5% yield.



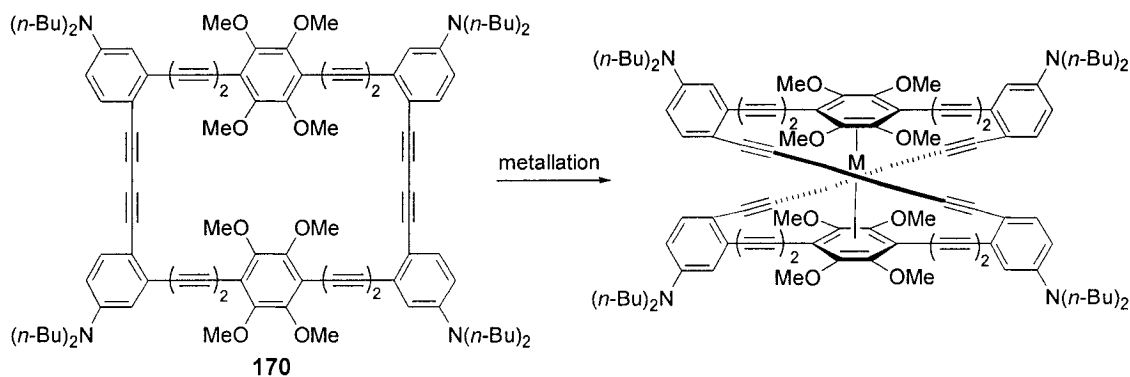
Scheme 39: [2,2]*paracyclophane* (**2**) as a η^{12} -bis(arene) ligand.

Although several cyclophanes and metals have been used to make bis(arene) complexes,¹⁰⁴ unsaturated cyclophanes have not been used, partly due to the lack of an efficient synthetic method. Undeterred, we set out to prepared an η^{12} -cyclophane complex.

3.5 Synthesis of (η^{12} -Cyclophane) Complexes

With cyclophane **170** in hand, we were ready to prepare an assortment of (η^{12} -cyclophane) complexes. The first synthetic procedure that was considered was metal vapour synthesis as (η^{12} -cyclophane)chromium complexes had been made using this method.¹⁰⁴ Geoffrey Cloke at the University of Sussex was contacted for his expertise in the metal vapour synthesis of organometallic compounds. Unfortunately, his apparatus would require over 1.5 g of cyclophane **170** so other synthetic methods were considered (Table 6).

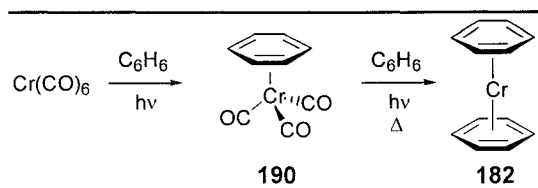
Table 6: Attempted metallation reactions of cyclophane **170**.



entry	metal source	reaction conditions	desired product	result
1	Cr(CO) ₆	DMSO, UV lamp, 24 h	171 [Cr(170) ₂]	formation of a bright yellow compound that rapidly decomposed
2	Cr(benzene) ₂	DMSO, 160 °C, 48 h	171 [Cr(170) ₂]	green, paramagnetic compound formed
3	Fe(H ₂ O) _x (BF ₄) ₂	MeNO ₂ , 80 °C, 96 h	188 [Fe(170)(BF ₄) ₂]	mixture of 170 and a yellow solid
4	FeCl ₃	1) Al/AlCl ₃ , MeNO ₂ , 60 °C, 16 h 2) NaBArF ^a	189 [Fe(170)(BArF) ₂]	formation of a yellow solid

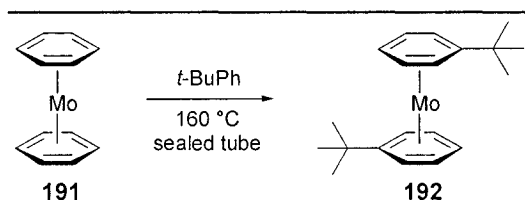
^a NaBArF = sodium tetrakis(3,5-bistrifluoromethylphenyl)borane

Photolysis of Cr(CO)₆ in the presence of an arene is known to form stable (arene)Cr(CO)₃ piano stool complexes.⁹⁹ Replacement of the remaining carbonyl ligands with a second arene would lead to a bis(arene) chromium complexes (Scheme 40). Although this is not a common method used in the preparation of bis(arene) complexes, it was an attractive starting point as cyclophane **170** was not expected to decompose under the reaction conditions. Cyclophane **170** was mixed with Cr(CO)₆ in degassed DMSO and photolyzed (Table 6, entry 1).¹⁰⁵ After 24 h, cyclophane **170** was consumed and a yellow compound had formed that was presumed to be a piano stool complex. Further photolysis did not lead to the desired (η¹²-cyclophane) chromium complex **171**.



Scheme 40: Potential preparation of bis(arene) chromium complexes by photolysis.

Recently, bis(arene)molybdenum complexes were prepared by an arene metathesis reaction (Scheme 41).¹⁰⁶ Many bis(arene) molybdenum complexes are pyrophoric¹⁰⁷ so an arene metathesis reaction with bis(η^6 -C₆H₆)₂Cr (**182**) was attempted. Cyclophane **170** and complex **182** were combined in DMSO in a sealed tube and the reaction was heated at 160 °C for 48 h (Table 6, entry 2). A green, paramagnetic material was formed, but it rapidly decomposed prior to characterization.



Scheme 41: Arene metathesis of bis(arene) molybdenum complexes.

Bis(arene)iron(II) complexes are known and in some cases are more stable than their chromium(0) counterparts.¹⁰⁸ Iron is the only metal other than chromium that has been used to make cyclophane complexes.¹⁰⁴ Although the Fischer-Hafner method has been the only method used for the preparation of bis(arene)Fe(II) complexes with cyclophanes, a ligand displacement reaction was attempted first as cyclophane **170** may react with AlCl₃. A solution of Fe(H₂O)_x(BF₄)₂ was added to a solution of cyclophane **170** in nitromethane and the mixture was heated at 80 °C for 96 h (Table 6, entry 3). A mixture of **170** and a dark yellow solid that could not be characterized was obtained.

In a last attempt at synthesizing a (η^{12} -cyclophane)Fe(II) complex, the Fischer-Böttcher method (similar to the Fischer-Hafner method for chromium) was used.¹⁰⁹ Ferric chloride (FeCl₃), AlCl₃, Al(0), and cyclophane **170** were combined in nitromethane and heated to 60 °C for 16 h (Table 6, entry 4). The reaction was cooled and poured into water. An orange solid was formed after the addition of NaBARf, which was recovered by filtration. Unfortunately, the orange solid slowly decomposed and characterization could not be achieved.

The difficulty in preparing bis(arene) complexes with cyclophane **170** forced us to consider other metal locking strategies. π -Coordination complexes were attractive targets due to their ease of preparation and air and moisture stability. The remainder of this chapter describes the synthesis of cyclophane π -coordination complexes.

3.6 1,10-Phenanthroline-Based Compounds

Many heterocycles could be chosen as a cyclophane capping group to facilitate the preparation of π -coordination complexes. However, 1,10-phenanthroline (**197**) is a particularly attractive candidate as it is a C_2 -symmetric ligand that can be pseudo *para*-substituted (3,8-disubstituted) to mimic our *para*-aryl capping groups. Furthermore, 1,10-phenanthroline is known to form air and moisture stable complexes with a variety of metals.¹¹⁰

A number of interesting phenanthroline-based copper(I) compounds have recently been synthesized including molecular grids that are prepared by self-assembly (**193**)¹¹¹ and catenanes (**194**)¹¹² that may be used as molecular machines (Figure 32).

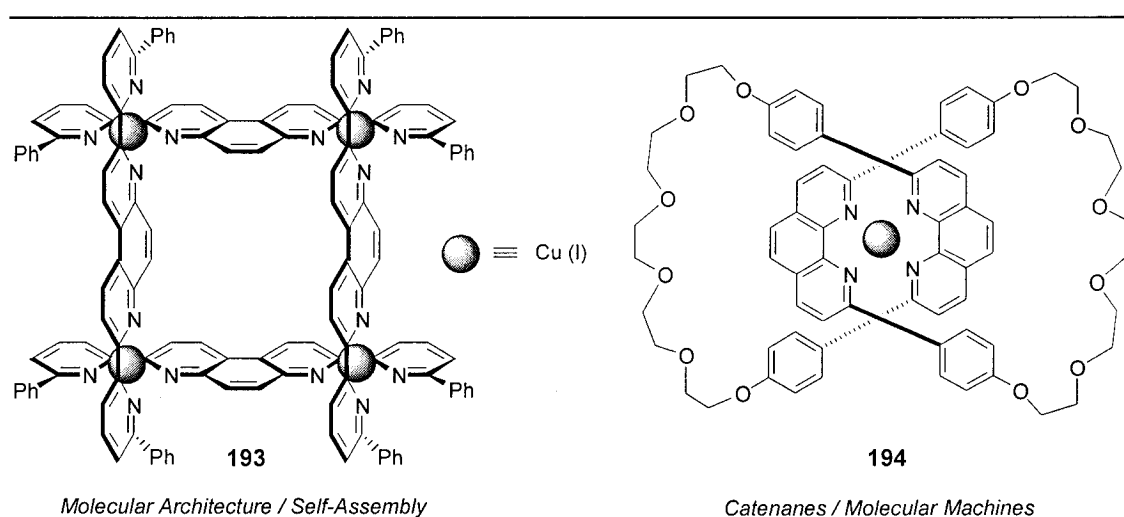


Figure 32: Phenanthroline based copper(I) compounds.

Luminescent Cu(I) phenanthroline compounds have received considerable attention for chemical recognition, sensing, and tagging applications.¹¹³ Optimized luminescence occurs when: (a) the two phenanthroline groups are perpendicular to one another to form a pseudotetrahedral coordination site for the copper(I) ion; (b) the copper ion is sufficiently

hindered to reduce flattening and rocking distortions and attack from solvent molecules; and (c) there is increased ligand π -electron delocalization (Figure 33).¹¹⁴

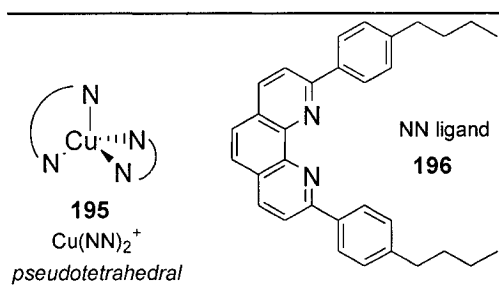
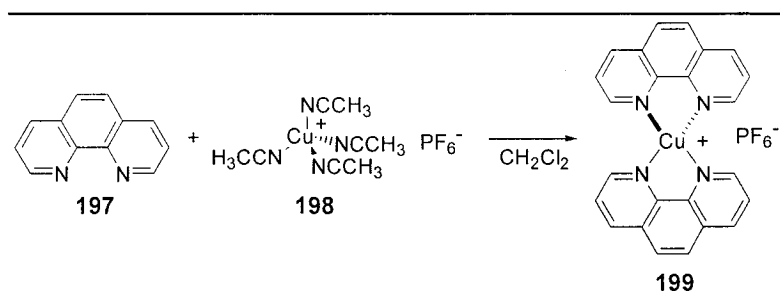


Figure 33: A luminescent Cu(I)-phenanthroline complex.^{113b}

1,10-Phenanthroline based compounds have been shown to intercalate within the major groove of DNA and catalyze the oxidative cleavage of ribose linkages.¹¹⁵ Thus, phenanthroline based molecules may be promising targets for pharmaceuticals. Also, chiral Cu(I) phenanthroline complexes have been used as asymmetric homogeneous catalysts.¹¹⁶

The synthesis of π -coordination complexes is much more straightforward than bis(arene) complexes. For example, $\text{Cu}(\text{phen})_2^+$ complexes can be prepared by combining 1,10-phenanthroline (**197**) and tetrakis(acetonitrile)copper(I) hexafluorophosphate (**198**)¹¹⁷ in methylene chloride (Scheme 42). Concentration of the solvent gives the crude $\text{Cu}(\text{phen})_2\text{PF}_6$ complex **199**, which can be purified by recrystallization.



Scheme 42: Preparation of $\text{Cu}(\text{I})(\text{phen})_2$ complexes.

A cyclophane that has 3,8-disubstituted, 1,10-phenanthroline capping groups should be helical, easy to prepare, and bind copper(I) ions to afford a luminescent compound that would be of interest for a variety of applications. The design and syntheses of phenanthroline cyclophanes and their copper(I) complexes are described in the following sections.

3.7 Synthesis of Phenanthroline Cyclophanes **200** and **217**

A number of phenanthroline cyclophane (phenanthrolineophane)¹¹⁸ targets were considered. Molecular modeling was used to predict whether the compounds would adopt a helical conformation with perpendicular phenanthroline moieties to allow metal coordination. The resulting copper-complexed phenanthrolineophane should be highly luminescent as the bridges could sufficiently protect the metal center from solvent molecules and the phenanthroline groups are favorably orientated. Phenanthrolineophane **200** was chosen as the first synthetic target as it adopts a helical conformation (Figure 34) and could be rapidly synthesized.

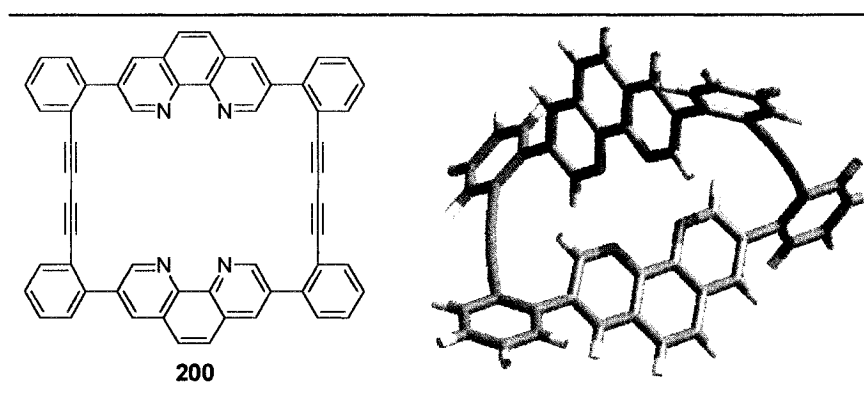


Figure 34: Molecular model of phenanthrolineophane 200.

Retrosynthetic disconnections of copper(phenanthrolineophane) complex **201** is shown in Figure 35. In a similar strategy to the bis(arene) complexes, metallation will be done in the last step. Phenanthrolineophane **200** would be prepared by our desilylation/dimerization protocol from dimerization precursor **202**. Compound **202** is rapidly synthesized from 3,8-dibromo-1,10-phenanthroline (**203**) and commercially available bromide **204**.

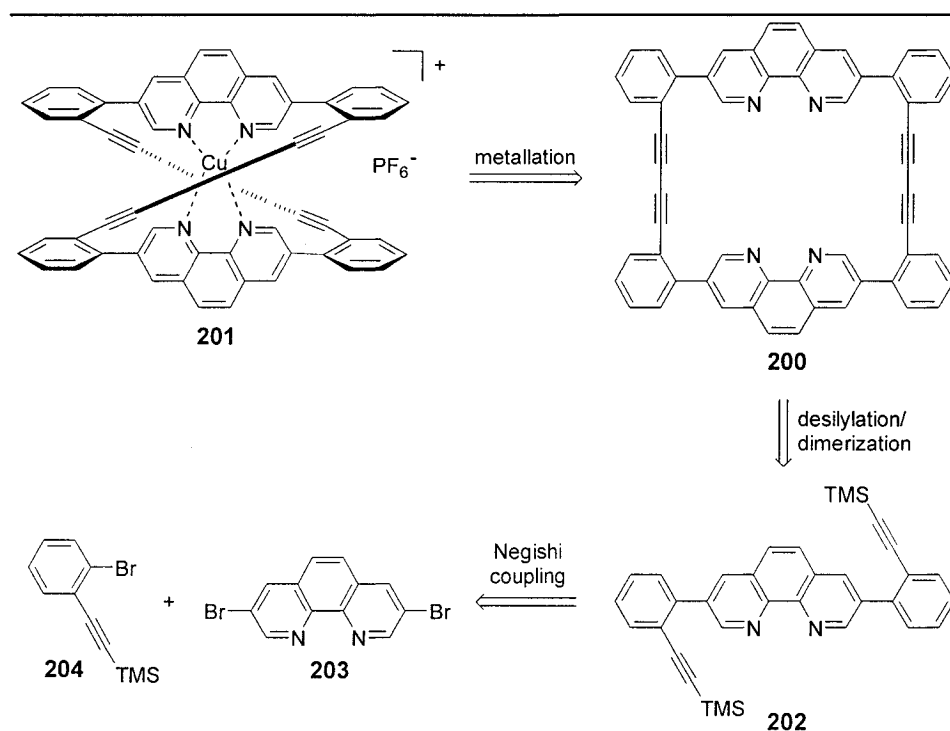
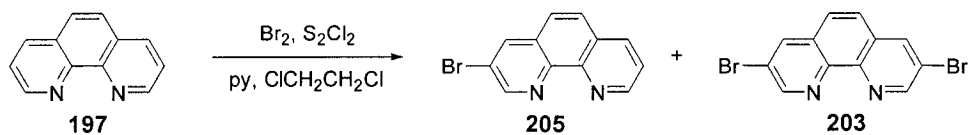


Figure 35: Retrosynthetic analysis of copper(phenanthroline) complex 201.

A number of procedures have been reported for the bromination of 1,10-phenanthroline (**197**) in the 3 and 8 positions.¹¹⁹ However, the best reported yield for the reaction was 32% so attempts were made to optimize the reaction (Table 7). Siegel and coworkers reported a preparation of 3,8-dibromo-1,10-phenanthroline (**203**) using 1,10-phenanthroline (**197**) and elemental bromine.^{119a} A mixture of monobromide **205** and dibromide **203** was obtained under these reaction conditions and were difficult to separate (entry 1). A second procedure included the use of a complexing agent, sulfur monochloride (S₂Cl₂), which led to an improved 38% yield of **203** (entry 2).^{119b} This method was based on a preparation of 3-bromopyridine.¹²⁰

The proposed mechanism for this bromination involved the initial coordination of sulfur monochloride to pyridine (Scheme 43). Bromination would take place on the resulting 1,2- or 1,4-dihydropyridine followed by the release of sulfur monochloride to afford 3-bromopyridine. The preparation of dibromide **203** would follow the same mechanism with bromination occurring on each heterocyclic ring.

Table 7: Bromination of 1,10-phenanthroline reaction conditions.

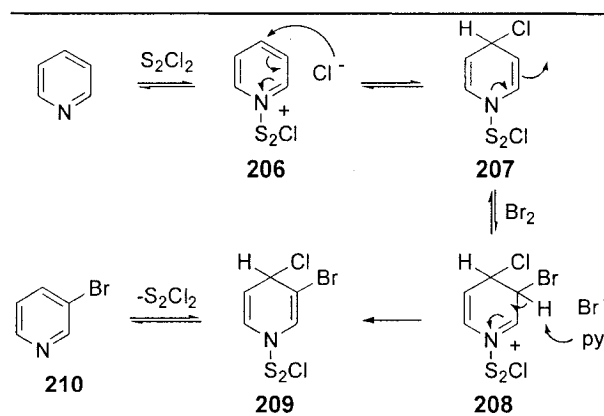


entry	S ₂ Cl ₂ (eq)	pyridine (eq)	Br ₂ (eq)	time (h)	result (% yield)
1	-	-	1.5	3	mixture of 205 and 203 ^a
2	3.28	3.62	3.16	18	203 (38) ^b
3	-	2	2	24	no reaction
4	TsCl 3.28	3.28	3.16	18	203 (45%) (complex mixture)
5	Br ₂ SO 3.28	3.28	3.16	18	203 (39%) (complex mixture)
6	2.05	DIPEA 2.05	2.3	18	black oil
7	2.05	2.05	I ₂ 2.05	18	no reaction
8	3.28	excess	3.16	18	203 (59) ^c

^a nitrobenzene was the solvent

^b 1-chlorobutane was the reaction solvent, 1,10-phenanthroline (**197**) was not very soluble.

^c crude product was obtained in 88% yield and looks good by ¹H NMR but contains a sulfur impurity.



Scheme 43: Proposed mechanism for the bromination of pyridine in the 3 position.¹²⁰

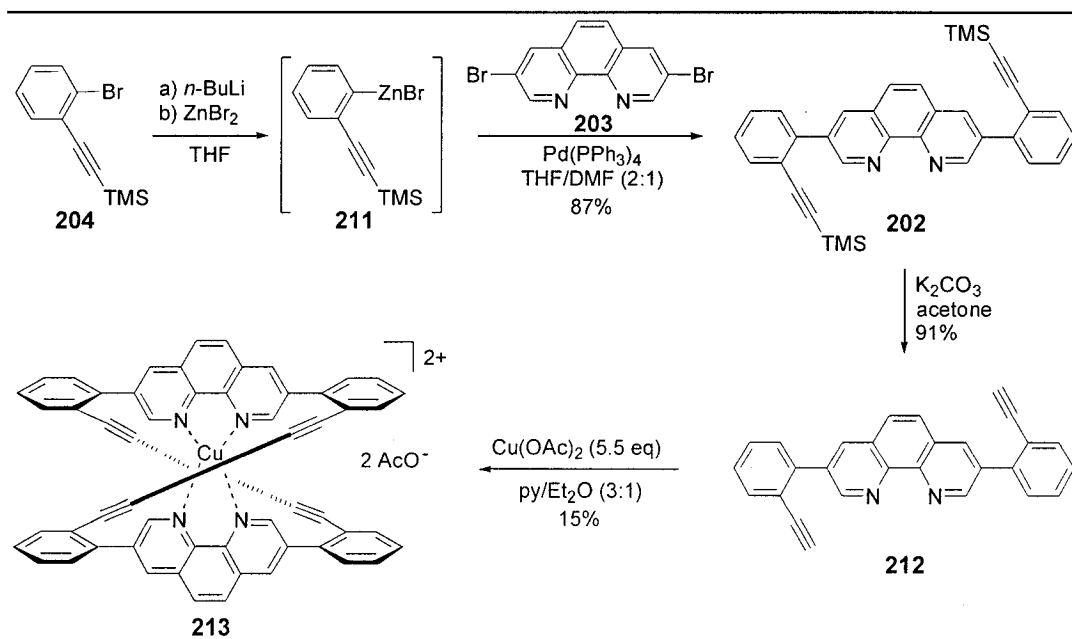
In order to gain further mechanistic insight, the reaction was performed with 1,2-dichloroethane-d₄ and pyridine-d₅ and monitored by ¹H NMR. When pyridine-d₅ was added to the phenanthroline-sulfur monochloride complex, uncoordinated

1,10-phenanthroline was observed (based on ^1H chemical shifts). This suggested that sulfur monochloride readily disassociated from 1,10-phenanthroline, leading to the bromination of both pyridine and phenanthroline. Based on these results, we felt that improvements could be made to the procedure.

First, the effect of the complexing agent was studied. A reaction without a complexing agent (no S_2Cl_2) resulted in the recovery of starting material (entry 3). The use of tosylchloride (entry 4) or thionylbromide (entry 5) gave complex mixtures with little to no dibromide **203**. Second, replacing pyridine with a base that would not compete for the complexing agent or undergo bromination itself was investigated. The use of diisopropylethylamine resulted in a viscous black oil that was discarded (entry 6). Finally, the reaction was attempted with elemental iodine in order to prepare 3,8-diiodo-1,10-phenanthroline, but no reaction took place (entry 7).

Modifications to Yamamoto's procedure,^{119b} such as using 1,2-dichloroethane instead of 1-chlorobutane as the reaction solvent and using flash chromatography (SiO_2) instead of recrystallization during purification, gave 3,8-dibromo-1,10-phenanthroline (**203**) in 88% yield (entry 8). Although the product looked pure by ^1H and ^{13}C NMR, a sulfur impurity remained. Further purification led to analytically pure **203** in 59% yield. The improved purification was also found independently by Sauvage's group.¹²¹

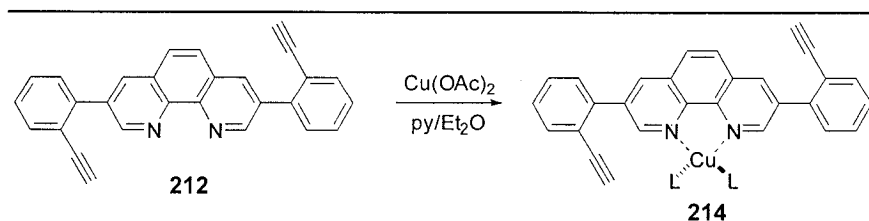
Despite the modest yields that were obtained in the preparation of **203**, we continued the synthesis of phenanthroline **200**. Bromide **204** was converted to organozincate **211** *in situ* by lithium-halogen exchange with *n*-BuLi followed by transmetalation with zinc bromide.¹²² Addition of a solution of 3,8-dibromo-1,10-phenanthroline (**203**) and a catalytic amount of $\text{Pd}(\text{PPh}_3)_4$ to the reaction afforded **202** in low yield (< 20%). However, when DMF was used as a co-solvent,¹²³ the yield improved dramatically to give **202** in 87% yield (Scheme 44).



Scheme 44: Synthesis of copper(phenanthroline) complex **213**.

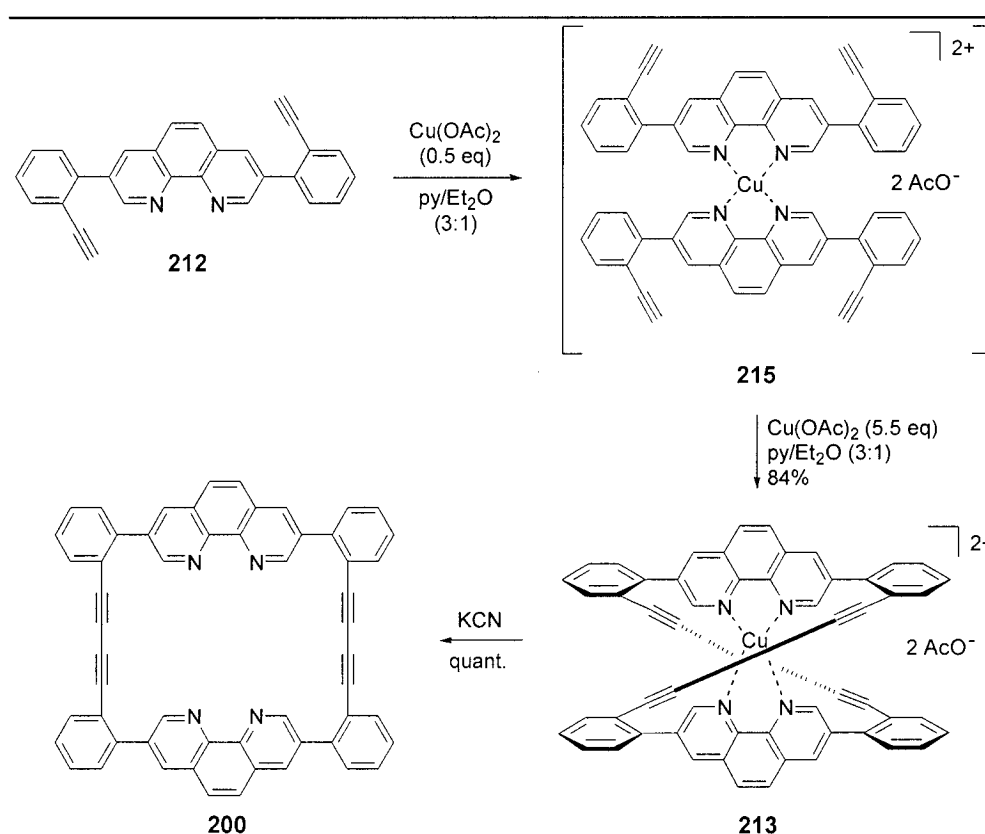
Attempted desilylation of **202** using the standard conditions of wet MeOH/THF with K_2CO_3 was unsuccessful as **202** was not soluble in the solvent mixture. Dimerization precursor **212** was obtained in 91% yield by changing the solvent to wet acetone. Dimerization of **212** was achieved using Eglinton coupling conditions [$Cu(OAc)_2$, pyridine/ Et_2O (3:1)] to give copper(phenanthroline) complex **213** in 15% yield instead of phenanthroline **200**.

Isolation of copper(phenanthroline) complex **213** demonstrated the stability of copper(phenanthroline) complexes. The low yield that was obtained for the dimerization reaction could be explained by the formation of a copper(phenanthroline) complex, such as **214**, prior to dimerization, which would then retard or inhibit the dimerization reaction (Scheme 45).



Scheme 45: Proposed formation of complex **214** during the dimerization of **212**.

We thought that if complex **214** was indeed being formed, copper could be used to template the reaction.¹²⁴ This strategy was expected to circumvent the formation of complex **214** and reduce the formation of side-products that are often observed during the dimerization reaction. Experimentally, addition of half an equivalent of $\text{Cu}(\text{OAc})_2$ to a solution of **212** led to the formation of complex **215** (Scheme 46). The dimerization was then carried out by the addition of excess $\text{Cu}(\text{OAc})_2$ to give copper(phenanthroline) complex **213** in a much improved 84% yield. Phenanthroline **200** was then quantitatively prepared by treating a solution of complex **213** in dichloromethane with aqueous KCN.



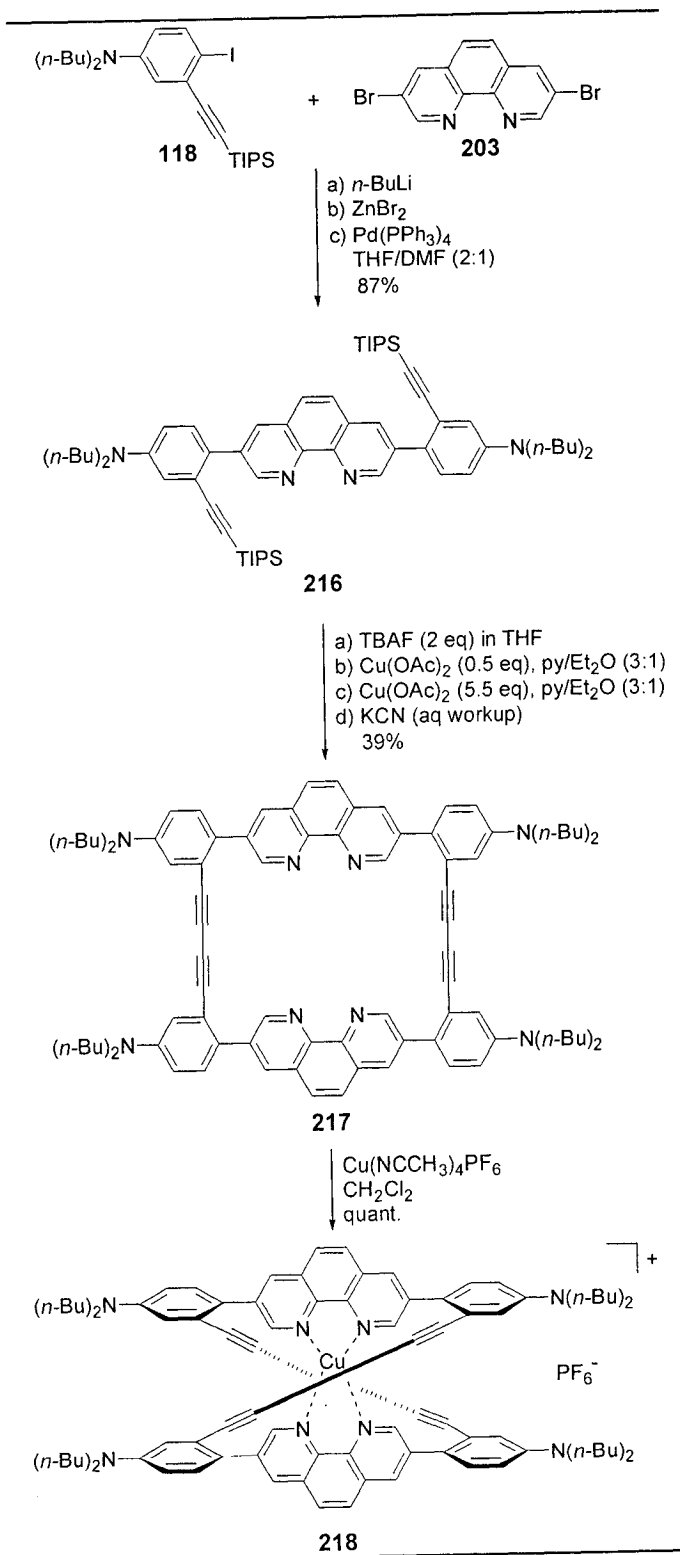
Scheme 46: Copper-template synthesis of phenanthroline **200**.

The poor solubility of phenanthroline **200** in common organic solvents prevented the synthesis of its copper(I) complex. The addition of dibutylamino-substituents on the bridging aryl rings would solve the solubility problems as they did for cyclophanes **113** and **123**. Thus, a second generation phenanthroline, **217**, was designed that had dibutylamino-substituents on the bridging aryl rings. In this case the dibutylamino

substituents were expected to have the additional benefit of providing insight into the phenanthroline's conformation.¹²⁵

The synthetic approach to phenanthroline **217** was the same one that was used for the preparation of **200** except that the synthesis required iodide **118** instead of bromide **204** (Figure 35). Our one-pot Negishi coupling method was used to combine iodide **118** and 3,8-dibromo-1,10-phenanthroline (**203**) to give **216** in 87% yield. Phenanthroline **217** was prepared directly from **216** using the copper-templated modification of our *in situ* desilylation/dimerization procedure described earlier. Dimerization precursor **216** was initially treated with two equivalents of TBAF to remove the triisopropylsilyl groups, and half an equivalent of Cu(OAc)₂ to establish the copper template. This solution was added by syringe pump to a solution of an excess of Cu(OAc)₂ to effect the dimerization and was worked up with an excess of potassium cyanide, which removed the copper and afforded phenanthroline **217** as a yellow foam in 39% yield (>80% yield for each bond breaking/forming step). Phenanthroline **217** was readily soluble in organic solvents (CH₂Cl₂, Et₂O, acetone) unlike its unsubstituted predecessor. Copper(I) phenanthroline complex **218** was easily prepared by adding a stoichiometric amount of Cu(CH₃CN)₄PF₆ to a solution of phenanthroline **217** in methylene chloride.

Phenanthrolines **200** and **217** and their corresponding copper(I) and copper(II) complexes were studied photochemically and by variable temperature NMR. These results are discussed in the following section.



Scheme 47: Synthesis of phenanthroline 217 and its copper(I) complex 218.

3.8 Properties of Phenanthrolineophanes **200** and **217**

UV/Vis spectra were obtained for the various phenanthrolineophanes (Figure 36). Phenanthrolineophane **200** was nearly colourless and had a $\pi\text{-}\pi^*$ transition at 360 nm. The two copper(II) complexes, **213** and **215**, had λ_{max} values of 462 and 473 nm respectively, which are typical of Cu(II)(phen) complexes.¹²⁶ Phenanthrolineophane **217** and its copper(I) complex **218** both had $n\text{-}\pi^*$ transitions, with the copper(I) complex λ_{max} red shifted relative to **217** by 24 nm.

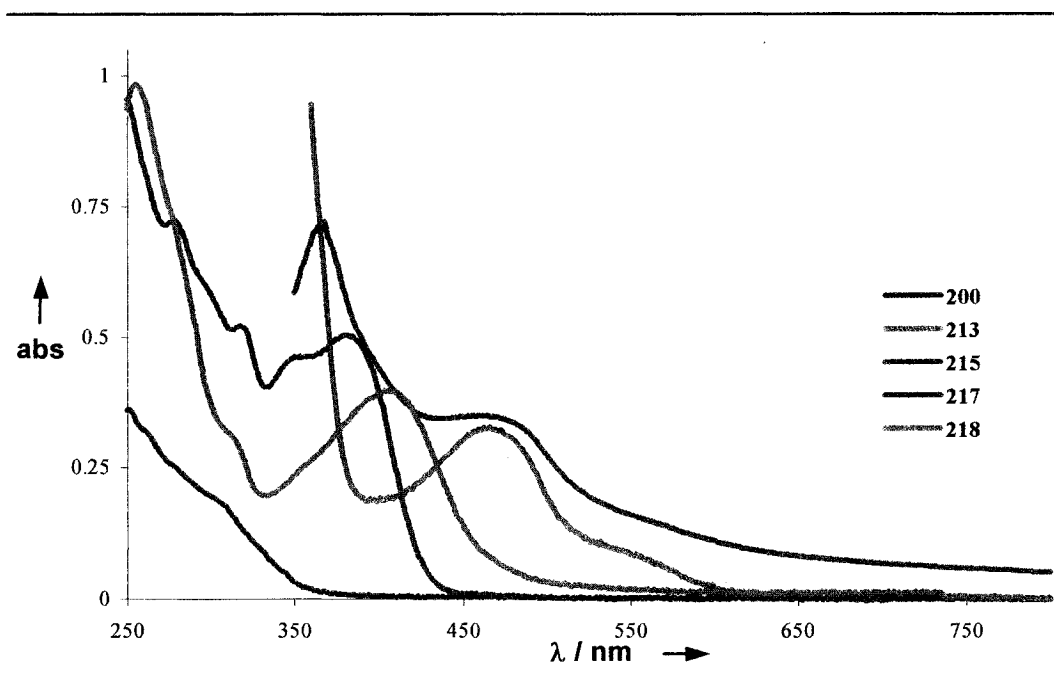


Figure 36: UV-VIS spectra of the phenanthrolineophanes in methylene chloride.

Phenanthrolineophanes **200** and **217** and dimerization precursor **216** were excited at 320, 451, and 451 nm respectively and their emission spectra were recorded (Figure 37). Phenanthrolineophane **217** is red shifted with respect to its precursor, **216**, by 21 nm. Emission quantum yields and lifetimes were not determined.

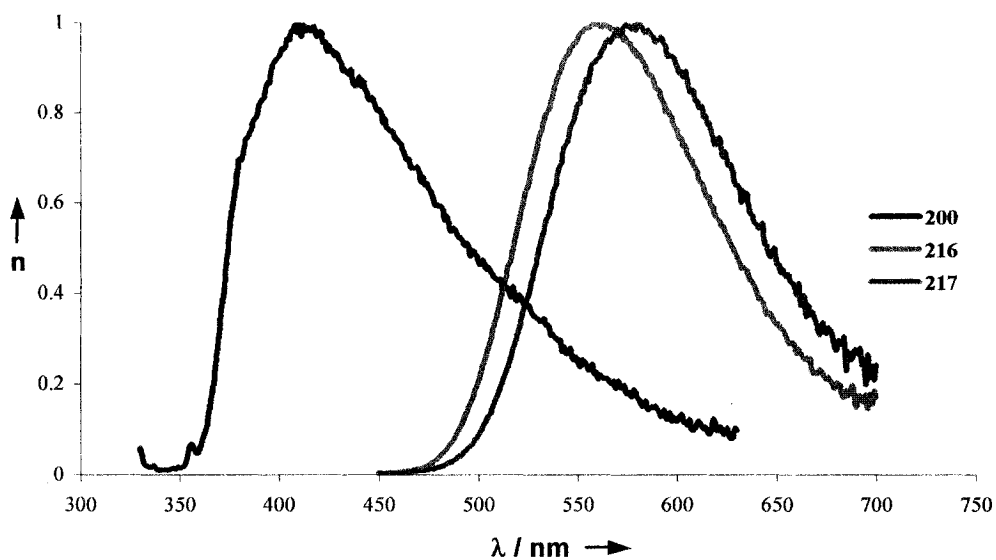
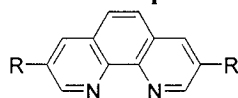


Figure 37: Normalized emission spectra of 200, 216, and 217 in methylene chloride.

The photochemical properties of various phenanthroline, synthetic intermediates, and copper complexes were compared to relevant literature examples (Table 8). Phenanthroline derivatives **200** and **217** had similar absorption and emission characteristics to related compounds **219** and **220** that were reported by Tor's group.^{84a}

Table 8: UV-VIS and fluorescent spectra maxima of the phenanthrolinephanes and selected reference spectra.



compound	$\lambda_{\max}(\text{abs}) / \text{nm}$	$\lambda_{\max}(\text{em}) / \text{nm}$
197 ¹²⁷	440	
199 ¹²⁸	458	
219 (R = C≡C-Ph) ^{84a}	346	376, 395
220 (R = C≡C-(<i>p</i> -PhNMe ₂)) ^{84a}	410	523
200	307 (sh)	416
213	473, 553 (sh)	
215	462	
217	383	584
218	407	563

Variable temperature ¹³C NMR was used to probe the helical nature of phenanthrolinephane **217** and its copper(I) complex, **218**. At low temperature both nitrogen inversion and helical isomerization were slow on the NMR timescale and the butyl groups of the dibutylamino substituents were diastereotopic. As the sample was heated, the butyl groups coalesced and became enantiotopic.

Phenanthrolinephane **217** was cooled to -90 °C (183 K) in CD₂Cl₂ and its ¹³C NMR spectrum was obtained. The methyl carbon atoms of the butyl groups were a single, broad signal indicating that helical interconversion was still fast compared to the NMR timescale. This set an upper limit on the coalescence temperature, and in turn, the isomerization barrier height of 3.4 kcal/mol.

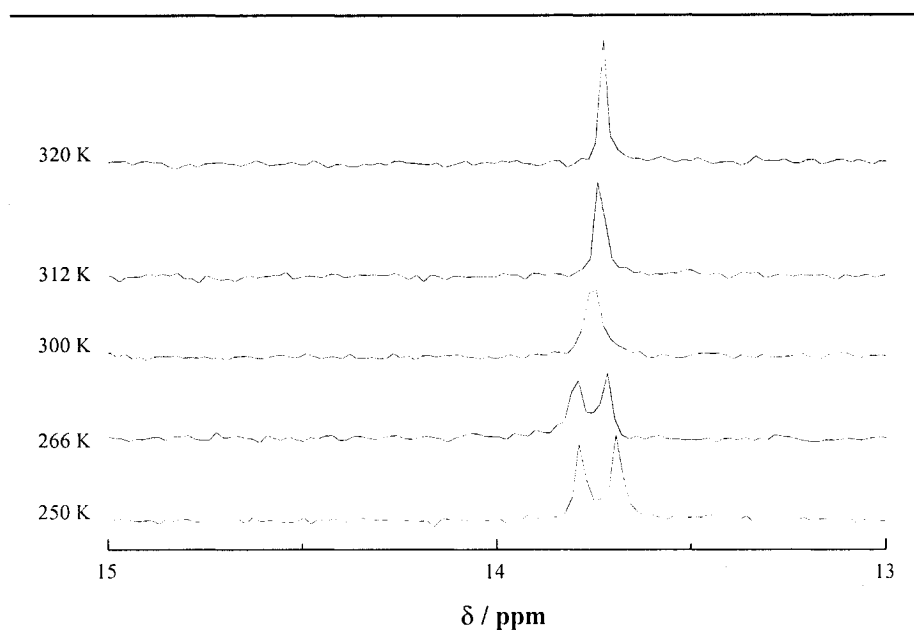


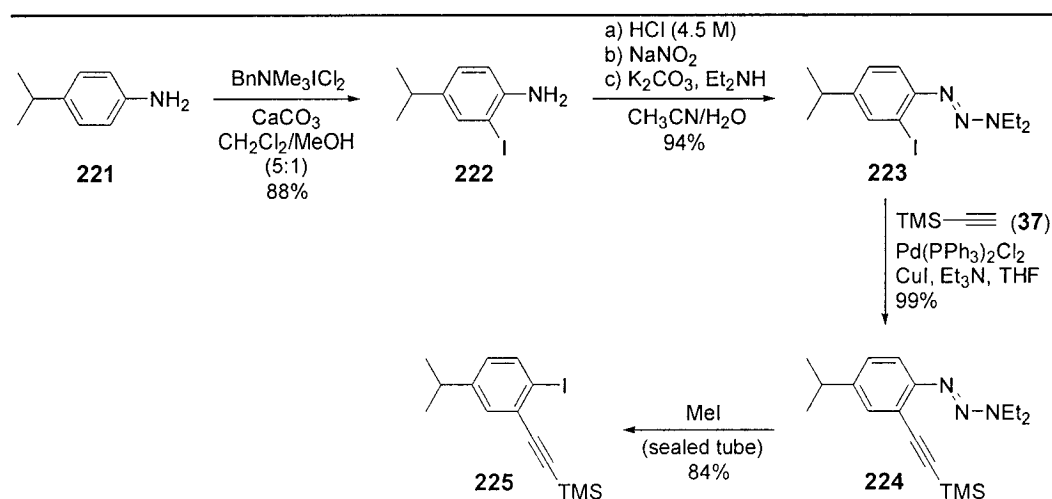
Figure 38: Stacked variable temperature ^{13}C NMR spectra of copper(phenanthroline) complex **218.**

The same NMR experiment was conducted on the copper(phenanthroline) complex **218**. At $-90\text{ }^{\circ}\text{C}$ (183 K) the methyl carbon atoms of the butyl groups were diastereotopic with a 32.6 ppm chemical shift difference between the two signals (Figure 39). When the sample was warmed, the methyl group coalesced at 300 K ($27\text{ }^{\circ}\text{C}$). This corresponds to an barrier height of 13.6 kcal/mol. Unfortunately, this could be due to either helical interconversion or nitrogen inversion. Typical nitrogen inversion values of substituted anilines lie in the range of 12 to 17 kcal/mol.¹²⁹ This experiment was useful as it illustrated that our hypothesis was correct in that metal coordination would raise the helical isomerization barrier height. However, to unambiguously assign which exchange process was responsible for the coalescence of the butyl groups, an isopropyl-substituted phenanthroline was synthesized (Section 3.9).

3.9 Preparation of Phenanthroline **227**

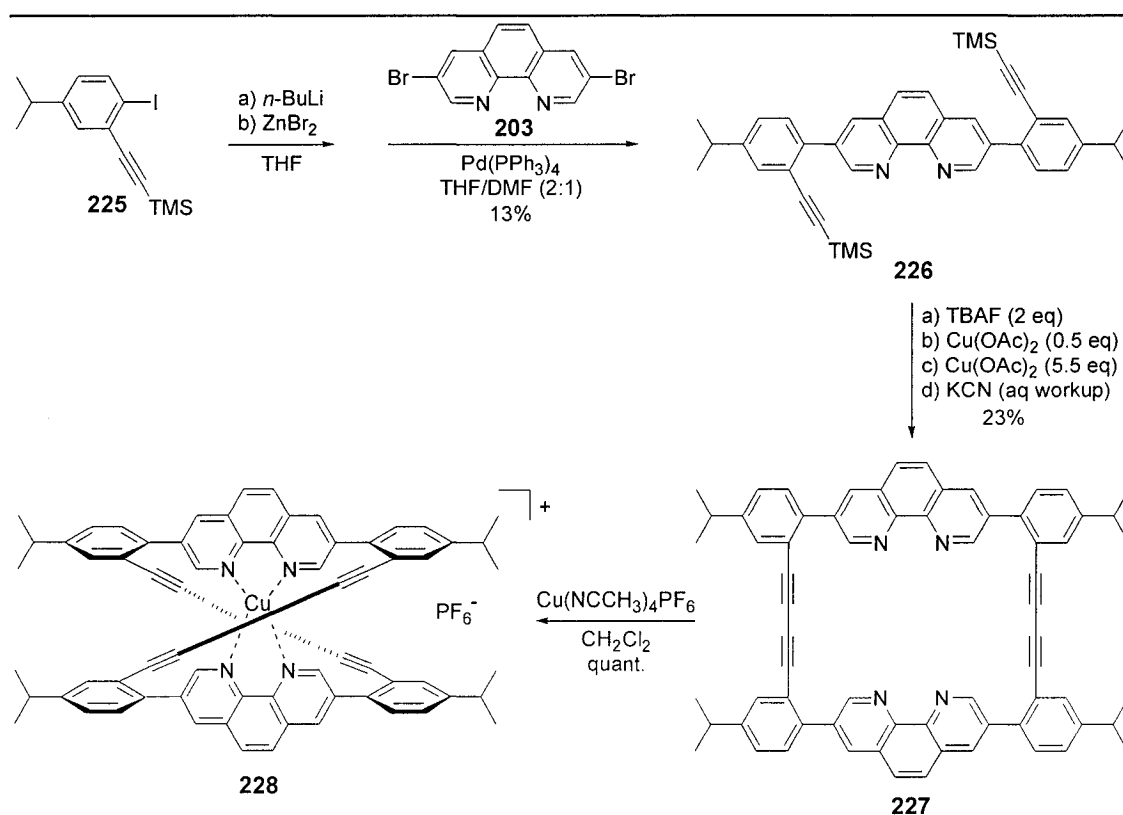
A new phenanthroline with isopropyl substituents, **227**, was designed so that variable temperature NMR studies would allow for the unambiguous determination of the helical isomerization barrier. Iodide **225** was required for the Negishi coupling reaction and could be prepared from 4-isopropylaniline (**221**).

4-Isopropylaniline (**221**) was iodinated with Kajigaeshi's reagent ($\text{BnNMe}_3\text{ICl}_2$)⁶⁸ and calcium carbonate to give iodide **222** in 88% yield (Scheme 48). Iodide **222** was converted to diethyltriazeno **223** in 94% yield using HCl (4.5 M, aq), sodium nitrite (NaNO_2), diethylamine, and K_2CO_3 .¹³⁰ A Sonogashira reaction of **223** with TMS-acetylene (**37**) using standard conditions afforded silylalkyne **224** in 99% yield. Finally, heating silylalkyne **224** in the presence of methyl iodide in a sealed tube gave iodide **225** in 84% yield.



Scheme 48: Preparation of iodide **225**.

Iodide **225** was subjected to our *in situ* Negishi coupling protocol with 3,8-dibromo-1,10-phenanthroline (**203**) to give dimerization precursor **226** in 13% yield (unoptimized) (Scheme 49). The copper-templated desilylation/dimerization method give phenanthroline **227** in 23% yield. Copper(phenanthroline) complex **228** was prepared quantitatively by treating a solution of **227** in CH_2Cl_2 with $\text{Cu}(\text{NCMe})_4\text{PF}_6$.



Scheme 49: Synthesis of phenanthroline **227**.

Variable temperature ¹³C NMR experiments were conducted on phenanthroline **227** and its copper(I) complex in order to determine the helical isomerization barrier height. Phenanthroline **227** was cooled to -90 °C (183 K) and the methyl carbon atoms of the isopropyl groups were a single, broad signal, indicating that they were enantiotopic. Copper(I)(phenanthroline) complex **228** was cooled to -20 °C (253 K). In this experiment the methyl groups of the isopropyl substituent were diastereotopic, indicating that helical isomerization was slow on the NMR timescale. The sample was warmed and the methyl signals coalesced at 57 °C (330 K) to give a helical isomerization barrier energy of 16.2 kcal/mol.

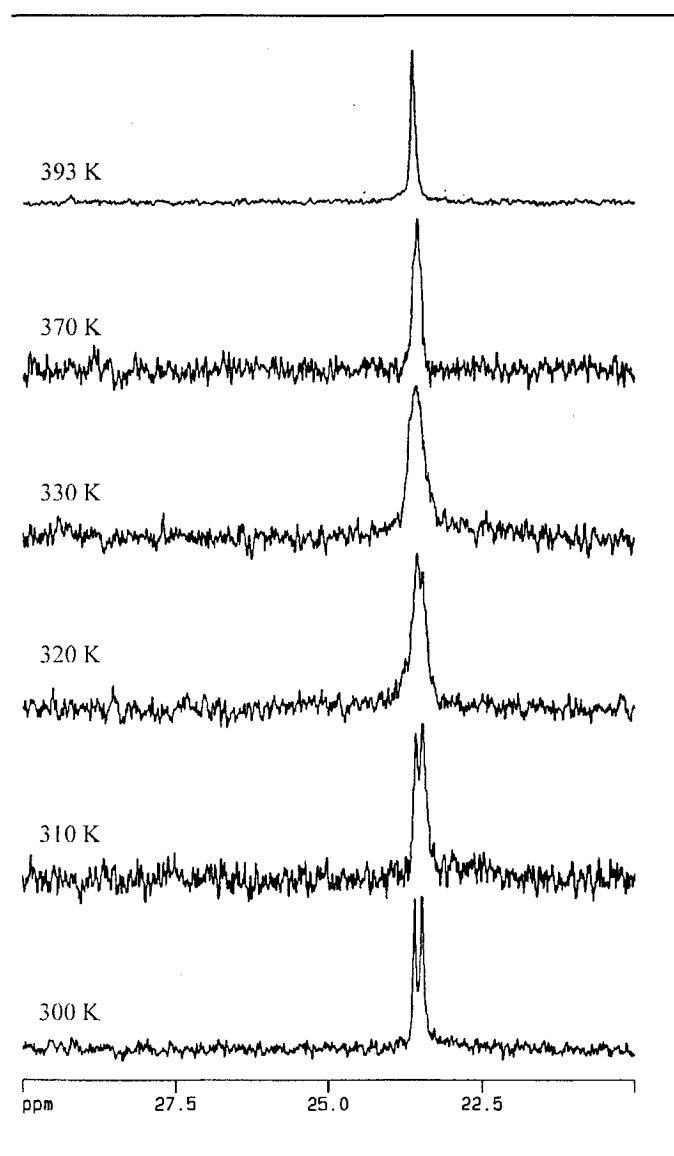


Figure 39: Stacked variable temperature ^{13}C NMR spectra of copper(phenanthroline) complex **228**.

This confirmed that metal coordination did indeed increase the helical inversion barrier as predicted. Copper coordination raised the helical inversion barrier height of phenanthroline **227** by 7.0 kcal/mol (Figure 40). Unfortunately, helical isomerization still occurred to a small extent at room temperature so enantiopure phenanthroline derivatives could not be obtained.

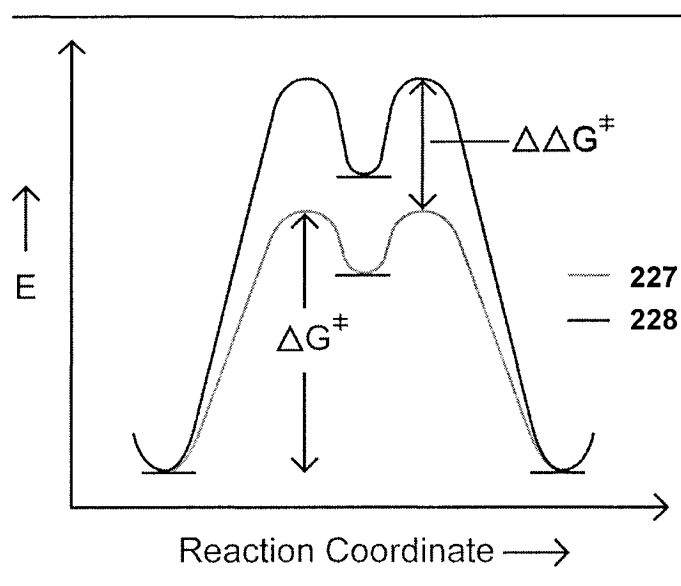


Figure 40: A potential energy diagram illustrating the difference in isomerization barrier heights ($\Delta\Delta G^\ddagger$) of phenanthroline 227 and its copper(I) complex, 228.

Helical isomerization of complex **228a** could occur *via* two pathways (Figure 41). The first pathway involves uncoordination of one phenanthroline moiety, isomerization by passing through a planar intermediate, **228c**, and recoordination to give the enantiomer **228b**. The other pathway involves elongation of the copper-nitrogen bonds to pass through planar intermediate **228d**, which can lead to the other helical enantiomer, **228b**. However, in order to preserve molecular orbital symmetry at the metal center, helical interconversion most likely takes place *via* the first pathway.

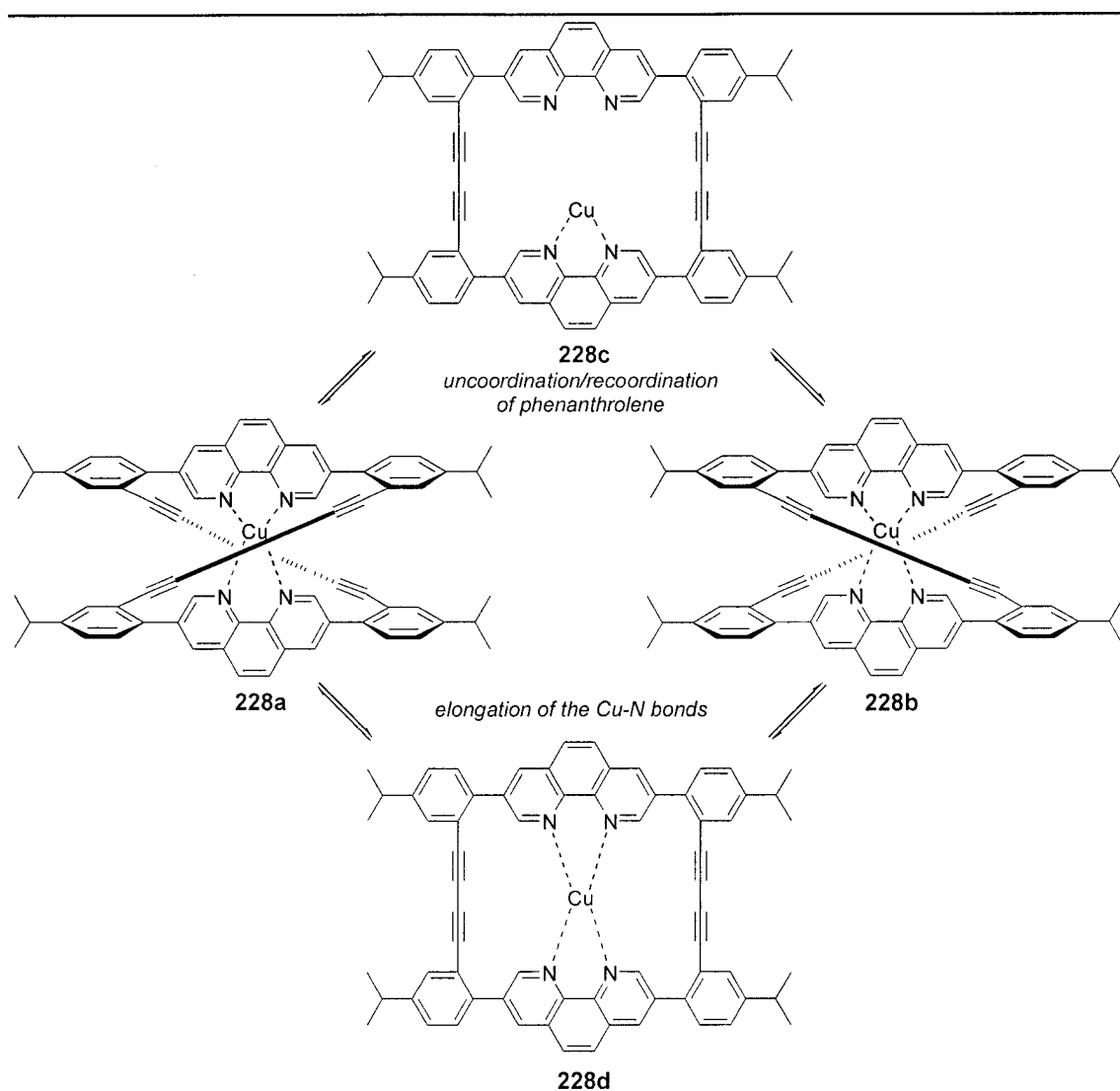


Figure 41: Proposed mechanisms for phenanthroline helical inversion.

3.10 Summary

Two classes of unsaturated π -compounds were synthesized as ligands for the preparation of chiral, non-racemic helical complexes: a tetramethoxybenzene-capped, C60 acetylenic cyclophane as a potential η^{12} -bis(arene) ligand, and phenanthroline derivatives as tetradentate coordination ligands. Cyclophane **170** was successfully prepared and a low resolution X-ray crystal structure confirmed that cyclophane **170** adopted a helical conformation with face-to-face π -stacked capping aromatic rings. Although cyclophane **170** should have been a very good η^{12} -bis(arene) ligand candidate, metal complexes of **170** could not be prepared. Phenanthroline derivatives **200**, **217**, and **227** were also prepared. A copper(I)

complex of the parent compound, **201**, could not be prepared due to **200**'s poor solubility in organic solvents, but copper(I) complexes of **217** and **227** were readily prepared. Copper coordination was found to raise the helical isomerization barrier height by over 7.0 kcal/mol; however, the isomerization still occurred at room temperature so enantiopure phenanthrolinephanes could not be obtained.

Chapter

2,9- AND 2,10-DISUBSTITUTED PENTACENE-BASED MOLECULES

- 4.1 Organic Semiconductors
 - 4.2 Disubstituted Pentacene Retrosynthetic Analysis
 - 4.3 Synthesis of 1,4,5,8-Anthraquinone (**249**)
 - 4.4 Synthesis of Silyl Ethers **247** and **268**
 - 4.5 Preparation of Ditriflates **246** and **271**
 - 4.6 2,9- and 2,10-Disubstituted Pentacenes
 - 4.7 Summary
-

4. 2,9- and 2,10-Disubstituted Pentacene-Based Molecules

The previous chapter summarized our work on helical, unsaturated cyclophanes and phenanthrolinephanes that resulted from *para*-substituted capping groups. Our work on C60 cyclophanes (Chapter 2) suggested that cyclophanes with *meta*-substituted capping rings and appropriate bridges would lead to planar cyclophanes. In order to test our hypothesis, a planar acetylenic cyclophane was designed with pentacene as the capping group (pentacenophane, **229**) (Figure 42). Planar, unsaturated carbon-rich compounds have been studied for a variety of applications, including molecular electronics, molecular wires, and semiconductors.

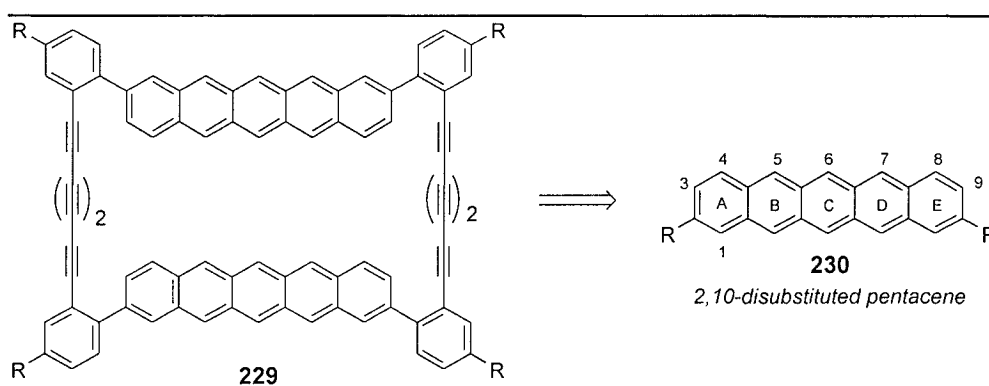


Figure 42: Pentacenophane **229** and a 2,10-disubstituted pentacene building block (**230**).

In order to synthesize pentacenophane **229**, a pseudo *meta*-substituted pentacene (2,10-disubstituted pentacene) building block was required. However, literature searches revealed that there were no reported syntheses of 2,10-disubstituted pentacenes or any pentacene compounds with substituents solely on the A and E rings. We learned more about pentacene and its use as an organic semiconductor as this research progressed and consequently our research focus shifted from preparing pentacenophane **229** to the synthesis of pentacene derivatives that had functionality on the terminal A and E rings. This chapter provides a brief introduction into organic semiconductors and describes the design and synthesis of 2,9- and 2,10-disubstituted pentacene derivatives.

4.1 Organic Semiconductors

Semiconductors are materials that have electronic properties between insulators and conductors, resulting from the nature of their band gap (Figure 43).¹³¹ Intrinsic

semiconductors have a small band gap and electrons can be thermally promoted to the conduction gap, leaving a hole in the valence band. When an external field is applied, the electrons move into the conduction band and the holes move in the valence band. Materials with larger band gaps can be made semiconducting by the addition of dopants. These materials are known as doped semiconductors.

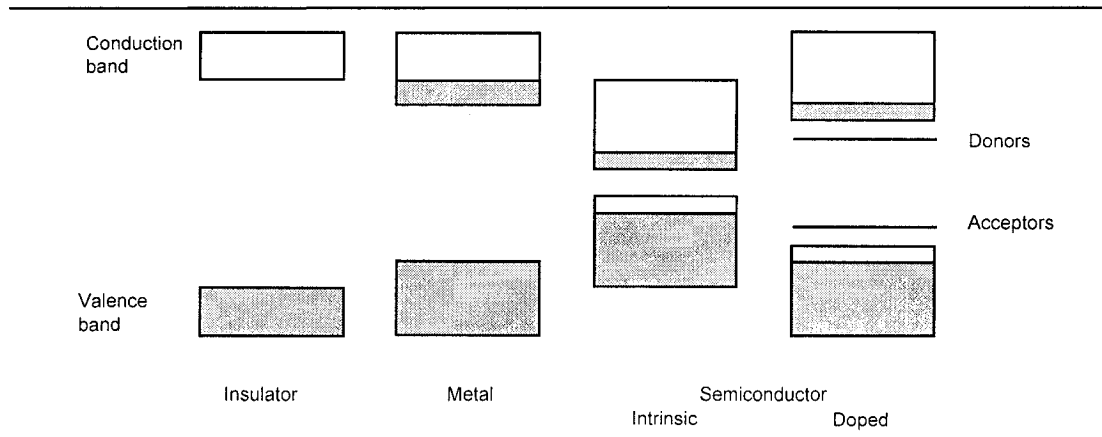


Figure 43: Energy band diagram illustrating insulators, metals, and semiconductors.

Semiconducting materials are predominately used in field effect transistors (FET), which are the integral part of computer chips. There are five main components in a FET device: The source, drain, semiconductor, dielectric, and gate (Figure 44).¹³² In the absence of an applied field to the gate, little to no current flows between the source and the drain. This is the "off" state of the transistor. When a voltage is applied to the gate, electrons are promoted from the valence band of the semiconductor to the conduction band, providing charge carriers. As a result, current flows from the source to the drain. This is the "on" state of the transistor. The number of charge carriers, and hence the performance of the semiconductor, is highly dependent on the applied gate voltage. On/off ratios of greater than $10^6:1$ and field effect mobilities of greater than $0.1 \text{ cm}^2\text{V}^{-1}\text{s}^{-1}$ are required to drive liquid crystal display circuits.

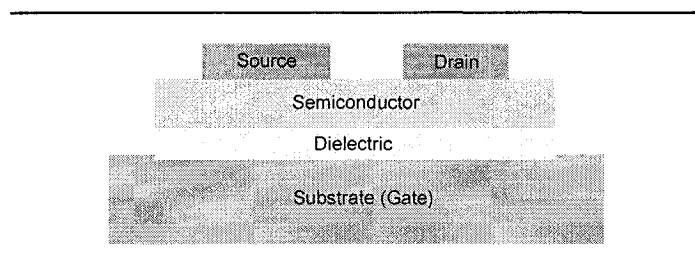


Figure 44: Diagram of a typical FET device.

The efficiency of a semiconducting material is determined by how easily the electron and hole can move through the material, *i.e.* the electron and hole mobilities (μ_e or μ_h). Highly conjugated organic compounds have overlapping atomic orbitals that form valence and conducting bands similar to metals. Organic semiconductors do not have the same electron or hole mobilities as single-crystalline silicon (Table 9),¹³³ but they are advantageous during fabrication as solution processing techniques such as lithography can be used. The lower fabrication costs make organic semiconductors desirable for single use devices such as smartcards, luggage tags, and anti-theft devices.¹³⁴

Table 9: Electron (μ_e) and hole (μ_h) mobilities of organic semiconductors.¹³³

semiconductor	$\mu_e / \text{cm}^2\text{V}^{-1}\text{s}^{-1}$	$\mu_h / \text{cm}^2\text{V}^{-1}\text{s}^{-1}$
single-crystalline silicon	1500	480
amorphous silicon	0.1 - 1	< 0.1
tetracene (231)	~2	~2
pentacene (232)	1.7	2.7
α -sexithiophene (233)	0.7	1.1
perfluorinated copper phthalocyanine (234)	1.7	-
C ₆₀ (41)	2.1	1.8

Organic semiconductors can be subdivided into two groups: Polymer-based organic semiconductors and molecular semiconductors. Linear acenes (tetracene (**231**) and pentacene (**232**)), oligiothiophenes (α -sexithiophene (**233**)), copper phthalocyanines (**234**), and naphthalenebisimides (**235**) are the current leading classes of molecular organic semiconductors (Figure 45).¹³⁵ These compounds are all electron-rich and highly

conjugated. Of all these organic semiconductors, pentacene (**232**) has the best electron and hole mobilities.

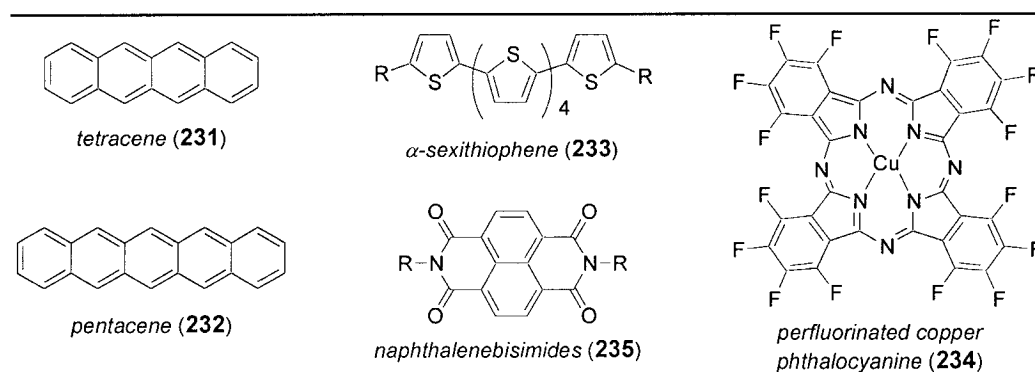
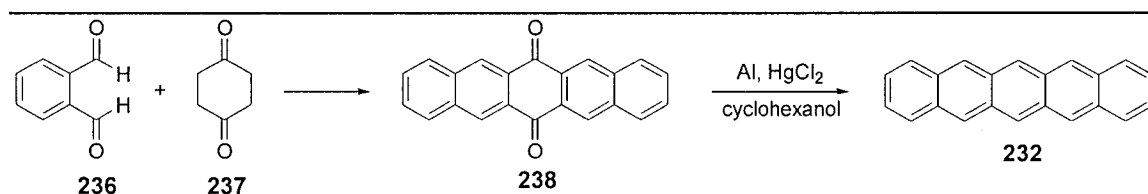


Figure 45: Molecular organic semiconductors.

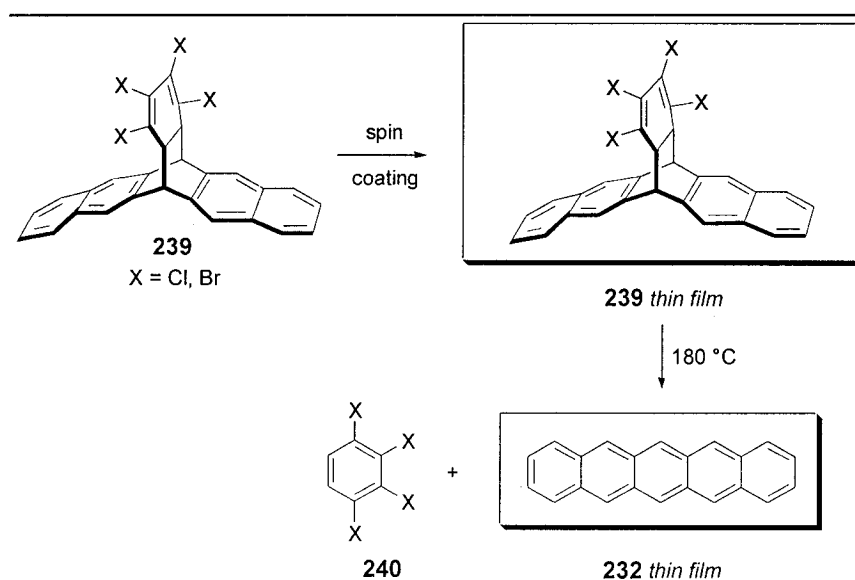
A rapid two-step synthesis of pentacene (**232**) was reported in 1972 (Scheme 50)¹³⁶ and pentacene was found to be both light and air sensitive. However, a greater liability is the virtual insolubility of pentacene in common organic solvents, preventing solution-based processing.¹³⁷ Desired spin-coating, dip-coating, and printable/lithographic processing all require the semiconducting compound to be in solution. As a result, pentacene thin films are prepared by evaporation/deposition.¹³⁷ The resulting pentacene crystals have molecules packed in a "herringbone" fashion and not the face-to-face π -stacking arrangement found in graphite.¹³⁸ As a result, there is poor intermolecular orbital overlap and reduced electron and hole mobilities.



Scheme 50: Synthesis of pentacene (**232**).

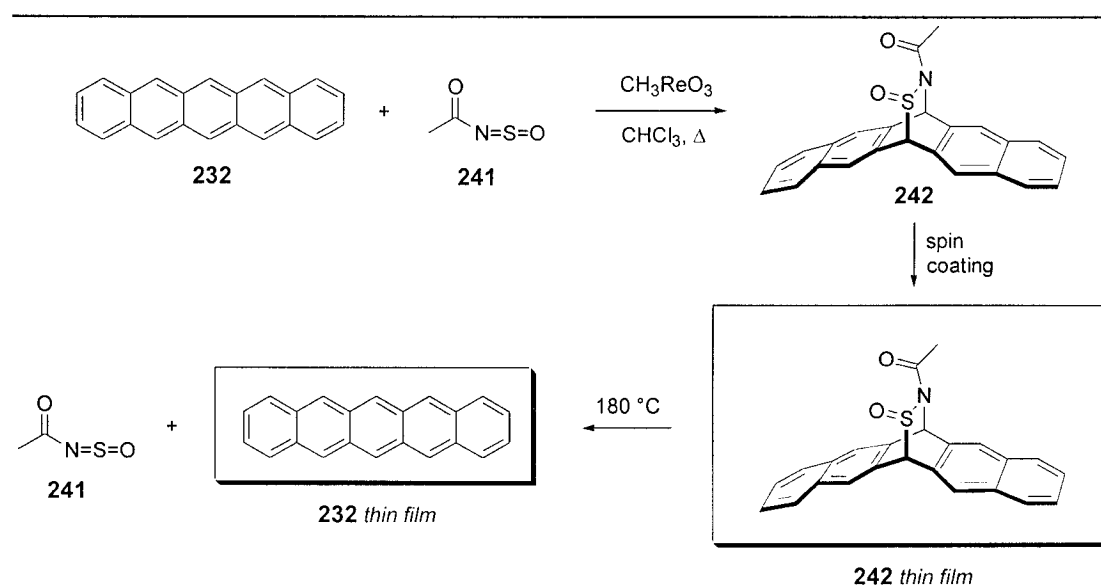
A variety of pentacene derivatives have been prepared to aid its processability, increase its solubility, or alter its solid-state packing. One of the more promising techniques involves the preparation of a pentacene precursor, **239**, that is capable of undergoing a retro Diels-Alder reaction when heated to generate pentacene (Scheme 51).¹³⁹ Precursor **239** was readily soluble in methylene chloride and thin films of **239** were prepared by spin-coating.

Subsequent heating of these films affected the retro Diels-Alder reaction, leaving a pentacene thin film. One drawback of this procedure was the lengthy synthesis of precursor **239**.



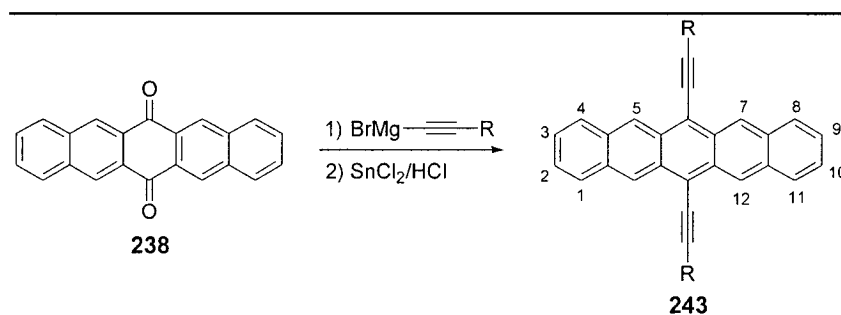
Scheme 51: Retro Diels-Alder approach to pentacene thin films.¹³⁹

An improved method in which the thin film precursor, **242**, could be prepared directly from pentacene was reported by Afzali and coworkers at the IBM research labs (Scheme 52).¹⁴⁰ A rhenium-catalyzed Diels-Alder reaction of pentacene (**232**) and *N*-sulfinylacetamide (**241**) gave precursor **242**. A spin-coated thin film of **242** was then prepared and heated to give a pentacene thin film.



Scheme 52: Synthesis of pentacene thin films by a Diels-Alder/retro Diels-Alder approach.¹⁴⁰

A different approach was taken by Anthony's group. Functionalized pentacenes, **243**, were synthesized that had solubilizing substituents (Scheme 53).¹⁴¹ Ethynyl substituents were chosen to limit electronic disruption of the pentacene core. Furthermore, the rapid preparation of pentacene derivatives allowed for a number of analogues to be prepared and screened (R = Me, *t*-Bu, TMS, TES, TBS, TIPS, and TPS).



Scheme 53: Synthesis of 6,13-disubstituted pentacene derivatives.

The 6,13-disubstituted pentacene derivatives were readily soluble in a variety of organic solvents and they had much better intermolecular π -stacking in the solid-state than pentacene (**232**) itself (Figure 46).¹⁴² These compounds have been studied for both their semiconducting performance and their photoresponse.¹⁴³

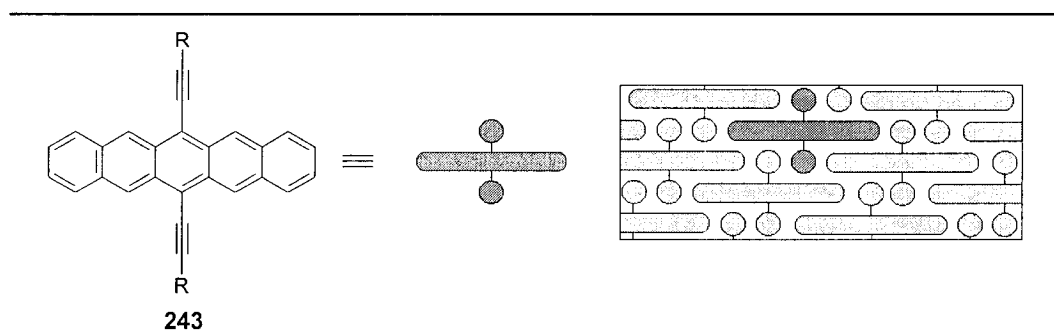


Figure 46: Packing diagram of 6,13-disubstituted pentacene (**243**).

Functionalized pentacene compounds with substituents on the terminal A and E rings are predicted to have better intermolecular π -stacking than compounds with substituents on the central C ring (Figure 47).¹⁴¹ However, no synthetic routes to pentacenes with substituents on the A and E rings are currently known.

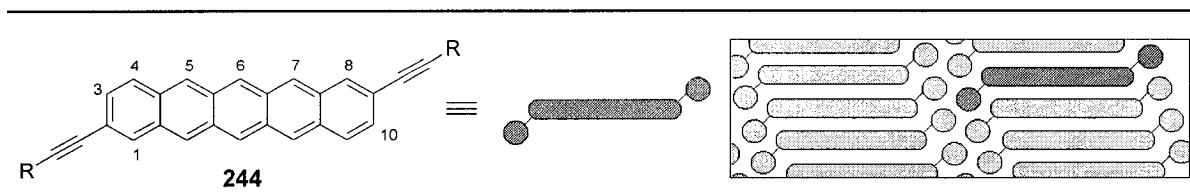


Figure 47: Proposed packing diagram of 2,9-disubstituted pentacene derivatives.¹⁴¹

Pentacene has greater electron density and reactivity at the central C ring¹⁴⁴ making selective functionalization of pentacene on the A and E rings difficult. Thus, a different synthetic approach was necessary with the introduction of functional groups on the A and E rings early in the synthesis. The remainder of this chapter describes the design and synthesis of 2,9- and 2,10-disubstituted pentacene compounds.

4.2 Disubstituted Pentacene Retrosynthetic Plan

Our synthetic plan to 2,9- and 2,10-disubstituted pentacene derivatives was to build a pentacyclic scaffold with appropriate functional groups in place to introduce a variety of substituents. These substituents could be used to tune the electronic properties or affect the solid-state packing of the pentacene derivatives. Subsequent oxidation or reduction of the pentacyclic compound would lead to pentacene. A proposed retrosynthetic route to 2,9-disubstituted pentacene **244** is shown in Figure 48. Substituted pentacene **244** would be formed from the reduction of a functionalized diquinone precursor, **245**. A variety of substituents could be introduced using palladium coupling reactions, such as a Sonogashira reaction, with ditriflate **246**. The ditriflate could be prepared by desilylation and triflation of silyl ether **247**. Silyl ether **247** would result from a double Diels-Alder reaction with Danishefsky's diene **248** and known anthraquinone **249**.

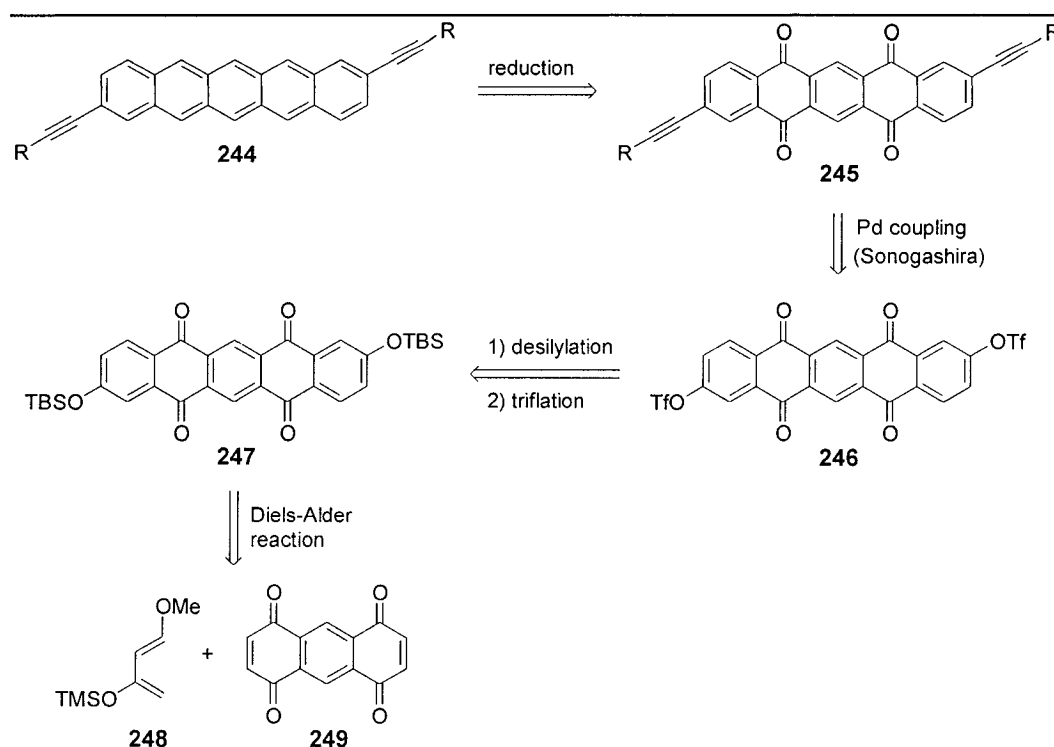
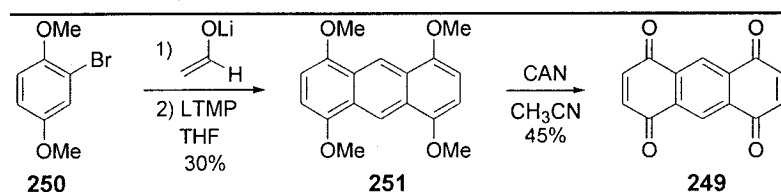


Figure 48: Retrosynthetic plan for the preparation of 2,9-disubstituted pentacenes (**244**).

One foreseeable problem with this synthetic plan was that the second Diels-Alder reaction would not be regioselective and two isomers would likely be formed. Thus, an efficient way of separating the two isomers from the double Diels-Alder reaction would be required. One isomer would lead to 2,9-disubstituted pentacene **244** (as shown in Figure 48), while the other isomer would lead to the 2,10-disubstituted compound *via* the same synthetic strategy. Although a regioselective synthesis would eventually be desired, the preparation of both pentacene isomers would be beneficial for initial semiconducting screening.

4.3 Synthesis of 1,4,5,8-Anthraquinone (**249**)

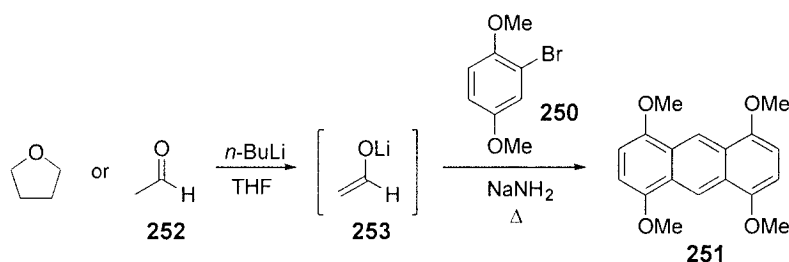
Two lengthy synthetic routes (> 5 steps) to the desired 1,4,5,8-anthraquinone (**249**) starting material have been reported, but large amounts of high purity material could not be obtained.¹⁴⁵ An alternative two-step preparation of anthraquinone **249** was reported by Cory's group (Scheme 54);¹⁴⁶ however, the yields for each reaction were below 50%. 1,4,5,8-Anthraquinone (**249**) was a key intermediate in our route to pentacene, thus an optimized preparation of **249** was desired.



Scheme 54: Cory's preparation of 1,4,5,8-anthraquinone (**249**).

The first reaction that was attempted was the original procedure reported by Fitzgerald (Table 10, entry 1). A solution of lithium 2,2,6,6-tetramethylpiperidine (LTMP, **254**) in THF was prepared by the addition of methyl lithium to 2,2,6,6-tetramethylpiperidine (TMP). The LTMP solution was heated to reflux, bromide **250** was added, and heating was continued for one hour. The reaction was cooled to room temperature and poured into HCl (10% aq). A small amount (16% yield) of 1,4,5,8-tetramethoxyanthracene (**251**) was obtained. A violent evolution of gases occurred when bromide **250** was added to the boiling LTMP solution, preventing the reaction from being conducted on a larger scale. When bromide **250** was added to the LTMP solution at room temperature (23 °C) and then heated, little to no product was obtained.

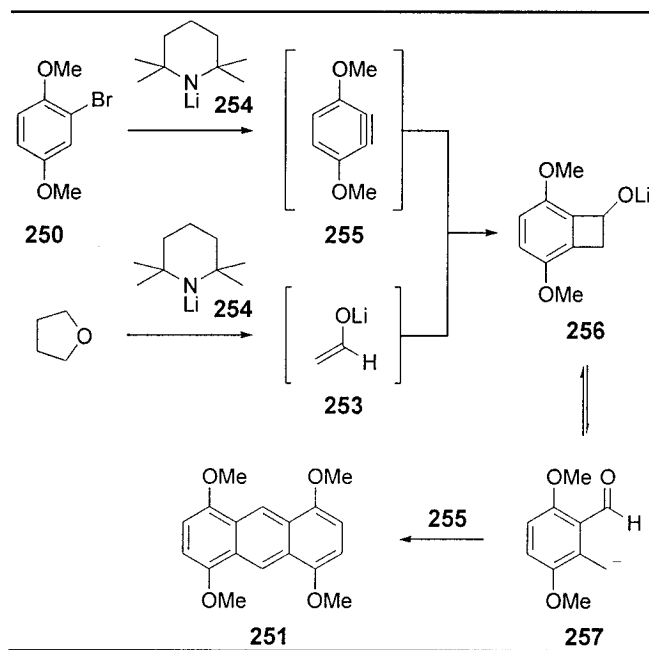
Table 10: Reaction conditions for the preparation of 1,4,5,8-tetramethoxyanthracene (**251**).



entry	reaction conditions	yield (%)
1 ^a	TMP was treated with MeLi to form LTMP and 250 was added at reflux	16
2	enolate 253 was preformed from THF, transferred to a suspension of NaNH ₂ , and treated with 250 at reflux	10-32
3	enolate 253 was preformed from 252 , transferred to a suspension of NaNH ₂ , and 250 was added at reflux	28
4	as entry 2, but toluene was used as the solvent instead of an excess of THF	< 5
5	NaNH ₂ was suspended in toluene, treated with THF (1 eq), and 250 (2.2 eq) was added at reflux	< 5

^aLTMP was the base

The proposed mechanism for the transformation of bromide **250** to 1,4,5,8-tetramethoxyanthracene (**251**) is shown in Scheme 55.¹⁴⁷ Benzyne **255** is formed from bromide **250** and is quenched with the lithium enolate of acetaldehyde (**253**) to give benzocyclobutane **256**. Benzocyclobutane **256** could either be isolated (after protonation) or reacted *in situ* with a second equivalent of benzyne **255** to give 1,4,5,8-tetramethoxyanthracene (**251**) after dehydration and aromatization.



Scheme 55: Proposed mechanism for the preparation of **251** *via* a benzyne intermediate.¹⁴⁷

Cory's group obtained 1,4,5,8-tetramethoxyanthracene (**251**) in better yield (30%) when *n*-butyllithium was used to form enolate **253** from THF and sodium amide (NaNH_2) was used to generate benzyne **255** from bromide **250**.¹⁴⁸ When these reaction conditions were used with sodium amide pellets, no reaction occurred. A similar result was obtained with freshly powdered NaNH_2 . When a suspension of NaNH_2 in toluene (commercially available from Aldrich) was used, varying amounts (10-32% yield) of 1,4,5,8-tetramethoxyanthracene (**251**) were obtained (Table 10, entry 2). Similar yields of **251** were obtained when acetaldehyde (**252**) was used as the enolate precursor instead of THF (entry 3).

In each of the procedures described above, THF was used as both a precursor for the lithium enolate of acetaldehyde (**253**) and as the reaction solvent. Lithium 2,2,6,6-tetramethylpiperidine (**254**) was shown to be a strong enough base to ring-open THF. If sodium amide has a similar reactivity toward THF, then an excess of enolate **253** would be

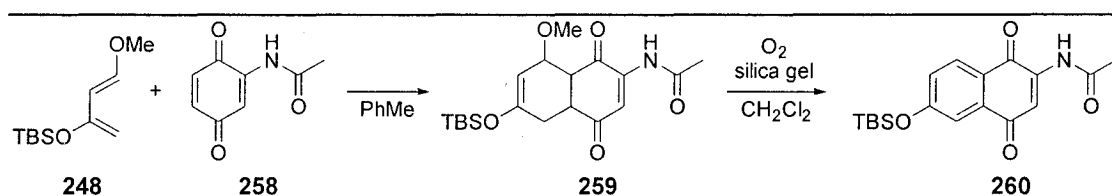
formed and would react with benzyne **255** to give cyclobutane **256**. This would result in a shortage of benzyne **255** for the reaction with anion **257** and lead to lower yields of **251**.

The reaction solvent was changed from THF to toluene and stoichiometric amounts of THF and *n*-butyllithium were used to generate enolate **253** (Table 10, entry 4). Unfortunately, only a small amount of **251** (< 5%) was obtained. The last optimization attempt involved using sodium amide to generate enolate **253** from THF and benzyne **255** from bromide **250**. In this reaction sodium amide was suspended in toluene and THF (1 eq) was added to the reaction (entry 5). The reaction was heated to form enolate **253** and bromide **250** was added to the boiling reaction. Once again, only a small amount of **251** (< 5%) was isolated. Despite numerous unsuccessful attempts at optimizing the synthesis of 1,4,5,8-tetramethoxyanthracene (**251**), we continued the synthesis using the material we could obtain using Cory's reaction conditions.

Oxidation of **251** to 1,4,5,8-anthraquinone (**249**) using ceric ammonium nitrate (CAN) proceeded consistently in 40-60% yields, similar to the reported yield for the reaction. Optimization of this reaction is currently being explored by another Fallis group member.

4.4 Synthesis of Silyl Ethers **247** and **268**

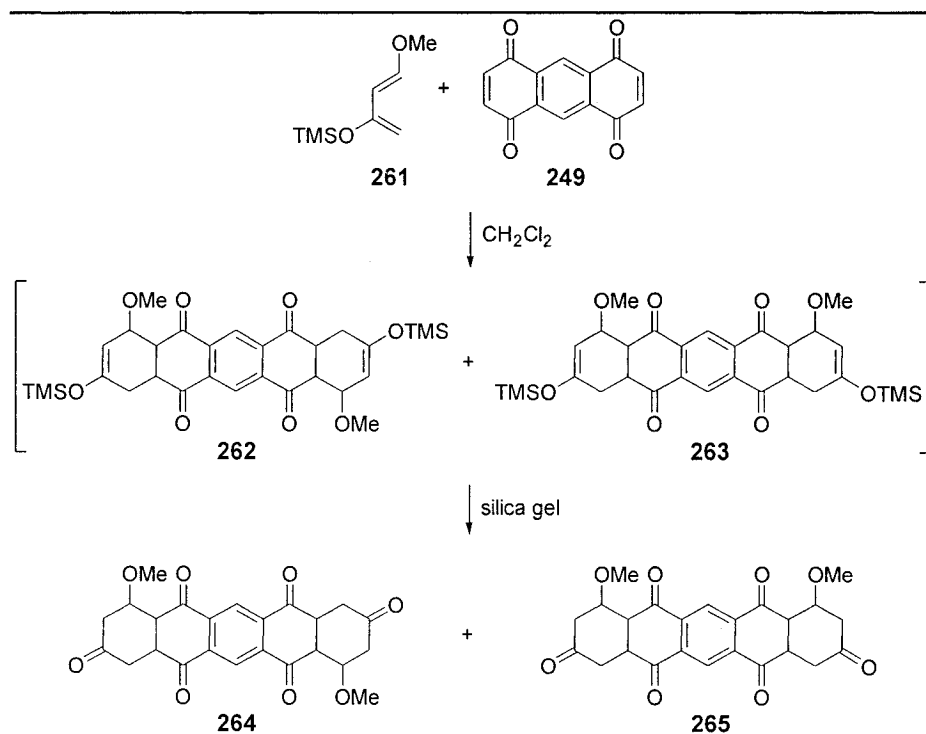
With anthraquinone **249** in hand we began studying the double Diels-Alder reaction and the inevitable separation of the resulting regioisomers. Danishefsky-type dienes readily undergo [4+2] cycloadditions with quinones and the reaction products are known to oxidize on silica gel in the presence of oxygen to the corresponding aromatic product (Scheme 56).¹⁴⁹



Scheme 56: [4+2] Cycloaddition/aromatization strategy to naphthaquinones.

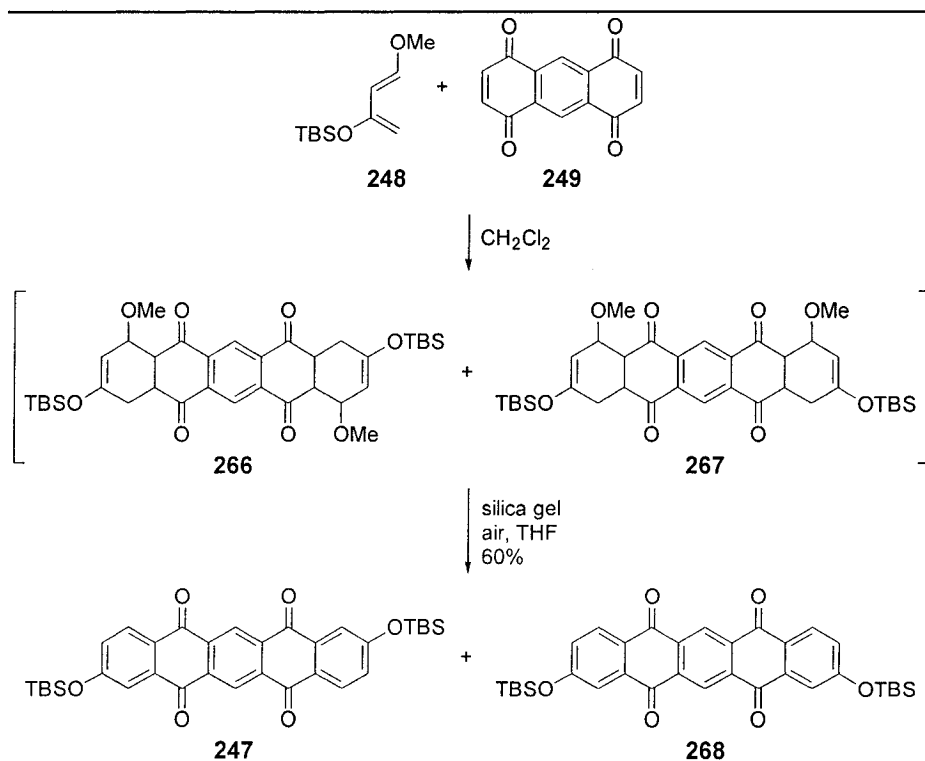
The first reaction that was conducted was a reaction of anthraquinone **249** with Danishefsky's diene **261** (Scheme 57). After stirring the reaction overnight at room temperature all of anthraquinone **249** was consumed, but the desired silyl ethers were not formed when the reaction was treated with silica gel. A proton NMR spectrum of the

reaction product suggested that desilylation had occurred to give a mixture of **264** and **265** instead of elimination of methoxide and aromatization as desired.



Scheme 57: Double Diels-Alder reaction of anthraquinone **249** and diene **261**.

The double Diels-Alder reaction was repeated with a bulkier *t*-butyldimethylsilyl Danishefsky's diene, **248**, which was not as prone to hydrolysis as the trimethylsilyl ether (Scheme 58). Diene **248** and anthraquinone **249** were combined in methylene chloride and stirred overnight at room temperature. Silica gel was added to the reaction and stirred open to air for 12 hours and two, less-polar spots were present on the TLC plate. The less polar compounds were isolated and determined to be silyl ethers **247** and **268**, which were formed as a 1:1 mixture in varying 20-42% yields. The reaction yield was increased to 60% by changing the solvent from methylene chloride to THF prior to adding silica gel to the reaction. A simple filtration of the crude reaction mixture through a silica gel plug with methylene chloride gave silyl ethers **247** and **268**. The overall transformation of diquinone **249** to the silyl ethers involved two cycloaddition reactions, elimination of two methoxy substituents, and aromatization of the two peripheral rings all in one pot.



Scheme 58: Double Diels-Alder reaction of diene **248** and anthraquinone **249**.

Separation of silyl ethers **247** and **268** proved to be difficult. Flash chromatography gave only one fraction of pure **247**. Repeated chromatography did not afford a pure sample of **268**, which was the second compound to elude. Preparative HPLC successfully separated the two isomers (Figure 49); however, the poor solubility of the silyl ethers in the mobile phase allowed only 25 mg of the mixture to be separated in a 45 minute run.

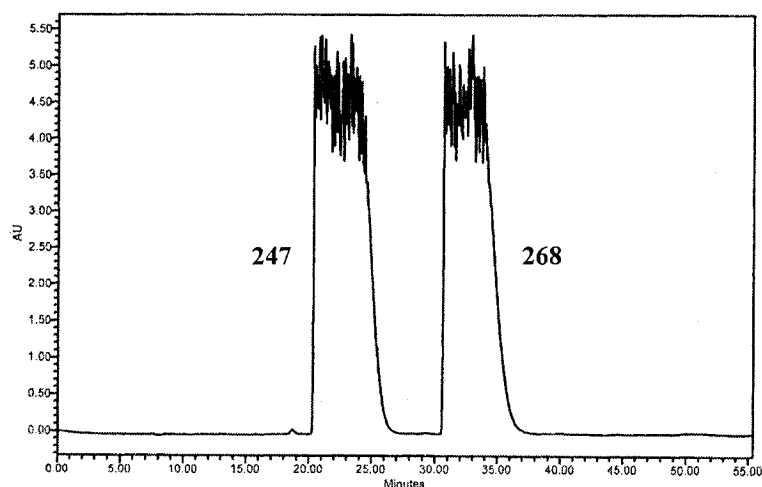


Figure 49: Preparative HPLC chromatogram illustrating the separation of silyl ethers 247 and 268.

To separate the two isomers, a supersaturated solution of silyl ethers **247** and **268** was filtered and injected into the preparative HPLC. Over the course of ten injections, the ratio of **247** and **268** changed from 1:1 to 1:1.2, suggesting that silyl ether **247** was less soluble in the mobile phase than the other isomer. Encouraged by this finding, a fractional crystallization separation of the silyl ethers was attempted. The mixture of silyl ethers was heated in chloroform and cooled to 0 °C for 18 h. The crystals that were recovered were predominately silyl ether **247**. After three recrystallizations, analytically pure silyl ether **247** was obtained. Silyl ether **268** was enriched in the mother liquor. Although the purity of **268** was not as high (> 90%), it was sufficiently pure to be used in future reactions as the minor impurity could be removed later in the synthesis.

The different symmetry of the two isomers allowed them to be identified by their ^1H and ^{13}C NMR spectra. Silyl ether **247** had C_{2h} symmetry, was the less polar isomer (higher spot on TLC), and less soluble in chloroform than silyl ether **268**. In contrast, silyl ether **268** had lower C_{2v} symmetry.

A single crystal X-ray structure of silyl ether **247** was obtained by the slow evaporation of a chloroform solution and proved that the structural assignment of the two silyl ethers was correct.¹⁴⁷ The pentacyclic core of the molecule is planar and forms sheets of edge-to-face π -stacked dimers (Figure 50).

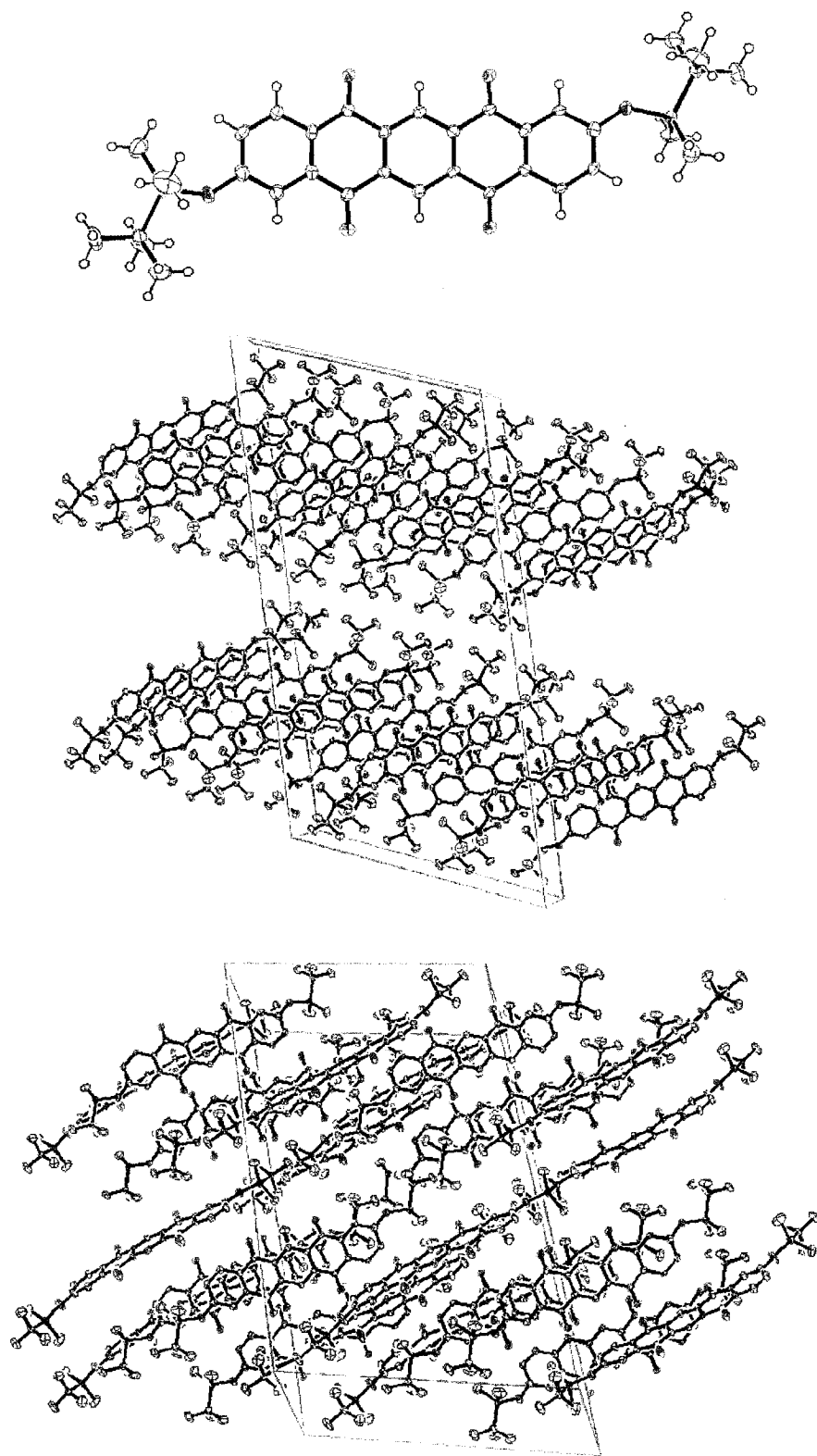
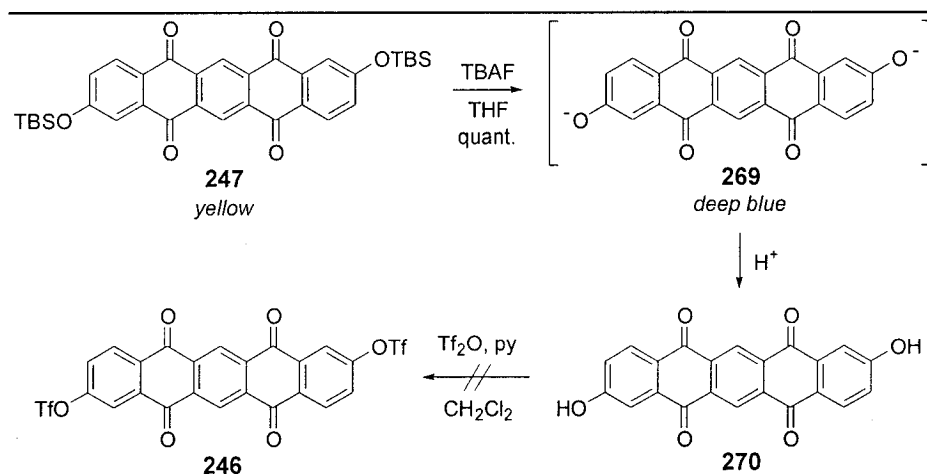


Figure 50: Single crystal X-ray structure of silyl ether 247.

4.5 Preparation of Ditriflates **246** and **271**

With the anticipated troublesome steps in our 2,9- and 2,10-disubstituted pentacene synthesis behind us, we turned our focus to the preparation of ditriflates **246** and **271**. These key intermediates would allow a multitude of substituted pentacene derivatives to be prepared in order to study the effect of various functional groups on the electronics and solid-state packing of these compounds.

Treatment of a solution of silyl ether **247** in THF with TBAF at room temperature resulted in a deep blue solution that gave diol **270** as a pale yellow solid after the addition of water (Scheme 59). Diol **270** was recovered by filtration and was not soluble in organic solvents. In fact, diol **270** was only soluble in aqueous NaOH (10%), giving a deep blue solution. Diol **270** could not be characterized due to its poor solubility.

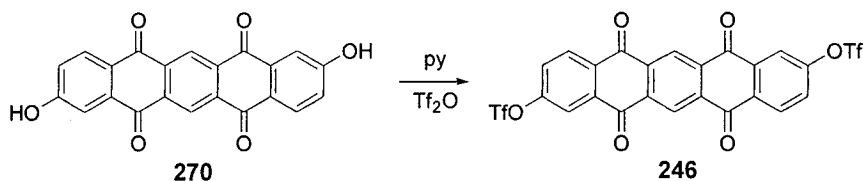


Scheme 59: Preparation of diol **270**.

Numerous attempts to convert diol **270** to ditriflate **246** were unsuccessful (Table 11). When diol **270** was suspended in methylene chloride and treated with triflic anhydride (Tf_2O), both with and without a catalytic amount of DMAP, only the diol starting material was recovered (Table 11, entries 1 and 2). The reaction was attempted using pyridine as both the base and the reaction solvent with DMAP and triflic anhydride; however, starting material was recovered for reactions conducted at both room and elevated temperatures (entries 3 and 4). The same result was obtained when 2,6-lutidine was used in place of pyridine (entry 5). Numerous organic bases were surveyed in an attempt to solublize diol

270 and generate the necessary anion, but in each case diol **270** did not react. This indicated that diol **270** was not in solution in any of these reactions.

Table 11: Attempted conversion of diol 270 to ditriflate 246.



entry	reaction conditions	result/yield (%)
1	CH ₂ Cl ₂ , 12 h, rt	recovered 270
2	CH ₂ Cl ₂ , DMAP (cat.), 12 h, rt	recovered 270
3 ^a	DMAP (cat.), 12 h, rt	recovered 270
4 ^a	DMAP (cat.), 12 h, Δ	recovered 270
5 ^{a,b}	DMAP (cat.), 12 h, rt	recovered 270
6 ^c	TBAF, CH ₂ Cl ₂ , 12 h, rt	mixture of 246 and 270
7 ^c	HF·py, CH ₂ Cl ₂	270
8 ^{c,d}	TBAF, THF, 12 h, rt	246 (78)

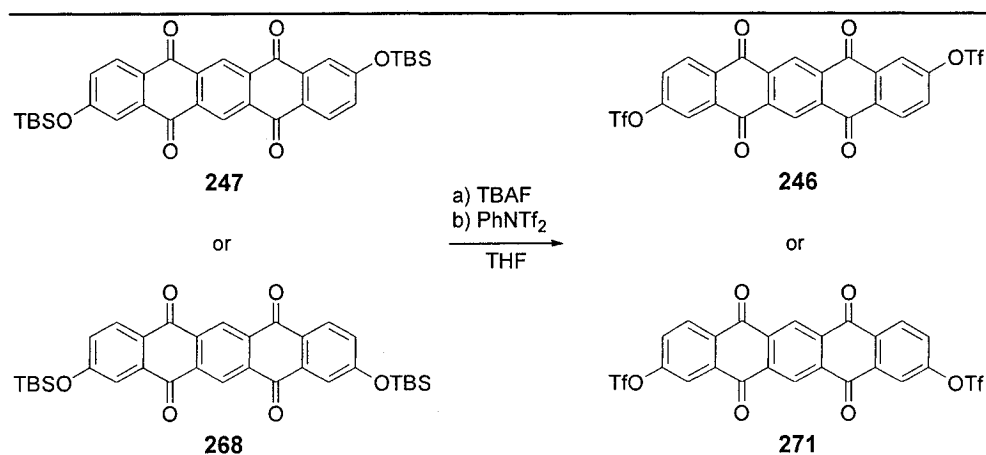
^a the base was used as the reaction solvent

^b lutidine was used instead of pyridine

^c silyl ether **247** was the substrate, not diol **270**

^d PhNTf₂ was used instead of Tf₂O

A new strategy for forming ditriflate **246** was devised. The conversion of silyl ether **247** to diol **270** must pass through a dianion **269** intermediate. This same intermediate was required for the formation of ditriflate **246**. Thus, silyl ether **247** was treated with two equivalents of TBAF to form the deep blue dianion, **269**, which was then treated with triflic anhydride to give a mixture of diol **270**, mono triflate, and ditriflate **246** (Table 11, entry 6). Encouraged by these results, the fluoride source was changed from TBAF¹⁵¹ to HF·pyridine, but only diol **270** was obtained. The best results were obtained when dianion **269** was formed from silyl ether **247** using TBAF in THF followed by treatment with *N,N*-bis(trifluoromethylsulfonyl)aniline,¹⁵² which is a triflating reagent that is compatible with THF (Table 11, entry 8 and Scheme 60). Ditriflate **246** was only sparingly soluble in THF and virtually insoluble in all other organic solvents.



Scheme 60: Desilylation/triflation of silyl ethers 247 and 268 to afford ditriflates 246 and 271.

One puzzling observation was that either diol **270** or monotriflate was present in the crude product mixture, regardless of the amount of TBAF or triflating reagent that was used. Workup of the one-pot desilylation/triflation reaction involved suspending the reaction in a mixture of THF/ether and successively washing with HCl (10% aq), NaOH (10% aq) and water. The organic phase was concentrated to give ditriflate **246** in varying yields. During the NaOH wash the aqueous phase turned blue, which was indicative of anion formation.

The varying yields obtained in desilylation/triflation reaction prompted an examination of the workup. One concern was that the hydroxide ion was nucleophilic enough to react with ditriflate **246**, either by attacking one of the quinone carbonyls or the triflate. When the reaction was worked up with a NaHCO₃ (sat. aq) wash instead of the NaOH (10% aq) wash, ditriflate **246** was isolated in greater than 90% yield. When an authentic sample of ditriflate **246** was suspended in THF/ether and treated with NaOH (10% aq), a blue solution characteristic of dianion **269** formed. Treatment of this solution with acid afforded diol **270**. This provided conclusive evidence that the hydroxide ion was reacting with ditriflate **246**.

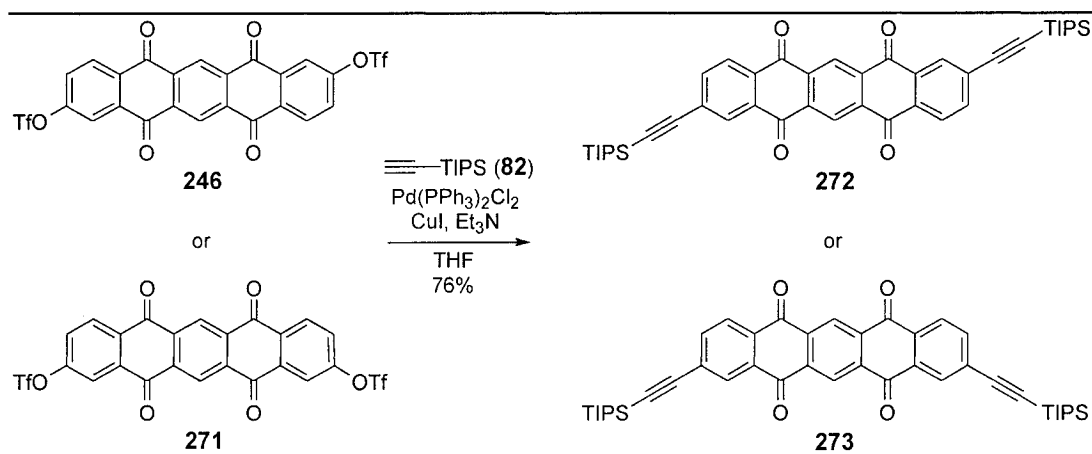
Ditriflates **246** and **271** could both be made by the desilylation/triflation procedure to give crude material in nearly quantitative yield. This product was used without further purification in the palladium coupling reactions described in the next section.

4.6 2,9- and 2,10-Disubstituted Pentacenes

The rapid route to ditriflates **246** and **271** was a major milestone in the synthesis of 2,9- and 2,10-disubstituted pentacenes, as an assortment of functionalized pentacene compounds could be accessed from ditriflates **246** and **271** *via* palladium coupling reactions. Pentacenes

274 and **275** possessing triisopropylsilylethynyl substituents in the 2,9 or 2,10 positions were the first targets. Anthony's group predicted pentacene **274** would be well-organized in the solid-state, allowing for significant intermolecular orbital overlap, and in turn, possess higher electron and hole mobilities.¹⁴¹

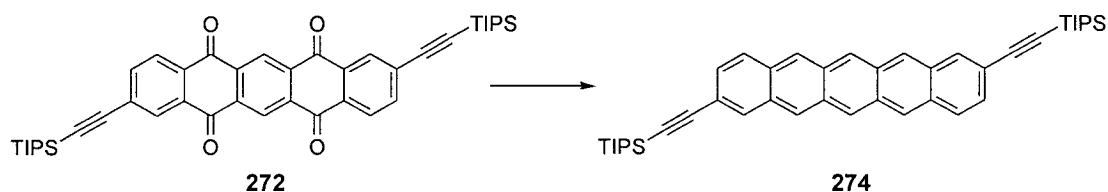
A Sonogashira reaction of ditriflate **246**¹⁵³ and TIPS-acetylene (**82**) in the presence of Pd(PPh₃)₂Cl₂, CuI, and Et₃N in THF gave diquinone **272** (Scheme 61). Ditriflate **246** was sparingly soluble in THF (1 mg/5 mL) and decent yields (76%) of diquinone **272** were obtained only when **246** was completely dissolved prior to the addition of the other reagents. The use of DMF as a cosolvent did not improve the solubility of **246** or the reaction yield. Diquinones **272** and **273** were readily soluble in THF and chlorinated solvents and could be purified by recrystallization from ether.



Scheme 61: Preparation of diquinones **272** and **273**.

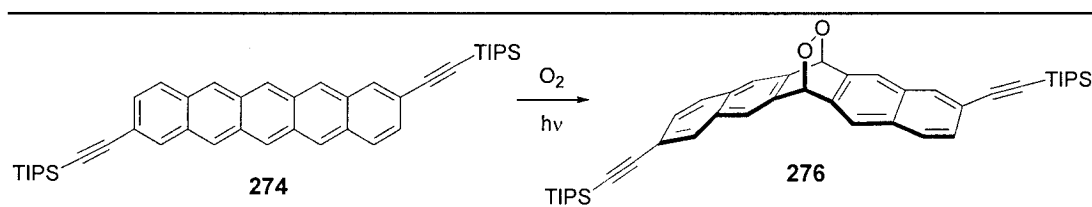
A number of procedures are known for the reduction of anthraquinones (and related compounds) to their corresponding deoxygenated, aromatic species. The most common procedures are zinc powder and catalytic copper(II) sulphate in ammonium hydroxide¹⁵⁴ or aluminum amalgam in ammonium hydroxide.¹⁵⁵ When these reaction conditions were used to reduce diquinone **272**, a complex mixture was obtained (Table 12, entries 1 and 2). However, when diquinone **272** was treated with a large excess of sodium borohydride in refluxing isopropanol,¹⁵⁶ pentacene **274** was isolated in an excellent yield (88%) (Table 12, entry 3). Reaction workup and product purification remains to be optimized.

Table 12: Reaction conditions for the reduction of diquinone **272** to pentacene **274**.



entry	reaction conditions	result (%)
1	Zn(s), Cu(II)SO ₄ (cat.), NH ₄ OH, Δ	mixture
2	Al/Hg, NH ₄ OH, Δ	mixture
3	NaBH ₄ , <i>i</i> -PrOH, Δ	274 (88)

During the preparation of an NMR sample of pentacene **274**, the initial purple solution rapidly turned bright yellow. The resulting ¹H NMR spectrum contained a peak at δ 4.19, which is characteristic of a methyne, bridgehead proton. There are numerous reports of acenes reacting with oxygen to give endoperoxides.¹⁵⁷ With this in mind, we suspected that pentacene **274** acted as its own photooxygenation sensitizer leading to the formation of endoperoxide **276** (Scheme 62).¹⁵⁸ To test this hypothesis, a solution of pentacene **274** was prepared in an inert atmosphere (glovebox) and the methylene chloride solution remained purple.



Scheme 62: Reaction of pentacene **274** with O₂ to give endoperoxide **276**.

4.7 Summary

We have developed a rapid, four-step synthesis of 2,9- and 2,10-bis(triisopropylsilylethynyl)pentacenes, **274** and **275**, from 1,4,5,8-anthraquinone **249**. A double Diels-Alder reaction of Danishefsky's diene **248** with anthraquinone **249** gave a mixture of silyl ethers **247** and **268** (1:1), which could be separated by fractional crystallization. The key ditriflate intermediates, **246** and **271**, were obtained from a one-pot desilylation/triflation of the corresponding silyl ether. Ditriflate **246** (or **271**) underwent a

palladium catalyzed coupling reactions to give diquinones **272** and **273**. This procedure may be used to introduce a number of substituents at the 2,9- or 2,10-positions. Finally, a sodium borohydride reduction of diquinones **272** and **273** gave pentacenes **274** and **275** respectively. A highlight of this synthetic route to 2,9- and 2,10-disubstituted pentacenes is that the entire synthesis could be conducted without chromatographic purification.

The performance of pentacenes **274** and **275** as organic field effect semiconductors is currently being explored through a collaboration with the Stacey Institute of the National Research Council of Canada. An outline of future work is discussed in Chapter 5.

Chapter

CONCLUSIONS, FUTURE WORK, AND CLAIMS TO ORIGINAL RESEARCH

5.1 New Methods

5.2 Synthesis of New Compounds

5.3 Future Work

5.3.1 *Chiral, Non-Racemic Cyclophanes*

5.3.2 *Substituted Pentacene Compounds for use as
Organic Semiconductors*

5.4 Claims to Original Research

5. Conclusions

The purpose of this research project was to synthesize new acetylenic cyclophanes and to study their spectroscopic and physical properties. In order to accomplish these goals, several new synthetic strategies and methods were developed. These new methods and the completed syntheses are highlighted in this chapter.

The synthesis of two new C₆₀ acetylenic cyclophanes revealed that the substitution pattern of the capping group affected the conformation of the molecule. Cyclophane **113** with *para*-substituted capping groups adopted a helical (chiral) conformation and the isomeric *meta*-capped cyclophane **123** had a different molecular folding pattern with the potential to be planar.

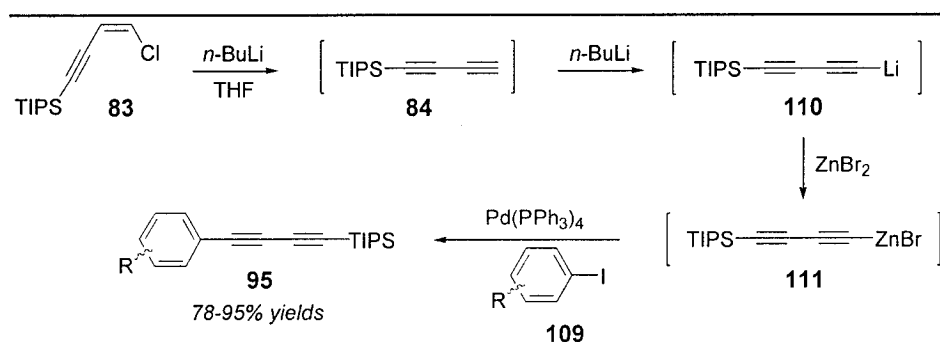
Two classes of unsaturated cyclophanes were synthesized as ligands for the preparation of chiral, non-racemic helical complexes: A tetramethoxybenzene-capped, C₆₀ acetylenic cyclophane as a potential η^{12} -bis(arene) ligand, and phenanthrolinephanes as tetradentate π -coordination ligands. Cyclophane **170** was successfully prepared and a low resolution X-ray crystal structure confirmed **170** adopted a helical conformation with face-to-face π -stacked capping aromatic rings. Although cyclophane **170** seemed to be a good η^{12} bis(arene) ligand candidate, metal complexes of **170** could not be prepared. Phenanthrolinephanes **200**, **217**, and **227** were synthesized and copper complexes were prepared. Coordination of copper was found to raise the helical isomerization barrier height by over 7 kcal/mol; however, isomerization still occurred at room temperature so enantiopure phenanthrolinephanes could not be isolated.

The first pentacene molecules with substituents on the A and E rings have also been synthesized. The rapid, four-step synthesis of pentacenes **274** and **275** was highlighted by the absence of column chromatographic purification. The commercial potential of these new pentacene compounds as organic semiconductors is being investigated in collaboration with the National Research Council of Canada.

5.1 New Methods

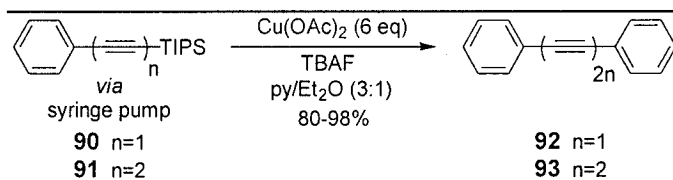
Several new methods were developed in order to achieve our synthetic objectives. These methods are summarized in the schemes below.

A new one-pot preparation of arylbutadiynes **95** was developed. Chloroenyne **83** was converted to organozincate **111**, which was reacted *in situ* via a Negishi-type coupling with aryl halides **109** to give arylbutadiynes **95** (Scheme 63). This procedure eliminated the isolation and purification of unstable butadiyne **84** and generated arylbutadiynes in significantly higher yields.



Scheme 63: Preparation of arylbutadiynes from chloroenyne **83** (Section 2.4).

A second method that was developed was an *in situ* desilylation/dimerization of bulky silylbutadiynes **91** (Scheme 64). Unprotected arylbutadiynes are known to be unstable and this new procedure facilitated the *in situ* dimerization of arylbutadiynes protected with bulky silyl protecting groups.



Scheme 64: *In situ* desilylation/dimerization of bulky, silyl-protected arylbutadiynes (Section 3.7).

A molecular modeling study provided insight into the observed dimerization reaction products of α,ω -dialkyne precursors (Figure 51). For example, when the termini separation distance (r) was less than 7 Å, intramolecular coupling occurred unless the transition state was too strained for the intramolecular reaction to occur. Conversely, termini separation distances greater than 10 Å resulted in intermolecular reactions. Mixtures of intra- and

intermolecular reaction products were obtained when the termini separation distance was between 7 and 10 Å.

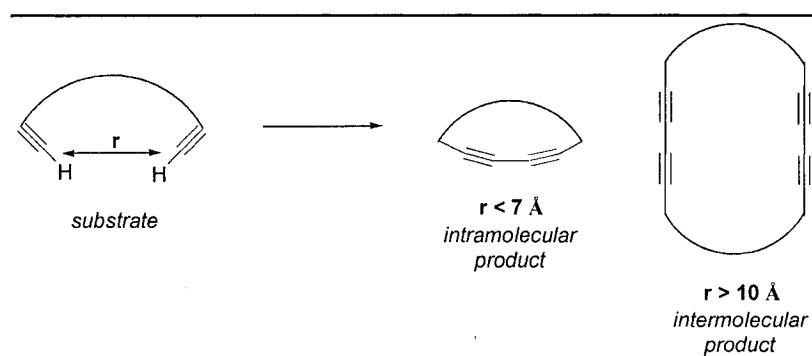
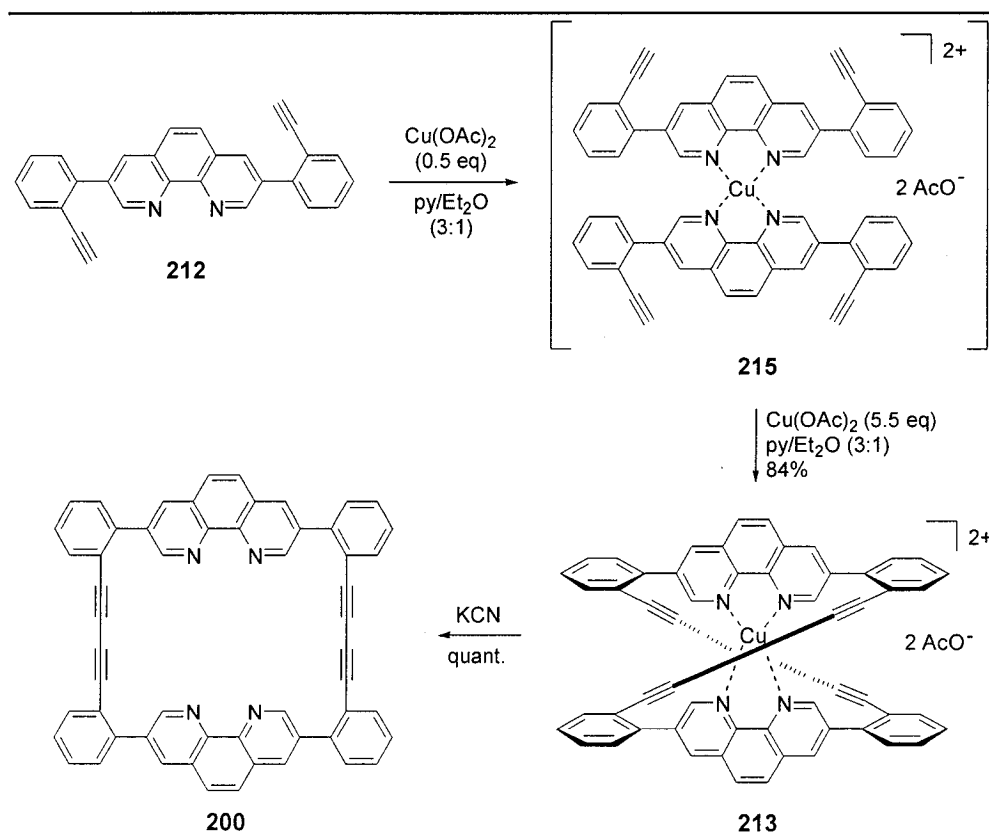


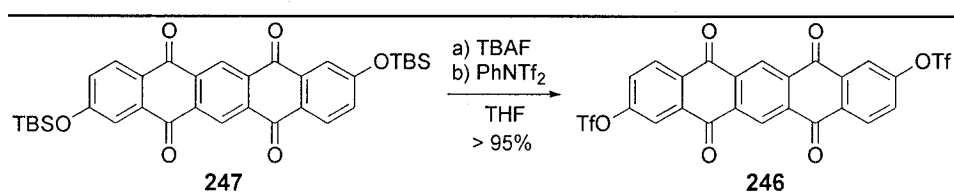
Figure 51: Molecular modeling study used to predict dimerization reaction products (Section 2.6).

A copper-templated dimerization reaction was also developed during the synthesis of phenanthrolinephanes (Scheme 65). Dimerization precursor **212** was treated with half an equivalent of $\text{Cu}(\text{OAc})_2$ to establish copper template **215**, which was then dimerized with an excess of $\text{Cu}(\text{OAc})_2$. The templated dimerization reaction resulted in a six-fold increase in reaction yield, from 15 to 84%.



Scheme 65: Copper-templated dimerization reaction (Section 3.7).

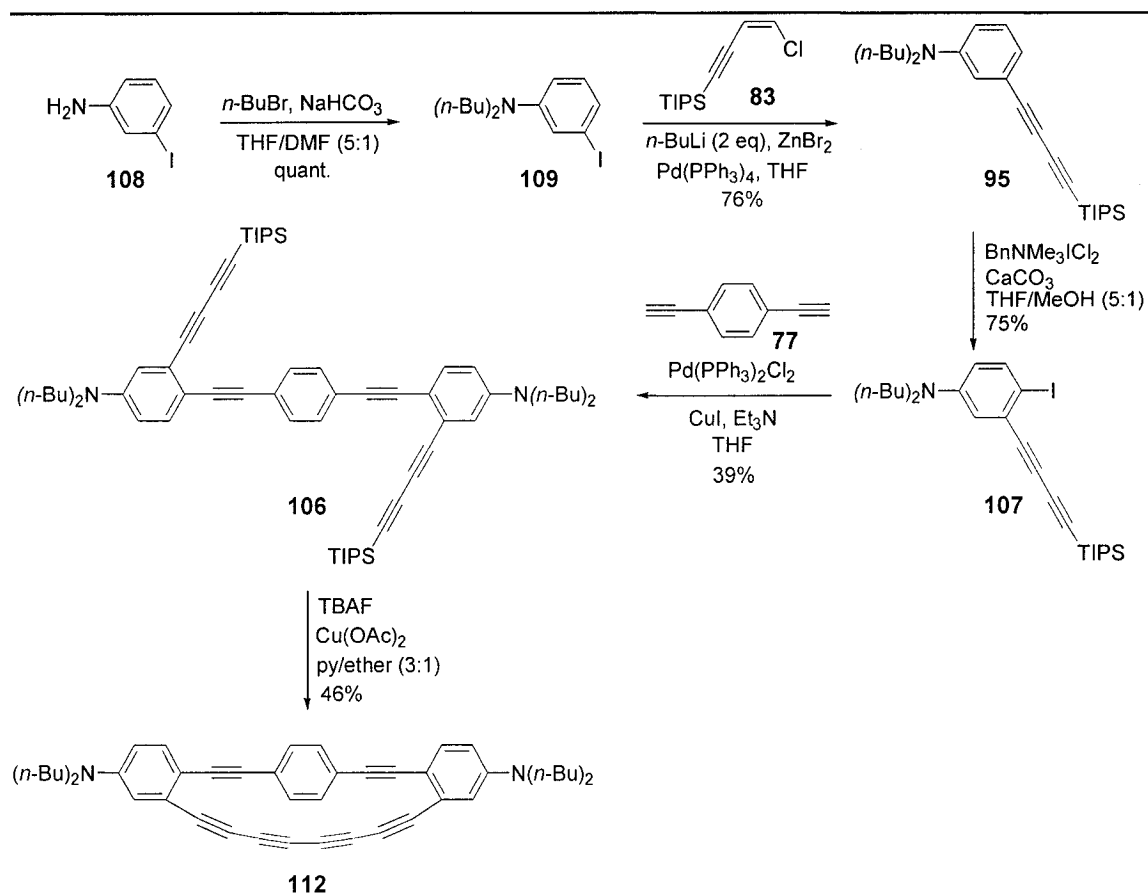
The last method developed was an *in situ* desilylation/triflation reaction (Scheme 66). The diol that resulted from the deprotection of silyl ether **247** was not soluble in organic solvents and could not be transformed to ditriflate **246** under standard reaction conditions. This new method provided an efficient route to key ditriflate intermediates **246** and **271**.



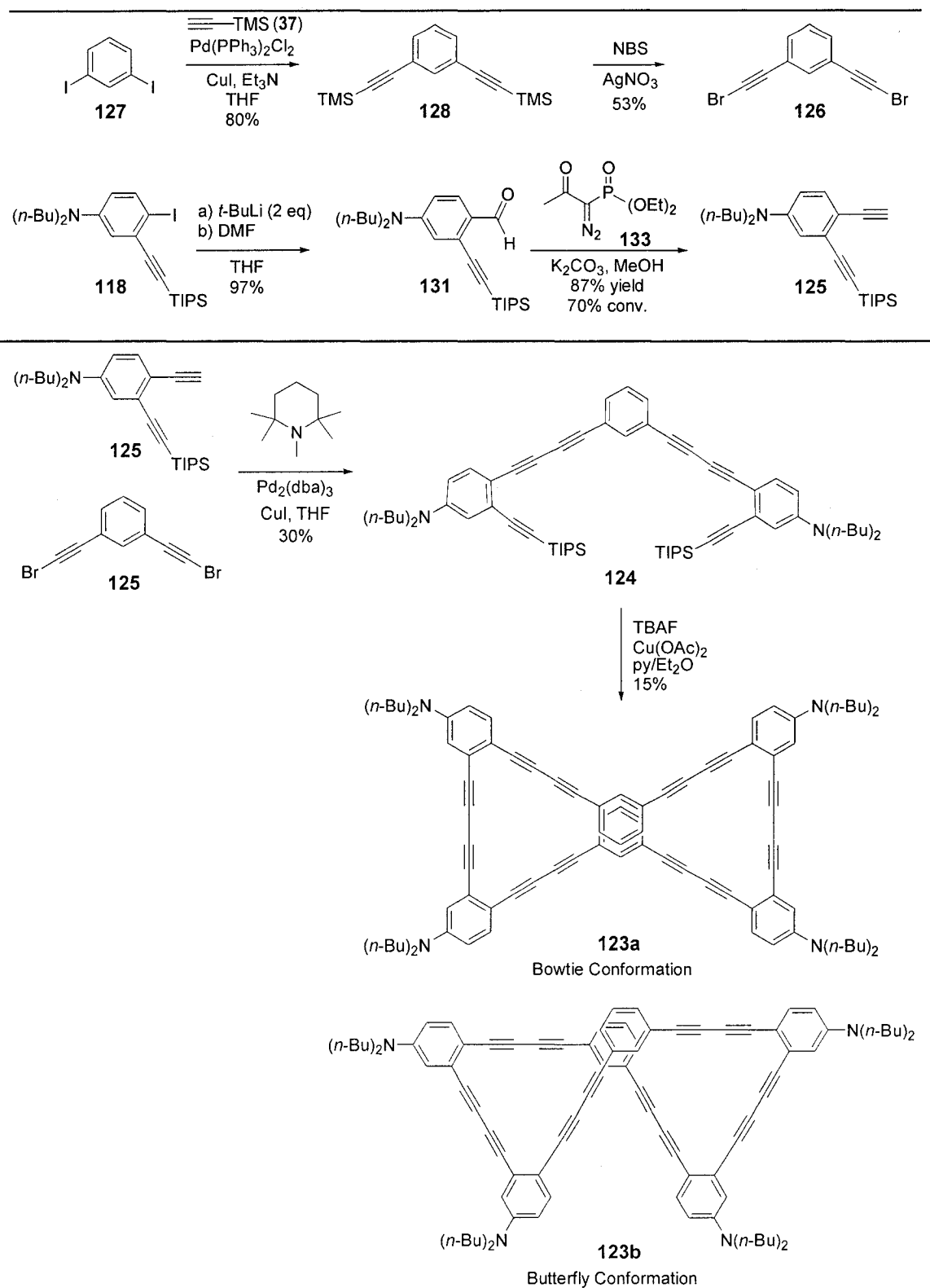
Scheme 66: *In situ* desilylation/triflation route to ditriflates **246** and **271** (Section 4.5).

5.2 Synthesis of New Compounds

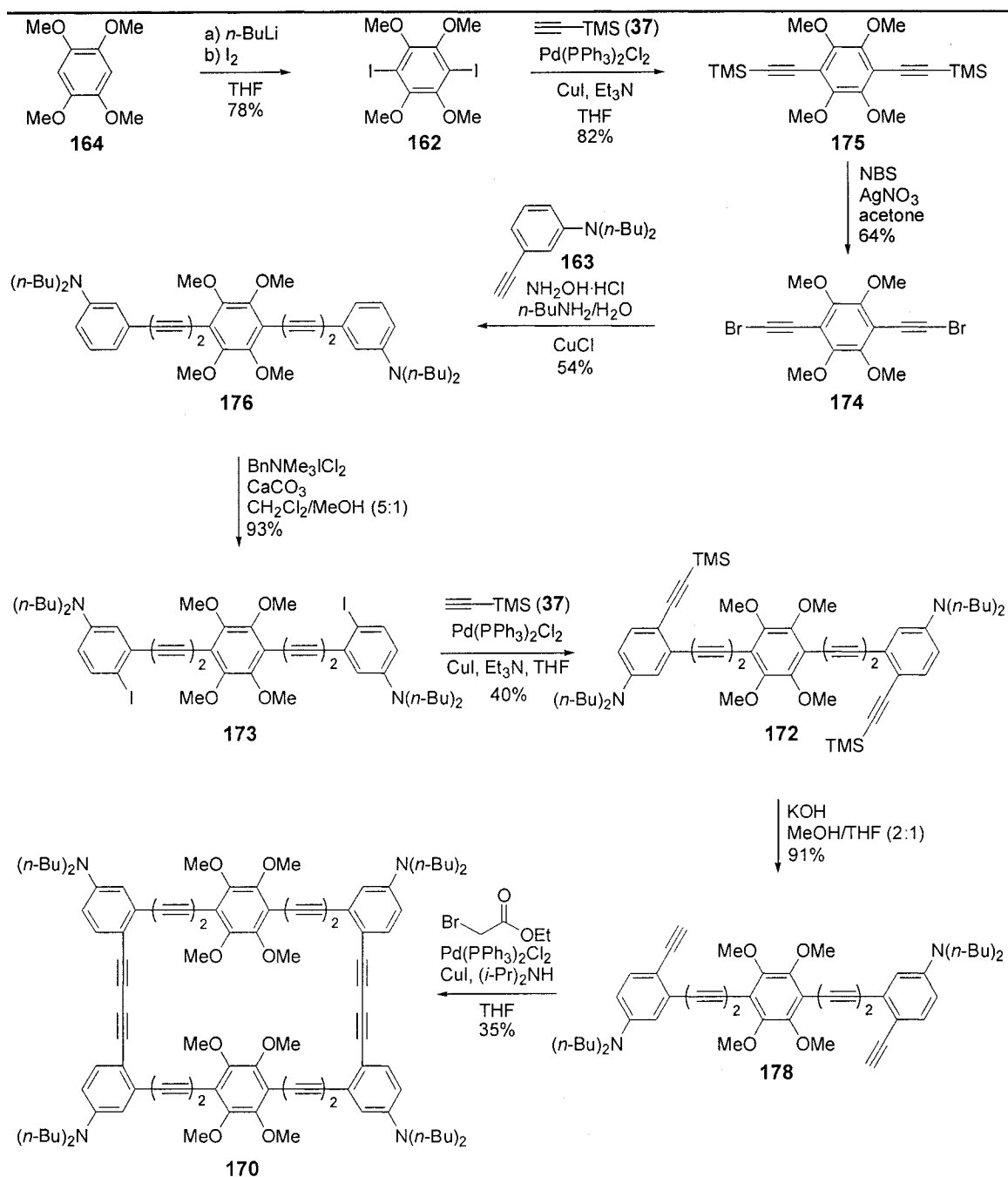
The synthetic routes to new unsaturated cyclophanes, phenanthrolinephanes, and disubstituted pentacenes is presented here.



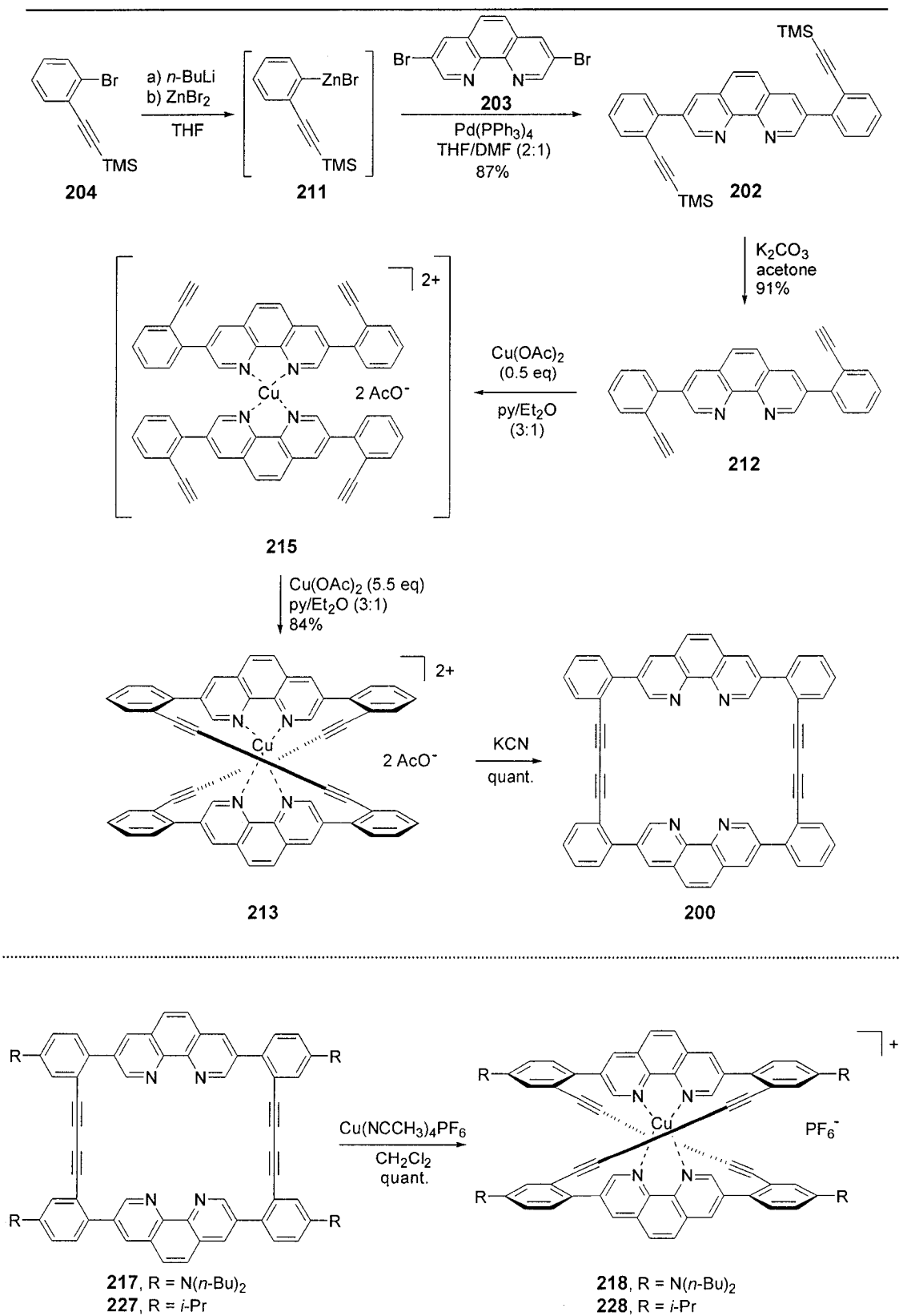
Scheme 67: Synthesis of cyclophane 112 (Section 2.4).



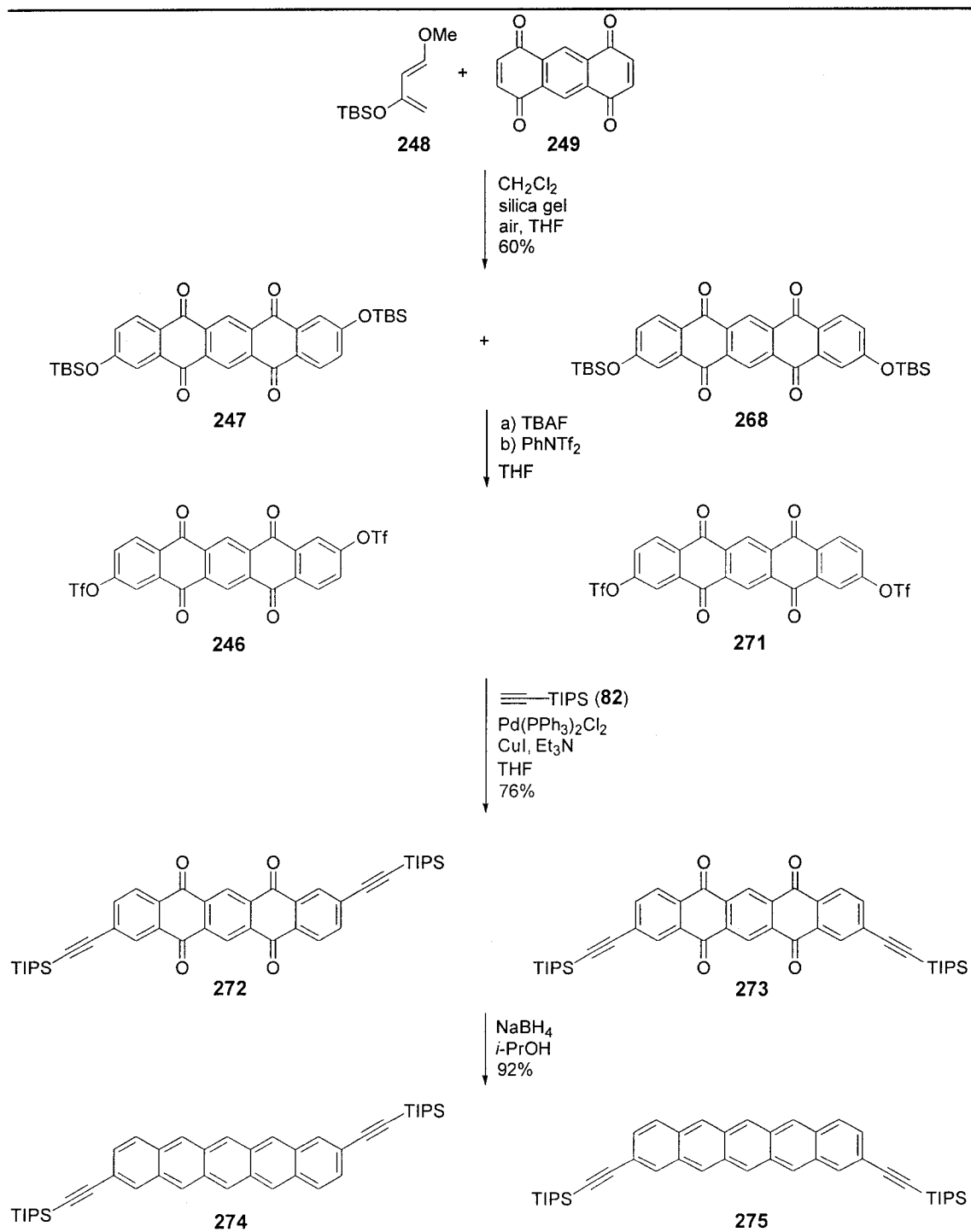
Scheme 69: Synthesis of C₆₀ *meta*-cyclophanes 123a and 123b (Section 2.7).



Scheme 70: Synthesis of cyclophane 170 as a potential η^{12} - bis(arene) ligand (Section 3.3).



Scheme 71: Synthesis of phenanthrolinephanes (Sections 3.7 and 3.9).



Scheme 72: Synthesis of disubstituted pentacenes **274** and **275** (Section 4.6).

5.3 Future Work

Further investigations are warranted in two areas: a) the synthesis of chiral, non-racemic cyclophanes; and b) the synthesis of new pentacene derivatives as organic semiconducting compounds. Potential future work pertaining to each of these areas is presented below.

5.3.1. Chiral, Non-Racemic Cyclophanes

Two strategies toward the preparation of chiral, non-racemic cyclophanes are worth pursuing. The first is an extension of the phenanthroline chemistry that has been described in this thesis. The preparation of new phenanthroline derivatives with acetylene spacers may reduce the strain of the molecule in twisted conformations and thus allow metal ions to inhibit helical isomerization (Figure 52). In addition, phenanthroline derivatives with long alkyl chains [R = C₁₂H₂₅, OC₁₂H₂₅, N(C₁₂H₂₅)₂] should be prepared and studied as potential liquid crystals.

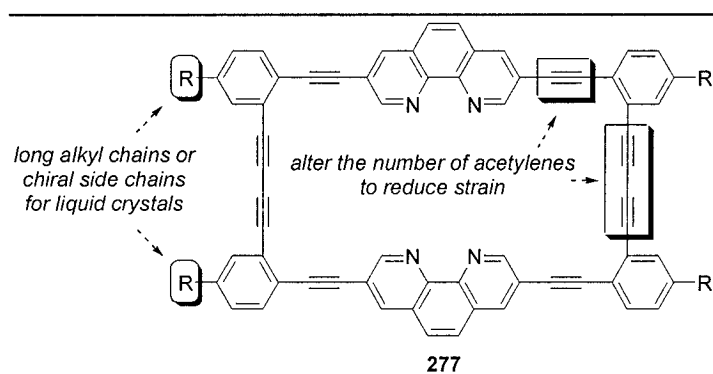


Figure 52: Second generation phenanthroline derivatives.

A second strategy to chiral, non-racemic cyclophanes is to use allenes as chiral directing groups (Figure 53). Although this strategy has been previously explored with other chiral building blocks, only one macrocycle containing more than one allene has been prepared and it was obtained as a racemate. The synthesis of chiral allene cyclophanes, such as **278**, would allow the molecular conformation and electronic properties of these compounds to be explored.

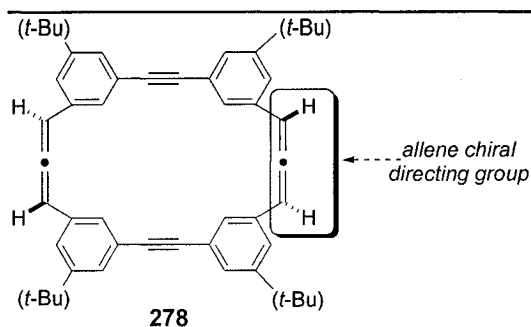


Figure 53: An allene cyclophane synthetic target.

5.3.2. Substituted Pentacene Compounds for use as Organic Semiconductors

New disubstituted pentacene compounds should be prepared to probe the electronic properties and the solid-state packing of these molecules. Also, new synthetic routes to A and E ring disubstituted pentacenes should be explored as an efficient route to required diquinone **249** remains unknown. One potential new synthetic route is shown in Figure 54.

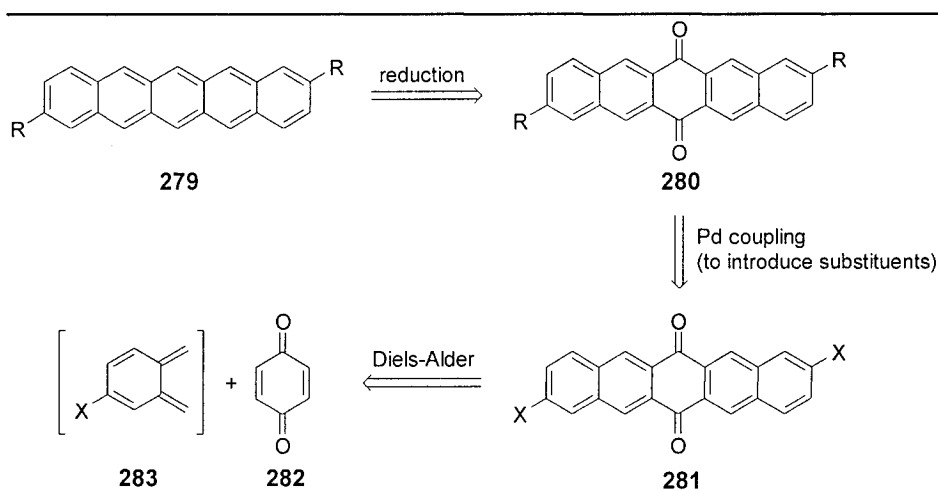


Figure 54: A new synthetic route to 2,9- and 2,10-disubstituted pentacenes.

Unsymmetrically-substituted, unsaturated molecules with electron-donating and electron-withdrawing substituents have been studied for their potential use as molecular wires and their photoelectric/photochemical properties. Thus, a pentacene derivative with electron-withdrawing and electron-donating substituents in the 2 and 9 positions may have interesting photoelectric and photochemistry properties (Figure 55).

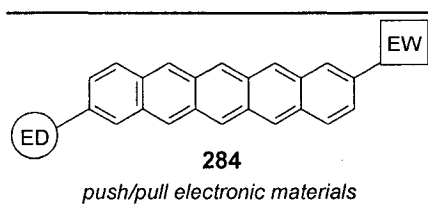


Figure 55: Unsymmetrically disubstituted pentacenes with electron-donating (ED) and withdrawing (EW) substituents for molecular electronics.

Anthracene oligomers have recently been shown to be better organic semiconductors (better electron and holes mobilities) than anthracene itself.¹⁵⁹ Thus, oligo pentacenes would be interesting targets as potential organic semiconductors (Figure 56).

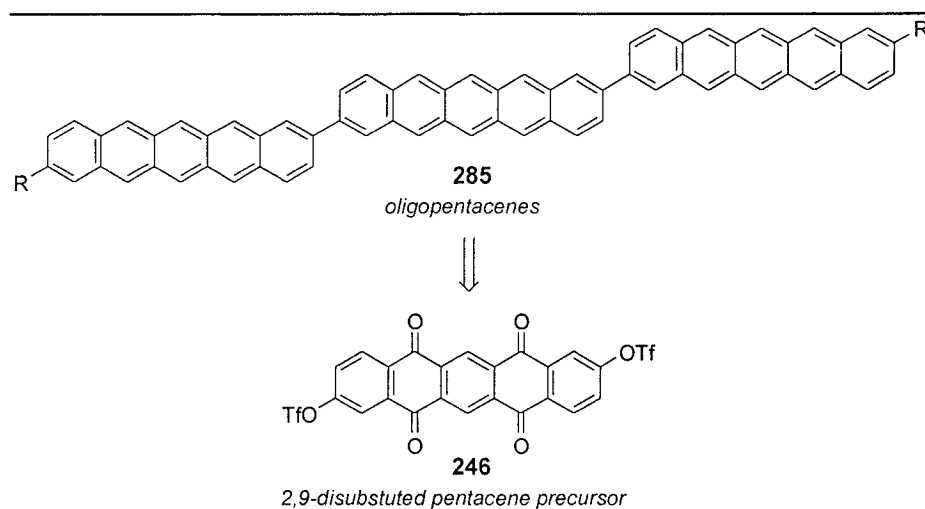


Figure 56: Oligopentacenes as organic semiconductors.

Pentacenophane **229** could be synthesized from ditriflate **271**. The 2,10-disubstituted pentacene precursor would lead to a pseudo *meta*-substituted pentacene and the synthesis of pentacenophane **229** would allow us to test our hypothesis that *meta*-capped cyclophanes can adopt planar conformations.

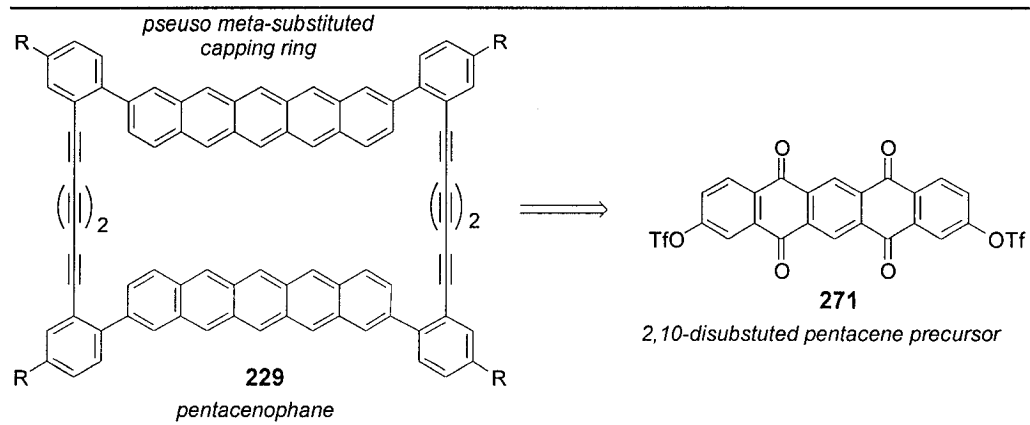


Figure 57: Pseudo *meta*-capped, planar pentacenophane 229.

5.4 Claims to Original Research

1. Co-developed an *in situ* desilylation/dimerization reaction for the synthesis of symmetrical butadiynes and octatetraynes.
2. Established a method for predicting the dimerization reaction products of α,ω -dialkynes *via* a molecular modeling study based on the termini separation distance.
3. Synthesized *para*- and *meta*-capped C₆₀ acetylenic cyclophanes (**113** and **123**) and demonstrated that the substitution pattern of the capping groups determines the molecular folding.
4. Synthesized a tetramethoxybenzene-capped C₆₀ acetylenic cyclophane (**170**) as a potential η^{12} bis(arene) ligand.
5. Synthesized a series of double helical phenanthrolinephanes by a copper-templated dimerization reaction. Phenanthrolinephane copper complexes were prepared and copper incorporation was found to reduce the rate of helical isomerization.
6. The first 2,9- and 2,10-disubstituted pentacene compounds were synthesized. These compounds are currently being studied as new organic semiconductors in collaboration with the National Research Council of Canada.

Chapter

EXPERIMENTAL SECTION

6.1 General Experimentals

6.2 Detailed Experimental Procedures

6. Experimental Section

6.1 General Experimental

All non-aqueous reactions were performed under a positive pressure of dry nitrogen in flame-dried glassware using dry solvents. Tetrahydrofuran and diethyl ether were distilled from sodium/benzophenone. Methylene chloride, toluene, and triethylamine were distilled from calcium hydride. Standard inert atmosphere techniques were employed in handling air and moisture sensitive reagents. Copper(II) acetate was prepared from the dihydrate $\text{Cu}(\text{OAc})_2 \cdot 2\text{H}_2\text{O}$ by refluxing in acetic anhydride for 15 h prior to use.¹⁶⁰ Commercially available *n*-BuLi solutions in hexanes were used from the Aldrich Chemical Company and titrated prior to use against diphenylacetic acid. All TBAF solutions were in THF solvent. All starting materials were purchased from Aldrich Chemical Company and used without further purification unless otherwise stated.

Reactions were monitored by thin layer chromatography (TLC) using commercial aluminum-backed silica gel sheets coated with silica gel 60 F₂₅₄ (E. Merck). TLC spots were visualized under ultraviolet light and developed by heating the plate after treatment with a 5% solution of ammonium molybdate in 10% aqueous sulphuric acid. Room temperature (rt) corresponds to 21 °C. Anhydrous magnesium sulfate (MgSO_4) was used to dry solutions of organic solvents. Excess solvents were removed (concentrated) *in vacuo* at pressures obtained by a water or air aspirator connected to a rotary evaporator. Trace solvents were removed on a vacuum pump. Product purification by flash chromatography was performed with silica gel 60 (230-400 mesh, E. Merck). Petroleum ether refers to a mixture of hydrocarbons with a boiling range of 30-60 °C.

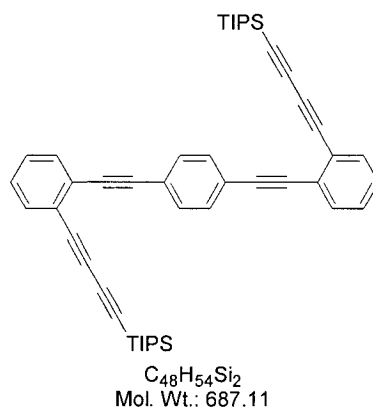
Melting points were determined with a Thomas-Hoover Unit melting point apparatus and are uncorrected. Infrared (IR) spectra were obtained as neat thin films or as a solution of the sample in CDCl_3 or CHCl_3 in a sodium chloride solution cell. All IR spectra were recorded on a Bomem Michelson 100 Fourier transform infrared spectrometer (FTIR). ^1H NMR (200 or 500 MHz) and ^{13}C NMR (125 MHz) spectra were run on a Gemini 200 spectrometer or Brüker AMX500 spectrometer. Chemical shifts are reported relative to tetramethylsilane (δ scale) in ppm. ^1H NMR data are reported as follows: chemical shift, multiplicity (s = singlet, d = doublet, t = triplet, q = quartet), coupling constants (Hz), and integration.

Low resolution mass spectroscopy (MS), using either electron impact (EI) or chemical ionization (CI), was performed on a V.G. Micromass 7070 HS mass spectrometer with an electron beam energy of 70 eV (for EI). High resolution mass spectroscopy (HRMS) was performed on a Kratos Concept-11A mass spectrometer with an electron beam energy of 70 eV. Electrospray mass spectra ES (MS) were determined on a Micromass Quattro LC with a pump rate of 20 $\mu\text{L}/\text{min}$. Elemental analyses were performed at M-H-W Laboratories, Phoenix, Arizona, USA. The purity of all title compounds was judged to be $> 95\%$ as determined by a combination of GC-MS, ^1H NMR and ^{13}C NMR analyses.

6.2 Detailed Experimental Procedures

Experimental procedures are presented for new compounds or for improved preparations and are in order of compound number as they appear in Chapters 1 to 5. Compounds that were prepared, but not included in the main text of the dissertation appear at the end of the experimental section.

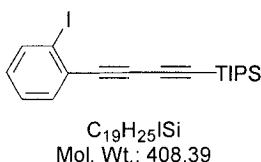
1,4-Bis-[2-(2-(4-triisopropyl-1,3-butadiynyl)phenyl)ethynyl]benzene (**76**)



A solution of iodide **86** (200 mg, 0.49 mmol, 2 eq) in THF (10 mL) was degassed by bubbling argon through the solution for 30 min. CuI (10 mg, 10 mol%), Pd(PPh₃)₂Cl₂ (30 mg, 5 mol%), and Et₃N (2 mL) were added to the degassed solution and stirred at rt for 10 min. Alkyne **77** (31 mg, 0.25 mmol, 1 eq) was added to the solution and the reaction was heated to reflux for 18 h. The reaction was cooled to rt, filtered through a silica gel plug, and concentrated. Chromatography (petroleum ether/Et₂O, 10:1) afforded **76** as a yellow solid (125 mg, 74%); mp: 120-121 °C; IR (CH₂Cl₂) ν 2945.5, 2867.1, 2099.7, 1511.9, 1262.1 cm^{-1} ; ^1H NMR (500 MHz, CDCl₃) δ 7.55 (s, 4H), 7.52 (d, $J = 8.1$ Hz, 4H), 7.33 (ddd,

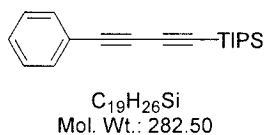
$J = 7.8, 7.7, 1.1$ Hz, 2H), 7.27 (ddd, $J = 7.7, 7.6, 1.1$ Hz, 2H), 1.14 (s, 42H); ^{13}C NMR (125 MHz, CDCl_3) δ 132.7 (d), 131.7 (d), 131.6 (d), 128.8 (d), 128.1 (d), 127.2 (s), 124.4 (s), 123.2 (s), 94.0 (s), 89.7 (s), 89.5 (s), 89.3 (s), 78.7 (s), 74.1 (s), 18.6 (q), 11.3 (d); MS (EI) m/z 686.4 (M^+ , 13), 482.3 (6), 397.1 (6), 267.0 (5), 143.0 (26); HRMS calcd for $\text{C}_{48}\text{H}_{54}\text{Si}_2$ 686.3766 (M^+), found 686.3750; Anal. calcd for $\text{C}_{48}\text{H}_{54}\text{Si}_2$ C 83.90%, H 7.92%, found C 84.06%, H 7.90%.

1-Iodo-2-(4-triisopropylsilyl-1,3-butadiynyl)benzene (**86**)



A solution of *n*-BuLi (2.13 M in THF, 3.25 mL, 6.92 mmol, 1 eq) was added to a -78 °C stirred solution of bromide **78** (2.50 g, 6.92 mmol, 1 eq) in THF (50 mL). The solution turned dark yellow upon addition of base. The reaction was quenched immediately by the addition of a solution of *N*-iodosuccinimide (1.56 g, 6.92 mmol, 1 eq) in THF (40 mL) and the reaction was warmed to rt with stirring for 2 h. The reaction mixture was diluted with petroleum ether, washed with H_2O and brine, dried, and concentrated to yield **86** as a dark yellow oil (2.74 g, 97%); ^1H NMR (500 MHz, CDCl_3) δ 7.81 (d, $J = 7.8$ Hz, 1H), 7.49 (d, $J = 7.8$ Hz, 1H), 7.28 (dd, $J = 7.7, 7.8$ Hz, 1H), 7.01 (dd, $J = 7.7, 7.7$ Hz, 1H), 1.12 (s, 21H); ^{13}C NMR (125 MHz, CDCl_3) δ 138.8 (d), 134.1 (d), 132.6 (s), 130.1 (d), 128.3 (s), 127.7 (d), 100.8 (s), 89.9 (s), 89.2 (s), 78.1 (s), 18.5 (q), 11.3 (d); MS (EI) m/z 408.1 (M^+ , 22), 365.0 (100), 336.9 (46), 294.8 (55), 239.1 (36); HRMS calcd for $\text{C}_{19}\text{H}_{25}\text{ISi}$ 408.0772 (M^+), found 408.0791.

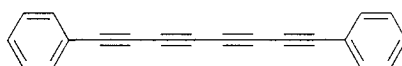
1-Phenyl-4-triisopropylsilyl-1,3-butadiyne (**91**)



A solution of *n*-BuLi (2.27 M, 15.8 mL, 35.8 mmol, 4.0 eq) was added in one portion to a -78 °C solution of *cis*-4-chloro-1-triisopropylsilyl-but-3-en-1-yne (**83**) (4.34 g, 17.9 mmol, 2.0 eq) in THF (40 mL). The resulting pale yellow coloured solution was stirred for 2 min followed by the addition of a solution of ZnBr_2 (4.12 g, 18.3 mmol, 2.05 eq) in THF (40 mL).

The colourless solution was stirred at $-78\text{ }^{\circ}\text{C}$ for 5 min then warmed to $0\text{ }^{\circ}\text{C}$ for 15 min. A mixture of iodobenzene (1.0 mL, 8.94 mmol, 1 eq), $\text{Pd}(\text{PPh}_3)_4$ (500 mg, 5 mol%) in THF (40 mL) was added by canula and the reaction was heated to reflux for 18 h. The reaction was cooled to rt, silica gel was added and the slurry was concentrated. Chromatography (petroleum ether) afforded **91** as a yellow oil (1.61 g, 64%); ^1H NMR (500 MHz, CDCl_3) δ 7.50 (dd, $J = 8.2, 1.3$ Hz, 2H), 7.37-7.29 (m, 3H), 1.13 (s, 21H); ^{13}C NMR (125 MHz, CDCl_3) δ 132.6 (d), 129.2 (d), 128.3 (d), 121.5 (s), 89.6 (s), 87.8 (s), 75.5 (s), 74.7 (s), 18.5 (q), 11.3 (d); HRMS calcd for $\text{C}_{19}\text{H}_{26}\text{Si}$ 282.1804 (M^+), found 282.1787.

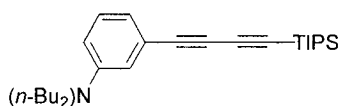
1,8-Diphenyl-oct-1,3,5,7-tetrayne (**92**)



$\text{C}_{20}\text{H}_{10}$
Mol. Wt.: 250.29

A solution of TBAF (1.0 M in THF, 355 μL) in THF (5 mL) was added over 2 h *via* syringe pump to a stirred solution of silylalkyne **91** (100 mg, 0.35 mmol) and $\text{Cu}(\text{OAc})_2$ (192 mg, 1.05 mmol) in pyridine/ Et_2O (3:1). The blue solution became emerald green once addition began. Once addition was complete, the solution was poured into Et_2O and HCl (1 M). The organic phase was washed excessively with HCl (1 M) until all pyridine was removed and the organic phase was dried and concentrated. Chromatography (petroleum ether) afforded **92** as a yellow solid (40 mg, 91%); ^1H NMR (500 MHz, CDCl_3) δ 7.54-7.51 (m, 2H), 7.42-7.37 (m, 1H), 7.36-7.32 (m, 2H); ^{13}C NMR (125 MHz, CDCl_3) δ 133.2 (d), 130.0 (d), 128.5 (d), 120.5 (s), 77.7 (s), 74.4 (s), 67.1 (s), 63.6 (s); HRMS calcd for $\text{C}_{20}\text{H}_{10}$ 250.0783 (M^+), found 250.0784.

N,N-Dibutyl-3-(4-triisopropylsilyl-1,3-butadiynyl)aniline (**95**)

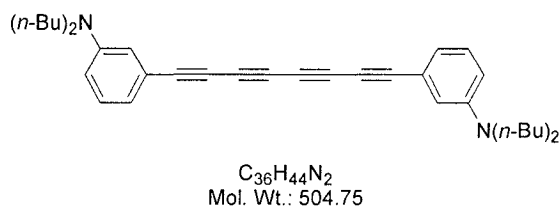


$\text{C}_{27}\text{H}_{43}\text{NSi}$
Mol. Wt.: 409.72

A solution of *n*-BuLi (2.04 M in THF, 22.4 mL, 45.6 mmol, 3.02 eq) was added in one portion to a $-78\text{ }^{\circ}\text{C}$ solution of *cis*-4-chloro-1-trimethylsilyl-but-3-en-1-yne (**83**) (5.50 g, 22.7 mmol, 1.5 eq) in THF (150 mL). The resulting yellow solution was stirred for 2 min followed by the addition of a solution of ZnBr_2 (5.27 g, 23.4 mmol, 1.55 eq) in THF

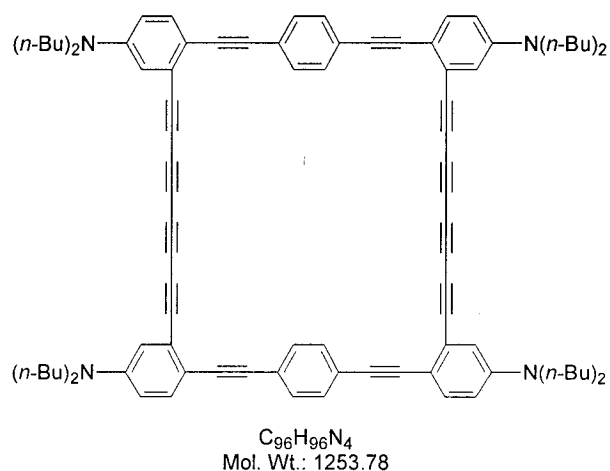
(100 mL). The colourless solution was stirred at -78 °C for 5 min then warmed to 0 °C for 15 min. A mixture of *N,N*-dibutyl-3-iodoaniline (**109**) (5.00g, 15.1 mmol, 1 eq), Pd(PPh₃)₄ (1.75 g, 10 mol%) in THF (150 mL) was added by canula and the reaction was heated to reflux for 18 h. The reaction was cooled to rt, silica gel was added to the reaction flask, and the slurry was concentrated. Chromatography (petroleum ether/CH₂Cl₂, 20:1) afforded **95** as a yellow oil (4.70 g, 76%); ¹H NMR (500 MHz, CDCl₃) δ 7.11 (dd, *J* = 7.9, 7.8 Hz, 1H), 6.79-6.76 (m, 3H), 3.24 (t, *J* = 7.7 Hz, 4H), 1.59-1.52 (m, 4H), 1.40-1.30 (m, 4H), 1.14 (s, 21H), 0.97 (t, *J* = 7.3 Hz, 6H); ¹³C NMR (125 MHz, CDCl₃) δ 147.9 (s), 129.1 (d), 121.9 (s), 119.7 (d), 115.3 (d), 113.0 (d), 90.0 (s), 86.7 (s), 73.3 (s), 65.8 (s), 50.7 (t), 29.0 (t), 20.4 (t), 18.4 (q), 13.9 (q), 11.3 (d); MS (EI) *m/z* 409.3 (M⁺, 5), 319.2 (66), 221.4 (33), 163.4 (100), 135.2 (52); HRMS calcd for C₂₇H₄₃NSi 409.3165. (M⁺), found 409.3157; Anal. calcd for C₂₇H₄₃NSi: C 79.15%, H 10.58%, found C 78.95%, H 10.68%.

1,8-Bis-(3-*N,N*-dibutylaminobenzene)-octa-1,3,5,7-tetrayne (**96**)



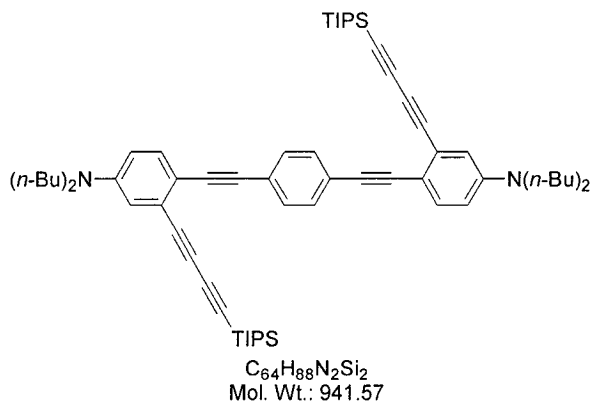
A solution of TBAF (1.0 M in THF, 100 μL) in THF (5 mL) was added over 2 h *via* syringe pump to a stirred solution of silylalkyne **95** (100 mg, 0.24 mmol) and Cu(OAc)₂ (133 mg, 0.73 mmol) in pyridine/Et₂O (3:1). The blue solution became emerald green once addition began. Once addition was complete, the solution was poured into Et₂O and HCl (1 M). The organic phase was washed excessively with HCl (1 M) until all pyridine was removed and the organic phase was dried and concentrated. Chromatography (petroleum ether) afforded **96** as a yellow oil (50 mg, 82%); ¹H NMR (200 MHz, CDCl₃) δ 7.12 (dd, *J* = 8.0, 8.0 Hz, 2H), 6.81-6.67 (m, 6H), 3.22 (t, *J* = 7.5 Hz, 8H), 1.63-1.42 (m, 8H), 1.42-1.22 (m, 8H), 0.97 (t, *J* = 7.1 Hz, 12H); ¹³C NMR (50 MHz, CDCl₃) δ 147.8 (s), 129.3 (d), 120.8 (s), 120.0 (d), 115.4 (d), 113.6 (d), 79.0 (s), 73.1 (s), 66.8 (s), 63.7 (s), 50.6 (t), 29.2 (t), 20.3 (t), 14.0 (q); HRMS calcd for C₃₆H₄₄N₂ 506.3504 (M⁺), found 506.3586.

11,28,41,58-Tetrakis-dibutylamino[8]1,3,5,7-tetraoctynylorthocyclo[2]15-ethynylparacyclo[2]23-ethynylorthocyclo[8]31,33,35,37-tetraoctynylorthocyclo[2]45-ethynylparacyclo[2]53-ethynylorthocyclophane (104)



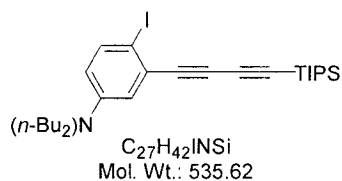
A solution of precursor **106** (508 mg, 0.54 mmol, 1 eq) and $Cu(OAc)_2$ (0.59 g, 3.23 mmol, 6 eq) were stirred in a mixture of pyridine/ Et_2O (3:1, 250 mL) for 15 min (Note: substrate concentration was 2.1 mM). A solution of TBAF (1 M in THF, 1.19 mL, 1.19 mmol, 2.2 eq) was added to the flask by syringe pump over 2 h. After stirring for an additional 1.5 h, no starting material remained by TLC (petroleum ether/ CH_2Cl_2 , 2:1). Silica gel (~ 1 g) was added and the slurry was concentrated. Chromatography (petroleum ether/ CH_2Cl_2 , 2:1) afforded **112** as a red solid (155 mg, 46%). When the substrate concentration was increased to 5.3 mM both cyclophane **112** (26%) and a small amount of a compound believed to be cyclophane **104** were obtained as a yellow glass (3 mg); 1H NMR (500 MHz, $CDCl_3$) δ 7.49 (s, 8H), 7.29 (d, $J = 8.9$ Hz, 4H), 6.73 (d, $J = 2.1$ Hz, 4H), 6.59 (d, $J = 6.8$ Hz, 4H), 3.24 (t, $J = 7.6$ Hz, 16H), 1.57-1.50 (m, 16H), 1.36-1.29 (m, 16H), 0.94 (t, $J = 7.3$ Hz, 24H); ^{13}C NMR (125 MHz, $CDCl_3$) δ 147.42 (s), 132.85 (d), 131.3 (d), 124.1 (s), 123.0 (s), 115.5 (s), 113.5 (d), 113.1 (d), 91.6 (s), 90.1 (s), 77.3 (s), 67.5 (s), 67.8 (s), 64.1 (s), 50.6 (t), 29.2 (t), 20.2 (t), 13.9 (q). The 1H and ^{13}C NMR spectra of cyclophane **104** was similar to, but differed from the corresponding spectra of cyclophane **112**.

1,4-Bis-2-(2-(4-triisopropylsilyl-1,3-butadiynyl)-4-*N,N*-dibutylaminophenyl)ethynylbenzene (106)



A solution of iodide **107** (4.00 g, 7.47 mmol, 2 eq) in THF (200 mL) was degassed by bubbling argon through the solution for 30 min. CuI (200 mg, 14 mol%), Pd(PPh₃)₂Cl₂ (600 mg, 10 mol%), and Et₃N (40 mL) were added to the degassed solution and stirred at rt for 10 min. 1,4-Diethynylbenzene (**77**) (460 mg, 3.64 mmol, 1 eq) was added to the solution and the reaction was heated at reflux for 18 h. The reaction was cooled to rt, filtered through a silica gel plug, and concentrated. Chromatography (hexanes/CH₂Cl₂, 5:2) afforded **106** as a bright yellow solid (1.31 g, 39%); IR (CH₂Cl₂) ν 2960.4, 2867.5, 2239.7, 1594.9, 1262.6 cm⁻¹; ¹H NMR (500 MHz, CDCl₃) δ 7.44 (s, 4H), 7.31 (d, *J* = 8.8 Hz, 2H), 6.72 (s, 2H), 6.56 (d, *J* = 7.6 Hz, 2H), 3.24 (t, *J* = 7.7 Hz, 8H), 1.57-1.51 (m, 8H), 1.37-1.30 (m, 8H), 1.12 (s, 42H), 0.95 (t, *J* = 7.3 Hz, 12H); ¹³C NMR (125 MHz, CDCl₃) δ 147.4 (s), 132.7 (d), 131.1 (d), 125.0 (s), 123.0 (s), 114.9 (d), 113.2 (s), 112.4 (d), 91.7 (s), 90.7 (s), 89.8 (s), 88.3 (s), 77.1 (s), 75.3 (s), 50.6 (t), 29.3 (t), 20.2 (t), 18.5 (q), 13.9 (q), 11.3 (d); MS (ES) *m/z* 941.3 (M⁺, 5), 734.1 (5), 610.1 (100), 285.9 (30).

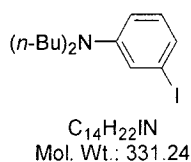
***N,N*-Dibutyl-4-iodo-3-(4-triisopropylsilyl-1,3-butadiynyl)aniline (107)**



Silylalkyne **95** (4.50 g, 11.0 mmol, 1 eq), BnNMe₃ICl₂ (3.83 g, 11.0 mmol, 1 eq), and CaCO₃ (1.54 g, 15.4 mmol, 1.4 eq) were combined in a mixture of CH₂Cl₂/MeOH (5:1, 90 mL) and stirred at rt for 3 h. Excess CaCO₃ was removed by filtration and the filtrate was concentrated. The crude yellow oil was dissolved in Et₂O and washed with Na₂S₂O₃ (10%

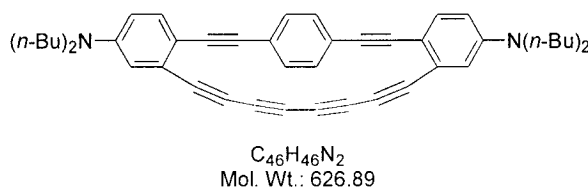
aq), H₂O, and brine, dried, and concentrated. Chromatography (hexanes/CH₂Cl₂, 2:1) afforded **107** as a yellow oil (4.41 g, 75%); ¹H NMR (500 MHz, CDCl₃) δ 7.48 (d, *J* = 8.5 Hz, 1H), 6.77 (s, 1H), 6.35 (s, 1H), 3.18 (t, *J* = 7.6 Hz, 4H), 1.53-1.47 (m, 4H), 1.35-1.28 (m, 4H), 1.11 (s, 21H), 0.93 (t, *J* = 7.3 Hz, 6H); ¹³C NMR (125 MHz, CDCl₃) δ 147.6 (s), 138.9 (d), 128.2 (s), 119.7 (s), 117.3 (d), 114.9 (d), 89.6 (s), 82.0 (s), 77.7 (s), 76.5 (s), 50.7 (t), 29.1 (t), 20.3 (t), 18.6 (q), 13.9 (q), 11.3 (d); MS (EI) *m/z* 535.2 (M⁺, 4), 388.6 (7), 345.1 (52), 319.7 (65), 162.3 (100); HRMS calcd for C₂₇H₄₂INSi 535.2131 (M⁺), found 535.2136.

***N,N*-Dibutyl-3-iodoaniline (109)**



3-Iodoaniline (4.26 mL, 35.4 mmol, 1 eq), NaHCO₃ (8.93 g, 106.2 mmol, 3 eq), 1-bromobutane (26.6 mL, 247.8 mmol, 7 eq), and NaI (1.00 g, 6.67 mmol, 19 mol%) were combined in a solution of THF/DMF (5:1, 225 mL) which was heated to reflux for 165 h. The reaction was cooled and poured into H₂O. The aqueous phase was extracted with Et₂O (2x) and the combined extracts were washed with H₂O (5x) and brine, dried, and concentrated. Chromatography (petroleum ether/CH₂Cl₂, 9:1) afforded **109** as a yellow oil (12.53 g, 99%); ¹H NMR (500 MHz, CDCl₃) δ 6.95-6.90 (m, 2H), 6.87 (dd, *J* = 7.9, 7.9 Hz, 1H), 6.56 (dd, *J* = 8.2, 1.9 Hz, 1H), 3.21 (t, *J* = 7.7 Hz, 4H), 1.57-1.49 (m, 4H), 1.38-1.29 (m, 4H), 0.95 (t, *J* = 7.4 Hz, 6H); ¹³C NMR (125 MHz, CDCl₃) δ 149.3 (s), 130.5 (d), 123.9 (d), 120.4 (d), 110.9 (d), 95.8 (s), 50.6 (t), 29.2 (t), 20.3 (t), 13.9 (q); MS (EI) *m/z* 331.1 (M⁺, 36), 288.0 (100), 246.3 (44), 232.0 (31), 161.1 (6); HRMS calcd for C₁₄H₂₃NI 332.0876 (M⁺ + H), found 332.0821. Characterization data of **109** agreed with the reported data.⁶⁰

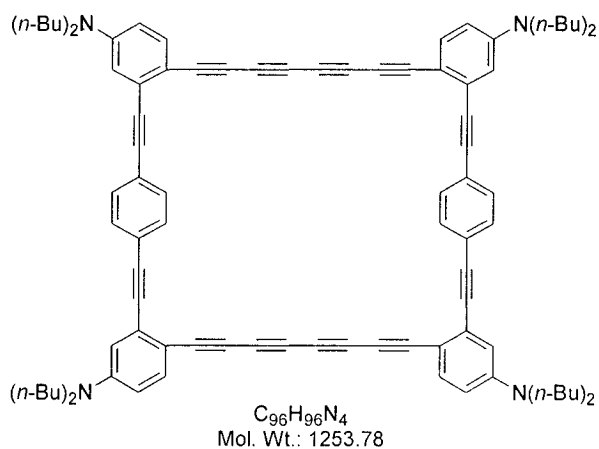
11,28-Bis-dibutylamino[8]1,3,5,7-tetraoctynylorthocyclo[2]15-ethynylparacyclo[2]23-ethynylorthocyclophane (112)



A solution of precursor **106** (508 mg, 0.54 mmol, 1 eq) and Cu(OAc)₂ (0.59 g, 3.23 mmol, 6 eq) were stirred in a mixture of pyridine/Et₂O (3:1, 250 mL) for 15 min (Note:

substrate concentration was 2.1 mM). A solution of TBAF (1 M in THF, 1.19 mL, 1.19 mmol, 2.2 eq) was added to the flask by syringe pump over 2 h. After stirring for an additional 1.5 h, no starting material remained by TLC (petroleum ether/CH₂Cl₂, 2:1). Silica gel (~ 1 g) was added and the slurry was concentrated. Chromatography (petroleum ether/CH₂Cl₂, 2:1) afforded **112** as a red solid (155 mg, 46%); mp: 155 °C (dec.); ¹H NMR (500 MHz, CDCl₃) δ 7.70 (s, 4H), 7.19 (d, *J* = 8.4 Hz, 2H), 6.54 (d, *J* = 8.4 Hz, 2H), 6.50 (s, 2H), 3.21 (t, *J* = 7.7 Hz, 8H), 1.54-1.48 (m, 8H), 1.35-1.28 (m, 8H), 0.93 (t, *J* = 7.3 Hz, 12H); ¹³C NMR (125 MHz, CDCl₃) δ 147.35 (s), 131.73 (d), 131.01 (d), 126.06 (s), 123.35 (s), 116.472 (s), 112.92 (d), 112.31 (d), 93.89 (s), 92.49 (s), 86.88 (s), 78.46 (s), 71.43 (s), 71.07 (s), 50.68 (t), 29.18 (t), 20.19 (t), 13.87 (q); MS (ES) *m/z* 627.1 (M⁺, 5), 314.3 (37), 144.8 (38), 72.9 (100).

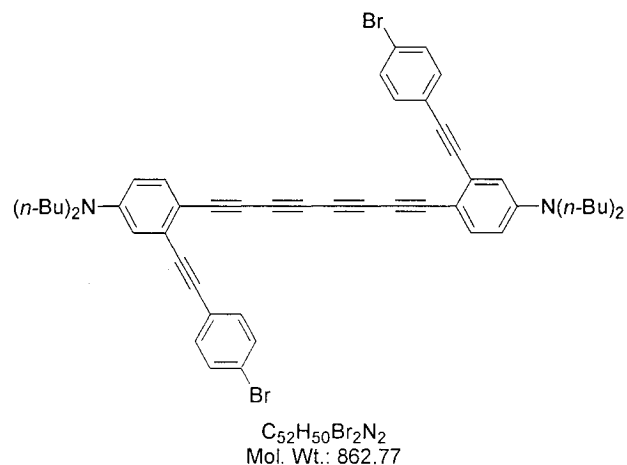
12,27,42,57-Tetrakis-dibutylamino[8]1,3,5,7-tetraoctynylorthocyclo[2]15-ethynylparacyclo[2]23-ethynylorthocyclo[8]31,33,35,37-tetraoctynylorthocyclo[2]45-ethynylparacyclo[2]53-ethynylorthocyclophane (113)



A solution of Pd(PPh₃)₂Cl₂ (25 mg, 10 mol%), CuI (5 mg, 5 mol%), 1-bromo-4-iodobenzene (**120**) (115 mg, 0.40 mmol, 2.0 eq), and Et₃N (5.0 mL) in THF (100 mL) was degassed with argon for 20 min. Hexyne **115** (112 mg, 0.20 mmol, 1 eq) was added to the reaction which was stirred at rt for 13 h. TLC (petroleum ether/CH₂Cl₂, 3:1) showed that the *in situ* formation of dibromide **114** was complete. A degassed solution of P(*t*-Bu)₃ (50 μL, 0.25 mmol), Pd(PhCN)₂Cl₂ (25 mg, 10 mol%), and hexyne **115** (112 mg, 0.20 mmol, 1 eq) in THF (100 mL) was added dropwise over 4 h and stirred at rt for an additional 13 h. The reaction was concentrated to 3 mL and diluted with CH₂Cl₂. The organics were washed with Na₂S₂O₃ (10% aq) and filtered through a silica gel plug. Chromatography (petroleum

ether/benzene, 2:1) afforded **113** as a yellow glass (6 mg, 2%); ^1H NMR (500 MHz, CDCl_3) δ 7.49 (d, $J = 8.4$ Hz, 4H), 7.42 (d, $J = 8.4$ Hz, 4H), 7.33 (d, $J = 6.7$ Hz, 2H), 7.32 (d, $J = 6.7$ Hz, 2H) 6.69 (d, $J = 2.5$, 4H), 6.52 (dd, $J = 2.5$, 2.5 Hz, 2H), 6.50 (dd, $J = 2.5$, 2.5 Hz, 2H), 3.30 (m, 16H), 1.63-1.52 (m, 16H), 1.41-1.29 (m, 16H), 0.94-0.91 (m, 24H); ^{13}C NMR (125 MHz, CDCl_3) δ 148.5 (s), 148.4 (s), 135.1 (d), 134.8 (d), 133.2 (d), 131.6 (d), 128.7 (s), 127.5 (s), 122.7 (s), 122.0 (s), 115.1 (d), 113.9 (d), 111.9 (d), 111.6 (d), 108.7 (s), 108.5 (s), 91.9 (s), 89.6 (s), 82.3 (s), 80.3 (s), 78.6 (s), 78.2 (s), 76.6 (s), 76.3 (s), 68.40 (s), 68.37 (s), 65.1 (s), 65.0 (s), 50.6 (t), 29.3 (t), 20.2 (t), 13.9 (q); MS (ES) m/z 1253.1 (M^+ , 1), 892.9 (5), 605.0 (5), 381.0 (25).

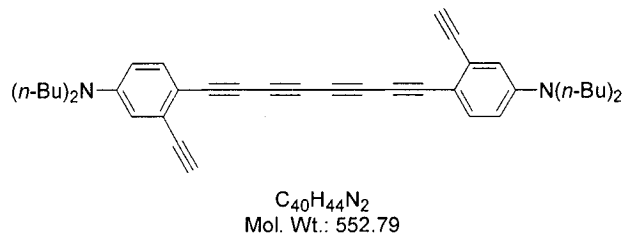
***N,N,N',N'*-Tetrabutyl-1,8-bis-[4-amino-2-(4-bromophenyl)ethynylphenyl]-1,3,5,7-tetraoctyne (114)**



A solution of $\text{Pd}(\text{PPh}_3)_2\text{Cl}_2$ (10 mg, 5 mol%), CuI (3 mg, 2.5 mol%), 1-bromo-4-iodobenzene (**120**) (48.4 mg, 0.171 mmol, 2.05 eq), and Et_3N (0.50 mL) in THF (10 mL) was degassed with argon for 20 min. Hexyne **115** (46.0 mg, 83.2 μmol , 1 eq) was added to the reaction, which was stirred at rt for 13 h. Silica gel was added to the reaction mixture and the slurry was concentrated. Chromatography (petroleum ether/ CH_2Cl_2 , 7:1 with significant dec.) afforded **114** as an orange solid (19 mg, 26%); mp: 135-140 $^\circ\text{C}$ (dec.); IR (CH_2Cl_2) ν 2960.0, 2149.7, 1597.9, 1368.8, 1133.2 cm^{-1} ; ^1H NMR (500 MHz, CDCl_3) δ 7.48 (d, $J = 8.5$ Hz, 4H), 7.43 (d, $J = 8.5$ Hz, 4H), 7.35 (d, $J = 8.9$ Hz, 2H), 6.67 (br s, 2H), 6.50 (br d, $J = 7.7$ Hz, 2H), 3.27 (t, $J = 7.6$ Hz, 8H), 1.58-1.52 (m, 8H), 1.38-1.31 (m, 8H), 0.95 (t, $J = 7.4$ Hz, 12H); ^{13}C NMR (125 MHz, CDCl_3) δ 148.5 (s), 134.9 (d), 133.3 (d), 131.7(d), 128.7 (s), 122.8 (s), 122.0 (s), 114.1 (d), 111.7 (d), 108.4 (s), 91.9 (s), 89.6 (s), 78.8 (s), 76.7 (s), 68.5

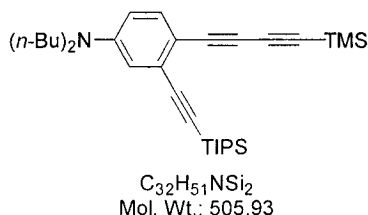
(s), 65.3 (s), 50.7 (t), 29.3 (t), 20.3 (t), 13.9 (q); MS (ES) m/z 862.8 (M^+ , 1), 237.7 (4), 176.7 (10), 70.7 (100).

***N,N,N',N'*-Tetrabutyl-1,8-bis-(4-amino-2-ethynylphenyl)- octa-1,3,5,7-tetrayne (115)**



A solution of TBAF (1 M in THF, 0.49 mL, 0.49 mmol, 2.7 eq) and silylalkyne **119** (151 mg, 0.17 mmol, 1 eq) were combined in THF (10 mL) and stirred at rt for 18 h. The reaction mixture was diluted with CH_2Cl_2 and was washed with $NaHCO_3$ (10% aq), H_2O , dried, and concentrated (not chromatographed due to decomposition on silica gel) to afford **115** as a red solid (94.3 mg, 97%); mp: 151 °C (dec.); IR (CH_2Cl_2) ν 2961.8, 2186.6, 1591.4, 1368.4, 1050.9 cm^{-1} ; 1H NMR (500 MHz, $CDCl_3$) δ 7.31 (d, $J = 8.8$ Hz, 2H), 6.67 (br s, 2H), 6.51 (br d, $J = 7.6$ Hz, 2H), 3.26 (s, 2H), 3.25 (t, $J = 7.9$ Hz, 8H), 1.56-1.50 (m, 8H), 1.36-1.30 (m, 8H), 0.98 (t, $J = 7.3$ Hz, 12H); ^{13}C NMR (125 MHz, $CDCl_3$) δ 148.3 (s), 135.1 (d), 127.6 (s), 115.2 (d), 112.0 (d), 107.6 (s), 82.3 (s), 80.4 (s), 78.2 (s), 76.4 (s), 68.4 (s), 65.1 (s), 50.7 (t), 29.3 (t), 20.2 (t), 13.9 (q); MS (ES) m/z 552.6 (1), 241.9 (40), 112.6 (13), 60.7 (89), 55.8 (100).

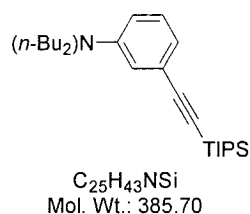
***N,N*-Dibutyl-4-(4-trimethylsilyl-1,3-butadiynyl)-3-(2-triisopropylsilylethynyl)-1-aniline (116)**



A solution of *n*-BuLi (2.36 M, 17.5 mL, 41.4 mmol, 3.02 eq) was added in one portion to a -78 °C solution of *cis*-4-chloro-1-trimethylsilyl-but-3-en-1-yne (**83a**) (3.26 g, 20.5 mmol, 1.5 eq) in THF (100 mL). The resulting yellow coloured solution was stirred for 2 min followed by the addition of a solution of $ZnBr_2$ (4.78 g, 21.2 mmol, 1.55 eq) in THF (100 mL). The colourless solution was stirred at -78 °C for 5 min then warmed to 0 °C for 15

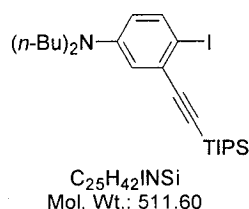
min. A mixture of iodide **118** (7.00 g, 13.7 mmol, 1.0 eq) and Pd(PPh₃)₄ (1.60 g, 10 mol%) in THF (350 mL) was added by canula and the reaction was heated at reflux for 48 h. Once cooled to rt, silica gel was added to the reaction flask and the slurry was concentrated. Chromatography (petroleum ether/CH₂Cl₂, 5:1) afforded **116** as a dark orange oil (5.52 g, 80%); ¹H NMR (500 MHz, CDCl₃) δ 7.25 (d, *J* = 8.8 Hz, 1H), 6.63 (br s, 1H), 6.45 (br d, *J* = 7.7 Hz, 1H), 3.24 (t, *J* = 7.6 Hz, 4H), 1.56-1.50 (m, 4H), 1.36-1.27 (m, 4H), 1.15 (s, 21H), 0.94 (t, *J* = 7.3 Hz, 6H), 0.19 (s, 9H); ¹³C NMR (125 MHz, CDCl₃) δ 148.0 (s), 134.0 (d), 128.7 (s), 114.7 (d), 111.5 (d), 109.9 (s), 105.7 (s), 94.4 (s), 94.1 (s), 89.6 (s), 89.2 (s), 75.7 (s), 50.6 (t), 29.5 (t), 20.2 (t), 18.7 (q), 13.7 (q), 11.4 (d), -0.3 (q); MS (EI) *m/z* 505.4 (M⁺, 4), 441.4 (20), 398.3 (50), 342.3 (100), 300.2 (31); HRMS calcd for C₃₂H₅₁NSi 505.3662 (M⁺), found 505.3586. Characterization data of **116** agreed with the reported data.⁶⁰

***N,N*-Dibutyl-3-(2-triisopropylsilylethynyl)aniline (**117**)**



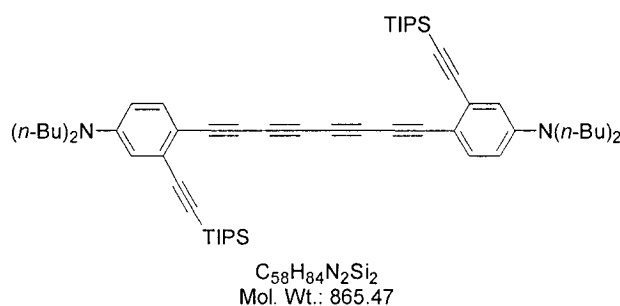
A solution of iodide **109** (10.01 g, 30.2 mmol, 1 eq) in THF (200 mL) was degassed by bubbling argon through the solution for 30 min. CuI (150 mg, 2.5 mol%), Pd(PPh₃)₂Cl₂ (500 mg, 2.5 mol%), and Et₃N (10 mL) were added to the degassed solution and stirred at rt for 10 min. Triisopropylsilyl-acetylene (**82**) (10.1 mL, 45.3 mmol, 1.5 eq) was added to the solution and the reaction was stirred for 18 h at rt. Silica gel was added to the reaction mixture and the slurry was concentrated. Chromatography (petroleum ether/CH₂Cl₂, 2:1) afforded **117** as a yellow oil (10.3 g, 88%); ¹H NMR (500 MHz, CDCl₃) δ 7.08 (dd, *J* = 7.8, 7.9 Hz, 1H), 6.76-6.69 (m, 2H), 6.57 (br d, *J* = 8.1 Hz, 1H), 3.23 (t, *J* = 7.5 Hz, 4H), 1.58-1.49 (m, 4H), 1.37-1.28 (m, 4H), 1.12 (s, 21H), 0.94 (t, *J* = 7.4 Hz, 6H); ¹³C NMR (125 MHz, CDCl₃) δ 147.9 (s), 128.9 (d), 124.0 (s), 119.0 (d), 115.1 (d), 112.2 (d), 108.5 (s), 88.7 (s), 50.6 (t), 29.2 (t), 20.2 (t), 18.6 (q), 13.9 (q), 11.3 (d); MS (EI) *m/z* 385.3 (M⁺, 2), 169.0 (4), 133.1 (11), 66.0 (100); HRMS calcd for C₂₅H₄₃NSi 385.3165 (M⁺), found 385.3154. Characterization data of **117** agreed with the reported data.⁶⁰

***N,N*-Dibutyl-4-iodo-3-(2-triisopropylsilylethynyl)aniline (118)**



Silylalkyne **117** (9.50 g, 24.6 mmol, 1 eq), $BnNMe_3ICl_2$ (8.57 g, 24.6 mmol, 1 eq), and $CaCO_3$ (3.45 g, 34.4 mmol, 1.4 eq) were combined in a mixture of $CH_2Cl_2/MeOH$ (5:1, 300 mL) and stirred at rt for 3 h. Excess $CaCO_3$ was removed by filtration and the filtrate was concentrated. The crude yellow oil was dissolved in Et_2O and washed with $Na_2S_2O_3$ (10% aq), H_2O , and brine, dried, and concentrated. Chromatography (hexanes/ CH_2Cl_2 , 2:1) afforded **118** as a yellow oil (9.82 g, 78%); 1H NMR (500 MHz, $CDCl_3$) δ 7.50 (d, $J = 8.8$ Hz, 1H), 6.76 (br s, 1H), 6.32 (br d, $J = 6.6$ Hz, 1H), 3.20 (t, $J = 7.6$ Hz, 4H), 1.55-1.47 (m, 4H), 1.37-1.27 (m, 4H), 1.15 (s, 21H), 0.93 (t, $J = 7.4$ Hz, 6H); ^{13}C NMR (125 MHz, $CDCl_3$) δ 147.7 (s), 138.7 (d), 130.0 (s), 116.7 (d), 114.2 (d), 109.0 (s), 93.3 (s), 81.8 (s), 50.6 (t), 29.1 (t), 20.2 (t), 18.7 (q), 13.9 (q), 11.4 (d); MS (EI) m/z 511.2 (M^+ , 11), 468.2 (16), 319.2 (100), 215.1 (75), 145.1 (48); HRMS calcd for $C_{25}H_{42}INSi$ 511.2134 (M^+), found 511.2158. Characterization data of **118** agreed with the reported data.⁶⁰

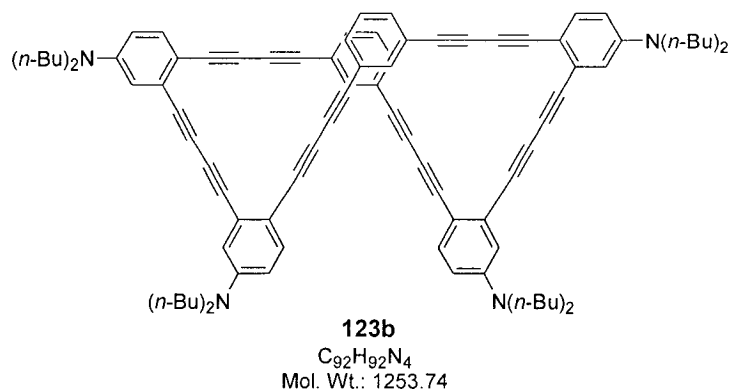
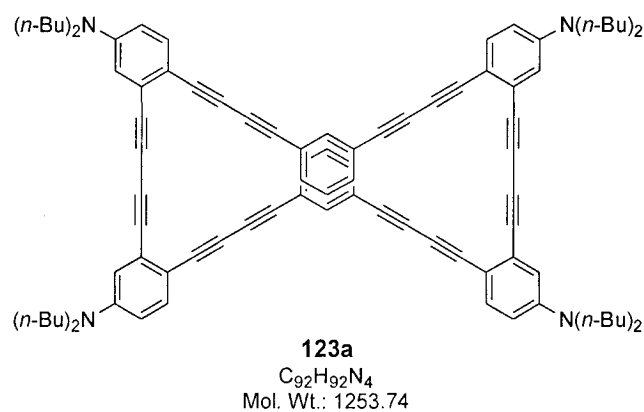
***N,N,N',N'*-Tetrabutyl-1,8-bis-[4-amino-2-(2-triisopropylsilylethynyl)phenyl]-1,3,5,7-tetraoctyne (119)**



Potassium carbonate (1.02 g, 7.38 mmol, 7.5 eq) and $Cu(OAc)_2 \cdot H_2O$ (1.97 g, 9.88 mmol, 10 eq) were stirred in a mixture of pyridine/ $MeOH$ (1:1, 180 mL) for 15 min. A solution of **118** (500 mg, 0.98 mmol, 1 eq) in pyridine/ $MeOH$ (1:1, 20 mL) was added to the reaction by syringe pump over 3 h and was further stirred at rt for 3 h. Silica gel was added to the reaction mixture and the slurry was concentrated. Chromatography (petroleum ether/ CH_2Cl_2 , 20:1) afforded **119** as an orange solid (395 mg, 92%); mp: 153-154 °C; IR

(CH₂Cl₂) ν 2960.3, 2186.3, 1589.7, 1368.2, 1121.6 cm⁻¹; ¹H NMR (500 MHz, CDCl₃) δ 7.29 (d, J = 8.9 Hz, 2H), 6.66 (s, 2H), 6.50 (s, 2H), 3.25 (t, J = 7.6 Hz, 8H), 1.56-1.50 (m, 8H), 1.36-1.29 (m, 8H), 1.15 (s, 42H), 0.94 (t, J = 7.3 Hz, 12H); ¹³C NMR (125 MHz, CDCl₃) δ 148.2 (s), 134.7 (d), 129.2 (s), 114.8 (d), 111.6 (d), 108.9 (s), 105.2 (s), 94.7 (s), 94.1 (s), 78.4 (s), 68.2 (s), 64.9 (s), 50.7 (t), 29.1 (t), 20.2 (t), 18.6 (q), 13.9 (q), 11.3 (d); MS (ES) m/z 865.3 (M⁺, 65), 442.2 (22), 366.1 (58), 191.8 (67).

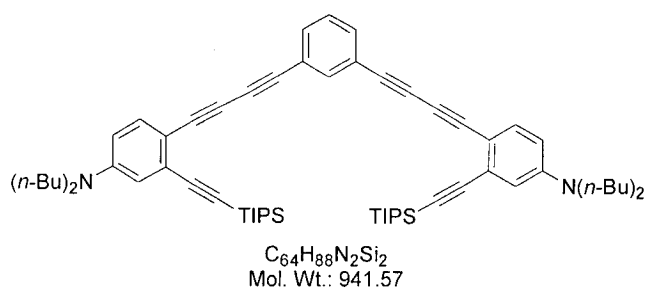
8,17,38,47-Tetrabutylamino[4]1,3-butadiynylorthocyclo[4]11,13-butadiynylorthocyclo[4]21,23-butadiynylmetacyclo[4]31,33-butadiynylorthocyclo[4]41,43-butadiynylorthocyclo[4]51,53-butadiynylmetacyclophane (123a and 123b)



A solution of TBAF (1 M in THF, 1.17 mL, 1.17 mmol, 2.2 eq) in a mixture of pyridine/Et₂O (3:1, 15 mL) was added by syringe pump to a stirred solution of silylalkyne **124** (500 mg, 0.53 mmol, 1 eq) in a mixture of pyridine/Et₂O (3:1, 250 mL) over 5 h. Once the addition was complete the reaction was stirred at rt for an additional 13 h. The reaction was diluted with CH₂Cl₂ and was washed with HCl (10% aq, 3x) and brine, dried, and

concentrated. Chromatography (petroleum ether/CH₂Cl₂, 9:1) afforded a yellow solid (50 mg, 15%) as a mixture of two compounds. Semi-preparative size exclusion chromatography (SEC) (Jordi Gel DVB 100A, MeOH/CHCl₃, 99:1) afforded **123a** and **123b**. Characterization of **123a**: yellow glass (24 mg, 8%); IR (CDCl₃) 2931.5, 2208.0, 1591.9, 1469.4, 1217.8 cm⁻¹; ¹H NMR (500 MHz, CDCl₃) δ 7.35 (d, *J* = 8.8 Hz, 4H), 7.30 (dd, *J* = 7.8, 1.6 Hz, 4H), 7.14 (br s, 2H), 7.00 (t, *J* = 7.8 Hz, 2H), 6.73 (br s, 4H), 6.56 (br s, 4H), 3.26 (t, *J* = 7.8 Hz, 16H), 1.58-1.52 (m, 16H), 1.38-1.28 (m, 16H), 0.96 (t, *J* = 7.4 Hz, 24H); ¹³C NMR (125 MHz, CDCl₃) δ 147.8 (s), 135.4 (d), 134.5 (d), 132.2 (d), 127.9 (d), 126.4 (d), 122.3 (d), 115.2 (s), 112.6 (s), 111.2 (s), 81.6 (s), 81.2 (s), 81.2 (s), 77.2 (s), 76.0 (s), 75.2 (s), 50.8 (t), 29.7 (t), 20.3 (t), 13.9 (q); MS (FAB) *m/z* 1254.0 (M⁺), 1195.4, 765.2, 306.1. Characterization of **123b**: yellow glass (8 mg, 3%) ¹H NMR (500 MHz, CDCl₃) δ 7.50 (s, 2H), 7.34-7.30 (m, 8H), 7.07 (dd, *J* = 7.8, 7.9 Hz, 2H), 6.73 (br s, 4H), 6.54 (br s, 4H), 3.24 (t, *J* = 7.5 Hz, 16H), 1.55-1.50 (m, 16H), 1.36-1.29 (m, 16H), 0.93 (t, *J* = 7.3 Hz, 24H); ¹³C NMR (125 MHz, CDCl₃) δ 147.89 (s), 147.82 (s), 135.9 (d), 134.6 (d), 132.3 (d), 128.3 (d), 126.3 (d), 122.7 (d), 122.6 (d), 115.4 (s), 112.4 (s), 110.7 (s), 110.3 (s), 81.8 (s), 81.7 (s), 81.6 (s), 81.4 (s), 81.1 (s), 80.9 (s), 80.87 (s), 80.84 (s), 75.9 (s), 75.8 (s), 75.52 (s), 75.49 (s), 50.7 (t), 29.6 (t), 20.2 (t), 13.9 (q). It should be noted that many of the aromatic carbon signals were broad and not resolved. MS (ES) *m/z* 1253.7 (M⁺), 941.2, 679.5, 351.2.

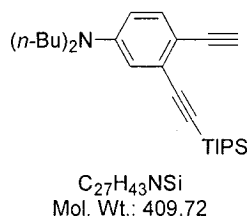
***N,N,N',N'*-Tetrabutyl-1,3-bis-[4-(2-triisopropylsilylethynyl-4-aminophenyl)-1,3-butadiynyl]benzene (**124**)**



A solution of Pd₂(dba)₃•CHCl₃ (202 mg, 10 mol%) and CuI (37 mg, 10 mol%) in benzene (50 mL) was degassed with argon. Alkyne **125** (2.00 g, 4.88 mmol, 2.5 eq), dibromide **126** (553 mg, 1.95 mmol, 1.0 eq), and 1,2,2,6,6-pentamethylpiperidine (1.41 mL, 7.80 mmol, 4.0 eq) were added sequentially to the reaction, which was stirred at rt for 16 h under an argon atmosphere. Silica gel was added to the reaction and the slurry was

concentrated and chromatographed twice (first with petroleum ether/CH₂Cl₂, 4:1 then with petroleum ether/Et₂O, 9:1) to afford **124** as a viscous yellow oil (556 mg, 30%) and **134** as a yellow foam (256 mg, 13%) resulting from the homocoupling of alkyne **125**. Characterization of **124**: IR (CDCl₃) ν 2957.0, 2207.0, 2138.4, 1588.8, 1365.7 cm⁻¹; ¹H NMR (500 MHz, CDCl₃) δ 7.54 (t, *J* = 1.6 Hz, 1H), 7.41 (dd, *J* = 7.7, 1.6 Hz, 2H), 7.30 (d, *J* = 8.8 Hz, 2H), 7.26 (d, *J* = 7.6 Hz, 1H), 6.67 (d, *J* = 2.2 Hz, 2H), 6.49 (dd, *J* = 8.8, 1.9 Hz, 2H), 3.26 (t, *J* = 7.6 Hz, 8H), 1.57-1.51 (m, 8H), 1.42-1.30 (m, 8H), 1.17 (s, 42H), 0.94 (t, *J* = 7.3 Hz, 12H); ¹³C NMR (125 MHz, CDCl₃) δ 148.1 (s), 135.3 (d), 134.0 (d), 132.2 (d), 128.5 (d), 128.4 (s), 123.2 (s), 114.7 (d), 111.6 (d), 110.1 (s), 105.7 (s), 94.2 (s), 82.7 (s), 80.1 (s), 76.0 (s), 75.2 (s), 50.5 (t), 29.3 (t), 20.2 (t), 18.7 (q), 13.9 (q), 11.4 (d); MS (ES) *m/z* 941.4 (M⁺, 0.1), 156.8 (2), 74.0 (58), 42.2 (100).

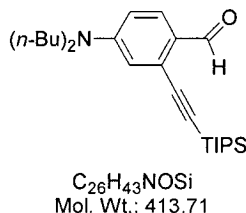
***N,N*-Dibutyl-4-ethynyl-3-(2-triisopropylsilylethynyl)aniline (**125**)**



Potassium carbonate (3.28 g, 23.8 mmol, 2.5 eq) was added to a 0 °C solution of aldehyde **131** (3.93 g, 9.5 mmol, 1.0 eq) and Ohira's reagent (**133**) (2.92 g, 15.2 mmol, 1.6 eq) in dry MeOH (50 mL) and the reaction was stirred vigorously at rt for 48 h. TLC (petroleum ether/Et₂O, 9:1) showed that starting material remained. More Ohira's reagent (~ 1 g) was added to the reaction and stirring was continued over the weekend (total reaction time was 6 days). The reaction was diluted with Et₂O, washed with NH₄Cl (sat. aq), H₂O, and brine, dried, and concentrated. Chromatography (petroleum ether/Et₂O, 9:1) afforded **125** as a yellow oil (2.38 g, 61%, starting material (**131**) was also recovered, 30%); IR (neat) ν 3310.8, 2958.0, 2155.1, 2101.9, 1597.7 cm⁻¹; ¹H NMR (500 MHz, CDCl₃) δ 7.27 (d, *J* = 8.8 Hz, 1H), 6.67 (d, *J* = 2.8 Hz, 1H), 6.49 (dd, *J* = 8.8, 2.8 Hz, 1H), 3.24 (t, *J* = 7.5 Hz, 4H), 3.09 (s, 1H), 1.56-1.50 (m, 4H), 1.37-1.29 (m, 4H), 1.13 (s, 21H), 0.94 (t, *J* = 7.4 Hz, 6H); ¹³C NMR (125 MHz, CDCl₃) δ 147.7 (s), 133.5 (d), 127.4 (s), 114.9 (d), 111.6 (d), 110.8 (s), 106.1 (s), 93.2 (s), 83.4 (s), 78.0 (s), 50.5 (t), 29.2 (t), 20.2 (t), 18.7 (q), 13.9 (q), 11.4 (d);

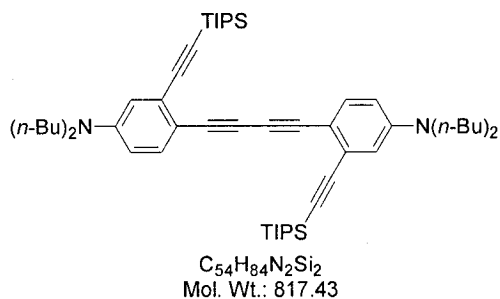
MS (EI) m/z 409.3 (M^+ , 60), 366.3 (100), 324.2 (22), 196.1 (7), 133.6 (7); HRMS calcd for $C_{27}H_{43}NSi$ 409.3165 (M^+), found 409.3184.

***N,N*-Dibutyl-4-amino-2-(2-triisopropylsilylethynyl)-1-benzaldehyde (131)**



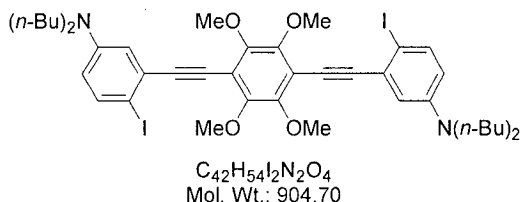
A solution of *t*-BuLi (1.7 M, 15.7 mL, 27.6 mmol, 2.1 eq) was added in one portion to a -78 °C solution of iodide **118** (6.50 g, 12.7 mmol, 1.0 eq) in THF (50 mL). The resulting yellow solution was stirred for 5 min followed by the addition *N,N*-dimethylformamide (4.0 mL, 62.1 mmol, 4.1 eq). The resulting colourless solution was stirred at -78 °C for 5 min, warmed to rt for 30 min, and heated at reflux for 12 h. The reaction was cooled to rt and quenched by adding NH_4Cl (sat. aq) and Et_2O . The organic phase was separated, washed with $Na_2S_2O_3$ (10% aq), H_2O , and brine, dried, and concentrated. Chromatography (petroleum ether/ Et_2O , 9:1) afforded **131** as a yellow oil (4.34 g, 97%); IR (neat) ν 2958.2, 2153.0, 1677.7, 1582.9 cm^{-1} ; 1H NMR (500 MHz, $CDCl_3$) δ 10.27 (s, 1H), 7.76 (d, $J = 9.0$ Hz, 1H), 6.65 (d, $J = 2.7$ Hz, 1H), 6.59 (dd, $J = 9.0, 2.4$ Hz, 1H), 3.31 (t, $J = 7.7$ Hz, 4H), 1.60-1.54 (m, 4H), 1.39-1.31 (m, 4H), 1.12 (s, 21H), 0.95 (t, $J = 7.4$ Hz, 6H); ^{13}C NMR (125 MHz, $CDCl_3$) δ 189.6 (d), 151.7 (s), 129.1 (s), 129.0 (d), 124.6 (s), 114.9 (d), 111.6 (d), 103.4 (s), 96.7 (s), 50.7 (t), 29.2 (t), 20.2 (t), 18.7 (q), 13.8 (q), 11.3 (d); MS (EI) m/z 413.3 (M^+ , 43), 370.3 (100), 328.2 (24), 200.1 (9), 114.5 (7); HRMS calcd for $C_{26}H_{43}NOSi$ 413.3114 (M^+), found 413.3118.

***N,N,N',N'*-Tetrabutyl-1,4-bis-[4-amino-2-(2-triisopropylsilylethynyl)phenyl]-1,3-butadiyne (134)**



Compound **134** was formed as a side product from the reaction of alkyne **125** and dibromide **126** (see **124** for experimental details). Characterization of **134**: 1H NMR (500 MHz, $CDCl_3$) δ 7.24 (d, $J = 8.8$ Hz, 2H), 6.65 (d, $J = 2.6$ Hz, 2H), 6.48 (dd, $J = 8.8, 2.5$ Hz, 2H), 3.24 (t, $J = 7.5$ Hz, 8H), 1.57-1.49 (m, 8H), 1.38-1.29 (m, 8H), 1.15 (s, 42H), 0.94 (t, $J = 7.4$ Hz, 12H); ^{13}C NMR (125 MHz, $CDCl_3$) δ 147.6 (s), 133.8 (d), 127.8 (s), 114.7 (d), 111.6 (d), 111.5 (s), 106.0 (s), 93.7 (s), 81.3 (s), 76.5 (s), 50.6 (t), 29.3 (t), 20.2 (t), 18.7 (q), 13.9 (q), 11.4 (d); MS (ES) m/z 817.4 (M^+ , 0.2), 504.3 (1), 410.2 (2), 114.9 (100).

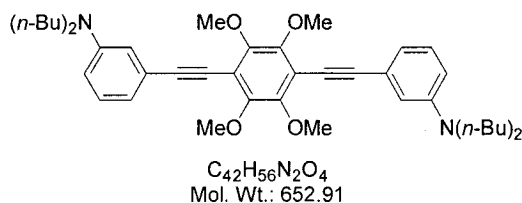
***N,N,N',N'*-Tetrabutyl-3,6-bis-[2-(5-amino-2-iodophenyl)ethynyl]-1,2,4,5-tetramethoxybenzene (160)**



Diamine **161** (1.00 g, 1.53 mmol, 1 eq), $BnNMe_3ICl_2$ (1.12 g, 3.22 mmol, 2.1 eq), and $CaCO_3$ (429 mg, 4.28 mmol, 2.8 eq) were combined in a mixture of $CH_2Cl_2/MeOH$ (5:1, 36 mL) and stirred at rt for 3.5 h. Excess $CaCO_3$ was removed by filtration through a silica gel plug and the filtrate was concentrated. The crude yellow oil was taken up in Et_2O and washed with $Na_2S_2O_3$ (10% aq), H_2O , and brine, dried, and concentrated. Chromatography (petroleum ether/ CH_2Cl_2 7:3 to 1:1) afforded **160** as a yellow solid (1.18 g, 85%); mp: 122-123 $^{\circ}C$; IR ($CDCl_3$) ν 3054.2, 2962.0, 2303.0, 1583.9, 1460.5 cm^{-1} ; 1H NMR (500 MHz, $CDCl_3$) δ 7.55 (d, $J = 8.8$ Hz, 2H), 6.85 (s, 2H), 6.36 (d, $J = 7.1$ Hz, 2H), 4.01 (s, 12H), 3.23 (t, $J = 7.3$ Hz, 8H), 1.59-1.49 (m, 8H), 1.37-1.28 (m, 8H), 0.94 (t, $J = 7.3$ Hz, 12H); ^{13}C NMR (125 MHz, $CDCl_3$) δ 150.5 (s), 147.7 (s), 138.9 (d), 129.9 (s), 116.5 (d), 114.4 (d),

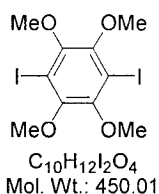
114.2 (s), 101.7 (s), 83.3 (s), 81.2 (s), 61.8 (q), 50.7 (t), 29.2 (t), 20.3 (t), 13.9 (q); MS (ES) m/z 905.0 (M^+ , 1.0), 779.2 (0.2), 453.1 (2.3), 115.0 (100).

***N,N,N',N'*-Tetrabutyl-3,6-bis-[2-(3-aminophenyl)ethynyl]-1,2,4,5-tetramethoxybenzene (161)**



A solution of diiodide **162** (990 mg, 2.22 mmol, 1 eq) in THF (200 mL) was degassed by bubbling argon through the solution for 30 min. CuI (125 mg, 30 mol%), Pd(PPh₃)₂Cl₂ (500 mg, 32 mol%), and Et₃N (10 mL) were added to the degassed solution and stirred at rt for 10 min. Alkyne **163** (1.40 g, 6.10 mmol, 2.75 eq) was added to the solution and the reaction was heated to reflux for 16 h. The reaction was cooled to rt, silica gel was added, and the slurry was concentrated. The residue was filtered through a silica gel plug (petroleum ether/CH₂Cl₂, 1:1) and the filtrate was concentrated. Chromatography (petroleum ether/CH₂Cl₂, 2:1) afforded **161** as an orange solid (842 mg, 78%); mp: 91-92 °C; IR (CDCl₃) ν 2961.0, 2936.3, 2213.3, 1592.6, 1495.0 cm⁻¹; ¹H NMR (500 MHz, CDCl₃) δ 7.16 (t, J = 7.9 Hz, 2H), 6.87-6.78 (m, 4H), 6.63 (dd, J = 8.3, 2.1 Hz, 2H), 3.98 (s, 12H), 3.26 (t, J = 7.4 Hz, 8H), 1.63-1.52 (m, 8H), 1.42-1.31 (m, 8H), 0.95 (t, J = 7.3 Hz, 12H); ¹³C NMR (125 MHz, CDCl₃) δ 150.2 (s), 148.0 (s), 129.1 (d), 123.8 (s), 118.7 (d), 114.6 (d), 114.1 (s), 112.4 (d), 110.7 (s), 80.0 (s), 61.4 (q), 50.7 (t), 29.4 (t), 20.3 (t), 14.0 (q); MS (ES) m/z 653.3 (M^+ , 0.4), 551.9 (0.4), 396.2 (0.2), 115.0 (100).

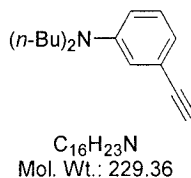
1,4-Diiodo-2,3,5,6-tetramethoxybenzene (162)



A solution of *n*-BuLi (2.5 M in hexanes, 25.2 mL, 63.1 mmol, 2.5 eq) was added to a -78 °C solution of 1,2,4,5-tetramethoxybenzene (**164**) (5.00 g, 25.2 mmol, 1 eq) in THF (500 mL). The reaction was stirred at -78 °C for 5 min then warmed to 0 °C for 1 h. The

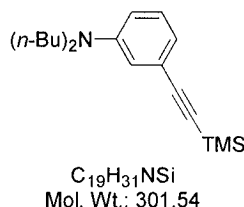
reaction was recooled to $-78\text{ }^{\circ}\text{C}$ and a solution of iodine (19.18 g, 75.6 mmol, 3 eq) in THF (100 mL) was added by canula over 20 min. The reaction was warmed to $0\text{ }^{\circ}\text{C}$ for 10 min then heated to reflux for 1 h. The reaction mixture was cooled to rt and quenched with a solution of sodium thiosulfate ($\text{Na}_2\text{S}_2\text{O}_3$, 10% aq). Ethyl acetate extracts (2x) were combined, washed with H_2O and brine, dried, and concentrated. Chromatography (petroleum ether/EtOAc, 9:1) gave **162** as a colourless solid (7.95 g, 70%); mp: $125\text{-}133\text{ }^{\circ}\text{C}$ (dec.); ^1H NMR (500 MHz, CDCl_3) δ 3.82 (s, 12H); ^{13}C NMR (125 MHz, CDCl_3) δ 149.6 (s), 91.6 (s), 60.6 (q); MS (EI) m/z 449.9 (M^+ , 100), 434.9 (31), 406.9 (33), 292.9 (11); HRMS calcd for $\text{C}_{10}\text{H}_{12}\text{I}_2\text{O}_4$ 449.8825 (M^+), found 449.8843. Characterization data of **162** agreed with the reported data.^{92c}

***N,N*-Dibutyl-3-ethynylaniline (163)**



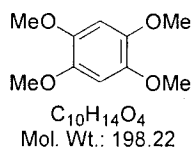
Silylalkyne **163a** (5.00 g, 16.6 mmol, 1 eq) and KOH (1.86 g, 33.2 mmol, 2 eq) were combined in MeOH (50 mL) and stirred at rt for 1h. NH_4Cl (sat. aq) was added until the solution was acidic by litmus paper. Et_2O extracts (3x) were washed with NaHCO_3 (sat. aq), H_2O , and brine, dried, and concentrated to afford **163** as a yellow oil (3.71 g, 98%) that did not require chromatography; IR (neat) ν 3313.2, 2957.7, 2872.8, 2107.2, 1594.2, 772.3 cm^{-1} ; ^1H NMR (500 MHz, CDCl_3) δ 7.13 (br dd, $J = 7.9, 8.0$ Hz, 1H), 6.76-6.73 (m, 2H), 6.61 (br d, $J = 6.5$ Hz, 1H), 3.23 (t, $J = 7.6$ Hz, 4H), 2.98 (s, 1H), 1.57-1.51 (m, 4H), 1.38-1.30 (m, 4H), 0.94 (t, $J = 7.3$ Hz, 6H); ^{13}C NMR (125 MHz, CDCl_3) δ 148.0 (s), 129.1 (d), 122.5 (s), 119.0 (d), 115.0 (d), 112.5 (d), 84.9 (s), 75.6 (s), 50.7 (t), 29.3 (t), 20.3 (t), 14.0 (q); MS (EI) m/z 229.2 (M^+ , 32), 186.1 (100), 144.1 (53), 130.1 (49); HRMS calcd for $\text{C}_{16}\text{H}_{23}\text{N}$ 229.1832 (M^+), found 229.1834.

***N,N*-Dibutyl-3-(2-trimethylsilylethynyl)aniline (163a)**



A solution of iodide **109** (10.01 g, 30.2 mmol, 1 eq) in THF (200 mL) was degassed by bubbling argon through the solution for 30 min. CuI (133 mg, 2.5 mol%), Pd(PPh₃)₂Cl₂ (500 mg, 2.5 mol%), and Et₃N (10 mL) were added to the degassed solution and stirred at rt for 10 min. Trimethylsilyl-acetylene (**37**) (6.4 mL, 45.3 mmol, 1.5 eq) was added to the solution and the reaction was stirred at rt for 16 h. The reaction was filtered through a silica gel plug and the filtrate was concentrated. The residue was dissolved in petroleum ether and washed with HCl (10% aq), Na₂S₂O₃ (10% aq), and brine (100 mL), dried, and concentrated. Chromatography (petroleum ether) afforded **163a** as a yellow oil (8.72 g, 96%); IR (neat) ν 2956.4, 2873.2, 2155.7, 1594.2, 843.0 cm⁻¹; ¹H NMR (500 MHz, CDCl₃) δ 7.09 (dd, J = 7.9, 8.0 Hz, 1H), 6.72 (d, J = 7.5 Hz, 1H), 6.70 (br s, 1H), 6.59 (dd, J = 8.4, 2.6 Hz, 1H), 3.23 (t, J = 7.5 Hz, 4H), 1.57-1.49 (m, 4H), 1.37-1.30 (m, 4H), 0.94 (t, J = 7.4 Hz, 6H), 0.24 (s, 9H); ¹³C NMR (125 MHz, CDCl₃) δ 148.0 (s), 128.9 (d), 123.5 (s), 119.1 (d), 114.9 (d), 112.2 (d), 106.4 (s), 92.4 (s), 50.6 (t), 29.3 (t), 20.3 (t), 14.0 (q), 0.1 (q); MS (EI) m/z 301.2 (M⁺, 26), 286.2 (10), 258.2 (100), 216.1 (36), 186.1 (24); HRMS calcd for C₁₉H₃₁NSi 301.2227 (M⁺), found 301.2216.

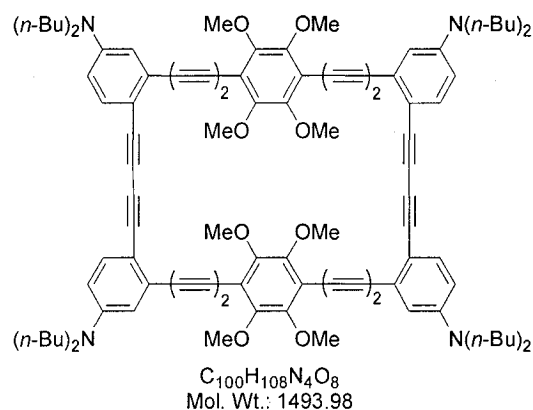
1,2,4,5-Tetramethoxybenzene (164)



1,4-Dihydroxy-2,5-dimethoxybenzene (13.2 g, 77.6 mmol, 1 eq), Me₂SO₄ (44 mL, 465 mmol, 6 eq), and sodium hydrosulphite (Na₂S₂O₄, 1.35 g, 7.76 mmol, 10 mol%) were combined in MeOH (30 mL) and the solution was cooled in an ice bath. A solution of NaOH (18.6 g, 465 mmol, 6 eq) in H₂O (40 mL) was added over 30 min. The reaction was then warmed to 70-80 °C for 30 min, diluted with H₂O (100 mL) and cooled in an ice bath. Filtration gave **164** as a colourless solid (13.1 g, 85%); mp: 97-98 °C; ¹H NMR (500 MHz,

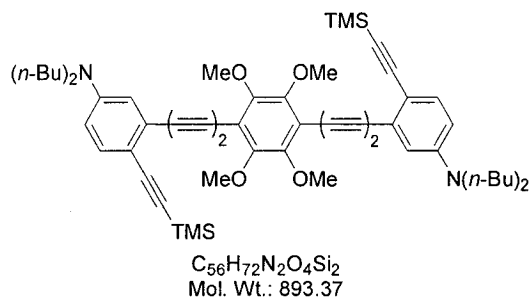
CDCl₃) δ 6.57 (s, 2H), 3.81 (s, 12H); ¹³C NMR (125 MHz, CDCl₃) δ 143.0 (s), 100.4 (d), 56.9 (q); MS (EI) *m/z* 198.1 (M⁺, 100), 183.1 (74), 155.1 (49), 125.0 (24); HRMS calcd for C₁₀H₁₄O₄ 198.0892 (M⁺), found 198.0900. Characterization data of **164** agreed with the reported data.^{92a}

17,28,47,58-tetrakis-dibutylamino-6,7,9,10,36,37,39,40-octamethoxy[4]1,3-butadiynylparacyclo[4]11,13-butadiynylorthocyclo[4]21,23-butadiynylorthocyclo[4]31,33-butadiynylparacyclo[4]41,43-butadiynylorthocyclo[4]51,53-butadiynylorthocyclophane (170)



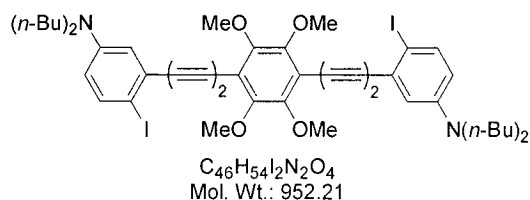
A solution of ethyl bromoacetate (192 μL, 1.74 mmol, 4 eq) in THF (100 mL) was degassed by bubbling argon through the solution for 30 min. CuI (10 mg, 3 mol%), Pd(PPh₃)₂Cl₂ (30 mg, 2.5 mol%), and diisopropylethylamine (605 μL, 3.47 mmol, 8 eq) were added to the degassed solution and stirred at rt for 10 min. A solution of dialkyne **178** (295 mg, 0.39 mmol, 1 eq) in THF (50 mL) was added dropwise by syringe pump over 10 h and the reaction was stirred at rt for an additional 14 h. The reaction was filtered through a silica gel plug and the filtrate was concentrated. Chromatography (petroleum ether/CH₂Cl₂, 1:1) afforded **170** as a yellow solid (102 mg, 35%); mp: 155-157 °C; IR (CH₂Cl₂) ν 2959.6, 2871.1, 2133.3, 1590.6, 1400.8 cm⁻¹; ¹H NMR (500 MHz, CDCl₃) δ 7.38 (d, *J* = 8.9 Hz, 4H), 6.78 (d, *J* = 2.4 Hz, 4H), 6.63 (dd, *J* = 9.0, 2.3 Hz, 4H), 3.88 (s, 24H), 3.30 (t, *J* = 7.6 Hz, 16H), 1.61-1.53 (m, 16H), 1.41-1.33 (m, 16H), 0.97 (t, *J* = 7.3 Hz, 24H); ¹³C NMR (125 MHz, CDCl₃) δ 151.8 (s), 148.5 (s), 135.8 (d), 125.3 (s), 116.2 (d), 114.1 (s), 113.6 (d), 111.1 (s), 84.04 (s), 83.98 (s), 82.6 (s), 76.9 (s), 76.6 (s), 75.1 (s), 62.1 (q), 51.3 (t), 29.8 (t), 20.8 (t), 14.3 (q); MS (ES) *m/z* 1494.7 (M⁺), 766.5, 748.2, 329.0.

***N,N,N',N'*-Tetrabutyl-3,6-bis-[4-(5-amino-2-(2-triisopropylsilylethynyl)phenyl)-1,3-butadiynyl]-1,2,4,5-tetramethoxybenzene (172)**



A solution of diiodide **173** (3.05 g, 3.20 mmol, 1 eq) in THF (250 mL) was degassed by bubbling argon through the solution for 30 min. CuI (60 mg, 10 mol%), Pd(PPh₃)₂Cl₂ (360 mg, 16 mol%), and Et₃N (15 mL) were added to the degassed solution and stirred at rt for 10 min. Trimethylsilyl-acetylene (**37**) (3.10 mL, 21.8 mmol, 6.8 eq) was added to the solution and the reaction was stirred at rt for 16 h. The reaction was diluted with petroleum ether (100 mL), filtered through a silica gel plug, and concentrated. Chromatography (petroleum ether/CH₂Cl₂, 1:1) afforded **172** as a yellow foam (1.14 g, 40%); IR (CDCl₃) ν 2961.3, 2874.9, 2147.0, 1594.8, 1465.3 cm⁻¹; ¹H NMR (500 MHz, CDCl₃) δ 7.25 (d, *J* = 8.7 Hz, 2H), 6.70 (d, *J* = 2.3 Hz, 2H), 6.51 (dd, *J* = 8.8, 2.2 Hz, 2H), 3.93 (s, 12H), 3.23 (t, *J* = 7.6 Hz, 8H), 1.55-1.49 (m, 8H), 1.37-1.29 (m, 8H), 0.94 (t, *J* = 7.4 Hz, 12H), 0.25 (s, 18H); ¹³C NMR (125 MHz, CDCl₃) δ 151.4 (s), 147.6 (s), 133.1 (d), 125.7 (s), 115.0 (d), 113.8 (s), 112.7 (s), 112.4 (d), 104.4 (s), 95.8 (s), 83.9 (s), 83.8 (s), 76.3 (s), 73.4 (s), 61.5 (q), 50.7 (t), 29.3 (t), 20.3 (t), 13.9 (q), 0.2 (q); MS (ES) *m/z* 893.4 (M⁺), 315, 210, 154.

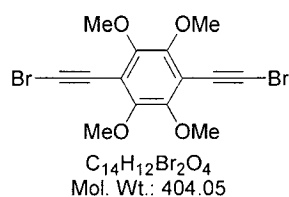
***N,N,N',N'*-Tetrabutyl-3,6-bis-[4-(5-amino-2-iodophenyl)-1,3-butadiynyl]-1,2,4,5-tetramethoxybenzene (173)**



Diamine **176** (1.10 g, 1.57 mmol, 1 eq), BnNMe₃ICl₂ (1.15 g, 3.30 mmol, 2.1 eq), and CaCO₃ (440 mg, 4.40 mmol, 2.8 eq) were combined in a mixture of CH₂Cl₂/MeOH (5:1, 30 mL) and stirred at rt for 4 h. The reaction mixture was poured into HCl (10% aq) and extracted with CH₂Cl₂ (2x). The organic extracts were washed with NaHCO₃ (10% aq) and H₂O, dried, and concentrated. Chromatography (petroleum ether/CH₂Cl₂, 1:1) afforded **173**

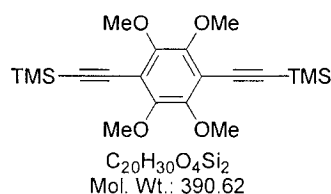
as a yellow solid (1.39 g, 93%); mp: 126-127 °C; IR (CDCl₃) ν 2964.6, 2876.7, 2244.2, 2238.6, 1578.6, 1457.6 cm⁻¹; ¹H NMR (500 MHz, CDCl₃) δ 7.50 (d, J = 9.0 Hz, 2H), 6.79 (d, J = 2.8 Hz, 2H), 6.36 (dd, J = 8.9, 2.8 Hz, 2H), 3.95 (s, 12H), 3.20 (t, J = 7.9 Hz, 8H), 1.54-1.48 (m, 8H), 1.36-1.28 (m, 8H), 0.93 (t, J = 7.3 Hz, 12H); ¹³C NMR (125 MHz, CDCl₃) δ 151.4 (s), 147.7 (s), 138.9 (d), 128.3 (s), 117.1 (d), 115.0 (d), 113.8 (s), 86.5 (s), 83.7 (s), 81.6 (s), 75.9 (s), 74.1 (s), 61.6 (q), 50.7 (t), 29.2 (t), 20.3 (t), 14.0 (q); MS (ES) m/z 953.0 (M⁺), 853.0, 811.0, 780.9, 685.1.

3,5-Bis-bromoethynyl-1,2,4,5-tetramethoxybenzene (174)



A solution of silylalkyne **175** (2.00 g, 5.12 mmol, 1 eq) and *N*-bromosuccinimide (2.10 g, 11.8 mmol, 2.3 eq) in acetone (30 mL) was stirred at rt for 10 min. Silver nitrate (157 mg, 1.02 mmol, 20 mol%) was added and the reaction was stirred at rt for 14 h. TLC (petroleum ether/EtOAc, 9:1) showed that starting material remained. Silver nitrate (163 mg) and NBS (200 mg) were added and the reaction was stirred for an additional 24 h. The reaction mixture was diluted with H₂O, extracted with EtOAc (3x), washed with H₂O and brine, dried, and concentrated. Chromatography (petroleum ether/EtOAc, 9:1) afforded **174** as an orange solid (1.33 g, 64%); mp: 124-126 °C; IR (CDCl₃) ν 2933.9, 2195.6, 1466.2, 1401.9 cm⁻¹; ¹H NMR (500 MHz, CDCl₃) δ 3.88 (s, 12H); ¹³C NMR (125 MHz, CDCl₃) δ 150.9 (s), 113.8 (s), 71.8 (s), 61.4 (q), 58.9 (s); MS (EI) m/z 405.9 (⁸¹Br₂, 48), 403.9 (⁸¹Br⁷⁹Br₂, 100), 401.9 (⁷⁹Br₂, M⁺, 49), 360.9 (31), 345.9 (45), 274.9 (6); HRMS calcd for C₁₄H₁₂Br₂O₄ 401.9102 (M⁺), found 401.9124.

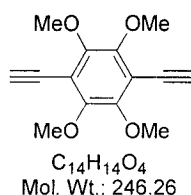
1,2,4,5-Tetramethoxy-3,6-bis-(trimethylsilylethynyl)benzene (175)



A solution of diiodide **162** (2.50 g, 5.56 mmol, 1 eq) in THF (200 mL) was degassed by bubbling argon through the solution for 30 min. CuI (125 mg, 12 mol%), Pd(PPh₃)₂Cl₂

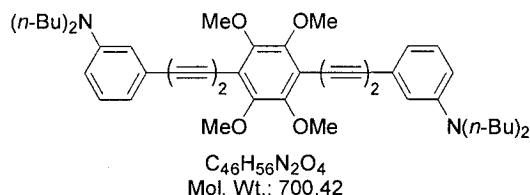
(500 mg, 12 mol%), and Et₃N (10 mL) were added to the degassed solution and stirred at rt for 10 min. Trimethylsilyl-acetylene (**37**) (1.81 mL, 12.8 mmol, 2.3 eq) was added to the solution and the reaction was heated at reflux for 16 h. GC/MS was used to determine the reaction had reached completion as TLC analysis was not conclusive. The reaction was cooled to rt and poured into H₂O. Et₂O extracts (2x) were combined and washed with brine, dried, and concentrated. Chromatography (petroleum ether/EtOAc, 99:1) afforded **175** as a colourless solid (1.79 g, 82%); mp: 99-101 °C; ¹H NMR (500 MHz, CDCl₃) δ 3.87 (s, 12H), 0.25 (s, 18H); ¹³C NMR (125 MHz, CDCl₃) δ 150.7 (s), 114.2 (s), 105.3 (s), 96.2 (s), 61.1 (q), -0.1 (q); MS (EI) *m/z* 390.2 (M⁺, 100), 347.2 (38), 332.1 (25), 317.1 (10); HRMS calcd for C₂₀H₃₀O₄Si₂ 390.1683 (M⁺), found 390.1707.

3,6-Diethynyl-1,2,4,5-tetramethoxybenzene (**175a**)



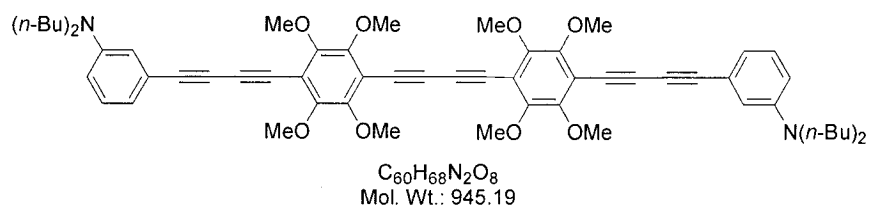
A solution of silylalkyne **175** (1.60 g, 4.10 mmol, 1 eq) and KOH (1.15 g, 20.0 mmol, 5 eq) in MeOH (25 mL) was stirred at rt for 18 h. TLC (petroleum ether/EtOAc, 97:3) showed no starting material remained. HCl (10% aq) was added until the reaction mixture was acidic by litmus paper. Ether extracts (3x) were washed with HCl (10% aq) and brine, dried, and concentrated. Chromatography (petroleum ether/EtOAc, 19:1) afforded **175a** as a near-colourless solid (0.69 g, 68%); mp: 109-110 °C; ¹H NMR (500 MHz, CDCl₃) δ 3.90 (s, 12H), 3.54 (s, 2H); ¹³C NMR (125 MHz, CDCl₃) δ 150.9 (s), 113.4 (s), 86.8 (d), 75.1 (s), 61.3 (q); MS (EI) *m/z* 246.1 (M⁺, 100), 231.1 (31), 203.1 (23), 188.0 (33); HRMS calcd for C₁₄H₁₄O₄ 246.0892 (M⁺), found 246.0881.

***N,N,N',N'*-Tetrabutyl-3,6-bis-[4-(3-aminophenyl)-1,3-butadiynyl]-1,2,4,5-tetramethoxybenzene (176)**



Hydroxylamine hydrochloride ($NH_2OH \cdot HCl$) (739 mg, 10.6 mmol, 3.3 eq) was dissolved in a mixture of *n*- $BuNH_2/H_2O$ (5:2, 30 mL) and was degassed by bubbling argon through the solution for 10 min. Alkyne **163** (1.48 g, 6.44 mmol, 2.1 eq) was added and degassing was continued for 10 min. Copper (I) chloride (255 mg, 2.58 mmol, 80 mol%) was added and the solution turned bright yellow. A solution of dibromide **174** (1.30 g, 3.22 mmol, 1 eq) in a mixture of *n*- $BuNH_2/THF$ (1:2, 30 mL) was added dropwise over 20 min and the reaction was stirred at rt for 14 h. The reaction was diluted with NH_4Cl (sat. aq), extracted with CH_2Cl_2 (2x), washed with H_2O (3x) and brine, dried, and concentrated. Chromatography (petroleum ether/ CH_2Cl_2 , 1:1) afforded **176** as a yellow wax (1.21 g, 58%); mp: 101-102 °C; IR ($CDCl_3$) ν 2961.2, 2937.5, 2212.9, 2144.2, 1591.4 cm^{-1} ; 1H NMR (500 MHz, $CDCl_3$) δ 7.12 (dd, $J = 8.0, 7.9$ Hz, 2H), 6.79 (d, $J = 7.5$ Hz, 2H), 6.76 (br s, 2H), 6.63 (dd, $J = 8.4, 2.3$ Hz, 2H), 3.94 (s, 12H), 3.23 (t, $J = 7.6$ Hz, 8H), 1.57-1.50 (m, 8H), 1.38-1.30 (m, 8H), 0.95 (t, $J = 7.4$ Hz, 12H); ^{13}C NMR (125 MHz, $CDCl_3$) δ 151.3 (s), 148.0 (s), 129.2 (d), 122.1 (s), 119.4 (d), 115.2 (d), 113.8 (s), 113.2 (d), 85.6 (s), 83.9 (s), 72.8 (s), 72.6 (s), 61.5 (q), 50.7 (t), 29.3 (t), 20.3 (t), 14.0 (q); MS (EI) m/z 700.4 (M^+ , 77), 657.3 (100), 615.3 (10), 307.2 (35); HRMS calcd for $C_{46}H_{56}N_2O_4$ 700.4240 (M^+), found 700.4258.

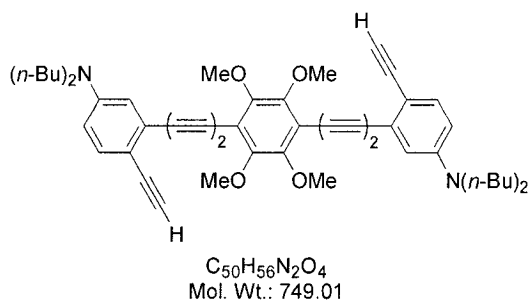
Compound 177



A yellow wax (197 mg, 13%) was also obtained from the reaction of alkyne **163** and dibromide **174** and was found to be **177**; mp: 143-147 °C; IR ($CDCl_3$) ν 2961.8, 2213.3, 2141.1, 1586.6, 1492.4 cm^{-1} ; 1H NMR (500 MHz, $CDCl_3$) δ 7.12 (dd, $J = 8.1, 7.9$ Hz, 2H), 6.79 (d, $J = 7.5$ Hz, 2H), 6.76 (br s, 2H), 6.63 (dd, $J = 8.3, 2.0$ Hz, 2H), 3.94 (s, 12H), 3.93 (s,

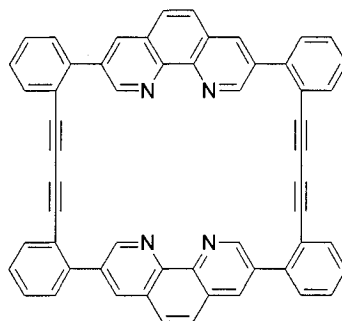
12H), 3.23 (t, $J = 7.6$ Hz, 8H), 1.57-1.51 (m, 8H), 1.38-1.30 (m, 8H), 0.94 (t, $J = 7.4$ Hz, 12H); ^{13}C NMR (125 MHz, CDCl_3) δ 151.4 (s), 148.0 (s), 129.2 (d), 122.0 (s), 119.4 (d), 115.2 (d), 114.2 (s), 113.5 (s), 113.2 (d), 86.8 (s), 85.8 (s), 84.1 (s), 83.4 (s), 75.7 (s), 72.7 (s), 72.5 (s), 61.6 (q), 50.7 (t), 29.3 (t), 20.3 (t), 14.0 (q); MS (ES) m/z 945.4 (M^+), 473.6, 210.1, 83.1.

***N,N,N',N'*-Tetrabutyl-3,6-bis-[4-(5-amino-2-ethynylphenyl)-1,3-butadiynyl]-1,2,4,5-tetramethoxybenzene (178)**



Silylalkyne **172** (659 mg, 0.74 mmol, 1 eq) and KOH (215 mg, 3.84 mmol, 3 eq) were combined in a mixture of THF/MeOH (2:1, 60 mL) with H_2O (3 drops). The reaction was stirred at rt for 3 h. HCl (10% aq) was added to the reaction until the solution was pH~3 by litmus paper. Et_2O extracts (3x) were combined and washed with H_2O and brine, dried, and concentrated. Chromatography (petroleum ether/ CH_2Cl_2 , 2:1) afforded **178** as a yellow solid (553 mg, 91%); mp: 139-141 $^\circ\text{C}$; IR (CDCl_3) ν 3306.0, 2956.9, 2098.4, 1594.6, 1400.1 cm^{-1} ; ^1H NMR (500 MHz, CDCl_3) δ 7.29 (d, $J = 8.8$ Hz, 2H), 6.73 (d, $J = 2.6$ Hz, 2H), 6.54 (dd, $J = 8.8, 2.6$ Hz, 2H), 3.94 (s, 12H), 3.24 (t, $J = 7.6$ Hz, 8H), 3.20 (s, 2H), 1.57-1.51 (m, 8H), 1.38-1.30 (m, 8H), 0.95 (t, $J = 7.4$ Hz, 12H); ^{13}C NMR (125 MHz, CDCl_3) δ 151.4 (s), 147.8 (s), 133.8 (d), 125.5 (s), 115.2 (d), 113.8 (s), 112.5 (s), 111.3 (d), 83.9 (s), 83.6 (s), 82.7 (s), 78.6 (d), 76.1 (s), 73.6 (s), 61.6 (q), 50.7 (t), 29.3 (t), 20.3 (t), 13.9 (q); MS (ES) m/z 749.3 (M^+), 375.3, 168.8, 102.0.

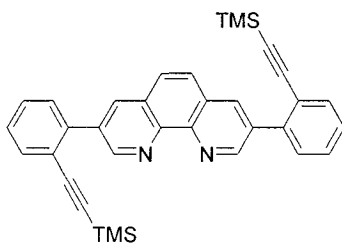
[4]1,3-Butadiynylorthocyclo[0](3,8)-1,10-phenanthroleno[0]orthocyclo[4]31,33-butadiynylorthocyclo[0](3,8)-1,10-phenanthroleno[0]orthocyclophane (200)



C₅₆H₂₈N₄
Mol. Wt.: 756.85

Copper(II)(phenanthroline) complex **213** (185 mg, 0.20 mmol, 1 eq) was dissolved in CH₂Cl₂ (25 mL) and was washed with KCN (10% aq, 25 mL), H₂O, and brine and concentrated to yield **200** as a yellow solid (149 mg, quant.). Poor solubility prevented further purification; mp: 150 °C (dec.); ¹H NMR (500 MHz, CDCl₃) δ 9.33 (br s, 4H), 8.87 (br s, 4H), 7.82-7.77 (m, 12H), 7.63 (br s, 4H), 7.40 (br s, 4H); ¹³C NMR (125 MHz, CDCl₃) δ 150.4 (d), 144.3 (s), 140.0 (s), 135.9 (d), 133.7 (s), 133.1 (d), 132.3 (d), 131.4 (d), 130.8 (d), 127.7 (s), 126.9 (d), 118.9 (s), 81.4 (s), 76.3 (s); MS (ES) *m/z* 757.0 (M⁺, 1), 579.1 (2), 279.0 (4), 141.9 (53).

3,8-Bis-[2-(2-trimethylsilylethynyl)phenyl]-1,10-phenanthroline (202)



C₃₄H₃₂N₂Si₂
Mol. Wt.: 524.80

A solution of *n*-BuLi (2.5 M in THF, 10.84 mL, 27.1 mmol, 3.05 eq) was added in one portion to a -78 °C solution of 2-bromo-1-(trimethylsilylethynyl)-benzene (**204**) (5.66 mL, 26.6 mmol, 3 eq) in THF (150 mL). After stirring at -78 °C for 15 min, a solution of ZnBr₂ (6.10 g, 27.1 mmol, 3.05 eq) in THF (50 mL) was added by canula. Once the addition was complete, the reaction was warmed to 0 °C and stirred for 20 min. A degassed solution of 3,8-dibromo-1,10-phenanthroline (**203**) (3.01 g, 8.88 mmol, 1 eq) and Pd(PPh₃)₄ (1.00 g, 11 mol%) in a mixture of THF/DMF (1:1, 300 mL) was added to the reaction by canula.

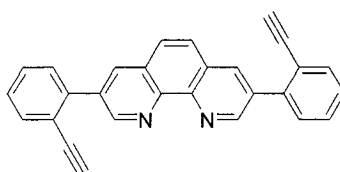
(Note: all of the phenanthroline must be dissolved before it is added to the reaction or poor yields are obtained). The reaction mixture was heated at reflux for 72 h. The reaction was concentrated, the dark residue was dissolved in CH₂Cl₂, washed with water (5x to remove residual DMF) and brine, and concentrated. Chromatography (CH₂Cl₂ to CH₂Cl₂/MeOH, 50:1) afforded **202** as a yellow oil (5.01 g) which could be crystallized from ether (4.12 g, 87%); mp: 140-143 °C; IR (CH₂Cl₂) ν 3054.5, 2963.2, 2156.0, 1260.4, 862.4 cm⁻¹; ¹H NMR (500 MHz, CDCl₃) δ 9.25 (s, 2H), 8.81 (d, *J* = 1.6 Hz, 2H), 7.95 (s, 2H), 7.58 (d, *J* = 7.6 Hz, 2H), 7.38-7.30 (m, 6H), 0.03 (s, 18H); ¹³C NMR (125 MHz, CDCl₃) δ 150.9 (d), 145.2 (s), 140.3 (s), 136.1 (d), 135.1 (s), 133.7 (d), 129.6 (d), 129.0 (d), 128.0 (d), 127.8 (s), 126.9 (d), 122.1 (s), 104.0 (s), 98.5 (s), -0.3 (q); MS (EI) *m/z* 524.2 (M⁺, 39), 277.1 (100), 262.1 (24), 201.0 (43); HRMS calcd for C₃₄H₃₂N₂Si₂ 524.2104 (M⁺), found 524.2056.

3,8-Dibromo-1,10-phenanthroline (**203**)



Sulfur monochloride (0.89 mL, 11.1 mmol, 2 eq) was added to a solution of 1,10-phenanthroline (**197**) (1.01 g, 5.55 mmol, 1 eq) in 1,2-dichloroethane (50 mL) and stirred at rt until a yellow precipitate formed. Addition of pyridine (0.99 mL, 12.2 mmol, 2.2 eq), led to a yellow homogeneous solution. Bromine (0.57 mL, 11.1 mmol, 2 eq) was added to the reaction and the reaction was heated at reflux for 72 h. The reaction was cooled to rt and quenched with a solution of HCl (10% aq) and stirred for 30 min. The reaction mixture was extracted with CHCl₃ (3x) and the combined extracts were washed with NaHCO₃ (10% aq) and brine, and concentrated. Chromatography (CH₂Cl₂ to CH₂Cl₂/MeOH, 50:1) afforded dibromide **203** as a colorless solid (1.10 g, 59%); ¹H NMR (500 MHz, CDCl₃) δ 9.15 (s, 2H), 8.36 (d, *J* = 2.2 Hz, 2H), 7.71 (s, 2H); ¹³C NMR (125 MHz, CDCl₃) δ 151.5 (d), 144.0 (s), 137.6 (d), 129.6 (s), 126.9 (d), 120.2 (s); Anal. calcd for C₁₂H₆Br₂N₂ C 42.64%, H 1.79%, found C 42.80%, H 1.86%. Characterization data of **203** agreed with the reported data.¹¹⁹

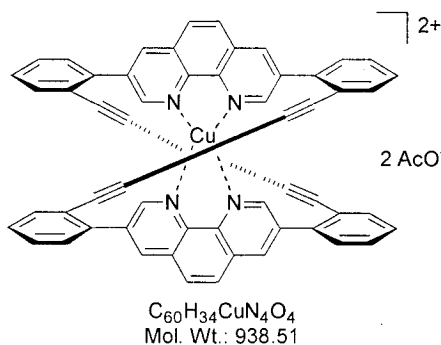
3,8-Bis-(2-ethynylphenyl)-1,10-phenanthroline (**212**)



$C_{28}H_{16}N_2$
Mol. Wt.: 380.44

Silylalkyne **202** (2.85 g, 5.43 mmol, 1 eq) and K_2CO_3 (300 mg) were combined in a mixture of $CH_2Cl_2/MeOH$ (3:2, 35 mL) with H_2O (3 drops) and stirred at rt for 72 h. The reaction mixture was poured into H_2O and extracted with CH_2Cl_2 (3x). The combined extracts were washed with H_2O and brine and concentrated. Chromatography ($CH_2Cl_2/MeOH$, 49:1) afforded **212** as a yellow solid (1.87 g, 91%); mp: 189 °C (dec.); IR ($CHCl_3$) ν 3021.2, 2400.4, 1424.5, 1219.4, 774.4 cm^{-1} ; 1H NMR (500 MHz, $CDCl_3$) δ 9.43 (d, $J = 2.2$ Hz, 2H), 8.43 (d, $J = 2.2$ Hz, 2H), 7.86 (s, 2H), 7.69 (dd, $J = 7.7, 1.1$ Hz, 2H), 7.54 (dd, $J = 7.7, 1.5$ Hz, 2H), 7.50 (ddd, $J = 7.5, 7.5, 1.3$ Hz, 2H), 7.41 (ddd, $J = 7.5, 7.5, 1.5$ Hz, 2H), 3.06 (s, 2H); ^{13}C NMR (125 MHz, $CDCl_3$) δ 151.1 (d), 145.1 (s), 140.6 (s), 135.7 (d), 135.2 (s), 134.0 (d), 129.8 (d), 129.4 (d), 128.13 (d), 128.10 (s), 126.9 (d), 121.1 (s), 104.0 (s), 98.5 (d); MS (ES) m/z 380 (M^+ , 77), 351 (6), 189 (11), 32 (100); HRMS calcd for $C_{28}H_{16}N_2$ 380.1313 (M^+), found 380.1329.

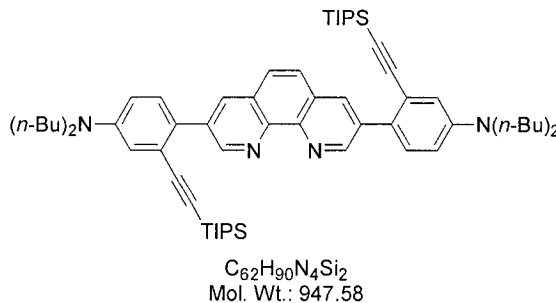
Copper(II){[4]1,3-butadiynylorthocyclo[0](1,10)phenanthroleno[0]orthocyclo[4]31,33-butadiynylorthocyclo[0](1,10)phenanthroleno[0]orthocyclophane} diacetate (**213**)



A solution of $Cu(OAc)_2$ (47.7 mg, 2.62 mmol, 0.5 eq) in pyridine/ Et_2O (3:1, 20 mL) was added over 2 h by syringe pump to a solution of **212** (200 mg, 5.26 mmol, 1 eq) in pyridine/ Et_2O (3:1, 225 mL) to template the oxidative dimerization. The solution turned from yellow to dark red. Additional $Cu(OAc)_2$ (525 mg, 2.89 mmol, 5.5 eq) was added to the reaction and the solution turned green immediately. The reaction was stirred at rt for 18 h

and poured into H₂O. The aqueous phase was extracted with CH₂Cl₂ (3x) and the combined extracts were filtered through Celite and concentrated to afford **213** as a red solid (172 mg, 70%); mp: > 260 °C; IR (CH₂Cl₂) ν 3049.9, 1604.0, 1436.7, 1266.8, 1119.7 cm⁻¹; ¹H NMR (500 MHz, DMSO-d₆) δ 9.25 (br s, 4H), 8.84 (br s, 4H), 8.37 (br s, 4H), 7.65 (br s, 4H), 7.41 (br s, 12H); ¹³C NMR (125 MHz, DMSO-d₆) δ 149.2 (d), 141.6 (s), 139.8 (s), 136.7 (d), 136.4 (s), 133.5 (d), 130.8 (d), 129.8 (d), 129.0 (d), 128.7 (s), 127.7 (d), 118.9 (s), 81.3 (s), 76.0 (s); MS (ES) 877.8 (M⁺-OAc, 73), 818.8 (M⁺-(OAc)₂, 100), 409.5 (39). Anal. calcd for C₆₀H₃₂N₄O₄ C 76.79%, H 3.65%; found C 76.59%, H 3.99%. Note: When KCN(aq) was included in the workup, copper-free cyclophane **200** was obtained.

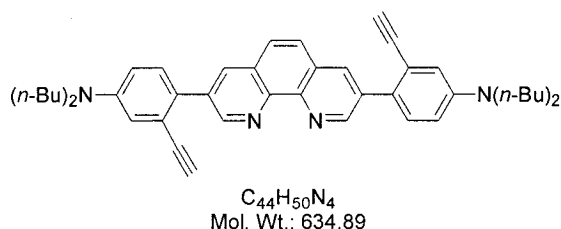
***N,N,N',N'*-Tetrabutyl-3,8-bis-[4-amino-2-(2-triisopropylsilylethynyl)phenyl]-1,10-phenanthroline (**216**)**



A solution of *n*-BuLi (1.60 M in THF, 5.65 mL, 9.03 mmol, 3.05 eq) was added in one portion to a -78 °C solution of iodide **118** (4.54 g, 8.88 mmol, 3 eq) in THF (150 mL). After stirring at -78 °C for 15 min a solution of ZnBr₂ (2.03 g, 9.03 mmol, 3.05 eq) in THF (50 mL) was added by canula. Once the addition was complete the reaction was warmed to 0 °C and stirred for 20 min. A degassed solution of 3,8-dibromo-1,10-phenanthroline (**203**) (1.00 g, 2.96 mmol, 1 eq) and Pd(PPh₃)₄ (175 mg, 10 mol%) in a mixture of THF/DMF (1:1, 300 mL) was added to the reaction by canula. (Note: all of the phenanthroline must be dissolved before it is added to the reaction or poor yields are obtained.) The reaction mixture was heated at reflux for 72 h. The reaction was concentrated, taken up in CH₂Cl₂, washed with H₂O (5x to remove residual DMF) and brine and concentrated. Chromatography (CH₂Cl₂/MeOH, 50:1) afforded **216** as a yellow foam (1.91 g, 70%); mp: 66-70 °C; IR (CH₂Cl₂) ν 2984.6, 2305.7, 1597.9, 1417.6, 1262.0 cm⁻¹; ¹H NMR (500 MHz, CDCl₃) δ 9.23 (s, 2H), 8.59 (s, 2H), 7.71 (s, 2H), 7.37 (d, *J* = 8.6 Hz, 2H), 6.92 (br s, 2H), 6.74 (d, *J* = 7.3 Hz, 2H), 3.32 (t, *J* = 7.5 Hz, 8H), 1.64-1.56 (m, 8H), 1.42-1.33 (m, 8H), 0.99-0.93 (m, 54H);

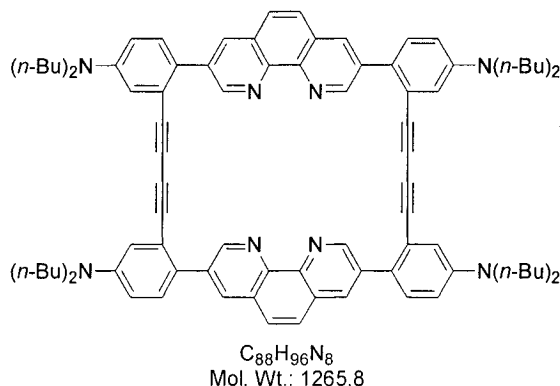
^{13}C NMR (125 MHz, CDCl_3) δ 150.6 (d), 147.5 (s), 144.6 (s), 135.5 (d), 135.2 (s), 130.5 (d), 127.6 (s), 126.7 (s), 126.5 (d), 122.8 (s), 116.8 (d), 112.6 (d), 107.2 (s), 92.9 (s), 50.7 (t), 29.3 (t), 20.4 (t), 18.5 (q), 13.9 (q), 11.2 (d); MS (ES) m/z 947.5 (M^+ , 100), 644.2 (34), 474.4 (32), 338.9 (26).

***N,N,N',N'*-Tetrabutyl-3,8-bis-(4-amino-2-ethynylphenyl)-1,10-phenanthroline (216a)**



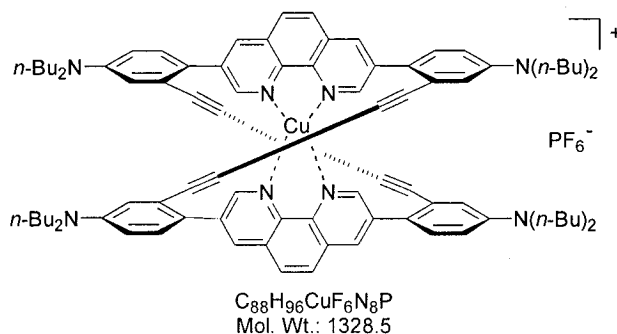
Silylalkyne **216** (605 mg, 0.64 mmol, 1 eq) and TBAF (1 M in THF, 1.34 mL, 1.34 mmol, 2.1 eq) were combined in THF (30 mL) and stirred at rt for 72 h. The reaction mixture was poured into H_2O and extracted with CH_2Cl_2 (3x). The combined extracts were washed with H_2O and brine and concentrated. Chromatography ($\text{CH}_2\text{Cl}_2/\text{MeOH}$, 49:1) afforded **216a** as a yellow foam (162 mg, 40%); mp: 72-74 °C; IR (CDCl_3) ν 2959.8, 2247.1, 1600.7, 1368.2, 811.6 cm^{-1} ; ^1H NMR (500 MHz, CDCl_3) δ 9.41 (s, 2H), 8.34 (s, 2H), 7.76 (s, 2H), 7.35 (d, $J = 8.6$ Hz, 2H), 6.90 (s, 2H), 6.74 (d, $J = 8.0$ Hz, 2H), 3.29 (t, $J = 7.3$ Hz, 8H), 3.00 (s, 2H), 1.62-1.54 (m, 8H), 1.40-1.32 (m, 8H), 0.95 (t, $J = 7.3$ Hz, 12H); ^{13}C NMR (125 MHz, CDCl_3) δ 151.2 (d), 147.6 (s), 144.3 (s), 135.1 (d), 134.7 (s), 130.7 (d), 127.9 (s), 127.0 (s), 126.6 (d), 121.3 (s), 116.4 (d), 112.9 (d), 83.7 (s), 79.4 (d), 50.6 (t), 29.3 (t), 20.2 (t), 13.9 (q); MS (ES) m/z 635.3 (M^+ , 100), 579.3 (14), 488.1 (22), 115.0 (63).

7,28,37,58-Tetrakis-dibutylamino-[4]1,3-butadiynylorthocyclo[0](1,10)phenanthroleno[0]orthocyclo[4]31,33-butadiynylorthocyclo[0](1,10)phenanthroleno[0]orthocyclophane (217)



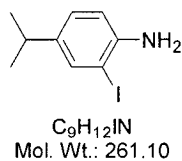
A solution of TBAF (1 M in THF, 1.32 mL, 1.32 mmol, 2.5 eq) was added in one portion to a stirred solution of # (500 mg, 0.53 mmol, 1 eq) in pyridine/Et₂O (3:1, 20 mL). After stirring for 15 min, a solution of Cu(OAc)₂ (48 mg, 0.26 mmol, 0.5 eq) in pyridine/Et₂O (3:1, 20 mL) was added over 2.5 h by syringe pump to establish the copper template. Once the addition was complete, additional Cu(OAc)₂ (530 mg, 2.92 mmol, 5.5 eq) was added to the reaction and the solution turned green immediately. The reaction was stirred for 18 h at rt and diluted with H₂O. The aqueous phase was extracted with CH₂Cl₂ (3x) and the combined extracts were washed with KCN (10% aq) and H₂O, filtered through a Celite plug and concentrated. Chromatography (CH₂Cl₂/MeOH, 30:1) afforded **217** as an orange solid (130 mg, 39%); mp: 138-140 °C; IR (CH₂Cl₂) ν 2960.9, 1596.2, 1369.8, 847.2 cm⁻¹; ¹H NMR (500 MHz, CDCl₃) δ 9.27 (s, 4H), 8.46 (s, 4H), 7.40 (d, *J* = 8.6 Hz, 4H), 7.03 (s, 4H), 6.91 (s, 4H), 6.75 (d, *J* = 6.9 Hz, 4H), 3.29 (t, *J* = 7.1 Hz, 16 H), 1.62-1.53 (m, 16H), 1.41-1.32 (m, 16H), 0.96 (t, *J* = 7.2 Hz, 24 H); ¹³C NMR (125 MHz, CDCl₃) δ 150.6 (d), 147.5 (s), 144.3 (s), 134.9 (d), 134.3 (s), 130.6 (d), 127.8 (s), 127.7 (s), 126.5 (d), 120.8 (s), 116.5 (d), 113.5 (d), 81.9 (s), 75.6 (s), 50.7 (t), 29.3 (t), 20.3 (t), 13.9 (q); MS (ES) *m/z* 1266.5 (M⁺, 1), 579 (1.2), 279.0 (48), 186.1 (100).

Copper(I){ 7,28,37,58-tetrakis-dibutylamino-[4]1,3-butadiynylorthocyclo[0](1,10)phenanthroleno[0]orthocyclo[4]31,33-butadiynylorthocyclo[0](1,10)phenanthroleno[0]orthocyclophane} hexafluorophosphate (218)



Phenanthroline **217** (50 mg, 39.5 μ mol, 1 eq) and $Cu(MeCN)_4PF_6$ (14.7 mg, 39.5 μ mol, 1 eq) were combined in CH_2Cl_2 (10 mL) and stirred at rt for 1 h and concentrated. The residue was dissolved in a minimal amount of CH_2Cl_2 and pentane was added slowly to crystallize the complex. The red crystals were isolated by centrifugation and dried to give **218** (58.8 mg, quant.); mp: > 250 $^{\circ}C$ (dec.); IR (CH_2Cl_2) ν 2960.9, 1596.2, 1369.8, 847.2, 769.8 cm^{-1} ; 1H NMR (500 MHz, $CDCl_3$) δ 9.18 (br s, 4H), 8.30 (br s, 4H), 8.08 (br s, 4H), 7.19 (br s, 4H), 6.71 (s, 4H), 6.62 (br s, 4H), 3.21 (br s, 16 H), 1.51 (br s, 16H), 1.32 (br s, 16H), 0.92 (br s, 24 Hz); ^{13}C NMR (125 MHz, $CDCl_3$) δ 150.0 (d), 148.1 (s), 141.6 (s), 137.8 (s), 134.8 (d), 130.5 (d), 128.9 (s), 127.3 (d), 126.6 (s), 120.5 (s), 115.4 (d), 113.7 (d), 81.9 (s), 75.4 (s), 50.6 (t), 29.6 (t)*, 29.3 (t)*, 20.2 (t), 13.9 (q); MS (ES) m/z 1328.5 (M^+ , 6), 342.1 (10), 186.2 (24). * Peak is split due to hindered helical interconversion. Confirmed by variable temperature ^{13}C NMR.

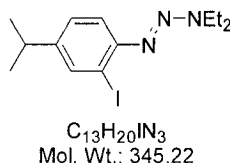
2-Iodo-4-isopropyl-1-aniline (222)



4-Isopropylaniline (**221**) (8.98 g, 66.4 mmol, 1 eq), $BnNMe_3ICl_2$ (26.1 g, 75.1 mmol, 1.1 eq), and $CaCO_3$ (9.30 g, 93.0 mmol, 1.4 eq) were combined in a mixture of $CH_2Cl_2/MeOH$ (5:1, 150 mL) and stirred at rt for 4 h. The reaction was poured into HCl (10% aq) and extracted with CH_2Cl_2 (3x). The combined organic phases were washed with

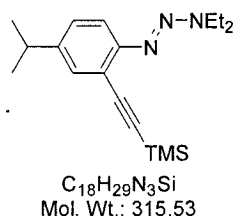
NaHCO₃ (10% aq.) and H₂O, dried, and concentrated. Chromatography (petroleum ether) afforded **222** as a yellow oil (9.49 g, 88%); IR (neat) ν 3457.4, 3360.0, 2950.0, 1614.6, 1497.7 cm⁻¹; ¹H NMR (500 MHz, CDCl₃) δ 7.48 (d, J = 2.0 Hz, 1H), 6.99 (dd, J = 8.2, 2.0 Hz, 1H), 6.69 (d, J = 8.2 Hz, 1H), 3.87 (br s, 2H, exchanges with D₂O), 2.75 (sept, J = 6.9 Hz, 1H), 1.18 (d, J = 6.9 Hz, 6H); ¹³C NMR (125 MHz, CDCl₃) δ 144.3 (s), 141.5 (s), 136.9 (d), 127.7 (d), 115.4 (d), 85.0 (s), 33.1 (d), 24.3 (q); MS (EI) m/z 261.0 (M⁺, 54), 246.0 (100), 119.1 (28), 91.1 (8); HRMS calcd for C₉H₁₂IN 261.0014 (M⁺), found 261.0035.

***N,N*-Diethyl-*N'*-(2-iodo-4-isopropylphenyl)triazine (223)**



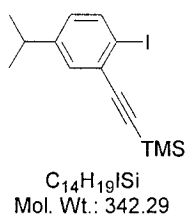
Hydrochloric acid (4.5 M aq, 74 mL, 334 mmol, 9 eq) was added to a solution of iodide **222** (9.70 g, 37.1 mmol, 1 eq) in a mixture of Et₂O/THF/CH₃CN (7:6:1, 75 mL) and the reaction was cooled to 0 °C. A solution of NaNO₂ (8.70 g, 126.1 mmol, 3.4 eq) in CH₃CN/H₂O (2:3, 65 mL) was added dropwise to the reaction and stirring was continued at 0 °C for 2 h. The mixture was then poured into a solution of K₂CO₃ (25.6 g, 185.5 mmol, 5 eq) and Et₂NH (19.2 mL, 185.5 mmol, 5 eq) in CH₃CN/H₂O (2:1, 370 mL) and stirred for 1.5 h. The mixture was extracted with Et₂O (2x), washed with brine, dried, and concentrated. Chromatography (petroleum ether/CH₂Cl₂, 4:1) afforded **223** as an orange oil (12.13 g, 94%); IR (neat) ν 2961.4, 2870.6, 1462.6 cm⁻¹; ¹H NMR (500 MHz, CDCl₃) δ 7.68 (d, J = 2.0 Hz, 1H), 7.25 (d, J = 8.2 Hz, 1H), 7.12 (dd, J = 8.2, 2.0 Hz, 1H), 3.76 (q, J = 7.3 Hz, 4H), 2.82 (sept, J = 6.9 Hz, 1H), 1.29 (t, J = 7.1 Hz, 6H), 1.21 (d, J = 6.9 Hz, 6H); ¹³C NMR (125 MHz, CDCl₃) δ 148.7 (s), 147.7 (s), 137.0 (d), 127.1 (d), 117.5 (d), 96.9 (s), 42.4 (t), 33.1 (d), 24.3 (q), 13.7 (q); MS (EI) m/z 345.1 (M⁺, 36), 273.0 (34), 245.0 (100), 117.1 (64); HRMS calcd for C₁₃H₂₀IN₃ 345.0702 (M⁺), found 345.0686.

***N,N*-Diethyl-*N'*-(4-isopropyl-2-(2-trimethylsilylethynyl)phenyl)triazine (224)**



A solution of iodide **223** (10.0 g, 28.8 mmol, 1 eq) in THF (200 mL) was degassed by bubbling argon through the solution for 30 min. CuI (550 mg, 10 mol%), Pd(PPh₃)₂Cl₂ (1.01 g, 5 mol%), and Et₃N (10 mL) were added to the degassed solution and stirred at rt for 10 min. Trimethylsilyl-acetylene (**37**) (5.71 mL, 40.4 mmol, 1.4 eq) was added to the solution and the reaction was stirred at rt for 18 h. Petroleum ether (200 mL) was added to the reaction and the reaction was filtered through a silica gel plug and concentrated. Chromatography (petroleum ether/CH₂Cl₂, 4:1) afforded **224** as a yellow oil (9.26 g, 99%); IR (neat) ν 2960.8, 2151.4, 1403.1, 1247.4 cm⁻¹; ¹H NMR (500 MHz, CDCl₃) δ 7.31 (d, J = 2.1 Hz, 1H), 7.28 (d, J = 8.2 Hz, 1H), 7.09 (dd, J = 8.3, 2.1 Hz, 1H), 3.75 (q, J = 7.2 Hz, 4H), 2.82 (sept, J = 6.9 Hz, 1H), 1.28 (t, J = 7.1 Hz, 6H), 1.20 (d, J = 6.9 Hz, 6H), 0.22 (s, 9H); ¹³C NMR (125 MHz, CDCl₃) δ 150.9 (s), 145.2 (s), 130.9 (d), 127.6 (d), 117.7 (s), 116.7 (d), 104.0 (s), 97.2 (s), 41.8 (t), 33.5 (d), 23.9 (q), 13.6 (q), 0.1 (q); MS (EI) m/z 315.2 (M⁺, 8), 243.2 (10), 215.1 (100), 187.1 (19); HRMS calcd for C₁₈H₂₉N₃Si 315.2131 (M⁺), found 315.2167.

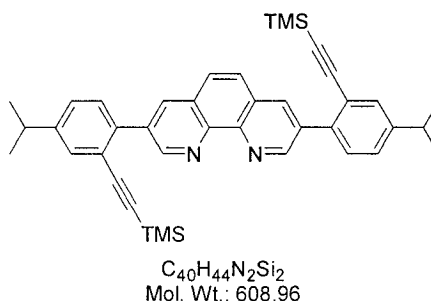
1-Iodo-4-isopropyl-3-(2-trimethylsilylethynyl)benzene (225)



Diethyltriazine **224** (3.31 g, 10.5 mmol, 1 eq) was mixed with iodomethane (30 mL) in a sealed tube fitted with a septa and the solution was degassed with argon for 15 min. The tube was sealed and heated at 120 °C for 4.25 h. The reaction was then cooled to rt and transferred to a flask with CH₂Cl₂ and concentrated. Chromatography (petroleum ether) afforded **225** as a colourless oil (2.99 g, 84%); IR (neat) ν 2960.8, 2157.5, 1467.0, 1249.2 cm⁻¹; ¹H NMR (500 MHz, CDCl₃) δ 7.70 (d, J = 8.2 Hz, 1H), 7.33 (d, J = 2.3 Hz, 1H), 6.84

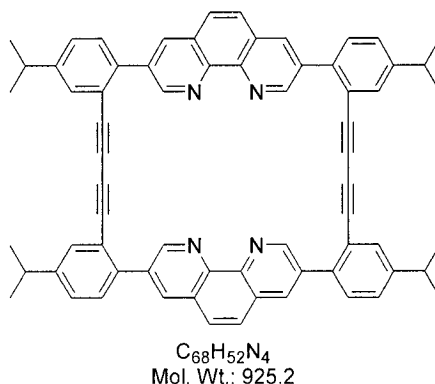
(dd, $J = 8.2, 2.3$ Hz, 1H), 2.80 (sept, $J = 6.9$ Hz, 1H), 1.19 (d, $J = 6.9$ Hz, 6H), 0.27 (s, 9H); ^{13}C NMR (125 MHz, CDCl_3) δ 158.8 (s), 138.5 (d), 131.0 (d), 129.4 (s), 128.3 (d), 106.9 (s), 98.1 (s), 97.5 (s), 33.6 (d), 23.9 (q), -0.2 (q); MS (EI) m/z 342.0 (M^+ , 45), 327.0 (100), 185.1 (9), 156.0 (7); HRMS calcd for $\text{C}_{14}\text{H}_{19}\text{Si}$ 342.0301 (M^+), found 342.0325.

3,8-Bis-(4-isopropyl-2-(2-trimethylsilylethynyl)phenyl)-1,10-phenanthroline (**226**)



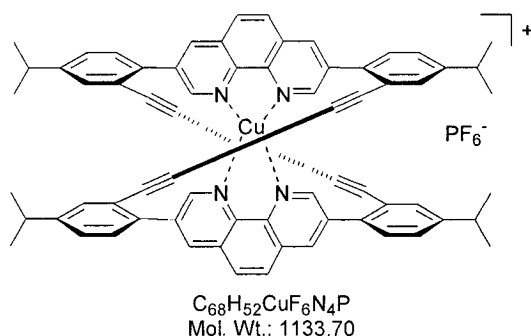
A solution of *n*-BuLi (2.5 M in THF, 3.02 mL, 7.55 mmol, 2.55 eq) was added in one portion to a -78 °C solution of **203** (2.53 g, 7.40 mmol, 2.5 eq) in THF (30 mL). After stirring at -78 °C for 15 min a solution of ZnBr_2 (1.70 g, 7.55 mmol, 2.55 eq) in THF (30 mL) was added by canula. Once the addition was complete, the reaction was warmed to 0 °C and stirred for 20 min. A degassed solution of 3,8-dibromo-1,10-phenanthroline (**203**) (1.00 g, 2.96 mmol, 1 eq) and $\text{Pd}(\text{PPh}_3)_4$ (341 mg, 10 mol%) in a mixture of THF/DMF (1:1, 110 mL) was added to the reaction by canula. (Note: all of the phenanthroline must be dissolved before it is added to the reaction or poor yields are obtained.) The reaction mixture was heated to reflux for 72 h and was concentrated. The dark residue was dissolved in CH_2Cl_2 and washed with H_2O (5x to remove residual DMF) and brine and concentrated. Chromatography (CH_2Cl_2 to $\text{CH}_2\text{Cl}_2/\text{MeOH}$, 50:1) afforded **226** as an orange solid (238 mg, 13%); mp: $236\text{--}237$ °C; IR (CDCl_3) 2963.9, 2153.4, 1426.6, 1250.8 cm^{-1} ; ^1H NMR (500 MHz, CDCl_3) δ 9.32 (d, $J = 2.3$ Hz, 2H), 8.55 (d, $J = 2.2$ Hz, 2H), 7.81 (s, 2H), 7.53 (d, $J = 1.9$ Hz, 2H), 7.47 (d, $J = 7.9$ Hz, 2H), 7.33 (dd, $J = 7.9, 1.9$ Hz, 2H), 2.95 (sept, $J = 6.9$ Hz, 2H), 1.30 (d, $J = 6.9$ Hz, 12H), 0.06 (s, 18H); ^{13}C NMR (125 MHz, CDCl_3) δ 150.9 (d), 148.9 (s), 145.1 (s), 137.9 (s), 135.9 (d), 135.0 (s), 131.7 (d), 129.6 (d), 127.8 (s), 127.5 (d), 126.8 (d), 121.9 (s), 104.5 (s), 97.8 (s), 33.8 (d), 23.9 (q), -0.2 (q); MS (ES) m/z 608 (M^+), 565, 535, 289.

7,28,37,58-Tetraisopropyl-[4]1,3-butadiynylorthocyclo[0](3,8)-1,10-phenanthroleno[0]orthocyclo[4]31,33-butadiynylorthocyclo[0](3,8)-1,10-phenanthroleno[0]orthocyclophane (227)



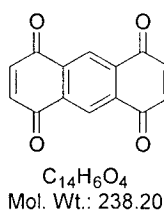
Copper(II) acetate (23.2 mg, 0.13 mmol, 0.5 eq) was added to a solution of **226** (156 mg, 0.23 mmol, 1 eq) in pyridine/Et₂O (3:1, 40 mL) and was stirred at rt for 30 min. This solution was added by syringe pump to a stirred solution of Cu(OAc)₂ (279 mg, 1.54 mmol, 6 eq) and K₂CO₃ (354 mg, 2.56 mmol, 10 eq) in pyridine/Et₂O (3:1, 200 mL) with MeOH (1 mL) over 8 h. The reaction was stirred at rt for a total of 14 h. A solution of TBAF (1 M in THF, 1 mL) was added to ensure complete desilylation of **226** and the reaction was stirred for 1 h and concentrated. The residue was dissolved in CH₂Cl₂ and washed with HCl (10% aq, 3x), NaOH (10% aq), KCN (500 mg in H₂O, 100 mL), and brine, and concentrated. Chromatography (CH₂Cl₂/MeOH, 10:1) afforded **227** as a yellow solid (54 mg, 23%); mp: > 280 °C; IR (CDCl₃) ν 2964.5, 2928.8, 2215.5, 1426.9 cm⁻¹; ¹H NMR (500 MHz, CDCl₃) δ 9.31 (d, *J* = 2.2 Hz, 4H), 8.54 (d, *J* = 2.2 Hz, 4H), 7.57 (d, *J* = 1.6 Hz, 4H), 7.52 (d, *J* = 8.0 Hz, 4H), 7.37 (dd, *J* = 8.0, 1.8 Hz, 4H), 7.11 (s, 4H), 2.96 (sept, *J* = 6.9 Hz, 4H), 1.29 (d, *J* = 6.9 Hz, 24 Hz); ¹³C NMR (125 MHz, CDCl₃) δ 150.7 (d), 149.1 (s), 145.0 (s), 138.4 (s), 135.8 (d), 134.3 (s), 132.5 (d), 129.7 (d), 128.5 (d), 128.0 (s), 126.7 (d), 120.3 (s), 81.4 (s), 76.5 (s), 33.7 (d), 23.7 (q); MS (ES) *m/z* 925.1 (M⁺, 100), 279.0 (12), 74.0 (43).

Copper(I){ 7,28,37,58-tetraisopropyl-[4]1,3-butadiynylorthocyclo[0](3,8)-1,10-phenanthroleno[0]orthocyclo[4]31,33-butadiynylorthocyclo[0](3,8)-1,10-phenanthroleno[0]orthocyclophane} hexafluorophosphate (228**)**



Phenanthroline **227** (67 mg, 72.4 μ mol, 1 eq) and $Cu(MeCN)_4PF_6$ (27 mg, 72.4 μ mol, 1 eq) were combined in methylene chloride (10 mL), stirred at rt for 30 min, and concentrated. The residue was dissolved in a minimal amount of CH_2Cl_2 and pentane was slowly added to precipitate the complex. The red crystals were isolated by centrifugation and dried to give **228** (81 mg, 99%); 1H NMR (500 MHz, $CDCl_3$) δ 9.44 (br s, 4H), 8.56 (br s, 4H), 8.19 (br s, 4H), 7.55 (d, $J = 7.8$ Hz, 4H), 7.51 (s, 4H), 7.43 (d, $J = 7.8$ Hz, 4H), 2.98-2.93 (m, 4H), 1.27 (d, $J = 6.8$ Hz, 24H); $^{13}C\{^1H\}$ NMR (125 MHz, $CDCl_3$) δ 150.1, 149.9, 142.3, 137.7, 137.6, 135.6, 131.4, 129.8, 129.1, 129.0, 127.3, 119.8, 81.3, 76.4, 33.5, 23.6,* 23.5*; MS (ES) 987.0 ($M^+ - PF_6$, 100). * Peak is split due to hindered helical interconversion. Confirmed by variable temperature ^{13}C NMR.

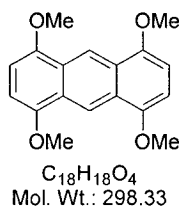
1,4,5,8-Anthraquinone (249**)**



An aqueous solution (20 mL) of ceric ammonium nitrate (CAN) (4.60 g, 8.40 mmol, 5 eq) was added dropwise over 5 min to a suspension of 1,4,5,8-tetramethoxyanthracene (**251**) (500 mg, 1.68 mmol, 1 eq) in acetonitrile (50 mL). The reaction was stirred at rt for 2 h, diluted with water (60 mL), and filtered to afford **249** as a yellow solid (235 mg, 59%); mp: > 168-169 $^{\circ}C$; IR (CH_2Cl_2) ν 1678.4 cm^{-1} ; 1H NMR (500 MHz, $CDCl_3$) δ 8.78 (s, 2H), 7.12 (s, 4H); ^{13}C NMR (125 MHz, $CDCl_3$) δ 183.2 (s), 139.2 (d), 135.0 (d), 125.6 (d); MS

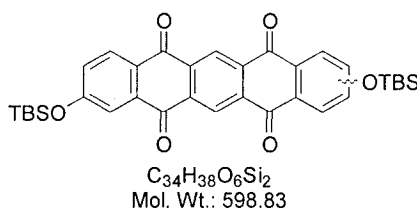
(EI) m/z 238.0266 (M^+ , 100), 184.0 (34), 156.0 (17), 128.0 (18); HRMS calcd for $C_{14}H_6O_4$ 238.0266 (M^+), found 238.0263. Characterization data of **249** agreed with the reported data.¹⁴⁶

1,4,5,8-Tetramethoxyanthracene (**251**)



A solution of *n*-butyllithium (2.5 M in hexanes, 17 mL, 6.8 mmol) was added to THF (175 mL) and was heated to 40 °C for 3.5 h to form the enolate of acetaldehyde (**253**). This solution was added to sodium amide (1:1 w/w in toluene, 12.4 g, 158 mmol) and heated to 100 °C. 2-Bromo-1,4-dimethoxybenzene (**250**) (10.0 g, 46.1 mmol) was added neat over 1 min (caution: the reaction is very exothermic!), the reaction was stirred at 100 °C for 30 min, and then cooled in an ice bath. Ice cold water (300 mL) was added and **251** was obtained as a yellow by filtration (1.62 g, 23%, yields typically ranged from 20 to 40%); mp: > 270 °C; 1H NMR (500 MHz, $CDCl_3$) δ 9.08 (s, 2H), 6.61 (s, 4H), 4.01 (s, 12H); ^{13}C NMR (125 MHz, $CDCl_3$) δ 149.9 (s), 125.3 (s), 115.2 (d), 101.4 (d), 55.6 (q); MS (EI) m/z 298.1 (M^+ , 100), 283.1 (82), 253.0 (51), 162.0 (30); HRMS calcd for $C_{18}H_{18}O_4$ 298.1205 (M^+), found 298.1211. Characterization data of **251** agreed with the reported data.¹⁴⁶

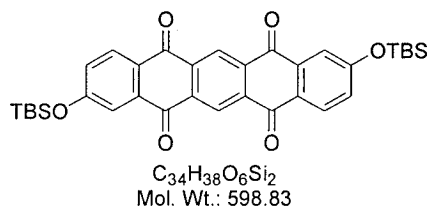
2,9/2,10-Bis(*t*-butyldimethylsiloxy)-5,7,12,14-pentacenediquinone (**247** and **268**)



1,4,5,8-Anthraquinone (**249**) (2.45 g, 10.3 mmol, 1 eq) and *trans*-3-(*t*-butyldimethylsilyloxy)-1-methoxy-1,3-butadiene (**248**) (5.14 mL, 21.6 mmol, 2.1 eq) were combined in methylene chloride and stirred at rt for 20 h. The reaction was concentrated, taken up in THF, silica gel was added, and the suspension was stirred open to air for 24 h. The reaction was filtered through a silica gel plug with CH_2Cl_2 to afford a mixture of **247** and **268** and then flushed with THF to recover unaromatized material (**266** and **267**). Silica gel

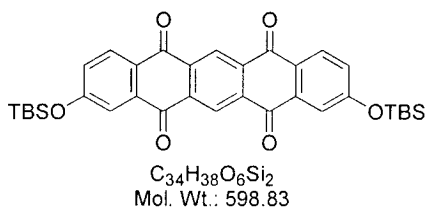
was added to the THF fraction and was stirred open to air for an additional 24 h. Filtration through a silica gel plug with CH₂Cl₂ afforded more **247** and **268**. The silica gel oxidation/filtration was repeated until all of **266** and **267** was converted to **247** and **268**. The silyl ethers were isolated as a yellow solid (3.72 g, 60%) and a mixture of **247** and **268** (1:1). Isomers **247** and **268** could be separated by fractional crystallization from chloroform.

2,9-Bis(*t*-butyldimethylsiloxy)-5,7,12,14-pentacenediquinone (**247**)



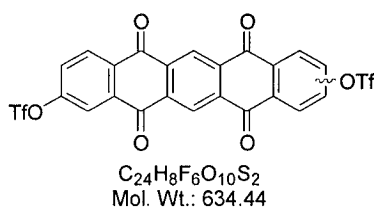
Mp: > 270 °C; IR (CDCl₃) ν 2957.6, 2930.7, 1677.7, 1591.9 cm⁻¹; ¹H NMR (500 MHz, CDCl₃) δ 9.15 (s, 2H), 8.28 (d, J = 8.6 Hz, 2H), 7.70 (d, J = 2.5 Hz, 2H), 7.24 (dd, J = 8.5, 2.6 Hz, 2H), 1.01 (s, 18 H), 0.30 (s, 12H); ¹³C NMR (125 MHz, CDCl₃) δ 181.8 (s), 180.7 (s), 161.9 (s), 136.9 (s), 136.7 (s), 135.6 (s), 130.4 (d), 127.5 (s), 127.0 (d), 126.5 (d), 117.7 (d), 25.5 (q), 18.3 (s), -4.3 (q); MS (EI) m/z 541.2 (M⁺ - *t*-Bu, 100), 485.1 (8), 242.0 (19), 162.0 (34); HRMS calcd for C₃₀H₂₉O₆Si₂ 541.1502 (M⁺ - *t*-Bu), found 541.1510.

2,10-Bis(*t*-butyldimethylsiloxy)-5,7,12,14-pentacenediquinone (**268**)



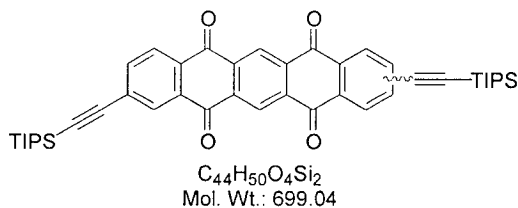
Mp: > 270 °C; IR (CDCl₃) ν 2955.8, 2927.2, 1675.0, 1590.9 cm⁻¹; ¹H NMR (500 MHz, CDCl₃) δ 9.18 (s, 1H), 9.14 (s, 1H), 8.28 (d, J = 8.6 Hz, 2H), 7.71 (d, J = 2.4 Hz, 2H), 7.24 (dd, J = 8.2, 2.6 Hz, 2H), 1.01 (s, 18 H), 0.30 (s, 12H); ¹³C NMR (125 MHz, CDCl₃) δ 181.8 (s), 180.7 (s), 161.9 (s), 137.0 (s), 136.6 (s), 135.6 (s), 130.4 (d), 127.5 (s), 127.1 (d), 127.0 (d), 126.5 (d), 117.7 (d), 25.5 (q), 18.3 (s), -4.3 (q); MS (EI) m/z 541.2 (M⁺ - *t*-Bu, 15), 504.9 (3), 162.0 (18), 57.1 (100); HRMS calcd for C₃₀H₂₉O₆Si₂ 541.1502 (M⁺ - *t*-Bu), found 541.1516.

2,9/2,10-Bis(trifluoromethylsulfonyloxy)-5,7,12,14-pentacenediquinone (268 and 271)



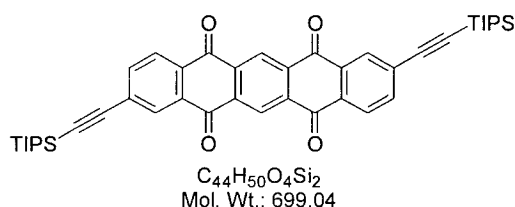
A solution of TBAF (1 M in THF, 1.81 mL, 1.81 mmol, 2.2 eq) was added to a 0 °C solution of silyl ether **247** (**268** was used to prepare the other isomer) (493 mg, 0.823 mmol, 1 eq) in THF (400 mL). The yellow solution turned deep blue immediately upon addition of TBAF. The reaction was stirred at 0 °C for 15 min followed by the addition of a solution of Tf₂NPh (882 mg, 2.47 mmol, 3 eq) in THF (5 mL). The reaction was warmed to rt and stirred for 18 h, concentrated to ~100 mL and diluted with Et₂O (200 mL). The organic suspension was washed with HCl (10% aq), NaHCO₃ (sat. aq.), and water, concentrated to ~50 mL, and filtered to afford crude **268** (or **271** depending on the starting material used) as a nearly colourless solid (518 mg, 98%). This compound was not further purified or characterized, but used crude in subsequent reactions.

2,9/2,10-Bis(triisopropylsilylethynyl)-5,7,12,14-pentacenediquinone (272 and 273)



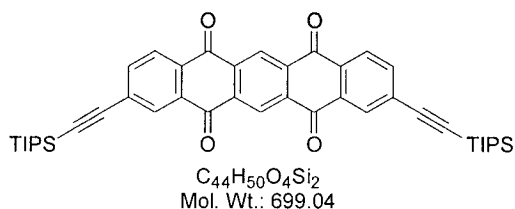
A solution of ditriflate **268** (or **271**) (500 mg, 0.788 mmol, 1 eq) in THF (250 mL) was degassed by bubbling argon through the solution for 30 min. CuI (30 mg, 20 mol%), Pd(PPh₃)₂Cl₂ (60 mg, 10 mol %), and Et₃N (7.5 mL) were added to the degassed solution and stirred at rt for 10 min. Triisopropylsilyl-acetylene (**82**) (438 μL, 1.97 mmol, 2.5 eq) was added to the solution and the reaction was heated to reflux for 16 h. The reaction was cooled to rt and concentrated. The residue was taken up in CH₂Cl₂ and washed with HCl (10% aq), NaHCO₃ (sat. aq), and water, dried, and concentrated. Chromatography (petroleum ether/CH₂Cl₂, 7:3) afforded **272** (or **273**) as a yellow solid (400 mg, 73% over two steps). If the ditriflate used in the reaction was a mixture of isomers, they could be separated by fractional crystallization from Et₂O.

2,9-Bis(triisopropylsilylethynyl)-5,7,12,14-pentacenediquinone (**272**)



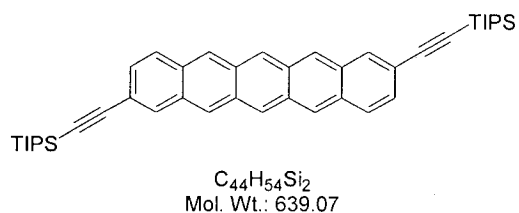
mp: > 272-273 °C; IR (neat) ν 2945.3, 2866.9, 1679.8, 1595.5 cm^{-1} ; 1H NMR (500 MHz, $CDCl_3$) δ 9.22 (s, 2H), 8.41 (d, $J = 1.6$ Hz, 2H), 8.31 (d, $J = 8.1$ Hz, 2H), 7.88 (dd, $J = 8.1, 1.7$ Hz, 2H), 1.15 (s, 42H); ^{13}C NMR (125 MHz, $CDCl_3$) δ 181.2 (s), 181.0 (s), 137.7 (d), 136.8 (s), 136.7 (s), 133.3 (s), 132.3 (s), 131.0 (d), 130.5 (s), 127.7 (d), 127.5 (d), 104.9 (s), 98.2 (s), 18.3 (q), 11.7 (d); MS (FAB) m/z 699.3 (M^+), 307.2, 154.1.

2,10-Bis(triisopropylsilylethynyl)-5,7,12,14-pentacenediquinone (**273**)



mp: 247-248 °C; IR (neat) ν 2945.7, 2866.9, 1679.2, 1595.8 cm^{-1} ; 1H NMR (500 MHz, $CDCl_3$) δ 9.22 (s, 1H), 9.21 (s, 1H), 8.41 (d, $J = 1.3$ Hz, 2H), 8.31 (d, $J = 8.0$ Hz, 2H), 7.88 (dd, $J = 8.1, 1.2$ Hz, 2H), 1.15 (s, 42H); ^{13}C NMR (125 MHz, $CDCl_3$) δ 181.2 (s), 181.0 (s), 137.0 (d), 136.9 (s), 136.7 (s), 133.3 (s), 132.3 (s), 131.0 (d), 130.5 (d), 130.2 (s), 127.7 (d), 127.6 (d), 104.9 (s), 98.2 (s), 18.6 (q), 11.3 (d); MS (FAB) m/z 699.3 (M^+), 307.2, 154.1.

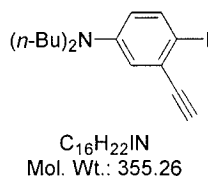
2,9-Bis(2-triisopropylsilylethynyl)pentacene (**274**)



Sodium borohydride (729 mg, 19.3 mmol, 20 eq) and diquinone **272** (674 mg, 0.96 mmol, 1 eq) were combined in degassed isopropanol (125 mL) and heated at reflux for 54 h. The reaction was cooled to rt and transferred to degassed HCl (5% aq., 100 mL). NOTE: pentacene **274** was very oxygen sensitive in solution so Schlenk techniques were used. The resulting purple solid was collected by filtration and dissolved in THF, dried, and

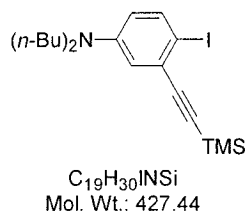
concentrated to give crude **274** as a purple solid (542 mg, 88%). Further purification was achieved by recrystallization by diffusion of *n*-decane into a solution of **274** in THF. Further optimization of the workup and purification is necessary.

***N,N*-Dibutyl-3-ethynyl-4-iodoaniline (286)**



A solution of TBAF (1 M in THF, 2.94 mL, 2.94 mmol, 1.5 eq) was added to a solution of silylalkyne **118** (1.00 g, 1.96 mmol, 1 eq) in THF (10 mL) and stirred at rt for 1 h. The reaction was diluted with CH_2Cl_2 and washed with H_2O and brine, dried, and concentrated. Chromatography (petroleum ether to petroleum ether/ Et_2O , 9:1) afforded **286** as a yellow oil (588 mg, 84%); IR (neat) ν 2956.0, 2108.7, 1582.7, 1462.1 cm^{-1} ; 1H NMR (500 MHz, $CDCl_3$) δ 7.50 (d, $J = 8.9$ Hz, 1H), 6.77 (d, $J = 2.4$ Hz, 1H), 6.35 (dd, $J = 8.9, 2.4$ Hz, 1H), 3.27 (s, 1H), 3.20 (t, $J = 7.6$ Hz, 4H), 1.54-1.47 (m, 4H), 1.36-1.27 (m, 4H), 0.93 (t, $J = 7.4$ Hz, 6H); ^{13}C NMR (125 MHz, $CDCl_3$) δ 147.7 (s), 138.8 (d), 128.5 (s), 116.7 (d), 114.5 (d), 86.0 (s), 81.3 (s), 79.3 (d), 50.7 (t), 29.1 (t), 20.3 (t), 13.9 (q); MS (EI) m/z 355.1 (M^+ , 45), 312.0 (100), 271.0 (4), 69.0 (57); HRMS calcd for $C_{16}H_{22}IN$ 355.0797 (M^+), found 355.0793.

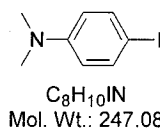
***N,N*-Dibutyl-4-iodo-3-(2-trimethylsilylethynyl)aniline (287)**



Ethyl magnesium bromide (1 M solution in THF, 1.83 mL, 1.83 mmol, 1.3 eq) was added to a solution of alkyne **286** (500 mg, 1.41 mmol, 1 eq) in THF (30 mL) which was heated at reflux for 15 h. The reaction was cooled to 0 °C and trimethylsilyl-chloride (290 μ L, 2.26 mmol, 1.6 eq) was added. Following heating at 50 °C for 3 h, the reaction was cooled to rt, diluted with Et_2O , washed with NH_4Cl (sat. aq), $NaHCO_3$ (10% aq), and brine, dried, and concentrated. Chromatography (petroleum ether/ Et_2O , 9:1) afforded **287** as a colourless oil (443 mg, 74%); IR (neat) ν 2957.7, 2872.4, 2158.0, 1582.2, 843.7 cm^{-1} ; 1H

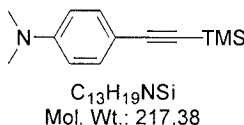
NMR (500 MHz, CDCl₃) δ 7.49 (d, *J* = 8.9 Hz, 1H), 6.73 (d, *J* = 3.1 Hz, 1H), 6.31 (dd, *J* = 8.9, 3.1 Hz, 1H), 3.19 (t, *J* = 7.6 Hz, 4H), 1.55-1.47 (m, 4H), 1.37-1.27 (m, 4H), 0.93 (t, *J* = 7.3 Hz, 6H), 0.27 (s, 9H); ¹³C NMR (125 MHz, CDCl₃) δ 147.8 (s), 138.7 (d), 129.4 (s), 116.0 (d), 114.3 (d), 107.7 (s), 96.9 (s), 82.5 (s), 50.6 (t), 29.2 (t), 20.3 (t), 13.9 (q), -0.1 (q); MS (EI) *m/z* 427.1 (M⁺, 42), 384.1 (100), 342.0 (25), 258.2 (6), 184.5 (6); HRMS calcd for C₁₉H₃₀INSi 427.1194 (M⁺), found 427.1180. Characterization data of **287** agreed with the reported data.⁶⁰

***N,N*-Dimethyl-4-iodoaniline (288)**



4-Iodoaniline (5.00 g, 22.8 mmol, 1 eq), MeI (3.13 mL, 50.2 mmol, 2.2 eq), and NaHCO₃ (5.75 g, 50.2 mmol, 3 eq) were combined in a mixture of THF/DMF (5:1, 50 mL) and heated to reflux for 4 h. The reaction turned from deep blue to yellow during the course of the reaction. The reaction was cooled to rt, diluted with H₂O and extracted with Et₂O (3x). The extracts were combined and washed with H₂O and brine, dried, and concentrated. Chromatography (petroleum ether/Et₂O, 19:1) afforded **288** as an off-white solid (3.73 g, 66%); mp: 79-80 °C; ¹H NMR (200 MHz, CDCl₃) δ 7.45 (d, *J* = 9.2 Hz, 2H), 6.48 (d, *J* = 9.1 Hz, 2H), 2.91 (s, 6H); MS (EI) *m/z* 247.0 (M⁺, 100), 231.0 (4), 162.0 (7), 119.1 (19); HRMS calcd for C₈H₁₀IN 246.9858 (M⁺), found 246.9857.

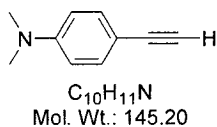
***N,N*-Dimethyl-4-(2-trimethylsilylethynyl)aniline (289)**



A solution of iodide **288** (3.25 g, 13.2 mmol, 1 eq) in THF (50 mL) was degassed by bubbling argon through the solution for 30 min. CuI (150 mg, 6 mol%), Pd(PPh₃)₂Cl₂ (410 mg, 5 mol%), and Et₃N (2.5 mL) were added to the degassed solution and stirred at rt for 10 min. Trimethylsilyl-acetylene (**37**) (2.42 mL, 17.1 mmol, 1.3 eq) was added to the solution and the reaction was stirred at rt for 12 h. The reaction mixture was filtered through a sand plug and the filtrate was concentrated. Chromatography (petroleum ether/Et₂O, 20:1) afforded **289** as a yellow solid (2.77 g, 96%); mp: 86-87 °C; ¹H NMR (200 MHz, CDCl₃) δ

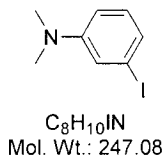
7.34 (d, $J = 9.1$ Hz, 2H), 6.57 (d, $J = 9.1$ Hz, 2H), 2.95 (s, 6H), 0.23 (s, 9H); MS (EI) m/z 217.1 (M^+ , 74), 202.1 (100), 186.1 (11), 162.0 (6); HRMS calcd for $C_{13}H_{19}NSi$ 217.1287 (M^+), found 217.1298.

***N,N*-Dimethyl-4-ethynylaniline (290)**



Silylalkyne **289** (1.97 g, 9.06 mmol, 1 eq) and KOH (760 mg, 13.6 mmol, 1.5 eq) were combined in MeOH (40 mL) with H_2O (5 drops) and stirred at rt for 2 h. The reaction was poured into NH_4Cl (sat. aq) and extracted with Et_2O (2x). The combined extracts were washed with H_2O and brine, dried, and concentrated. Chromatography (petroleum ether/ Et_2O , 19:1) afforded **290** as an orange solid (1.13 g, 86%); mp: 50-51 °C; 1H NMR (500 MHz, $CDCl_3$) δ 7.36 (d, $J = 9.0$ Hz, 2H), 6.60 (d, $J = 9.0$ Hz, 2H), 2.97 (s, 1H), 2.96 (s, 6H); ^{13}C NMR (125 MHz, $CDCl_3$) δ 150.4 (s), 133.2 (d), 111.7 (d), 108.9 (s), 84.9 (s), 74.8 (s), 40.1 (q); MS (EI) m/z 145.1 (M^+ , 100), 144.1 (90), 129.1 (18), 101.0 (10); HRMS calcd for $C_{10}H_{11}N$ 145.0891 (M^+), found 145.0888. Characterization data of **290** agreed with the reported data.¹⁶¹

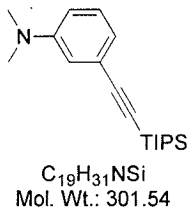
***N,N*-Dimethyl-3-iodoaniline (291)**



3-Iodoaniline (11.1 mL, 91.3 mmol, 1 eq), MeI (12.53 mL, 201 mmol, 2.2 eq), and $NaHCO_3$ (23.0 g, 274 mmol, 3 eq) were combined in a mixture of THF/DMF (5:1, 400 mL) and heated to reflux for 48 h. The reaction was cooled to rt, diluted with H_2O , and extracted with Et_2O (3x). The extracts were combined and washed with H_2O and brine, dried, and concentrated. Chromatography (petroleum ether/ Et_2O , 9:1) afforded **291** as a yellow solid (22.1 g, 98%); mp: 34-35 °C; 1H NMR (500 MHz, $CDCl_3$) δ 7.02 (d, $J = 1.6$ Hz, 1H), 7.01 (br s, 1H), 6.91 (dd, $J = 7.9, 7.9$ Hz, 1H), 6.66 (dd, $J = 7.9, 1.8$ Hz, 1H), 2.91 (s, 6H); ^{13}C NMR (125 MHz, $CDCl_3$) δ 151.6 (s), 130.4 (d), 125.3 (d), 121.2 (d), 111.6 (d), 95.6 (s), 40.3

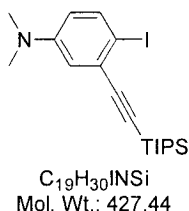
(q); MS (EI) m/z 247.0 (M^+ , 100), 169.0 (10), 143.0 (3), 119.1 (15); HRMS calcd for $C_8H_{10}IN$ 246.9858 (M^+), found 246.9846.

***N,N*-Dimethyl-3-(2-triisopropylsilylethynyl)aniline (292)**



A solution of iodide **291** (11.0 g, 44.5 mmol, 1 eq) in THF (200 mL) was degassed by bubbling argon through the solution for 30 min. CuI (230 mg, 5 mol%), Pd(PPh₃)₂Cl₂ (850 mg, 5 mol%), and Et₃N (10 mL) were added to the degassed solution and stirred at rt for 10 min. Triisopropylsilyl-acetylene (**82**) (13.6 mL, 60.7 mmol, 1.5 eq) was added to the solution and the reaction was stirred at rt for 12 h. Silica gel was added to the reaction mixture and the slurry was concentrated. Chromatography (petroleum ether/CH₂Cl₂, 2:1) afforded **292** as a yellow oil (12.7 g, 94%); IR (neat) ν 2942.7, 2865.1, 2153.4, 1596.6, 1495.9 cm^{-1} ; ¹H NMR (500 MHz, CDCl₃) δ 7.16 (dd, J = 8.1, 7.8 Hz, 1H), 6.88 (d, J = 7.4 Hz, 1H), 6.85 (br s, 1H), 6.73 (d, J = 7.9 Hz, 1H), 2.94 (s, 6H), 1.13 (s, 21H); ¹³C NMR (125 MHz, CDCl₃) δ 149.9 (s), 128.9 (d), 124.1 (d), 116.1 (d), 113.4 (d), 107.0 (s), 94.7 (s), 89.3 (s), 40.8 (q), 18.7 (q), 11.4 (d); MS (EI) m/z 301.2 (M^+ , 75), 258.2 (60), 216.1 (61), 188.1 (100); HRMS calcd for $C_{19}H_{31}NSi$ 301.2226 (M^+), found 301.2233.

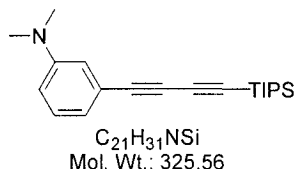
***N,N*-Dimethyl-4-iodo-3-(2-triisopropylsilylethynyl)aniline (293)**



Silylalkyne **292** (11.1 g, 36.5 mmol, 1 eq), BnNMe₃ICl₂ (13.9 g, 40.0 mmol, 1.1 eq), and CaCO₃ (5.10 g, 51.1 mmol, 1.4 eq) were combined in a mixture of CH₂Cl₂/MeOH (5:1, 200 mL) and stirred at rt for 4 h. The reaction mixture was diluted with CH₂Cl₂ and washed with HCl (10% aq), NaHCO₃ (10% aq), H₂O, and brine, dried, and concentrated. Chromatography (petroleum ether/CH₂Cl₂, 4:1) afforded **293** as a brown solid (13.7 g, 88%); mp: 77-79 °C; IR (CH₂Cl₂) ν 2944.3, 2865.5, 2153.8, 1586.4 cm^{-1} ; ¹H NMR (500 MHz,

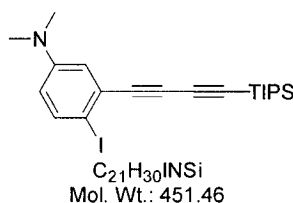
CDCl₃) δ 7.57 (d, J = 8.8 Hz, 1H), 6.85 (br s, 1H), 6.54 (br d, J = 7.0 Hz, 1H), 2.91 (s, 6H), 1.15 (s, 21H); ¹³C NMR (125 MHz, CDCl₃) δ 149.9 (s), 139.0 (d), 130.3 (s), 117.6 (d), 115.3 (d), 108.9 (s), 94.1 (s), 86.0 (s), 40.9 (q), 19.0 (q), 11.6 (d); MS (EI) m/z 427.1 (M⁺, 100), 384.1 (50), 314.0 (46), 215.1 (42); HRMS calcd for C₁₉H₃₀INSi 427.1192 (M⁺), found 427.1185.

***N,N*-Dimethyl-3-(4-triisopropylsilyl-1,3-butadiynyl)-aniline (294)**



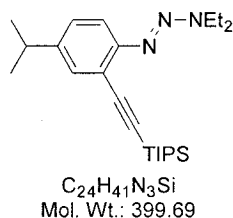
A solution of *n*-BuLi (2.5 M in THF, 68.0 mL, 170 mmol, 2.8 eq) was added in one portion to a -78 °C solution of *cis*-4-chloro-1-triisopropylsilyl-but-3-en-1-yne (**83**) (20.6 g, 85.0 mmol, 1.4 eq) in THF (500 mL). The resulting pale yellow coloured solution was stirred for 2 min followed by the addition of a solution of ZnBr₂ (19.1 g, 85.0 mmol, 1.4 eq) in THF (200 mL). The colourless solution was stirred at -78 °C for 5 min then warmed to 0 °C for 15 min. A mixture of *N,N*-dimethyl-3-iodoaniline (**291**) (15.0 g, 60.7 mmol, 1 eq) and Pd(PPh₃)₄ (3.50 g, 5 mol%) in THF (125 mL) was added by canula and the reaction was stirred at rt for 18 h. Silica gel was added to the reaction and the slurry was concentrated. Chromatography (petroleum ether/CH₂Cl₂, 9:1) afforded **294** as an off-white solid (15.0 g, 76%); mp: 75-76 °C; IR (CH₂Cl₂) ν 2945.6, 2866.9, 2201.4, 2098.4, 1595.5 cm⁻¹; ¹H NMR (500 MHz, CDCl₃) δ 7.11 (dd, J = 8.0, 7.9 Hz, 1H), 6.86 (d, J = 7.8 Hz, 1H), 6.85 (s, 1H), 6.73 (br d, J = 7.1 Hz, 1H), 2.92 (s, 6H), 1.10 (s, 21H); ¹³C NMR (125 MHz, CDCl₃) δ 150.7 (s), 132.3 (s), 129.3 (d), 122.0 (d), 116.5 (d), 114.0 (d), 90.0 (s), 87.4 (s), 76.9 (s), 73.8 (s), 40.7 (q), 18.8 (q), 11.6 (d); MS (EI) m/z 325.2 (M⁺, 100), 282.2 (96), 240.1 (65), 212.1 (91); HRMS calcd for C₂₁H₃₁NSi 325.2226 (M⁺), found 325.2238.

***N,N*-Dimethyl-4-iodo-3-(4-triisopropylsilyl-1,3-butadiynyl)aniline (295)**



Silylalkyne **294** (14.6 g, 44.7 mmol, 1 eq), $BnNMe_3ICl_2$ (17.6 g, 50.7 mmol, 1.1 eq), and $CaCO_3$ (6.46 g, 64.5 mmol, 1.4 eq) were combined in a mixture of $CH_2Cl_2/MeOH$ (5:1, 200 mL) and stirred at rt for 4 h. The reaction mixture was diluted with CH_2Cl_2 and washed with HCl (10% aq), $NaHCO_3$ (10% aq), H_2O , and brine, dried, and concentrated. Chromatography (petroleum ether/ CH_2Cl_2 , 9:1) afforded **295** as a brown solid (15.8 g, 78%); mp: 63-64 °C; IR (CH_2Cl_2) ν 2951.1, 2859.7, 2098.4, 1583.2 cm^{-1} ; 1H NMR (500 MHz, $CDCl_3$) δ 7.53 (d, $J = 8.9$ Hz, 1H), 6.84 (d, $J = 3.1$ Hz, 1H), 6.42 (dd, $J = 8.9, 3.1$ Hz, 1H), 2.90 (s, 6H), 1.10 (s, 21H); ^{13}C NMR (125 MHz, $CDCl_3$) δ 150.0 (s), 139.0 (d), 128.4 (s), 118.1 (d), 115.6 (d), 89.7 (s), 89.3 (s), 83.7 (s), 78.0 (s), 76.9 (s), 40.4 (q), 18.8 (q), 11.6 (d); MS (EI) m/z 451.1 (M^+ , 100), 408.1 (45), 337.9 (38), 176.0 (51); HRMS calcd for $C_{21}H_{30}INSi$ 451.1192 (M^+), found 451.1177.

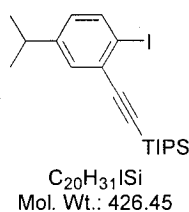
***N,N*-Diethyl-*N'*-[4-isopropyl-2-(2-triisopropylsilylethynyl)phenyl]triazene (296)**



A solution of iodotriazine **223** (975 mg, 2.81 mmol, 1 eq) in THF (75 mL) was degassed by bubbling argon through the solution for 30 min. CuI (20 mg, 4 mol%), $Pd(PPh_3)_2Cl_2$ (50 mg, 2.5 mol%), and Et_3N (3.75 mL) were added to the degassed solution and stirred at rt for 10 min. Triisopropylsilyl-acetylene (**82**) (0.94 mL, 4.22 mmol, 1.5 eq) was added to the solution and the reaction was heated at reflux for 24 h. TLC (petroleum ether) showed that starting material remained. Additional $Pd(PPh_3)_2Cl_2$ (25 mg, 1.25 mol%) and **82** (0.50 mL, 2.0 mmol) were added to the reaction and heating was continued for 24 h. The reaction was cooled to rt, silica gel was added, and the slurry was concentrated. Chromatography (petroleum ether/ CH_2Cl_2 , 20:1) afforded **296** as a red oil (428 mg, 38%);

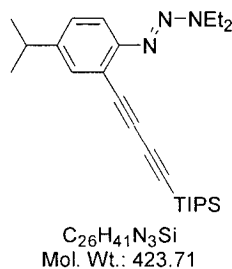
IR (neat) ν 2959.4, 2864.8, 2148.1, 1463.6, 1242.6 cm^{-1} ; ^1H NMR (500 MHz, CDCl_3) δ 7.33 (d, $J = 8.4$ Hz, 1H), 7.29 (d, $J = 2.1$ Hz, 1H), 7.08 (dd, $J = 8.4, 2.1$ Hz, 1H), 3.75 (q, $J = 7.2$ Hz, 4H), 2.83 (sept, $J = 6.9$ Hz, 1H), 1.20 (d, $J = 6.9$ Hz, 6H), 1.12 (s, 21H); ^{13}C NMR (125 MHz, CDCl_3) δ 150.9 (s), 145.4 (s), 131.9 (d), 127.4 (d), 118.4 (s), 117.0 (d), 106.2 (s), 93.5 (s), 42.4 (t), 33.7 (d), 24.1 (q), 19.0 (q), 18.9 (q), 11.7 (d); MS (EI) m/z 399.3 (M^+ , 8), 327.2 (15), 257.2 (45), 69.0 (100); HRMS calcd for $\text{C}_{24}\text{H}_{41}\text{N}_3\text{Si}$ 399.3070 (M^+), found 399.2964.

1-Iodo-4-isopropyl-2-(2-triisopropylsilylethynyl)benzene (297)



Triazine **296** (400 mg, 1.0 mmol, 1 eq) was mixed with iodomethane (5 mL) in a sealed tube fitted with a septa and the solution was degassed with argon for 15 min. The tube was sealed and heated to 120 $^\circ\text{C}$ for 5 h. The reaction was cooled to rt and transferred to a flask with CH_2Cl_2 and concentrated. Chromatography (petroleum ether/ CH_2Cl_2 , 9:1) afforded **297** as a yellow oil (352 mg, 83%); IR (neat) ν 2959.2, 2864.5, 2155.0, 1461.5, 1398.8 cm^{-1} ; ^1H NMR (500 MHz, CDCl_3) δ 7.71 (d, $J = 8.2$ Hz, 1H), 7.31 (d, $J = 2.2$ Hz, 1H), 6.85 (dd, $J = 8.2, 2.2$ Hz, 1H), 2.81 (sept, $J = 6.9$ Hz, 1H), 1.20 (d, $J = 6.9$ Hz, 6H) 1.15 (s, 21H); ^{13}C NMR (125 MHz, CDCl_3) δ 149.0 (s), 138.8 (d), 131.7 (d), 130.1 (s), 128.2 (d), 108.6 (s), 97.4 (s), 94.9 (s), 33.9 (d), 23.9 (q), 18.9 (q), 11.6 (d); MS (EI) m/z 426 (M^+ , 5), 383 (100), 341 (25), 313 (37), 171 (33); HRMS calcd for $\text{C}_{20}\text{H}_{31}\text{ISi}$ 426.1240 (M^+), found 426.1265.

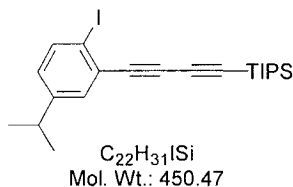
N,N-Diethyl-*N'*-[4-isopropyl-2-(4-triisopropylsilyl-1,3-butadiynyl)phenyl]triazene (298)



A solution of *n*-BuLi (2.5 M in THF, 55.8 mL, 139.4 mmol, 3 eq) was added in one portion to a -78 $^\circ\text{C}$ solution of *cis*-4-chloro-1-triisopropylsilyl-but-3-en-1-yne (**83**) (16.9 g,

69.7 mmol, 1.5 eq) in THF (150 mL). The resulting yellow solution was stirred for 2 min followed by the addition of a solution of ZnBr₂ (16.9 g, 75.0 mmol, 1.6 eq) in THF (100 mL). The colourless solution was stirred at -78 °C for 5 min then warmed to 0 °C for 15 min. A mixture of iodotriazine **223** (16.1 g, 46.6 mmol, 1 eq) and Pd(PPh₃)₄ (3.10 g, 5 mol%) in THF (100 mL) was added by canula and the reaction was stirred at rt for 18 h. The reaction was diluted with H₂O and extracted with Et₂O (2x). The combined extracts were washed with H₂O and brine, dried, and concentrated. Chromatography (petroleum ether/CH₂Cl₂, 9:1) afforded **298** as a dark red oil (15.0 g, 66%); IR (neat) ν 2961.7, 2866.4, 2199.6, 2096.6, 1464.3 cm⁻¹; ¹H NMR (500 MHz, CDCl₃) δ 7.37 (d, *J* = 2.1 Hz, 1H), 7.30 (d, *J* = 8.2 Hz, 1H), 7.16 (dd, *J* = 8.1, 2.1 Hz, 1H), 3.84 (q, *J* = 7.1 Hz, 4H), 2.92 (sept, *J* = 6.9 Hz, 1H), 1.40 (t, *J* = 7.1 Hz, 6H), 1.31 (d, *J* = 6.9 Hz, 6H), 1.20 (s, 21H); ¹³C NMR (125 MHz, CDCl₃) δ 152.7 (s), 145.2 (s), 132.0 (d), 128.3 (d), 117.3 (d), 115.7 (s), 90.4 (s), 87.0 (s), 77.9 (s), 75.0 (s), 42.1 (t), 33.4 (d), 23.8 (q), 18.4 (q) (2 peaks), 11.3 (d); MS (EI) *m/z* 380.3 (M⁺ - 43 (*i*-Pr), 4), 281.2 (11), 211.1 (10), 119.1 (14), 70.1 (100); HRMS calcd for C₂₃H₃₄N₃Si 380.2822 (M⁺ - 43 (*i*-Pr)), found 380.2825.

1-Iodo-4-isopropyl-2-(4-triisopropylsilyl-1,3-butadiynyl)benzene (**299**)



Triazine **298** (3.30 g, 7.79 mmol, 1 eq) was mixed with iodomethane (30 mL) in a sealed tube fitted with a septa and the solution was degassed with argon for 15 min. The tube was sealed and heated to 120 °C for 6 h. The reaction was cooled to rt and transferred to a flask with CH₂Cl₂ and concentrated. Chromatography (petroleum ether) afforded **299** as an orange oil (2.36 g, 67%); IR (neat) ν 2960.2, 2866.0, 2205.4, 2096.4, 1465.0 cm⁻¹; ¹H NMR (500 MHz, CDCl₃) δ 7.69 (d, *J* = 8.4 Hz, 1H), 7.37 (d, *J* = 2.8 Hz, 1H), 6.89 (dd, *J* = 8.3, 2.8 Hz, 1H), 2.81 (sept, *J* = 6.9 Hz, 1H), 1.19 (d, *J* = 6.9 Hz, 6H) 1.11 (s, 21H); ¹³C NMR (125 MHz, CDCl₃) δ 149.1 (s), 138.9 (d), 132.7 (d), 129.2 (s), 128.5 (d), 97.2 (s), 89.8 (s), 89.6 (s), 77.8 (s), 77.3 (s), 33.8 (d), 23.8 (q), 18.8 (q), 11.6 (d); MS (EI) *m/z* 450.1 (M⁺, 12), 407.1 (100), 379.0 (27), 365.0 (23); HRMS calcd for C₂₂H₃₁ISi 450.1240 (M⁺), found 450.1241. Reference: Moore, J. S.; Weinstein, E. J.; Wu, Z. *Tetrahedron Lett.* 1991, 32, 2465-2466.

7. References

1. Nicolaou, K. C.; Sorensen, E. J. *Classics in Total Synthesis*; VCH, New York, 1996.
2. Weber, E. *Top. Curr. Chem.* **1994**, *172*, preface.
3. Pellegrin, M. *Recl. Trav. Chim. Pays-Bas* **1899**, *18*, 457.
4. (a) Brown, C. J.; Farthing, A. C. *Nature*, **1949**, *164*, 915; (b) Brown, C. J. *J. Chem. Chem. Soc.* **1951**, *73*, 5691.
5. Cram, D. J.; Steinberg, H. *J. Am. Chem. Soc.* **1951**, *73*, 5691.
6. Vögtle, F.; Neumann, P. *Tetrahedron Lett.* **1969**, *60*, 5329; (b) Vögtle, F.; Neumann, P. *Tetrahedron* **1970**, *26*, 5847.
7. Bodwell, G. *Angew. Chem., Int. Ed. Engl.* **1996**, *35*, 2085.
8. Matohara, K.; Lim, C.; Yasutake, M.; Nogita, R.; Koga, T.; Sakamoto, Y.; Shinmyozu, T. *Tetrahedron Lett.* **2000**, *41*, 6803.
9. Aly, A. A.; Hopf, H.; Ernst, L. *Eur. J. Org. Chem.* **2000**, 3021.
10. Hermanns, N.; Dahmen, S.; Bolm, C.; Bräse, S. *Angew. Chem. Int. Ed.* **2002**, *41*, 3692.
11. Sato, M.; Uehara, F.; Sato, K.; Yamaguchi, M.; Kabuto, C. *J. Am. Chem. Soc.* **1999**, *121*, 8270.
12. Popova, E. L.; Rozenberg, V. I.; Starikova, Z. A.; Keuker-Baumann, S.; Kitzrow, H.-S.; Hopf, H. *Angew. Chem. Int. Ed.* **2002**, *41*, 3411.
13. Bodwell, G. J.; Satou, T. *Angew. Chem. Int. Ed.* **2002**, *41*, 4003.
14. (a) Stille, J. K. *Angew. Chem., Int. Ed. Engl.* **1986**, *25*, 508; (b) McKean, D. R.; Parrinello, G.; Renaldo, A. F.; Stille, J. K. *J. Org. Chem.* **1987**, *52*, 422; (c) Scott, W. J.; Stille, J. K. *J. Am. Chem. Soc.* **1986**, *108*, 3033.
15. Negishi, E.; Liu, F. In *Metal-Catalyzed Cross-coupling Reactions*; Deiderich, F.; Stang, P. J., Eds.; Wiley-VCH, Weinheim, Germany, 1998; pp 1- 48.
16. Tameo, K.; Miyaura, N. *Top. Curr. Chem.* **2002**, *219*, 1.

-
17. Amatore, C.; Jutand, A. *Acc. Chem. Res.* **2000**, *33*, 314.
 18. (a) Farina, V.; Krihnan, B.; Marshall, D. R.; Roth, G. P. *J. Org. Chem.* **1993**, *58*, 5434; (b) Farina, V.; Kapadia, S.; Krishnan, B.; Wang, C.; Liebeskind, L. S. *J. Org. Chem.* **1994**, *59*, 5905; (c) Segelstein, B. E.; Butler, T. W.; Chenard, B. L. *J. Org. Chem.* **1995**, *60*, 12; (d) Allred, G. D.; Liebeskind, L. S. *J. Am. Chem. Soc.* **1996**, *118*, 2748; (e) Roth, G. P.; Farina, V. *Tetrahedron Lett.* **1995**, *36*, 2191.
 19. Traditionally the reaction was limited to sp- and sp²-hybridized organohalides. The development of new catalysts has allowed saturated organohalides to be used in the reaction, see: Zhou, J.; Fu., G. C. *J. Am. Chem. Soc.* **2003**, *125*, 12527.
 20. Tsuji, J. *Palladium Reagents and Catalysts – Innovations in Organic Synthesis*; Wiley, Toronto, 1996.
 21. Hundertmark, T.; Littke, A. F.; Buchwald, S. L.; Fu, G. C. *Org. Lett.* **2000**, *2*, 1729 and references cited therein.
 22. Casado, A. L.; Espinet, P. *J. Am. Chem. Soc.* **1998**, *120*, 8978.
 23. Sonogashira, K.; Tohda, Y.; Higihara, N. *Tetrahedron Lett.* **1975**, *16*, 4467.
 24. Sonogashira K. In *Metal-catalyzed Cross-coupling Reactions*; Deiderich, F.; Stang, P. J., Eds.; Wiley-VCH, Weinheim, Germany, 1998; pp 203-227.
 25. (a) Glaser, C. *Ber. Dtsch. Chem. Ges.* **1869**, *2*, 422; (b) Glaser, C. *Ann. Chem. Pharm.* **1870**, *154*, 137.
 26. Eglinton, G.; Galbraith, A. R. *Chem. Ind. (London)* **1956**, 737.
 27. Hay, A. S. *J. Org. Chem.* **1962**, *27*, 3320.
 28. Siemsen, P.; Livingston, R. C.; Diederich, F. *Angew. Chem. Int. Ed.* **2000**, *39*, 2632.
 29. (a) Zalkind, Y. S.; Fundyler, F. B. *Ber. Dtsch. Chem.* **1936**, *69*, 128; (b) Zalkind, Y. S.; Fundyler, F. B. *J. Gen. Chem. USSR* **1957**, *27*, 3008.
 30. Bohlmann, F.; Schonowsky, H.; Inhoffen, E.; Grau, G. *Chem. Ber.* **1964**, *97*, 794.
 31. Rossi, R.; Carpita, A.; Bigelli, C. *Tetrahedron Lett.* **1985**, *26*, 523.

-
32. Liu, Q.; Burton, D. J. *Tetrahedron Lett.* **1997**, *38*, 4371.
 33. Lie, A.; Srivastava, M.; Zhang, X. *J. Org. Chem.* **2002**, *67*, 1969.
 34. Chodkiewicz, W.; Cadiot, P. *C. R. Hebd. Seances Acad. Sci.* **1955**, *241*, 1055.
 35. (a) Miyaoura, N.; Yamada, K.; Suzuki, A. *Tetrahedron Lett.* **1979**, *20*, 3437; (b) Wityak, J.; Chan, J. B. *Synth. Commun.* **1991**, *21*, 977.
 36. Romero, M. A.; Fallis, A. G. *Tetrahedron Lett.* **1994**, *35*, 4711.
 37. Fallis, A. G. *Can. J. Chem.* **1999**, *77*, 159.
 38. Collins, S. K.; Yap, G. P. A.; Fallis, A. G. *Angew. Chem. Int. Ed.* **2000**, *39*, 385.
 39. Collins, S. K.; Yap, G. P. A.; Fallis, A. G. *Org. Lett.* **2000**, *2*, 3189.
 40. Collins, S. K.; Yap, G. P. A.; Fallis, A. G. *Org. Lett.* **2002**, *4*, 11.
 41. (a) Eaton, P. E.; Cole, T. W. Jr. *J. Am. Chem. Soc.* **1964**, *86*, 962; (b) Eaton, P. E.; Cole, T. W. Jr. *J. Am. Chem. Soc.* **1964**, *86*, 3157.
 42. (a) Paquette, L. A.; Ternansky, R. J.; Balogh, D. W. *J. Am. Chem. Soc.* **1982**, *104*, 4502; (b) Ternansky, R. J.; Balogh, D. W.; Paquette, L. A. *J. Am. Chem. Soc.* **1982**, *104*, 4503.
 43. Kroto, H. W.; Heath, J. R.; O'Brien, R. F.; Curl, R. E.; Smalley, E. *Nature* **1985**, *318*, 162.
 44. Dresselhaus, M. S.; Dresselhaus, G.; Eklund, P. C. *Science of Fullerenes and Carbon Nanotubes*; Academic Press, London, 1996.
 45. Boese, R.; Matzger, A. J.; Vollhardt, K. P. C. *J. Am. Chem. Soc.* **1997**, *119*, 2052.
 46. Faust, R. *Angew. Chem. Int. Ed.* **1998**, *37*, 2825.
 47. (a) Rubin, Y.; Kahr, M.; Knobler, C. B.; Diederich, F.; Wilkins, C. L. *J. Am. Chem. Soc.* **1991**, *113*, 495; (b) McElvany, S. W.; Ross, M. M.; Goroff, N. S.; Diederich, F. *Science* **1993**, *259*, 1594.
 48. Ferrier, R. J.; Holden, S. G.; Gladkikh, O. *J. Chem. Soc., Perkin Trans. 1* **2000**, 3505.

-
49. Rubin, Y.; Parker, T. C.; Khan, S. I.; Holliman, C. L.; McElvany, S. W. *J. Am. Chem. Soc.* **1996**, *118*, 5308.
 50. Rubin, Y.; Parker, T. C.; Pastor, S. J.; Jalisatgi, S.; Boule, C.; Wilkins, C. L. *Angew. Chem. Int. Ed.* **1998**, *37*, 1226.
 51. Tobe, Y.; Nakagawa, N.; Naemura, K.; Wakabayashi, T.; Shida, T.; Achiba, Y. *J. Am. Chem. Soc.* **1998**, *120*, 4544.
 52. Scott, L. T.; Boorum, M. M.; McMahon, B. J.; Hagen, S.; Mack, J.; Blank, J.; Wegner, H.; de Meijere, A. *Science* **2002**, *295*, 1500.
 53. Haley, M. M.; Bell, M. L.; Brand, S. C.; Kimball, D. B.; Pak, J. J.; Wan, W. B. *Tetrahedron Lett.* **1997**, *38*, 7483.
 54. Collins, S. K. *Design, Synthesis, and Applications of Novel Phenyl/Acetylene Cyclophanes*; Ph.D. Thesis, University of Ottawa, Ottawa, Canada, 2001.
 55. (a) Lu, Y.-F.; Harwig, C. W.; Fallis, A. G. *J. Org. Chem.* **1993**, *58*, 4202; (b) Lu, Y.-F.; Harwig, C. W.; Fallis, A. G. *Can. J. Chem.* **1995**, *73*, 2253.
 56. (a) Brandsma, L. *Preparative Acetylene Chemistry*, 2nd ed., Elsevier: Amsterdam, 1988; (b) Haley, M. M. *Synlett* **1998**, 557; (c) Wan, W. B.; Haley, M. M. *J. Org. Chem.* **2001**, *66*, 3893.
 57. Moore, J. S. *Acc. Chem. Res.* **1997**, *30*, 402.
 58. Haley, M. M.; Brand, S. C.; Pak, J. J. *Angew. Chem. Int. Ed. Engl.* **1997**, *36*, 836.
 59. Lin, C.-H.; Tour, J. *J. Org. Chem.* **2002**, *67*, 7761.
 60. Pak, J. J.; Weakley, J. R.; Haley, M. M. *J. Am. Chem. Soc.* **1999**, *121*, 8192.
 61. Tobe, Y.; Utsumi, N.; Nagano, A.; Naemura, K. *Angew. Chem. Int. Ed.* **1998**, *37*, 1285.
 62. Ikegashira, K.; Nishihara, Y.; Hirabayashi, K.; Mori, A.; Hiyama, T. *Chem. Commun.* **1997**, 1039.
 63. Nishihara, Y.; Ikegashira, K.; Mori, A.; Hiyama, T. *Tetrahedron Lett.* **1998**, *39*, 4075.
 64. Heuft, M. A.; Collins, S. K.; Yap, G. P. A.; Fallis, A. G. *Org. Lett.* **2001**, *3*, 2883.

-
65. (a) Oda, H.; Sato, M.; Morizawa, Y.; Oshima, K.; Nozaki, H. *Tetrahedron* **1985**, *41*, 3257; (b) Johnson, T. R.; Walton, D. R. M. *Tetrahedron* **1972**, *28*, 5221.
66. (a) Chan, T. H.; Massuda, D. *Tetrahedron Lett.* **1975**, 3383; (b) Chan, T. H.; Ong, B. S. *J. Org. Chem.* **1978**, *43*, 2994.
67. Akiyama, S.; Nakasuji, K.; Akashi, K.; Nakagawa, M. *Tetrahedron Lett.* **1968**, 1121.
68. Kajigaeshi, S.; Kakinami, T.; Yamasaki, H.; Fujisaki, S.; Okamoto, T. *Bull. Chem. Soc. Jpn.* **1988**, *61*, 600.
69. X-ray data for cyclophane **112** including bond lengths and angles can be found in Appendix A4.
70. (a) Patel, G. N.; Chance, R. R.; Turi, E. A.; Khanna, Y. P. *J. Am. Chem. Soc.* **1978**, *100*, 6644; (b) Zhou, Q.; Carroll, P. J.; Swager, T. M. *J. Org. Chem.* **1994**, *59*, 1294.
71. Grave, C.; Schlüter, A. D. *Eur. J. Org. Chem.* **2002**, 3075; (b) Tobe, Y.; Utsumi, N.; Kawabata, K.; Nagano, A.; Adachi, K.; Araki, S.; Sonoda, M.; Hirose, K.; Naemura, K. *J. Am. Chem. Soc.* **2002**, *124*, 5350.
72. (a) Tovar, J. D.; Jux, N.; Jarrosson, T.; Khan, S. I.; Rubin, Y. *J. Org. Chem.* **1997**, *62*, 3432; (b) Bunz, U. H. F.; Enkelmann, V. *Chem. Eur. J.* **1999**, *5*, 263; (c) Baldwin, K. P.; Matzger, A. J.; Scheiman, D. A.; Tessier, C. A.; Vollhardt, K. P. C.; Youngs, W. J. *Synlett* **1995**, 1215; (d) Tobe, Y.; Kishi, J.-Y.; Ohki, I.; Sonoda, M. *J. Org. Chem.* **2003**, *68*, 3330.
73. Höger, S.; Bonrad, K.; Karcher, L.; Meckenstock, A.-D. *J. Org. Chem.* **2000**, *65*, 1588.
74. Modeling results were obtained using a DN basis set in the Cerius²-Dmol³ molecular modeling suite from Molecular Simulations Inc. San Diego, 1999.
75. Our more detailed study was rejected for publication twice prior to Tobe's report.
76. Rubin, Y.; Parker, T. C.; Pastor, S. J.; Jalisatgi, S.; Boule, C.; Wilkins, C. L. *Angew. Chem. Int. Ed.* **1998**, *37*, 1226.
77. Heuft, M. A.; Collins, S. K.; Fallis, A. G. *Org. Lett.* **2003**, *5*, 1911.

-
78. Hofmeister, H.; Annen, K.; Laurent, H.; Wiechert, R. *Angew. Chem. Int. Ed. Engl.* **1974**, *23*, 727.
79. Corey, E. J.; Fuchs, P. L. *Tetrahedron Lett.* **1972**, 3769.
80. Ohira, S. *Synth. Commun.* **1989**, *19*, 561.
81. See compound **134** in chapter 6 for the structure.
82. Semi-preparative size-exclusion chromatography (SEC) (Jordi Gel DVB 100A, CH₂Cl₂).
83. Hopf, H. *Classics in Hydrocarbon Chemistry*, Wiley-VCH: Toronto, 2000.
84. (a) Joshi, H. S.; Jamshidi, R.; Tor, Y. *Angew. Chem. Int. Ed.* **1999**, *38*, 2721; (b) Connors, P. J.; Tzalis, D.; Dunnick, A. L.; Tor, Y. *Inorg. Chem.* **1998**, *37*, 1121; (c) Tzalis, D.; Tor, Y. *Tetrahedron Lett.* **1995**, *36*, 6017.
85. Watson, J. D.; Crick, F. H. C. *Nature* **1953**, 171, 964.
86. (a) Nakano, T.; Okamoto, Y. *Chem. Rev.* **2001**, *101*, 4013; (b) Green, M. M.; Cheon, K.-S.; Yang, S.-Y.; Park, J.-W.; Swanburg, S.; Lui, W. *Acc. Chem. Res.* **2001**, *34*, 672.
87. Nuckolls, C.; Katz, T. J. Castellanos, L. *J. Am. Chem. Soc.* **1996**, *118*, 3767.
88. (a) Nuckolls, C.; Katz, T. J. *J. Am. Chem. Soc.* **1998**, *120*, 9541; (b) Nuckolls, C.; Katz, T. J.; Katz, G.; Collings, P. J.; Castellanos, L. *J. Am. Chem. Soc.* **1999**, *121*, 79.
89. Fox, J. M.; Lin, D.; Itagaki, Y.; Fujita, T. *J. Org. Chem.* **1998**, *63*, 2031.
90. Marsella, M. J.; Kim, I. T.; Tham, F. *J. Am. Chem. Soc.* **2000**, *122*, 974.
91. (a) An, D. L.; Nakano, T.; Orita, A.; Otera, J. *Angew. Chem. Int. Ed.* **2002**, *41*, 171; (b) Orita, A.; An, D. L.; Nakano, T.; Yaruva, J.; Ma, N.; Otera, J. *Chem. Eur. J.* **2002**, *8*, 2005.
92. (a) Kalamar, J.; Steiner, E.; Charollais, E.; Posternak, T. *Helv. Chim. Acta* **1974**, *57*, 2368; (b) Staab, H. A.; Weiser, J.; Futscher, M.; Voit, G.; Rückemann, A.; Anders, C. *Chem. Ber.* **1992**, *125*, 2285; (c) Rose, A.; Lugmair, C. G.; Miao, Y.-J.; Kim, J.;

-
- Levitsky, I. A.; Bpir, V. E.; Amicus, P. S. *Detection and Remediation Technologies for Mine and Minelike Targets V.*, **2000**, 512.
93. Benington, F.; Morin, R. D.; Clark, L. C. *J. Org. Chem.* **1955**, *20*, 102.
94. Hofmeister, H.; Annen, K.; Laurent, H.; Wiechert, R. *Angew. Chem., Int. Ed. Engl.* **1974**, *23*, 727.
95. Marino, J. P.; Nguyen, H. N. *J. Org. Chem.* **2002**, *67*, 6841.
96. See compound 177 in chapter 6 for the structure.
97. See Section 2.3.
98. Seyferth, D. *Organometallics* **2002**, *21*, 1520 and references therein.
99. Kirtley, S. W. in *Comprehensive Organometallic Chemistry*, Vol. 3; Eds. Wilkinson, G.; Stone, F. G. A.; Abel, E. W., Pergamon: 1982, Toronto.
100. (a) Hein, F. *Ber.* **1919**, *52*, 195; (b) Zeiss, H. H.; Wheatley, P. J.; Winkler, H. J. S. *Benzenoid-Metal Complexes*, Ronald Press: 1966, New York.
101. Fischer, E. O.; Hafber, W. *Naturforsch., Teil B* **1955**, *10*, 665.
102. Timms, P. L. *Chem. Commun.* **1969**, 1033.
103. Elschenbroich, C.; Möckel, R.; Zenneck, U. *Angew. Chem.* **1978**, *90*, 560.
104. Schulz, J.; Vögtle, F. *Top. Curr. Chem.* **1994**, *172*, 41.
105. Hannover medium pressure Hg arc lamp, 350 V.
106. Asirvatham, V. S.; Ashby, M. T. *Organometallics* **2001**, *20*, 1687.
107. Davis, R.; Kane-Maguire, L. A. P. in *Comprehensive Organometallic Chemistry*, Vol. 3; Eds. Wilkinson, G.; Stone, F. G. A.; Abel, E. W., Pergamon: 1982, Toronto.
108. Deeming, A. J. in *Comprehensive Organometallic Chemistry*, Vol. 4; Eds. Wilkinson, G.; Stone, F. G. A.; Abel, E. W., Pergamon: 1982, Toronto.
109. (a) Fischer, E. O.; Böttcher, R. *Chem Ber.* **1956**, *89*, 2397; (b) Elzinga, B.; Rosenblum, M. *Tetrahedron Lett.* **1982**, *23*, 1535.

-
110. (a) von Zelewsky, A. *Stereochemistry of Coordination Compounds*; Wiley: 1996, Chichester; (b) Constable, E. C. in *Comprehensive Supramolecular Chemistry*, Vol. 9; Eds. Atwood, J. L.; Davies, J. E. D.; MacNicol, D. D.; Vögtle, F.; Lehn, J.-M., Pergamon: 1996, Toronto.
111. (a) Baxter, P. N. W.; Lehn, J.-M.; Kneisel, B. O.; Fenske, D. *Angew. Chem. Int. Ed.* **1997**, *36*, 1978; (b) Toyota, S.; Woods, C. R.; Benaglia, M.; Haldimann, R.; Warnmark, K.; Hardcastle, K.; Siegel, J. S. *Angew. Chem. Int. Ed.* **2001**, *40*, 751.
112. Dietrich-Buchecker, C. O.; Sauvage, J.-P.; Kintzinger, J.-P. *Tetrahedron Lett.* **1983**, *24*, 5095.
113. (a) Loren, J. C.; Siegel, J. S. *Angew. Chem. Int. Ed.* **2001**, *40*, 754; (b) Felder, D.; Nierengarten, J.-F.; Barigelletti, F.; Ventura, B.; Armaroli, N. *J. Am. Chem. Soc.* **2001**, *123*, 6291; (c) MacLachlan, M. J.; Rose, A.; Swager, T. M. *J. Am. Chem. Soc.* **2001**, *123*, 9180; (d) Cuttell, D. G.; Kuang, S.-M.; Fanwick, P. E.; McMillin, D. R.; Walton, R. A. *J. Am. Chem. Soc.* **2002**, *124*, 6.
114. (a) Armaroli, N. *Chem. Soc. Rev.* **2001**, *30*, 113; (b) Scaltrino, D. V.; Thompson, D. W.; O'Callaghan, J. A.; Meyer, G. J. *Coord. Chem. Rev.* **2000**, *208*, 243; (c) Miller, M. T.; Gantzel, P. K.; Karpishin, T. B. *Inorg. Chem.* **1999**, *38*, 3414; (d) McMillin, D. R.; McNett, K. M. *Chem. Rev.* **1998**, *98*, 1201.
115. Tamilarasan, R.; McMillin, D. R. *Inorg. Chem.* **1990**, *29*, 2798.
116. Chelucci, G.; Thummel, R. P. *Chem. Rev.* **2002**, *102*, 3129.
117. Kubas, G. J. *Inorg. Syn.* **1990**, *28*, 68.
118. Only one phenanthrolinephane has previously been reported: Lüning, U.; Müller, M. *Chem. Ber.* **1990**, *123*, 643.
119. (a) Tzalis, D.; Tor, Y.; Failla, Siegel, J. S. *Tetrahedron Lett.* **1995**, *36*, 3489; (b) Saitoh, Y.; Koizumi, T.-A.; Osakada, K.; Yamamoto, T. *Can. J. Chem.* **1997**, *75*, 1336.
120. Garcia, E. E.; Greco, C. V.; Hunsberger, I. M. *J. Am. Chem. Soc.* **1960**, *82*, 4430.

-
121. Dietrich-Buchecker, C.; Jiménez, M. C.; Sauvage, J.-P. *Tetrahedron Lett.* **1999**, *40*, 3395.
122. Suzuki couplings have also been used to prepare 3,8-diaryl-1,10-phenanthrolines: Kimura, M.; Shiba, T.; Muto, T.; Hanabusa, K.; Shirai, H. *Tetrahedron Lett.* **2000**, *41*, 6809 and ref 121.
123. Sjoegren, M.; Hansson, S.; Norrby, P. O. Aakermark, B.; Cucciolito, M. E.; Vitagliano, A. *Organometallics* **1992**, *11*, 3954.
124. (a) Busch, D. H.; Vance, A. L.; Kolchinski, A. G. in *Comprehensive Supramolecular Chemistry*, Vol. 9; Eds. Atwood, J. L.; Davies, J. E. D.; MacNicol, D. D.; Vögtle, F.; Lehn, J.-M., Pergamon: 1996, Toronto; (b) *Templated Organic Synthesis*, Eds. Diederich, F.; Stang, P. J., Wiley-VCH: Weinheim, 2000.
125. The butyl groups are diastereotopic if helical isomerization and nitrogen inversion are slow. ¹³C NMR can be used to obtain conformational information. See reference 45.
126. Ozutsumi, K.; Kawashima, T. *Inorg. Chem. Acta* **1991**, *180*, 231.
127. Cunningham, C. T.; Cunningham, K. L. H.; Michalec, J. F.; McMillin, D. R. *Inorg. Chem.* **1999**, *38*, 4388.
128. Ruthkosky, M.; Castellano, F. N.; Mayer, G. J. *Inorg. Chem.* **1996**, *35*, 6406.
129. Shvo, Y.; Taylor, E. C.; Mislou, K.; Raban, M. *J. Am. Chem. Soc.* **1967**, *89*, 4910.
130. For a recent review on triazenes used in organic synthesis see: Kimball, D. B.; Haley, M. M. *Angew. Chem. Int. Ed.* **2002**, *41*, 3338.
131. Munn, B. Molecular Electronics in *The New Chemistry*, Nina Hall, Ed. Cambridge University Press, New York, 2000.
132. Bao, Z.; Rogers, J. A.; Katz, H. E. *J. Mater. Chem.* **1999**, *9*, 1895.
133. Kraft, A. *ChemPhysChem* **2001**, *2*, 163.
134. Würthner, F. *Angew. Chem. Int. Ed.* **2001**, *40*, 1037.
135. Katz, H. E.; Bao, Z.; Gilat, S. L. *Acc. Chem. Res.* **2001**, *34*, 359.

-
136. Goodings, E. P.; Mitchad, D. A.; Owen, G. *J. Chem. Soc., Perkin I* **1972**, 1310.
137. Mayer zu Heringdorf, F.-J.; Reuter, M. C.; Tromp, R. M. *Nature* **2001**, *412*, 517.
138. Cornil, J.; Calbert, J. P.; Brédas, J. L. *J. Am. Chem. Soc.* **2001**, *123*, 1250.
139. Herwig, P. T.; Müllen, K. *Adv. Mater.* **1999**, *11*, 480.
140. Afzali, A.; Dimitrakopoulos, C. D.; Breen, T. L. *J. Am. Chem. Soc.* **2002**, *124*, 8812.
141. Anthony, J. E.; Eaton, D. L.; Parkin, S. R. *Org. Lett.* **2002**, *4*, 15.
142. Anthony, J. E.; Brooks, J. S.; Eaton, D. L.; Parkin, S. R. *J. Am. Chem. Soc.* **2001**, *123*, 9482.
143. Tokumoto, T.; Brooks, J. S.; Clinite, R.; Wei, X.; Anthony, J. E.; Eaton, D. L.; Parkin, S. R. *J. Appl. Phys.* **2002**, *92*, 5208.
144. (a) Schleyer, P. R.; Manoharan, M.; Jiao, H.; Stahl, F. *Org. Lett.* **2001**, *3*, 3643; (b) Randić, M. *Chem. Rev.* **2003**, *103*, 3449.
145. (a) Boldt, P.; Vardakis, F. *Angew. Chem., Int. Ed. Engl.* **1965**, *4*, 1078; (b) Almlof, J. E.; Feyereisen, M. W.; Jozefiak, T. H.; Miller, L. L. *J. Am. Chem. Soc.* **1990**, *112*, 1206.
146. Cory, R. M.; McPhail, C. L.; Dikmans, A. J. *Tetrahedron Lett.* **1993**, *34*, 7533.
147. (a) Fitzgerald, J. J.; Drysdale, N. E.; Olofson, R. A. *Synth. Commun.* **1992**, *22*, 1807; (b) Fitzgerald, J. J.; Drysdale, N. E.; Olofson, R. A. *J. Org. Chem.* **1992**, *57*, 7122.
148. Cory, R. M. Personal Correspondence – April 11, 2002 (e-mail).
149. (a) Danishefsky, S. J.; Kitahara, T.; Yan, C. F.; Morris, J. *J. Am. Chem. Soc.* **1979**, *101*, 6996; (b) Danishefsky, S. J.; Yan, C. F.; Singh, R. K.; Gammill, R. B.; McCurry, P.; Fritsch, N.; Clardy, J. C. *J. Am. Chem. Soc.* **1979**, *101*, 7001.
150. X-ray data for silyl ether **247** including bond lengths and angles can be found in Appendix A4.

-
151. TBAF was used as a solution in THF. Tf_2O reacts with THF and reduces the effective amount of Tf_2O in the reaction. Better yields were obtained when excess Tf_2O was used.
152. Hendrickson, J. B.; Bergeron, R. *Tetrahedron Lett.* **1973**, *14*, 4747.
153. A review on the synthesis of aryl and vinyl triflates and their reactions including palladium couplings: Ritter, K. *Synthesis* **1993**, 735.
154. Rewcastle, G. W.; Atwell, G. J.; Palmer, B. D.; Boyd, P. D. W.; Baguley, B. C.; Denny, W. A. *J. Med. Chem.* **1991**, *34*, 491.
155. (a) Petti, M. A.; Shepodd, T. J.; Barrans Jr., R. E.; Dougherty, D. A. *J. Am. Chem. Soc.* **1988**, *110*, 6825; (b) Goodall, F. L.; Perkin, A. G. *J. Chem. Soc.* **1923**, 470; (c) Hall, J.; Perkin, A. G. *J. Chem. Soc.* **1923**, 2029.
156. Tius, M. A.; Gomez-Galeno, J.; Zaidi, J. H. *Tetrahedron Lett.* **1988**, *29*, 6909.
157. Aubry, J.-M.; Pierlot, C.; Rigaudy, J.; Schmidt, R. *Acc. Chem. Res.* **2003**, *36*, 668.
158. A crystal structure of a related endoperoxide was recently published: Schuster, I. I.; Craciun, L.; Ho, D. M.; Pascal, R. A. Jr. *Tetrahedron* **2002**, *58*, 8875.
159. Ito, K.; Suzuki, T.; Sakamoto, Y.; Kubota, D.; Inoue, Y.; Sato, F.; Tokito, S. *Angew. Chem. Int. Ed.* **2003**, *42*, 1159.
160. Spath, E. *Sitzungsber. Akad. Wiss. Wien. Math.-Naturwiss. Kl., Abt. 2B* **1911**, *120*, 117.
161. Chattopadhyay, N.; Serpa, C.; Pereira, M. M.; de Melo, J. S.; Arnaut, L. G.; Formosinho, S. J. *J. Phys. Chem. A* **2001**, *105*, 10025.

APPENDIX

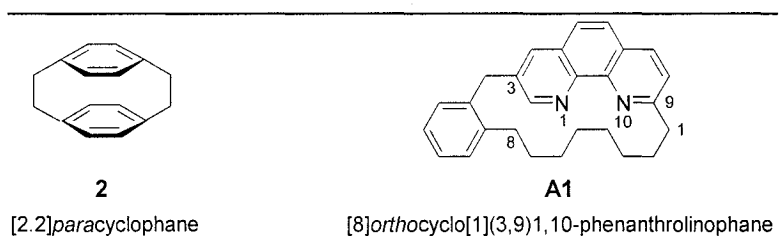
- A.1 Cyclophane Nomenclature
 - A.2 Phenanthrolinephane Helical Interconversion Barrier Height Determination
 - A.3 Selected ^1H , ^{13}C , and Mass Spectra
 - A.4 X-Ray Crystallographic Data
-

Appendix

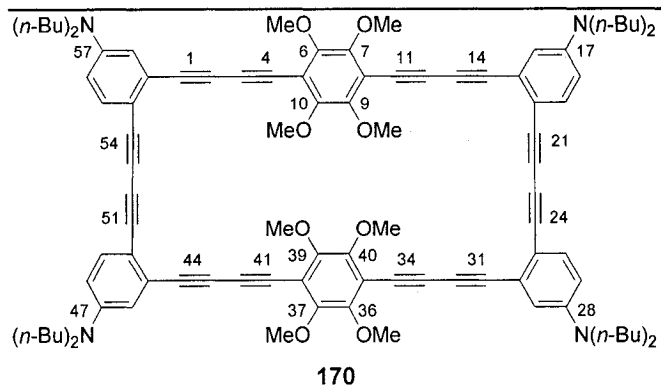
A.1 Cyclophane Nomenclature

An entire chapter could be written on the nomenclature of cyclophanes, but only a general introduction will be presented here. A systematic method for cyclophane nomenclature was introduced by Vögtle.⁶ "Phanes" are compounds that contain one or more aromatic nuclei (cap) and at least one aliphatic bridge. IUPAC nomenclature is used to name the aromatic segment(s) with the addition of the ending "-o". By definition "cyclo" is used for phenyl rings. Bridge attachment is denoted by either *ortho/meta/para* or by numbering the aromatic nuclei, depending on what is appropriate. The suffix "phane" is used after the last aromatic nuclei.

A bridge is defined by IUPAC as a "valence compound or atom or unbranched chain of atoms that connect two parts of a molecule." The number of aliphatic bridge members is indicated in square brackets, with each bridge separated by a period. Two examples are shown below.



Many of the cyclophanes in this thesis have several bridges of differing length as well as different substituted aromatic nuclei. In order to unambiguously name these compounds, we have developed our own nomenclature convention based on the accepted conventions used to name cyclophanes. First, the cyclophane is numbered beginning with the longest bridge and numbering is continued around the entire molecule. Cyclophane substituents are named first and then the number of bridge members is given in square brackets. The bridges of the compounds in this dissertation are not simply aliphatic, so each bridge is named. Finally, the aromatic nuclei is named according to cyclophane nomenclature rules. The naming of bridges and aromatic nuclei continues around the molecule and the suffix "-phane" is added at the end. The nomenclature of cyclophane **170** is described here in detail as an example.



17,28,47,58-tetrakis(dibutylamino)-6,7,9,10,36,37,39,40-octamethoxy-[4]1,3-butadiynyl*paracyclo*[4]11,13-butadiynyl*orthocyclo*[4]21,23-butadiynyl*orthocyclo*[4]31,33-butadiynyl*paracyclo*[4]41,43-butadiynyl*orthocyclo*[4]51,53-butadiynyl*orthocyclo*phane

All of the bridges in cyclophane **170** are the same length so one bridge was chosen as a starting point and the whole cyclophane was numbered. There are four dibutylamino substituents (one on each bridging aromatic ring) and these substituents are named first "17,28,47,58-tetrakis(dibutylamino)." This is followed by the methoxy-substituents (substituents are listed alphabetically) "6,7,9,10,36,37,39,40-octamethoxy." With all of the substituents named, the bridges and aromatic nuclei are named. The first bridge has four atoms (members) and is denoted by [4], but since it is a butadiyne, the bridge is named "[4]1,3-butadiynyl." The aromatic nuclei is a *para*-substituted phenyl ring and is named "*paracyclo*." The next bridge is also butadiynyl, but it begins at the 11th atom and is named "[4]11,13-butadiynyl." The next aromatic nuclei is *ortho*-substituted and is named "*orthocyclo*". This naming of bridges and aromatic nuclei continues around the molecule and the suffix "-phane" is added after the last aromatic nuclei.

A.2 Phenanthroline Helical Interconversion Barrier Height Determination

The rate of exchange is inversely proportional to the NMR timescale (τ) at coalescence which can be expressed as:

$$k_{ex} = \tau^{-1} = \frac{\pi(\nu_a - \nu_x)}{\sqrt{2}}$$

with ν_a and ν_x being the peak midpoint frequencies of the exchanging signals at slow interconversion. The enantiomerization barrier height (ΔG^\ddagger) can be found from the interconversion rate k_{ex} as:

$$k_{ex} = \kappa \frac{k_B T}{h} \exp(-\Delta G^\ddagger / RT)$$

Combining equations 1 and 2 allows for ΔG^\ddagger to be determined from the frequency difference between the coalescing peaks during slow exchange and the coalescence temperature:

$$\frac{\Delta G^\ddagger}{RT_c} = 22.96 + \ln\left(\frac{T_c}{\nu_a - \nu_x}\right)$$

Phenanthroline (217)

$\Delta\nu = 32.6$ Hz (assume that $\Delta\nu$ is the same for both compounds)

T_c is below 193 K

$$\Delta G^\ddagger < 22.96 RT + RT \ln(T / \Delta\nu)$$

$$< 22.96 (8.31451 \text{ J mol}^{-1} \text{ K}^{-1}) (193 \text{ K}) + (8.31451 \text{ J mol}^{-1} \text{ K}^{-1})(193 \text{ K}) \ln(193/32.6)$$

$$< 39.7 \text{ kJ/mol}$$

$$< 9.5 \text{ kcal/mol (193 K)}$$

Copper (I) Phenanthroline Complex (218)

$\Delta\nu = 32.6$ Hz (at 213 K)

T_c is between 273 and 253 K

$$\begin{aligned}\Delta G^\ddagger &= 22.96 RT + RT \ln (T / \Delta\nu) \\ &= 22.96 (8.31451 \text{ J mol}^{-1} \text{ K}^{-1}) (273 \text{ K}) + (8.31451 \text{ J mol}^{-1} \text{ K}^{-1})(273 \text{ K}) \ln (273/32.6) \\ &= 56.9 \text{ kJ/mol} \\ &= 13.6 \text{ kcal/mol (273 K)}\end{aligned}$$

$$\begin{aligned}\Delta G^\ddagger &= 22.96 RT + RT \ln (T / \Delta\nu) \\ &= 22.96 (8.31451 \text{ J mol}^{-1} \text{ K}^{-1}) (253 \text{ K}) + (8.31451 \text{ J mol}^{-1} \text{ K}^{-1})(253 \text{ K}) \ln (253/32.6) \\ &= 52.6 \text{ kJ/mol} \\ &= 12.6 \text{ kcal/mol (253 K)}\end{aligned}$$

Phenanthroline (227)

$\Delta\nu = 60.1$ Hz (assume that $\Delta\nu$ is the same for both compounds)

T_c is below 193 K

$$\begin{aligned}\Delta G^\ddagger &< 22.96 RT + RT \ln (T / \Delta\nu) \\ &< 22.96 (8.31451 \text{ J mol}^{-1} \text{ K}^{-1}) (193 \text{ K}) + (8.31451 \text{ J mol}^{-1} \text{ K}^{-1})(193 \text{ K}) \ln (193/60.1) \\ &< 38.7 \text{ kJ/mol} \\ &< 9.2 \text{ kcal/mol (193 K)}\end{aligned}$$

Copper(I) Phenanthroline Complex 228

$\Delta\nu = 60.1$ Hz (assume that $\Delta\nu$ is the same for both compounds)

T_c is 330 K

$$\begin{aligned}\Delta G^\ddagger &= 22.96 RT + RT \ln (T / \Delta\nu) \\ &= 22.96 (8.31451 \text{ J mol}^{-1} \text{ K}^{-1}) (330 \text{ K}) + (8.31451 \text{ J mol}^{-1} \text{ K}^{-1})(330 \text{ K}) \ln (330/60.1) \\ &= 67.7 \text{ kJ/mol} \\ &= 16.2 \text{ kcal/mol (193 K)}\end{aligned}$$

Phenanthroline **227** had a helical inversion barrier of less than 9.2 kcal/mol. Copper raises the inversion barrier by over 7.0 kcal/mol. However, helical interconversion still occurred at room temperature so the enantiomers could not be separated.

A.3 Selected ^1H , ^{13}C , and Mass Spectra

Cyclophane 112	^1H NMR ^{13}C NMR MS(ES)
Cyclophane 113	^1H NMR ^{13}C NMR + expansion
Cyclophane 123a	^1H NMR ^{13}C NMR
Cyclophane 123b	^1H NMR ^{13}C NMR
Cyclophane 170	^1H NMR ^{13}C NMR
Phenanthrolinephane 200	^1H NMR ^{13}C NMR MS(FAB)
Phenanthrolinephane 217	^1H NMR ^{13}C NMR MS(ES)
Phenanthrolinephane 218	^1H NMR ^{13}C NMR MS(ES)
Phenanthrolinephane 227	^1H NMR ^{13}C NMR MS(ES)
Phenanthrolinephane 228	^1H NMR ^{13}C NMR MS(ES)

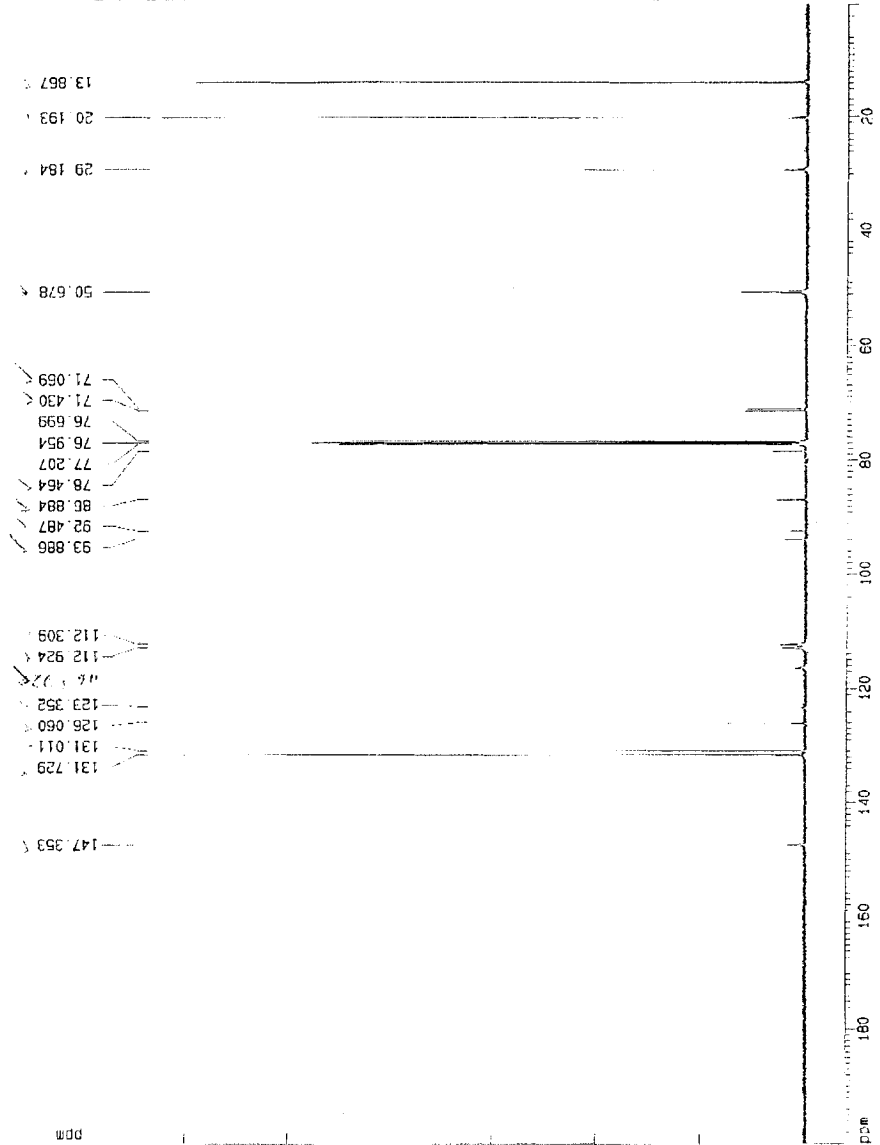
¹³C NMR Spectrum of Cyclophane 112

Current Data Parameters
 NAME nevft_134
 EXPNO 2
 PROCNO 1

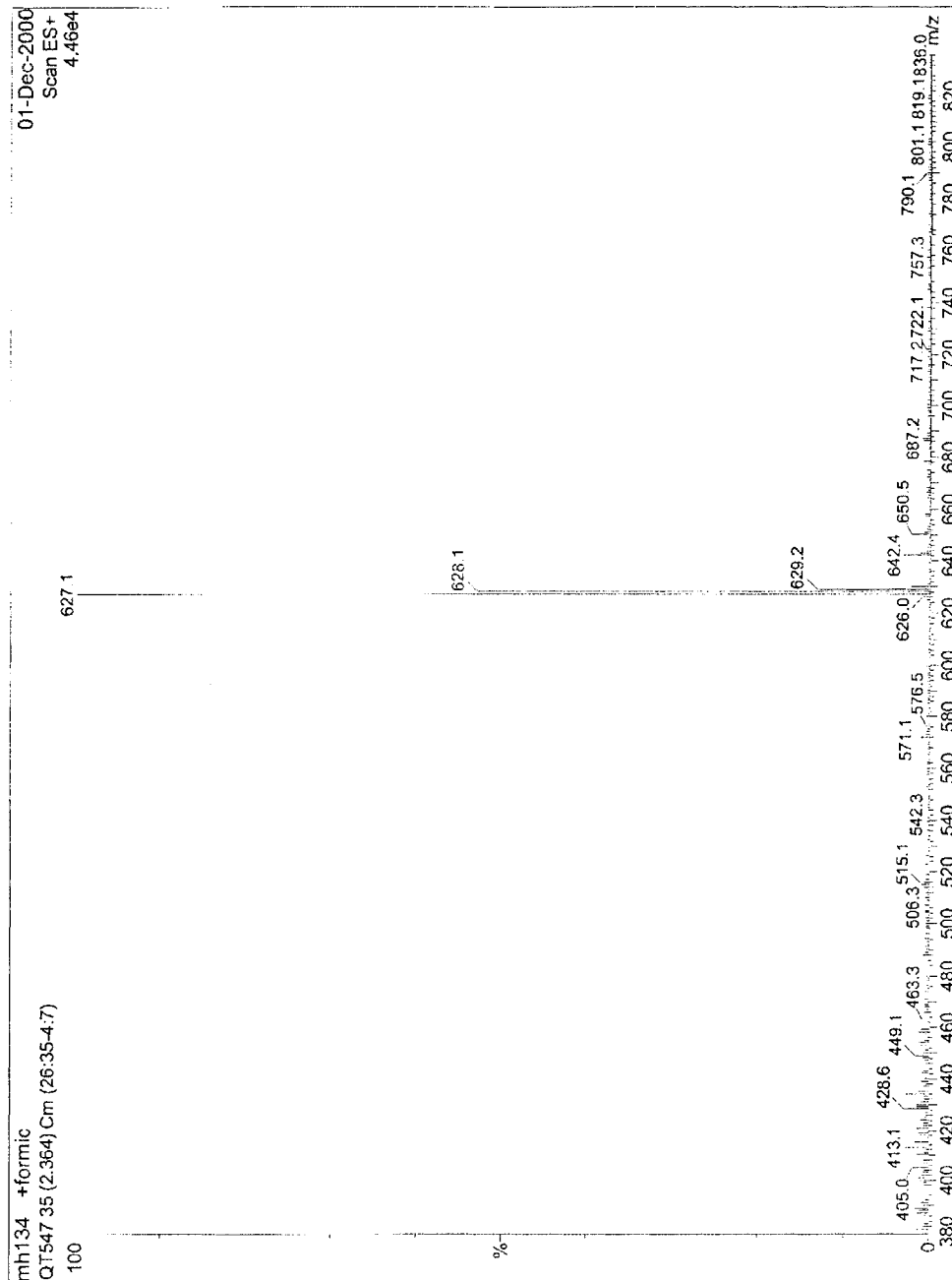
F2 - Acquisition Parameters
 Date_ 20001204
 Time 7.29
 PULPROG zgpg
 SOLVENT CDCl3
 AD 1.0485950
 FL3HS 0.478847
 DM 15.0
 RG 32758
 NUCLEUS 13C
 Q11 0.0300000
 Q31 70.0
 Q52 22
 Q71 22
 -L1 5.000000
 P1 5.0
 PC 20.0
 SF01 125.7724464
 SFR 31250.00
 TD 65536
 TO 6144
 BS 0

F1 - Processing parameters
 SI 32768
 MC2 0
 SF 125.7591571
 NCM EM
 SSB 0
 LB 1.00
 GB 0

1D NMR plot parameters
 CX 22.00
 FIP 200.000
 F1 25151.83
 F2 0.000
 FZ 0.00
 PPMCM 9.09091
 RZCM 1143.26501



MS(ES) Spectrum of Cyclophane 112

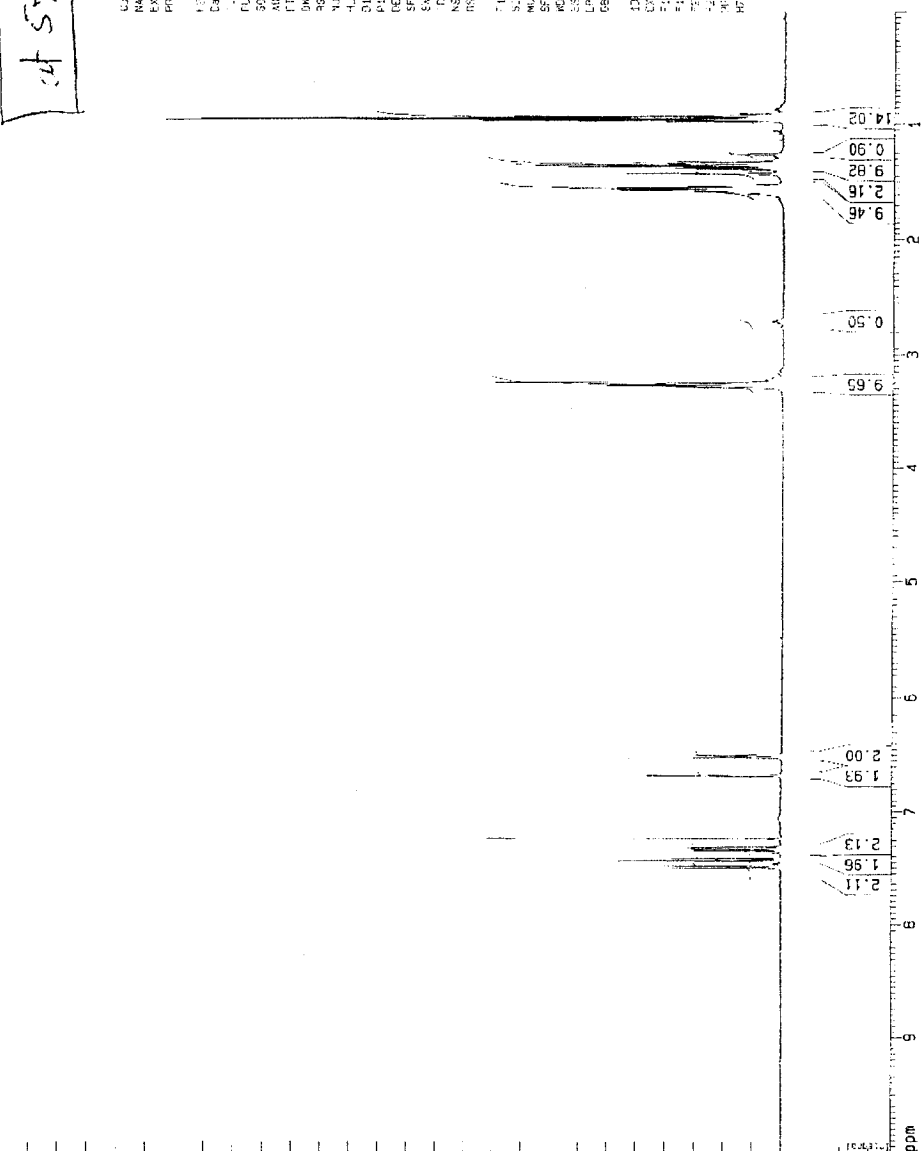


¹H NMR Spectrum of Cyclophane 113

at 57°C

```

Current Data Parameters
NAME:          113_113
EXPNO:        2
PROCNO:       1
Date_         20110304
Time:         12:55
INSTRUM:      spect
PROBHD:       5mm
PULPROG:      zgpg30
SOLVENT:      CDCl3
AQ:           4.955655 sec
RG:           6.107428 Hz
AQ:           21.0 usec
RG:           512
SOLVENT:      CDCl3
F2 - Acquisition Parameters
Date_         20110304
Time:         12:55
INSTRUM:      spect
PROBHD:       5mm
PULPROG:      zgpg30
SOLVENT:      CDCl3
AQ:           4.955655 sec
RG:           6.107428 Hz
AQ:           21.0 usec
RG:           512
SOLVENT:      CDCl3
F1 - Processing parameters
SI:           32768
SF:           500.135421 MHz
RG:           6.107428 Hz
AQ:           4.955655 sec
RG:           512
SOLVENT:      CDCl3
F2 - Processing parameters
SI:           32768
SF:           500.135421 MHz
RG:           6.107428 Hz
AQ:           4.955655 sec
RG:           512
SOLVENT:      CDCl3
  
```



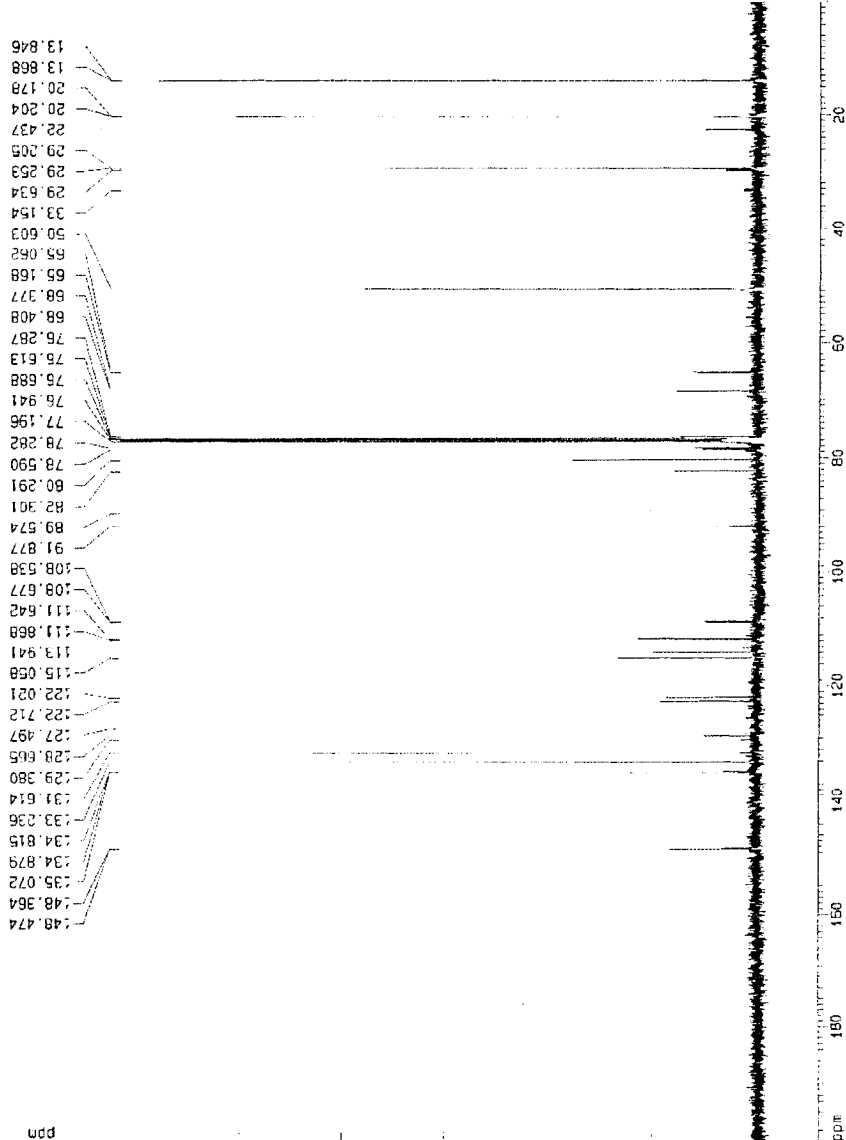
¹³C NMR Spectrum of Cyclophane 113

Current Data Parameters
 NAME hault_115
 EXPNO 4
 PROCNO 1

F2 - Acquisition Param
 Date 20010224
 Time 13.56
 PULPROG zgpg
 SOLVENT CDCl3
 AQ 1.048560
 FIDRES 0.472837
 DQ 16.0
 HZ 32768
 NUCLEUS 13C
 P1 70.0
 S2 22
 HL1 22
 D1 3.000000
 DE 20.0
 SF01 125.772464
 SWH 31250.00
 TD 65536
 NS 10240
 DS 0

F1 - Processing param
 SI 32768
 IC2 OF
 SF 125.7591571
 XGM EM
 SSB 0
 LB 1.00
 GB 0

1D NMR Plot Parameters
 CX 22.00
 F1P 154.023
 F1 19369.80
 F2P 106.207
 F2 13356.49
 PPKM 2.17345
 HZCN 273.33231



¹³C NMR Spectrum of Cyclophane 113 (expansion)

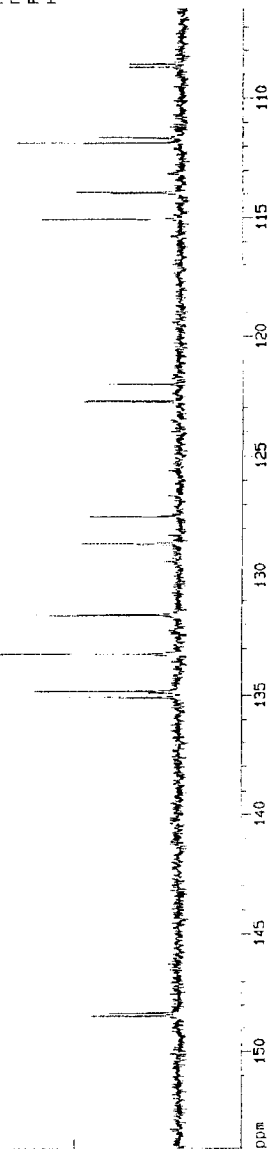
Current Data Parameters
 NAME neut_113
 EXPNO 4
 PROCNO 1

F2 - Acquisition Param
 Date_ 20010224
 Time 13:35
 ZGPGM zgpg
 SOLVENT CDCl3
 AQ 1.0469560
 FIDRES 0.476837
 SW 16.0
 RB 32768
 NUC1 13C
 NU1 0.0300000
 P1 70.0
 P2 22
 P3 22
 HL1 22
 D1 3.0000000
 P1 5.0
 P2 20.0
 SF01 125.7724464
 SWH 31250.00
 TO 65536
 NS 10240
 DS 0

F1 - Processing paramet
 SI 32768
 MC2 OF
 SF 125.7591571
 ACQ EM
 SSB 0
 LB 1.00
 GB 0

ID_VWR plot parameters
 CY 22.00
 F1P 154.023
 F1 19366.80
 F2P 106.207
 F2 13356.49
 PPKCN 2.17346
 HZCM 273.33231

148.474
 148.354
 135.072
 134.815
 134.815
 133.236
 131.614
 129.380
 128.665
 127.497
 122.712
 122.021
 115.058
 113.941
 111.868
 111.642
 108.677
 108.538



¹H NMR Spectrum of Cyclophane 123a

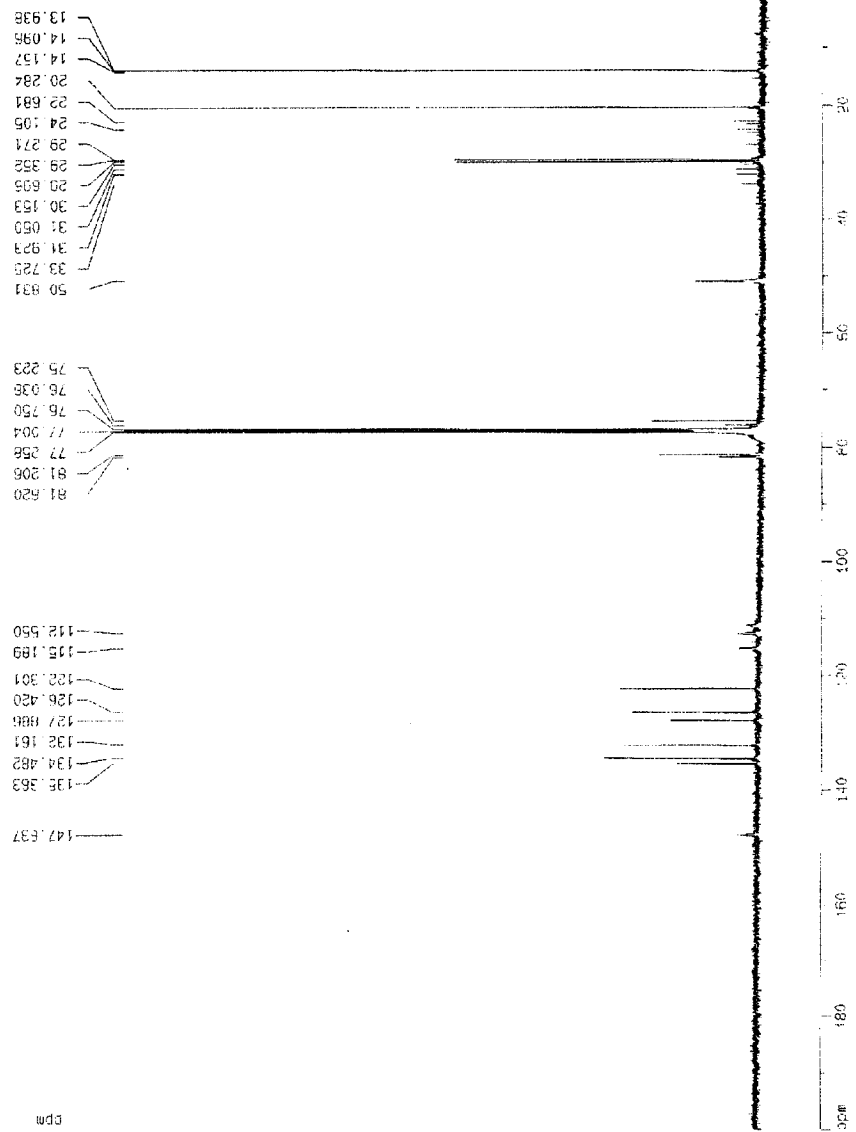
MAR 05 2002

Current Data Parameters
 NAME: test_123a
 EXPNO: 1
 F2 - Acquisition Parameters
 Date_ Time: 20020224 15:45
 PULPROG: zgpg30
 SOLVENT: DMSO-d6
 F1: 400.146000 MHz
 F2: 101.625000 MHz
 F3: 71.700000 MHz
 NUC1: 13C
 NUC2: 1H
 INSTRUM: spect
 P1: 12.00
 PL1: 0.00
 SFO1: 500.136411 MHz
 SR1: 2042.2342
 AS: 16
 DS: 4
 E1: Processing parameters
 SI: 32768
 SF: 500.136411 MHz
 AQA: 1
 LQ: 1
 LP: 1.00 Hz
 GB: 0
 F2 - MRF parameters
 CY: 32.000000
 F1: 500.136411 MHz
 F2: 101.625000 MHz
 F3: 71.700000 MHz
 N1: 13C
 N2: 1H
 N3: 1H

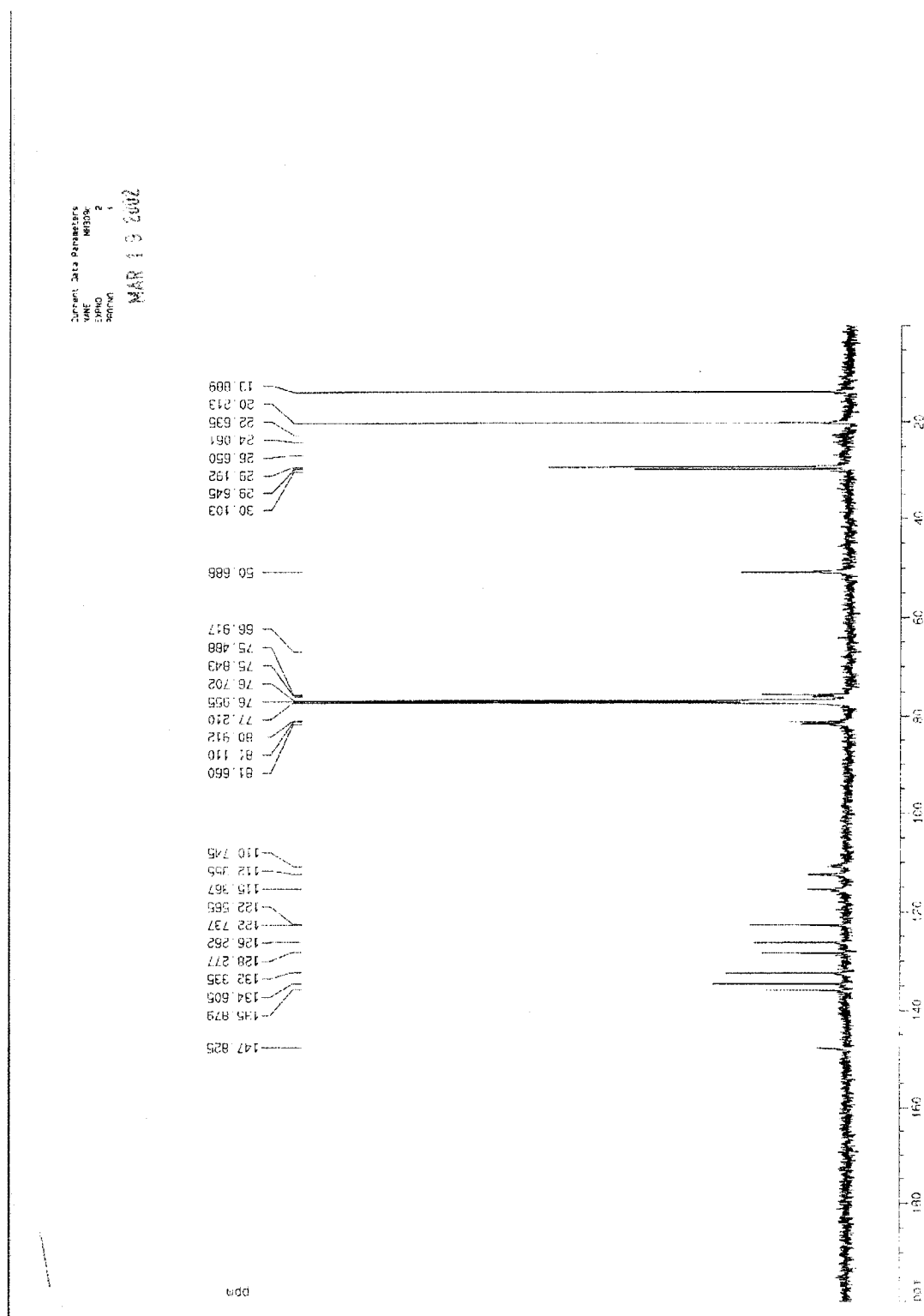


¹³C NMR Spectrum of Cyclophane 123a

Current Data Parameters
NAME: harr1_008
EXPNO: 2
PROCNO: 1
DATE_05_2002



¹³C NMR Spectrum of Cyclophane 123b



¹H NMR Spectrum of Cyclophane 170

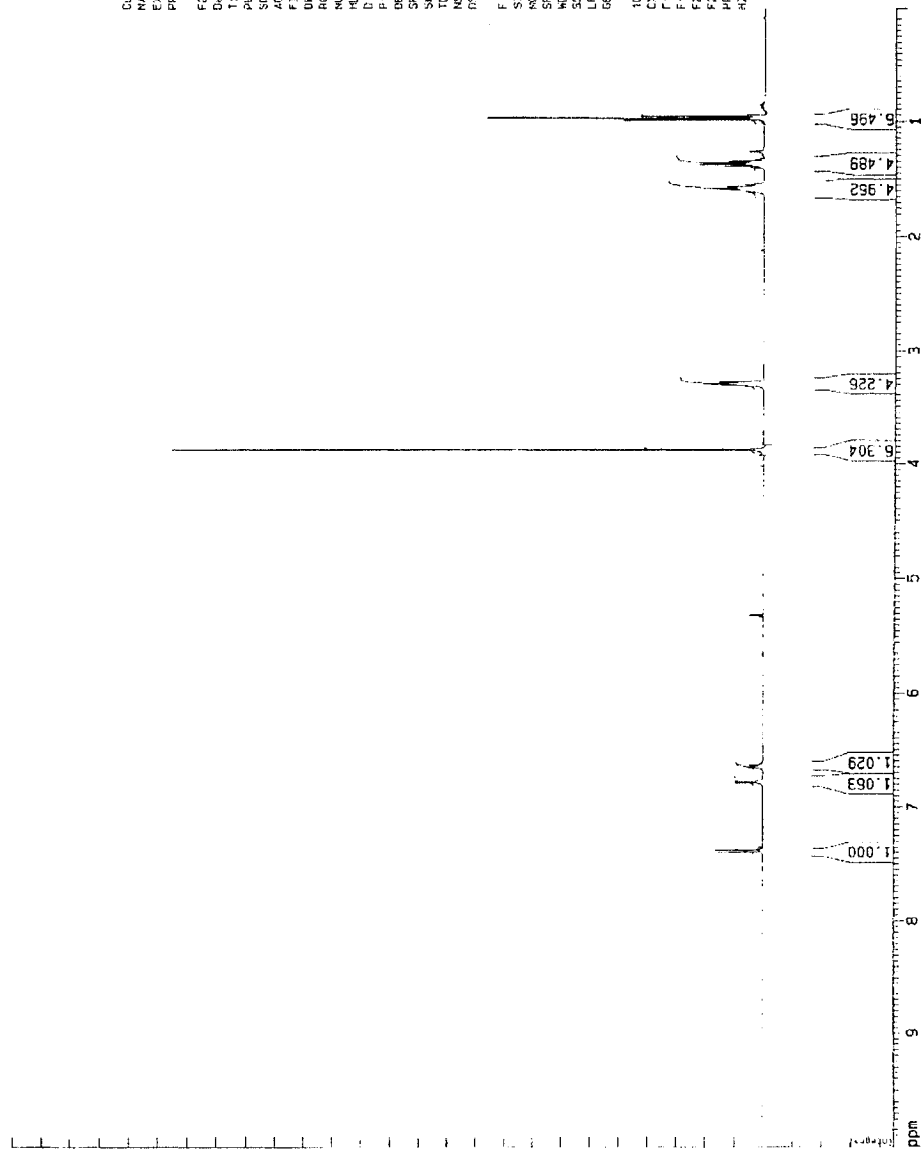
AUG 15 2002

Current Data Parameters
NAME meff_340p
EXPNO 1
PROCNO 1

F2 - Acquisition Parameters
Date_ 20020812
Time 18:17
PULPROG zgpg30
SOLVENT CDCl3
PROBHD 4.00mm QNP-1H
FIDRES 0.102466 Hz
AQ 0.102466 Hz
RG 320
AQ 0.102466 Hz
NUCLEUS 1H
P1 0.05
D1 0.00002 sec
P2 0.05
DE 0.00002 sec
SFO1 500.1362000 MHz
SFO2 125.7611500 MHz
TO 65.233
NS 16
DS 4
RS 0

F1 - Processing parameters
SI 32768
SF 500.1362000 MHz
WDW EM
SSB 0
LR 0.00 Hz
GB 0

1D F1F2 plot parameters
CX 22.00 cm
FLP 15.000 cm
F1 500.1362000 MHz
F2 125.7611500 MHz
PULPROG zgpg30
SOLVENT CDCl3
FIDRES 0.102466 Hz
AQ 0.102466 Hz
RG 320
AQ 0.102466 Hz
NUCLEUS 1H
P1 0.05
D1 0.00002 sec
P2 0.05
DE 0.00002 sec
SFO1 500.1362000 MHz
SFO2 125.7611500 MHz
TO 65.233
NS 16
DS 4
RS 0



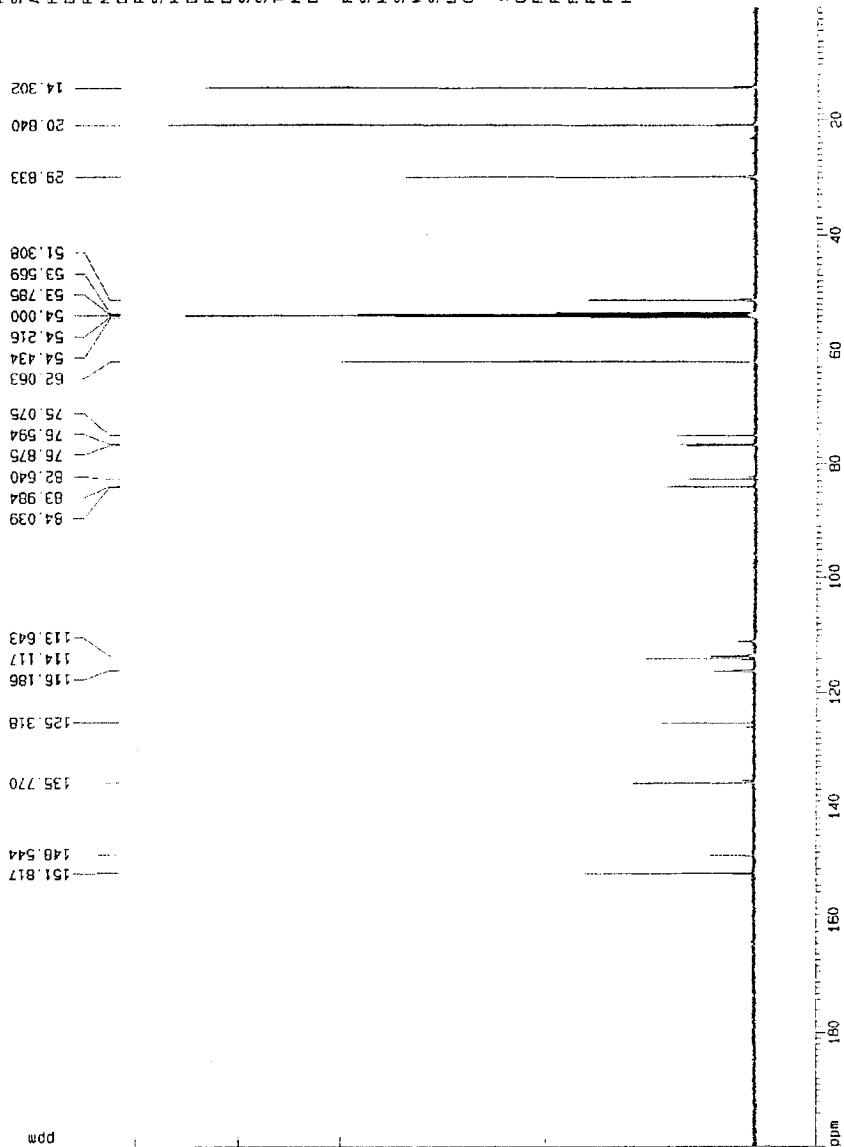
¹³C NMR Spectrum of Cyclophane 170

Current Data Parameters
 NAME heuft_340p
 EXPNO 2
 PROCNO 1

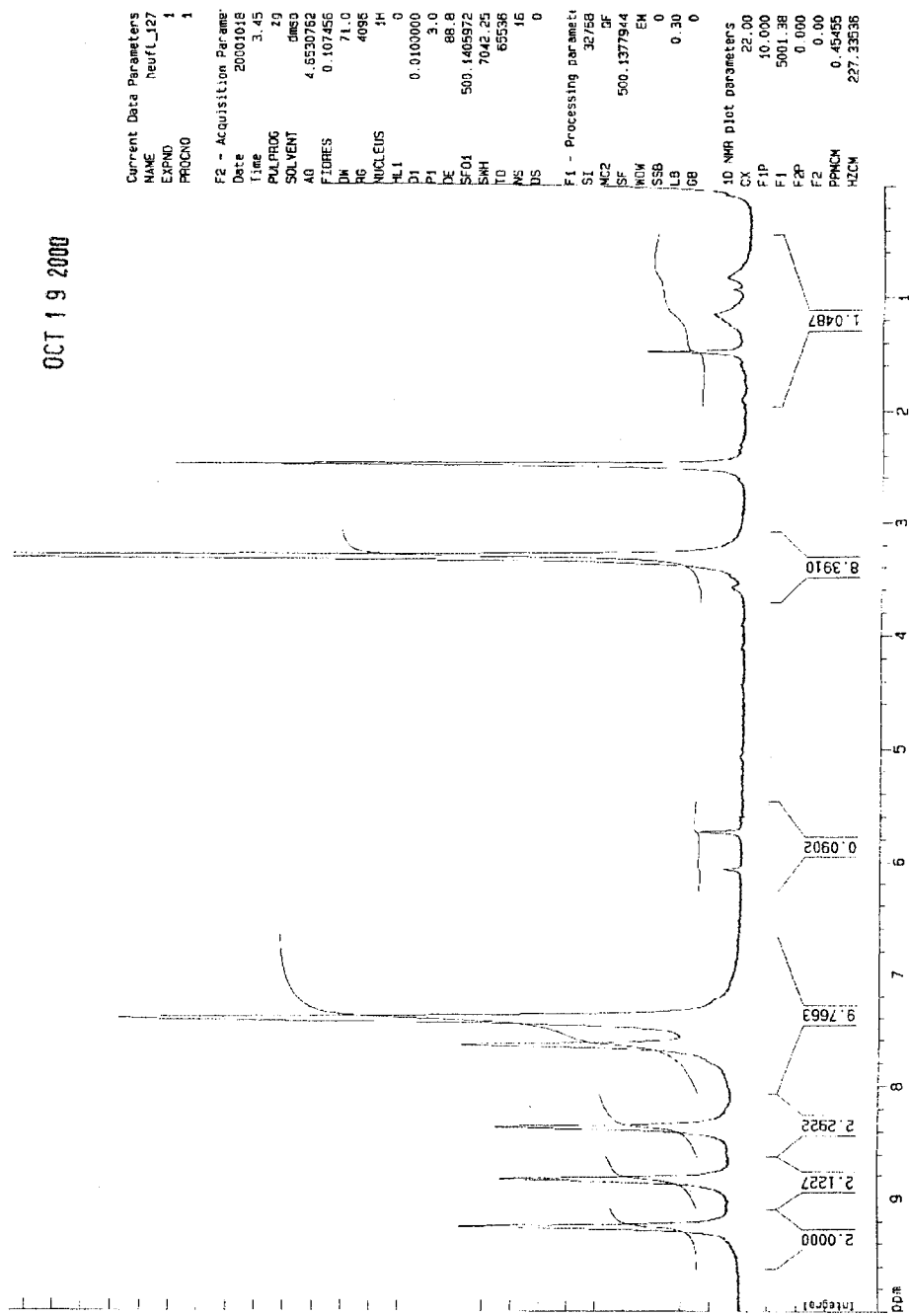
F2 - Acquisition Param
 Date 20020812
 Time 18.43
 PULPROG zgpg
 SOLVENT CDCl3
 AQ 0.0519860
 FIDRES 0.586877
 DM 13.0
 RG 32768
 NUCLEUS 13C
 D11 0.0300000
 P31 70.0
 S2 22
 HL1 22
 D1 1.0000000
 P1 5.0
 DE 18.6
 SFO1 125.7724464
 SWH 38461.54
 TD 65636
 NS 18000
 DS 0

F1 - Processing param
 SI 32768
 MC2 OF
 SF 125.7593124
 MDW EM
 SSB 0
 LB 1.00
 GB 0

ID NMR plot parameters
 CA 22.00
 F1P 200.000
 F1 25351.86
 F2P 0.000
 F2 0.00
 PPMCM 9.05091
 HZCM 1143.26648



¹H NMR Spectrum of Phenanthroline 200



¹³C NMR Spectrum of Phenanthroline 200

Current Data Parameters
 NAME Inuit_127
 EXPNO 2
 PROCNO 1
 C F2 - Acquisition Param:
 Date 2000.03.19
 Time 4.17
 PULPROG zgpg
 PCVENT dmsdms
 AQ 0.5243080
 FIDRES 0.953674
 DN 16.0
 F6 32758
 NUCLEUS 13C
 D11 0.0300000
 P31 70.0
 S2 22
 HL1 22
 D1 1.5000000
 P1 5.0
 DE 20.0
 SF01 125.7724454
 SWH 31250.00
 TD 32758
 NS 6328
 DS 0
 F1 - Processing param:
 SI 32758
 MC2 g
 SF 125.7536647
 WDW EM
 SSB 0
 LB 4.00
 GB 0
 ID NMR plot parameters
 CK 22.00
 FIP 200.000
 F1 25151.96
 F2 0.000
 F3 0.00
 PRIN 3.03031
 AZON 1143.27100

24.68
 39.09
 39.25
 39.42
 39.59
 39.75
 39.92
 40.09

75.99
 81.27

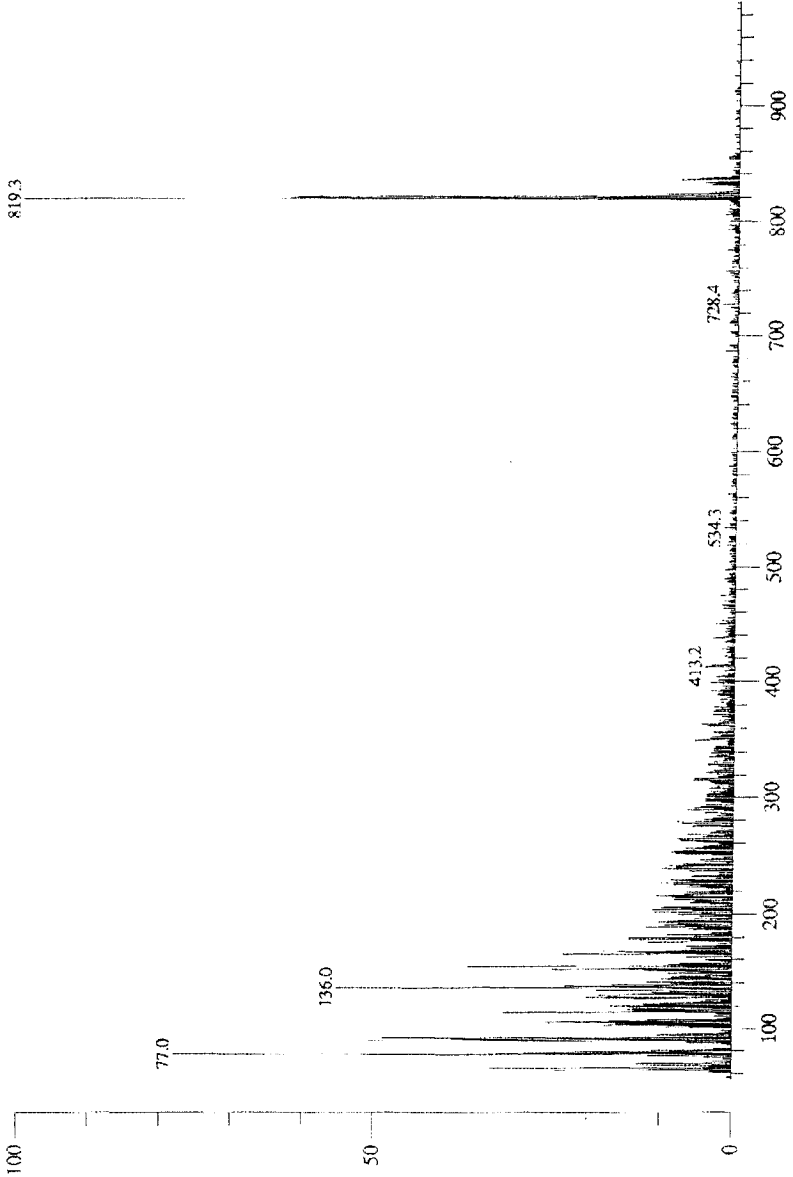
119.91
 127.68
 128.73
 129.09
 129.52
 130.77
 133.48
 136.42
 136.76
 139.81
 141.52
 149.22

ppm

ppm

MS(FAB) Spectrum of Phenanthrolineophane 200

1c2573 Scan 4 RT=1:02 100%=17021 mv 18 Oct 72 11:42
HRP +FAB 056-078



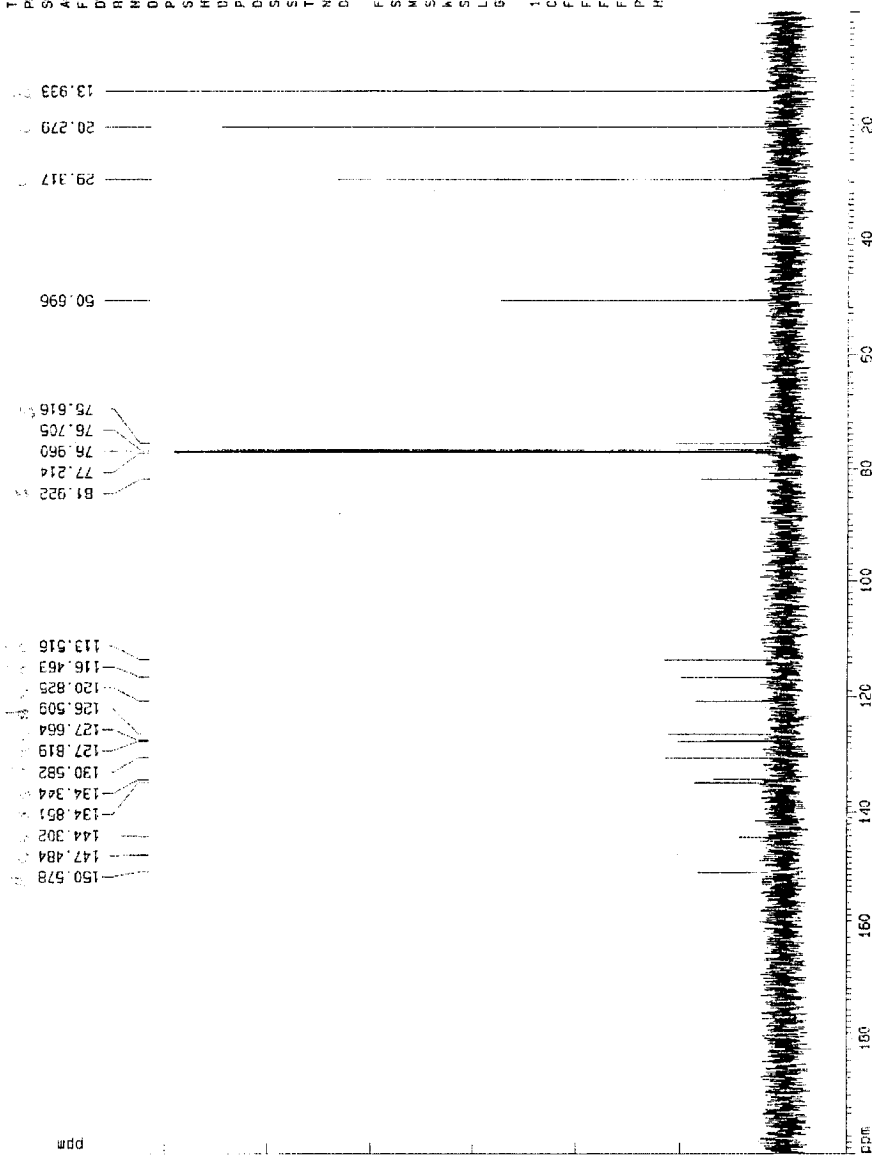
¹³C NMR Spectrum of Phenanthroline 217

Current Data Parameters
 NAME haurt_157c
 EXPHO 3
 PROCNO 1

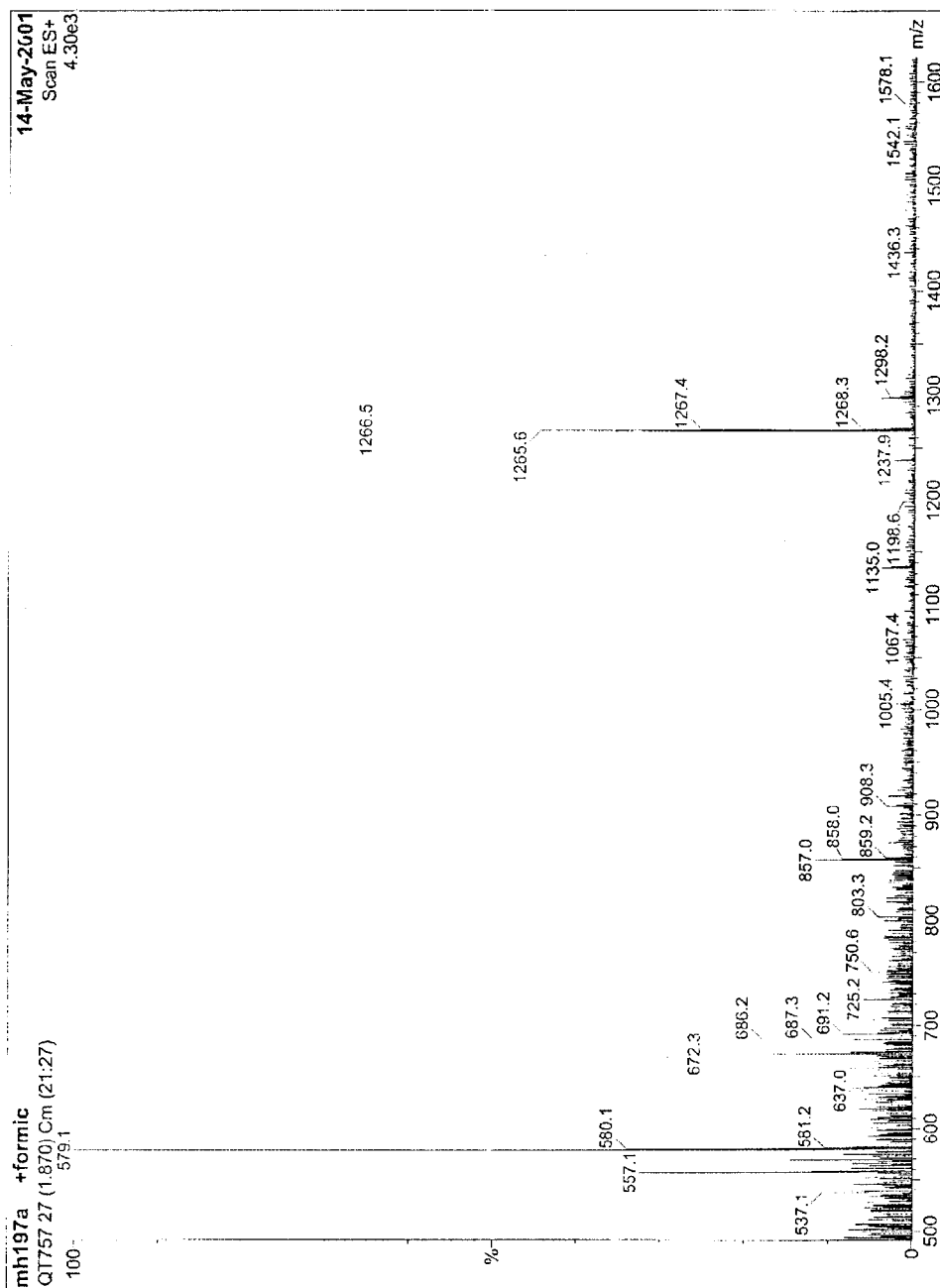
F2 Acquisition Param
 Date 20010516
 Time 10.49
 PULPROG zgpg
 SOLVENT CDCl3
 AQ 0.8519880
 FIDRES 0.568877
 DN 43.0
 RE 32768
 NUCLEUS 13C
 P1 70.0
 S2 22
 HL 22
 D1 1.0000000
 P1 5.0
 DE 18.6
 SF01 125.772464
 SNU 38461.54
 TC 65036
 NE 345
 DS 0

F1 - Processing param
 SI 32768
 MC2 DF
 SF 125.7591571
 ACW EM
 SSB 0
 LB 1.00
 GB 0

1C NMR plot parameters
 CX 22.00
 FIP 200.060
 F1 25151.83
 F2 0.060
 F2 0.00
 PRMCM 9.05091
 HZCM 1143.25501



MS(ES) NMR Spectrum of Phenanthrolinophane 217

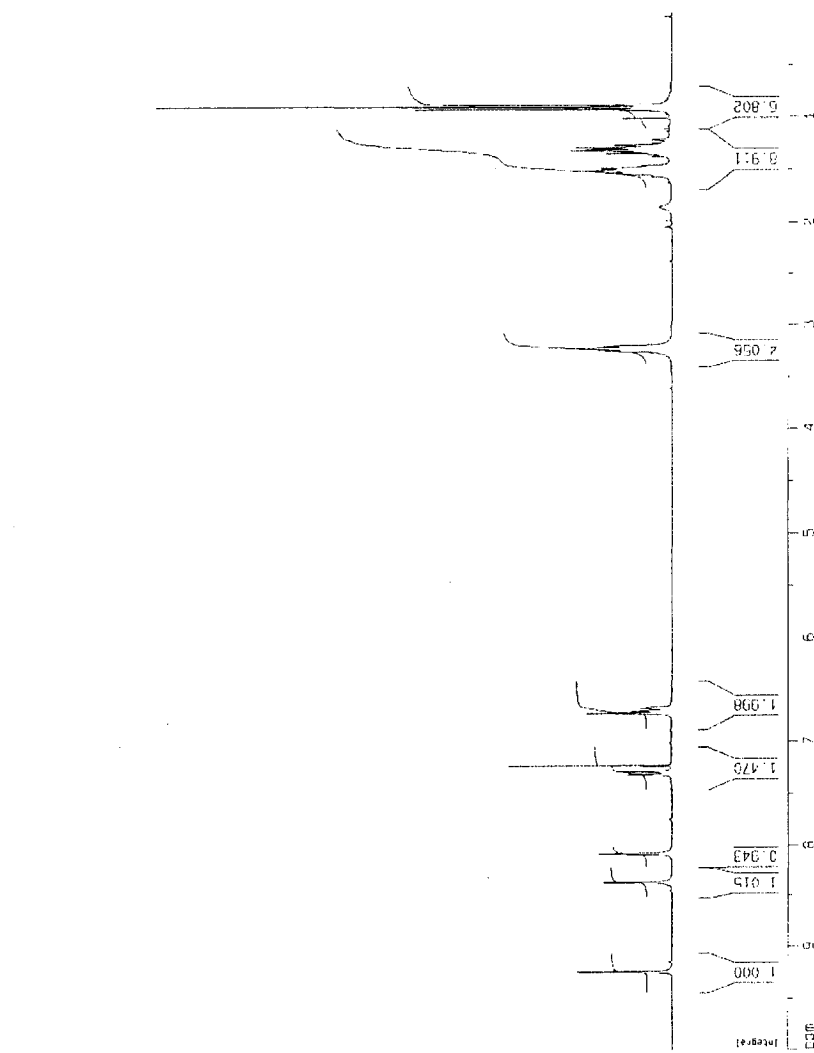


¹H NMR Spectrum of Phenanthroline 218

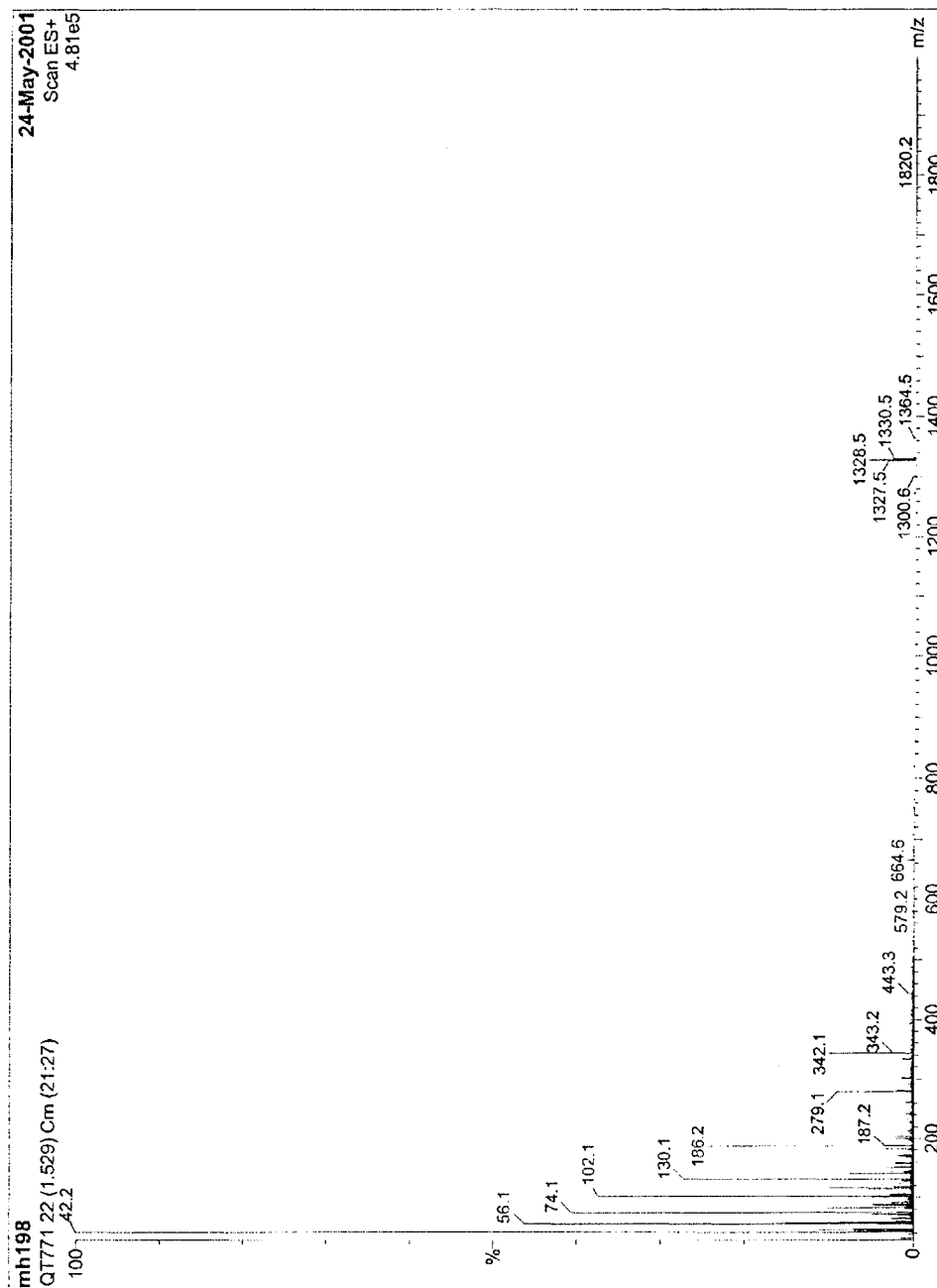
MH77b
 Current Data Parameters
 NAME :
 EXPNO :
 F2 (Hz) :

F2 - Acquisition Parameters
 Date_ : 20010512
 Time : 14.42
 INSTRUM : spect
 PROBRD : 5 mm QNP 1H/1
 PULPROG : zgpg30
 U :
 SOLVENT : CDCl3
 NS : 16
 DS : 4
 SWH : 5081.301 Hz
 FIDRES : 0.169407 Hz
 AQ : 3.0222880 sec
 RG : 322.5
 DM :
 DE : 98.400 usec
 DC : 5.00 usec
 TE : 290.0 K
 D1 : 1.30000000 sec

***** CHANNEL f1 *****
 NUCL1 : 1H
 P1 : 12.00 usec
 PL1 : 0.00 dB
 SFO1 : 300.1460000 MHz
 ZNU1 : 1H
 ZPL1 : 0.00 dB
 SFO2 : 100.6261260 MHz
 P2 : 1.00 usec
 PL2 : 0.00 dB
 SFO3 : 100.6261260 MHz
 P3 : 1.00 usec
 PL3 : 0.00 dB
 SFO4 : 100.6261260 MHz
 P4 : 1.00 usec
 PL4 : 0.00 dB
 SFO5 : 100.6261260 MHz
 P5 : 1.00 usec
 PL5 : 0.00 dB
 SFO6 : 100.6261260 MHz
 P6 : 1.00 usec
 PL6 : 0.00 dB
 SFO7 : 100.6261260 MHz
 P7 : 1.00 usec
 PL7 : 0.00 dB
 SFO8 : 100.6261260 MHz
 P8 : 1.00 usec
 PL8 : 0.00 dB
 SFO9 : 100.6261260 MHz
 P9 : 1.00 usec
 PL9 : 0.00 dB
 SFO10 : 100.6261260 MHz
 P10 : 1.00 usec
 PL10 : 0.00 dB
 SFO11 : 100.6261260 MHz
 P11 : 1.00 usec
 PL11 : 0.00 dB
 SFO12 : 100.6261260 MHz
 P12 : 1.00 usec
 PL12 : 0.00 dB
 SFO13 : 100.6261260 MHz
 P13 : 1.00 usec
 PL13 : 0.00 dB
 SFO14 : 100.6261260 MHz
 P14 : 1.00 usec
 PL14 : 0.00 dB
 SFO15 : 100.6261260 MHz
 P15 : 1.00 usec
 PL15 : 0.00 dB
 SFO16 : 100.6261260 MHz
 P16 : 1.00 usec
 PL16 : 0.00 dB
 SFO17 : 100.6261260 MHz
 P17 : 1.00 usec
 PL17 : 0.00 dB
 SFO18 : 100.6261260 MHz
 P18 : 1.00 usec
 PL18 : 0.00 dB
 SFO19 : 100.6261260 MHz
 P19 : 1.00 usec
 PL19 : 0.00 dB
 SFO20 : 100.6261260 MHz
 P20 : 1.00 usec
 PL20 : 0.00 dB
 SFO21 : 100.6261260 MHz
 P21 : 1.00 usec
 PL21 : 0.00 dB
 SFO22 : 100.6261260 MHz
 P22 : 1.00 usec
 PL22 : 0.00 dB
 SFO23 : 100.6261260 MHz
 P23 : 1.00 usec
 PL23 : 0.00 dB
 SFO24 : 100.6261260 MHz
 P24 : 1.00 usec
 PL24 : 0.00 dB
 SFO25 : 100.6261260 MHz
 P25 : 1.00 usec
 PL25 : 0.00 dB
 SFO26 : 100.6261260 MHz
 P26 : 1.00 usec
 PL26 : 0.00 dB
 SFO27 : 100.6261260 MHz
 P27 : 1.00 usec
 PL27 : 0.00 dB
 SFO28 : 100.6261260 MHz
 P28 : 1.00 usec
 PL28 : 0.00 dB
 SFO29 : 100.6261260 MHz
 P29 : 1.00 usec
 PL29 : 0.00 dB
 SFO30 : 100.6261260 MHz
 P30 : 1.00 usec
 PL30 : 0.00 dB
 SFO31 : 100.6261260 MHz
 P31 : 1.00 usec
 PL31 : 0.00 dB
 SFO32 : 100.6261260 MHz
 P32 : 1.00 usec
 PL32 : 0.00 dB
 SFO33 : 100.6261260 MHz
 P33 : 1.00 usec
 PL33 : 0.00 dB
 SFO34 : 100.6261260 MHz
 P34 : 1.00 usec
 PL34 : 0.00 dB
 SFO35 : 100.6261260 MHz
 P35 : 1.00 usec
 PL35 : 0.00 dB
 SFO36 : 100.6261260 MHz
 P36 : 1.00 usec
 PL36 : 0.00 dB
 SFO37 : 100.6261260 MHz
 P37 : 1.00 usec
 PL37 : 0.00 dB
 SFO38 : 100.6261260 MHz
 P38 : 1.00 usec
 PL38 : 0.00 dB
 SFO39 : 100.6261260 MHz
 P39 : 1.00 usec
 PL39 : 0.00 dB
 SFO40 : 100.6261260 MHz
 P40 : 1.00 usec
 PL40 : 0.00 dB
 SFO41 : 100.6261260 MHz
 P41 : 1.00 usec
 PL41 : 0.00 dB
 SFO42 : 100.6261260 MHz
 P42 : 1.00 usec
 PL42 : 0.00 dB
 SFO43 : 100.6261260 MHz
 P43 : 1.00 usec
 PL43 : 0.00 dB
 SFO44 : 100.6261260 MHz
 P44 : 1.00 usec
 PL44 : 0.00 dB
 SFO45 : 100.6261260 MHz
 P45 : 1.00 usec
 PL45 : 0.00 dB
 SFO46 : 100.6261260 MHz
 P46 : 1.00 usec
 PL46 : 0.00 dB
 SFO47 : 100.6261260 MHz
 P47 : 1.00 usec
 PL47 : 0.00 dB
 SFO48 : 100.6261260 MHz
 P48 : 1.00 usec
 PL48 : 0.00 dB
 SFO49 : 100.6261260 MHz
 P49 : 1.00 usec
 PL49 : 0.00 dB
 SFO50 : 100.6261260 MHz
 P50 : 1.00 usec
 PL50 : 0.00 dB
 SFO51 : 100.6261260 MHz
 P51 : 1.00 usec
 PL51 : 0.00 dB
 SFO52 : 100.6261260 MHz
 P52 : 1.00 usec
 PL52 : 0.00 dB
 SFO53 : 100.6261260 MHz
 P53 : 1.00 usec
 PL53 : 0.00 dB
 SFO54 : 100.6261260 MHz
 P54 : 1.00 usec
 PL54 : 0.00 dB
 SFO55 : 100.6261260 MHz
 P55 : 1.00 usec
 PL55 : 0.00 dB
 SFO56 : 100.6261260 MHz
 P56 : 1.00 usec
 PL56 : 0.00 dB
 SFO57 : 100.6261260 MHz
 P57 : 1.00 usec
 PL57 : 0.00 dB
 SFO58 : 100.6261260 MHz
 P58 : 1.00 usec
 PL58 : 0.00 dB
 SFO59 : 100.6261260 MHz
 P59 : 1.00 usec
 PL59 : 0.00 dB
 SFO60 : 100.6261260 MHz
 P60 : 1.00 usec
 PL60 : 0.00 dB
 SFO61 : 100.6261260 MHz
 P61 : 1.00 usec
 PL61 : 0.00 dB
 SFO62 : 100.6261260 MHz
 P62 : 1.00 usec
 PL62 : 0.00 dB
 SFO63 : 100.6261260 MHz
 P63 : 1.00 usec
 PL63 : 0.00 dB
 SFO64 : 100.6261260 MHz
 P64 : 1.00 usec
 PL64 : 0.00 dB
 SFO65 : 100.6261260 MHz
 P65 : 1.00 usec
 PL65 : 0.00 dB
 SFO66 : 100.6261260 MHz
 P66 : 1.00 usec
 PL66 : 0.00 dB
 SFO67 : 100.6261260 MHz
 P67 : 1.00 usec
 PL67 : 0.00 dB
 SFO68 : 100.6261260 MHz
 P68 : 1.00 usec
 PL68 : 0.00 dB
 SFO69 : 100.6261260 MHz
 P69 : 1.00 usec
 PL69 : 0.00 dB
 SFO70 : 100.6261260 MHz
 P70 : 1.00 usec
 PL70 : 0.00 dB
 SFO71 : 100.6261260 MHz
 P71 : 1.00 usec
 PL71 : 0.00 dB
 SFO72 : 100.6261260 MHz
 P72 : 1.00 usec
 PL72 : 0.00 dB
 SFO73 : 100.6261260 MHz
 P73 : 1.00 usec
 PL73 : 0.00 dB
 SFO74 : 100.6261260 MHz
 P74 : 1.00 usec
 PL74 : 0.00 dB
 SFO75 : 100.6261260 MHz
 P75 : 1.00 usec
 PL75 : 0.00 dB
 SFO76 : 100.6261260 MHz
 P76 : 1.00 usec
 PL76 : 0.00 dB
 SFO77 : 100.6261260 MHz
 P77 : 1.00 usec
 PL77 : 0.00 dB
 SFO78 : 100.6261260 MHz
 P78 : 1.00 usec
 PL78 : 0.00 dB
 SFO79 : 100.6261260 MHz
 P79 : 1.00 usec
 PL79 : 0.00 dB
 SFO80 : 100.6261260 MHz
 P80 : 1.00 usec
 PL80 : 0.00 dB
 SFO81 : 100.6261260 MHz
 P81 : 1.00 usec
 PL81 : 0.00 dB
 SFO82 : 100.6261260 MHz
 P82 : 1.00 usec
 PL82 : 0.00 dB
 SFO83 : 100.6261260 MHz
 P83 : 1.00 usec
 PL83 : 0.00 dB
 SFO84 : 100.6261260 MHz
 P84 : 1.00 usec
 PL84 : 0.00 dB
 SFO85 : 100.6261260 MHz
 P85 : 1.00 usec
 PL85 : 0.00 dB
 SFO86 : 100.6261260 MHz
 P86 : 1.00 usec
 PL86 : 0.00 dB
 SFO87 : 100.6261260 MHz
 P87 : 1.00 usec
 PL87 : 0.00 dB
 SFO88 : 100.6261260 MHz
 P88 : 1.00 usec
 PL88 : 0.00 dB
 SFO89 : 100.6261260 MHz
 P89 : 1.00 usec
 PL89 : 0.00 dB
 SFO90 : 100.6261260 MHz
 P90 : 1.00 usec
 PL90 : 0.00 dB
 SFO91 : 100.6261260 MHz
 P91 : 1.00 usec
 PL91 : 0.00 dB
 SFO92 : 100.6261260 MHz
 P92 : 1.00 usec
 PL92 : 0.00 dB
 SFO93 : 100.6261260 MHz
 P93 : 1.00 usec
 PL93 : 0.00 dB
 SFO94 : 100.6261260 MHz
 P94 : 1.00 usec
 PL94 : 0.00 dB
 SFO95 : 100.6261260 MHz
 P95 : 1.00 usec
 PL95 : 0.00 dB
 SFO96 : 100.6261260 MHz
 P96 : 1.00 usec
 PL96 : 0.00 dB
 SFO97 : 100.6261260 MHz
 P97 : 1.00 usec
 PL97 : 0.00 dB
 SFO98 : 100.6261260 MHz
 P98 : 1.00 usec
 PL98 : 0.00 dB
 SFO99 : 100.6261260 MHz
 P99 : 1.00 usec
 PL99 : 0.00 dB
 SFO100 : 100.6261260 MHz
 P100 : 1.00 usec
 PL100 : 0.00 dB



MS(ES) NMR Spectrum of Phenanthrolinophane 218



¹H NMR Spectrum of Phenanthroline 227

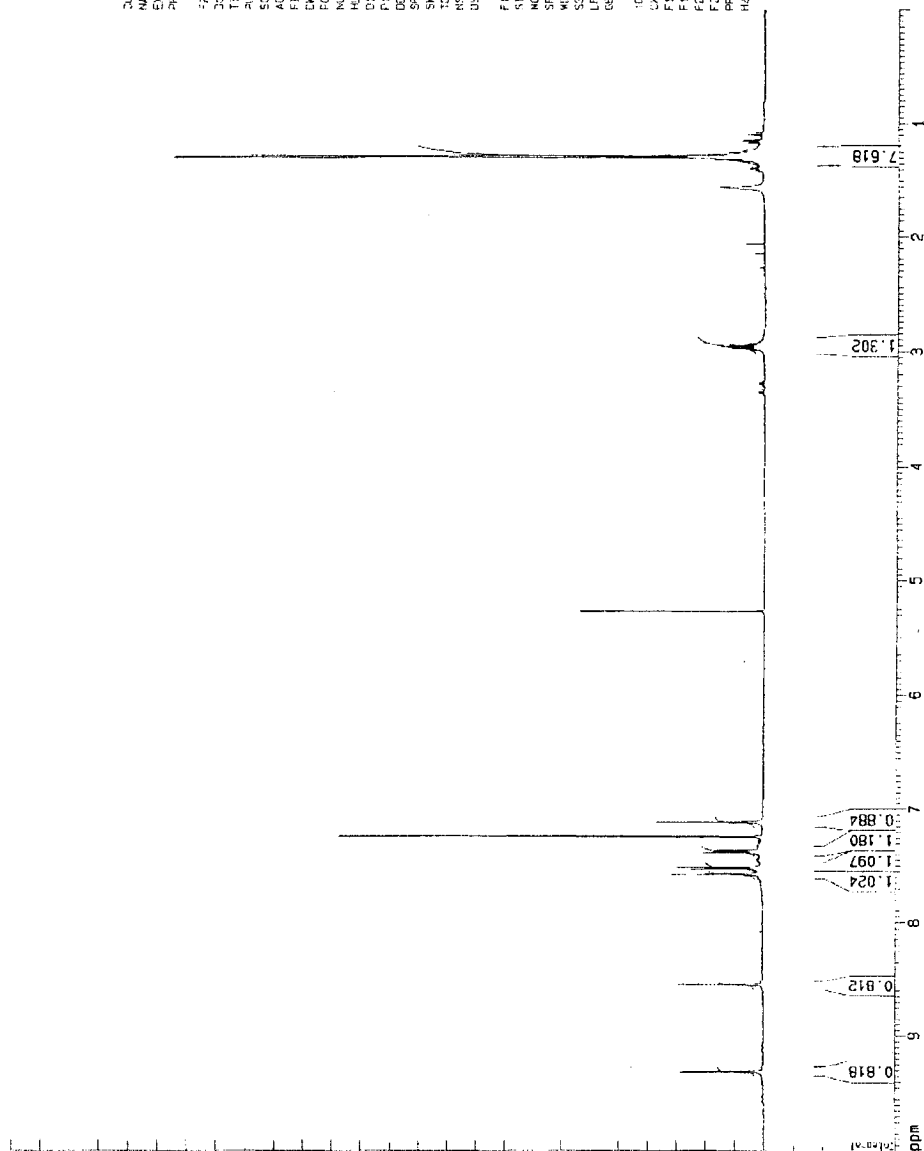
FEB 23 2003

Current Data Parameters
 NAME: FEH1_488
 EXPNO: 1
 PROCNO: 1

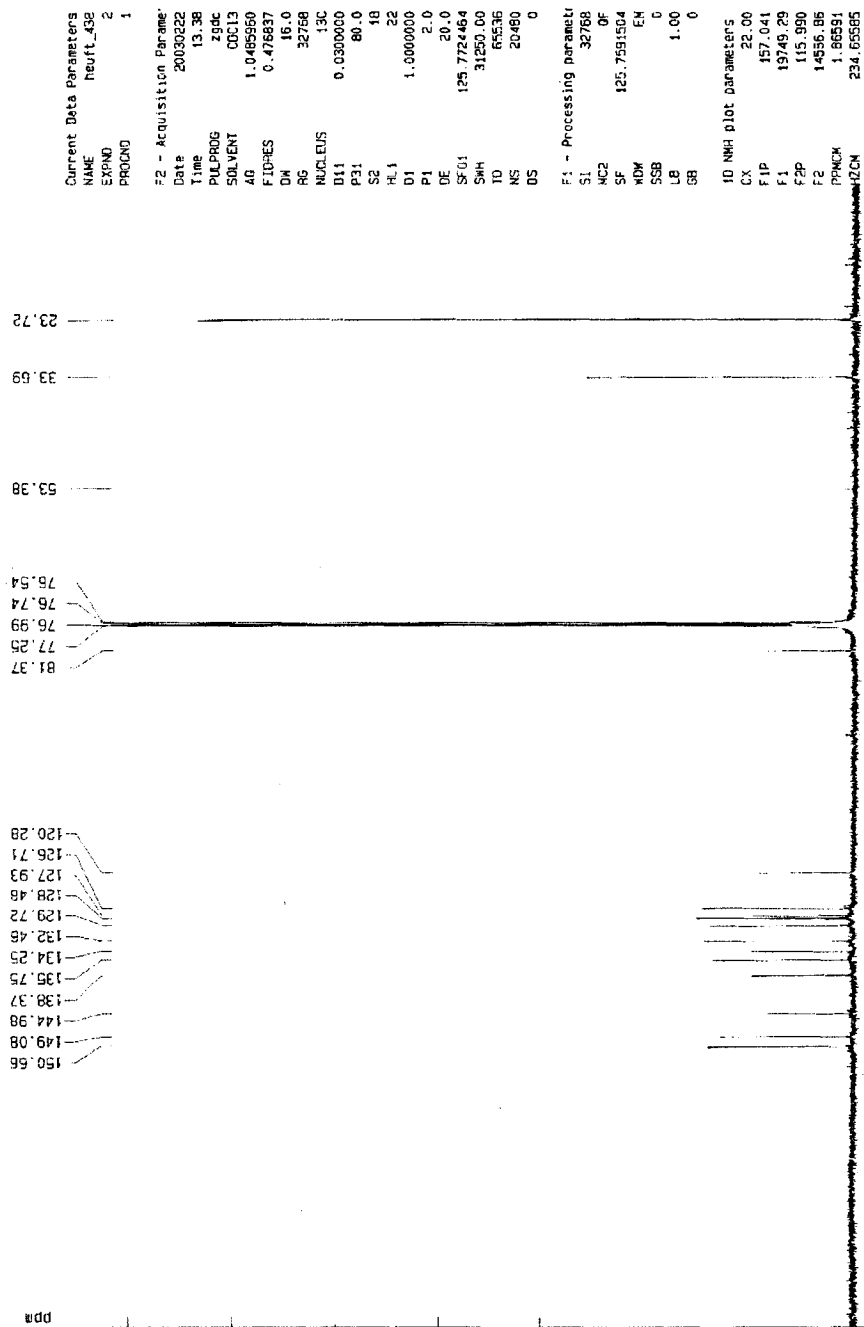
F2 - Acquisition Parameters
 Date_UTC: 20030224
 Time: 12.41
 PULPROG: zgpg30
 SOLVENT: DMSO-d6
 F2: 400.146000 MHz
 F1: 100.628150 MHz
 F0: 0.000000 MHz
 NUC1: ¹H
 NUC2: ¹³C
 P1: 12.00
 PL1: 0.00
 DC: 0.000000 VPP
 SFO1: 500.1361931 MHz
 SIH1: 7042.25 Hz
 TO: 655.96
 RS: 32
 US: C

F1 - Processing parameters
 SI: 32768
 SF: 500.1361931 MHz
 WDW: EM
 SSB: 0
 LB: 0.100 Hz
 GB: 0

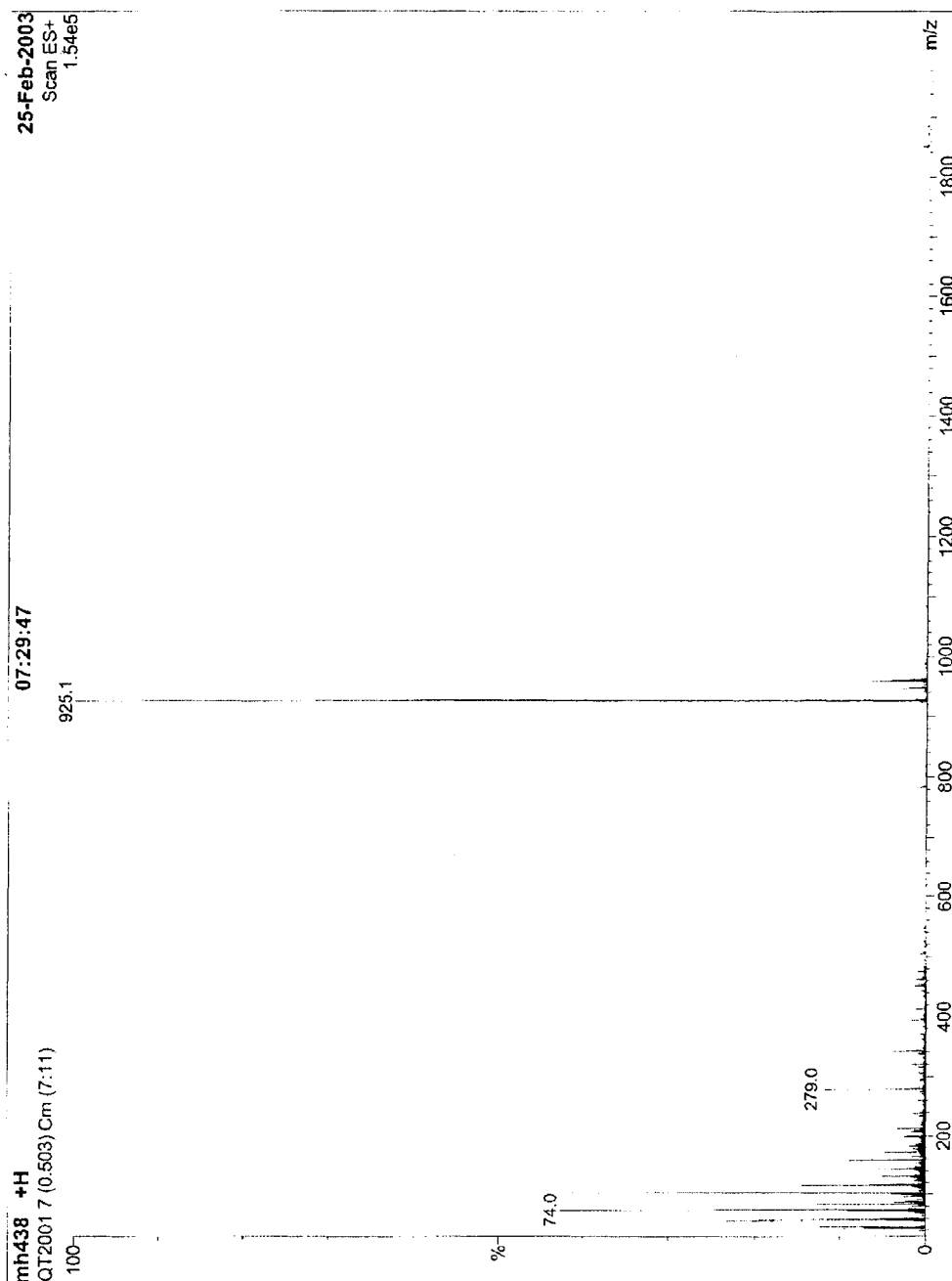
F0 - Reference parameters
 CX: 25.00 cm
 F1F: 10.000 DCM
 F1: 500.135150 MHz
 F2: 100.628150 MHz
 F2F: 10.000 DCM
 PPMH: 1.4545 DCM
 HZPM: 207.3840000 Hz



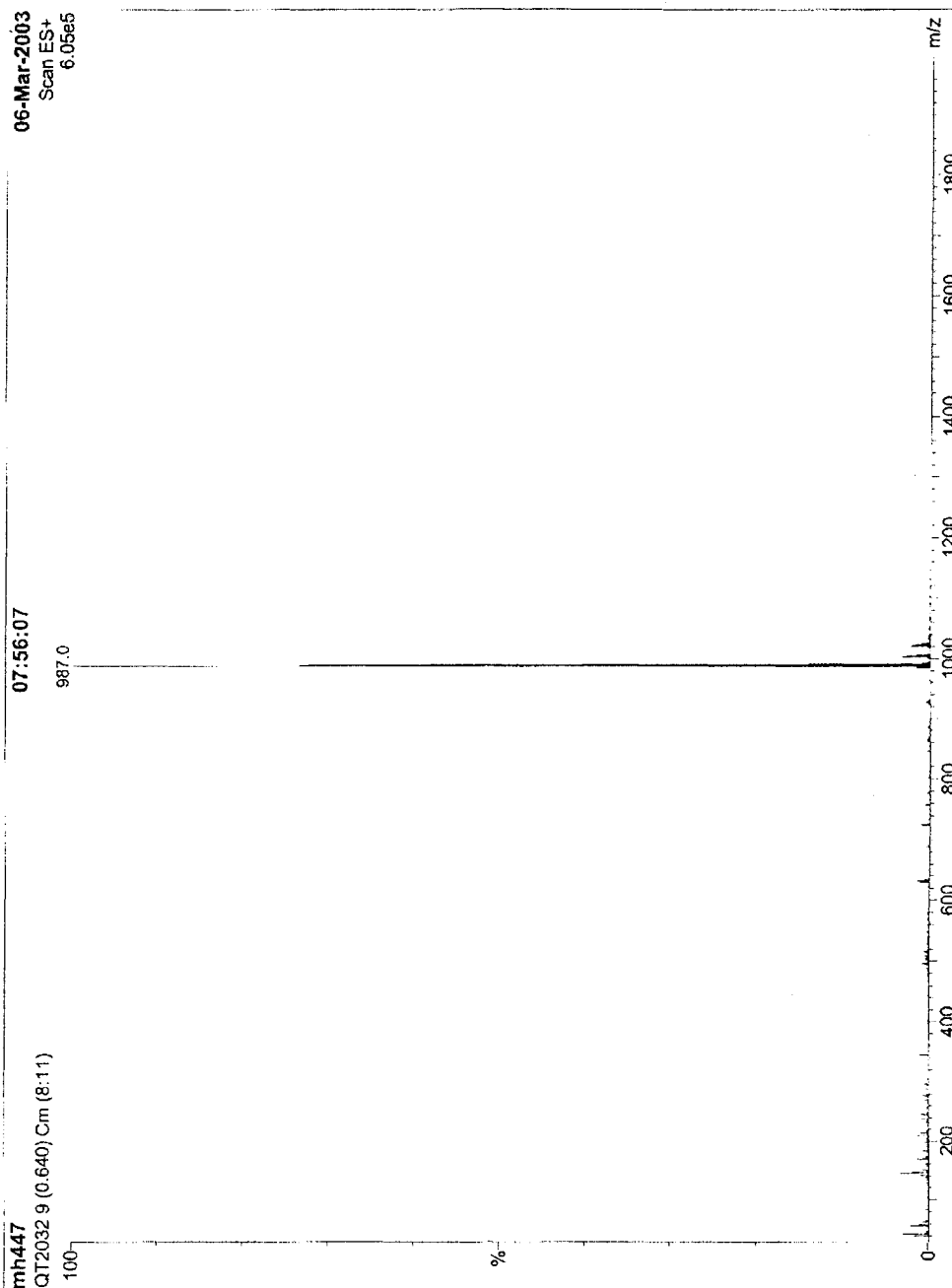
¹³C NMR Spectrum of Phenanthroline 227



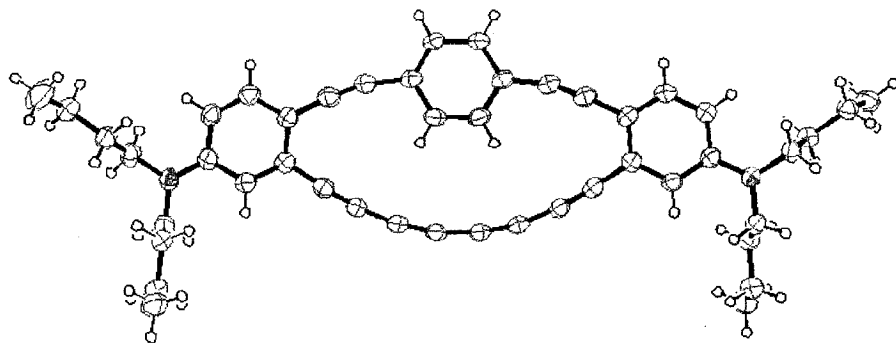
MS(ES) NMR Spectrum of Phenanthrolinophane 227



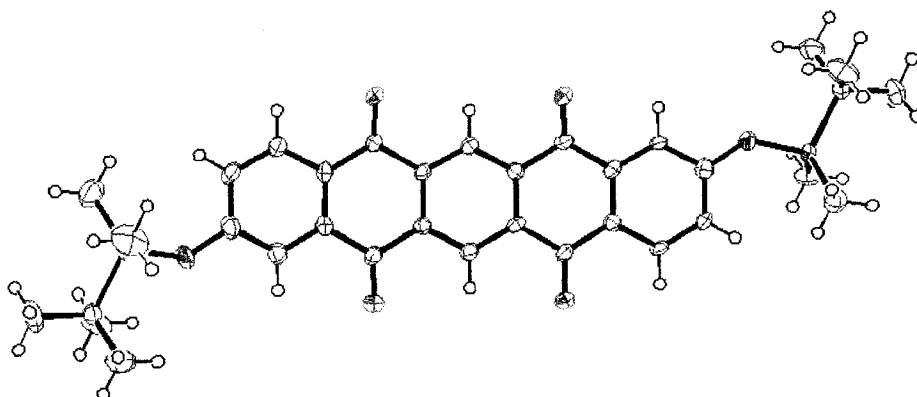
MS(ES) NMR Spectrum of Phenanthrolineophane 228



A.4 X-Ray Crystallographic Data



Cyclophane 112



Silyl Ether 247

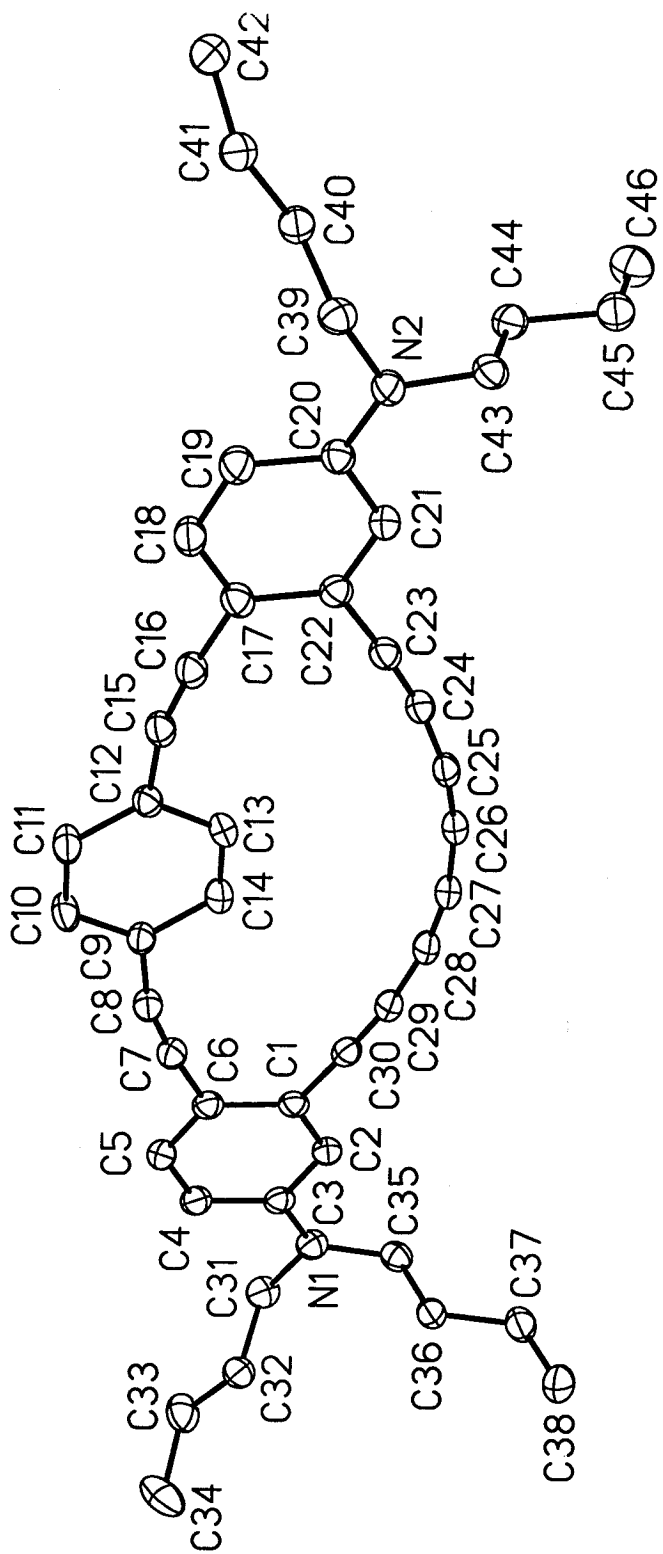


Table 1. Crystal data and structure refinement for af022.

Identification code	af022
Empirical formula	C ₄₆ H ₄₆ N ₂
Formula weight	626.85
Temperature	203(2) K
Wavelength	0.71073 Å
Crystal system, space group	Monoclinic, P2(1)/n
Unit cell dimensions	a = 9.3848(10) Å alpha = 90 deg. b = 15.8543(17) Å beta = 99.973(2) de c = 24.834(3) Å gamma = 90 deg.
Volume	3639.2(7) Å ³
Z, Calculated density	4, 1.144 Mg/m ³
Absorption coefficient	0.066 mm ⁻¹
F(000)	1344
Crystal size	0.05 x 0.08 x 0.30 mm
Theta range for data collection	1.53 to 28.76 deg.
Limiting indices	-12<=h<=12, 0<=k<=21, 0<=l<=33
Reflections collected / unique	31772 / 8764 [R(int) = 0.0520]
Completeness to theta = 28.76	92.7 %
Absorption correction	Semi-empirical from equivalents
Max. and min. transmission	0.928076 and 0.698124
Refinement method	Full-matrix least-squares on F ²
Data / restraints / parameters	8764 / 0 / 433
Goodness-of-fit on F ²	1.029
Final R indices [I>2sigma(I)]	R1 = 0.0487, wR2 = 0.0938
R indices (all data)	R1 = 0.1185, wR2 = 0.1084
Largest diff. peak and hole	0.151 and -0.181 e.Å ⁻³

Table 2. Atomic coordinates ($\times 10^4$) and equivalent isotropic displacement parameters ($\text{Å}^2 \times 10^3$) for AlO_2 . $U(\text{eq})$ is defined as one third of the trace of the orthogonalized U_{ij} tensor.

	x	y	z	$U(\text{eq})$
N(1)	11074 (1)	2516 (1)	-787 (1)	45 (1)
N(2)	-5828 (1)	772 (1)	1580 (1)	42 (1)
C(1)	7609 (2)	2487 (1)	-265 (1)	38 (1)
C(2)	8780 (2)	2228 (1)	-498 (1)	41 (1)
C(3)	9914 (2)	2777 (1)	-555 (1)	40 (1)
C(4)	9815 (2)	3605 (1)	-359 (1)	45 (1)
C(5)	8664 (2)	3859 (1)	-128 (1)	46 (1)
C(6)	7518 (2)	3322 (1)	-75 (1)	41 (1)
C(7)	6306 (2)	3572 (1)	170 (1)	44 (1)
C(8)	5262 (2)	3709 (1)	375 (1)	42 (1)
C(9)	3961 (2)	3641 (1)	600 (1)	39 (1)
C(10)	3240 (2)	4289 (1)	816 (1)	48 (1)
C(11)	1973 (2)	4140 (1)	1015 (1)	49 (1)
C(12)	1381 (2)	3332 (1)	1004 (1)	39 (1)
C(13)	2108 (2)	2688 (1)	784 (1)	48 (1)
C(14)	3361 (2)	2835 (1)	591 (1)	50 (1)
C(15)	66 (2)	3096 (1)	1184 (1)	43 (1)
C(16)	-985 (2)	2736 (1)	1280 (1)	43 (1)
C(17)	-2210 (2)	2246 (1)	1368 (1)	41 (1)
C(18)	-3311 (2)	2562 (1)	1619 (1)	47 (1)
C(19)	-4472 (2)	2083 (1)	1702 (1)	47 (1)
C(20)	-4627 (2)	1239 (1)	1525 (1)	39 (1)
C(21)	-3519 (2)	909 (1)	1275 (1)	40 (1)
C(22)	-2338 (2)	1393 (1)	1198 (1)	38 (1)
C(23)	-1245 (2)	1035 (1)	931 (1)	40 (1)
C(24)	-287 (2)	780 (1)	706 (1)	39 (1)
C(25)	872 (2)	609 (1)	460 (1)	39 (1)
C(26)	1969 (2)	590 (1)	263 (1)	39 (1)
C(27)	3215 (2)	728 (1)	72 (1)	39 (1)
C(28)	4323 (2)	998 (1)	-56 (1)	39 (1)
C(29)	5509 (2)	1428 (1)	-157 (1)	39 (1)
C(30)	6485 (2)	1896 (1)	-211 (1)	40 (1)
C(31)	12253 (2)	3094 (1)	-838 (1)	50 (1)
C(32)	11969 (2)	3704 (1)	-1317 (1)	50 (1)
C(33)	13184 (2)	4336 (1)	-1310 (1)	66 (1)
C(34)	12973 (3)	4902 (1)	-1809 (1)	101 (1)
C(35)	11016 (2)	1723 (1)	-1089 (1)	46 (1)
C(36)	10011 (2)	1733 (1)	-1639 (1)	45 (1)
C(37)	9965 (2)	903 (1)	-1941 (1)	56 (1)
C(38)	8962 (2)	922 (1)	-2489 (1)	71 (1)
C(39)	-6980 (2)	1124 (1)	1837 (1)	43 (1)
C(40)	-6729 (2)	1080 (1)	2459 (1)	43 (1)
C(41)	-7940 (2)	1495 (1)	2693 (1)	47 (1)
C(42)	-7830 (2)	1355 (1)	3303 (1)	53 (1)
C(43)	-5878 (2)	-131 (1)	1463 (1)	42 (1)
C(44)	-4932 (2)	-673 (1)	1885 (1)	44 (1)
C(45)	-4979 (2)	-1597 (1)	1732 (1)	49 (1)
C(46)	-4013 (2)	-2134 (1)	2149 (1)	62 (1)

Table 3. Bond lengths [Å] and angles [deg] for af022.

N(1)-C(3)	1.3799(19)
N(1)-C(35)	1.460(2)
N(1)-C(31)	1.4589(19)
N(2)-C(20)	1.3749(18)
N(2)-C(43)	1.4593(19)
N(2)-C(39)	1.4578(18)
C(1)-C(2)	1.390(2)
C(1)-C(6)	1.413(2)
C(1)-C(30)	1.434(2)
C(2)-C(3)	1.401(2)
C(3)-C(4)	1.410(2)
C(4)-C(5)	1.369(2)
C(5)-C(6)	1.396(2)
C(6)-C(7)	1.436(2)
C(7)-C(8)	1.200(2)
C(8)-C(9)	1.432(2)
C(9)-C(10)	1.387(2)
C(9)-C(14)	1.395(2)
C(10)-C(11)	1.385(2)
C(11)-C(12)	1.395(2)
C(12)-C(13)	1.391(2)
C(12)-C(15)	1.433(2)
C(13)-C(14)	1.364(2)
C(15)-C(16)	1.198(2)
C(16)-C(17)	1.436(2)
C(17)-C(18)	1.389(2)
C(17)-C(22)	1.417(2)
C(18)-C(19)	1.373(2)
C(19)-C(20)	1.408(2)
C(20)-C(21)	1.401(2)
C(21)-C(22)	1.388(2)
C(22)-C(23)	1.432(2)
C(23)-C(24)	1.208(2)
C(24)-C(25)	1.363(2)
C(25)-C(26)	1.214(2)
C(26)-C(27)	1.353(2)
C(27)-C(28)	1.217(2)
C(28)-C(29)	1.365(2)
C(29)-C(30)	1.204(2)
C(31)-C(32)	1.520(2)
C(32)-C(33)	1.516(2)
C(33)-C(34)	1.516(3)
C(35)-C(36)	1.521(2)
C(36)-C(37)	1.510(2)
C(37)-C(38)	1.516(2)
C(39)-C(40)	1.523(2)
C(40)-C(41)	1.514(2)
C(41)-C(42)	1.516(2)
C(43)-C(44)	1.518(2)
C(44)-C(45)	1.513(2)
C(45)-C(46)	1.515(2)
C(3)-N(1)-C(35)	120.66(13)
C(3)-N(1)-C(31)	120.82(14)
C(35)-N(1)-C(31)	117.31(13)
C(20)-N(2)-C(43)	120.46(13)

C(20)-N(2)-C(39)	121.35(13)
C(43)-N(2)-C(39)	117.48(12)
C(2)-C(1)-C(6)	120.90(14)
C(2)-C(1)-C(30)	119.61(14)
C(6)-C(1)-C(30)	119.49(14)
C(1)-C(2)-C(3)	121.89(15)
N(1)-C(3)-C(2)	121.62(15)
N(1)-C(3)-C(4)	121.84(15)
C(2)-C(3)-C(4)	116.54(15)
C(5)-C(4)-C(3)	121.54(15)
C(4)-C(5)-C(6)	122.50(16)
C(5)-C(6)-C(1)	116.63(15)
C(5)-C(6)-C(7)	123.42(15)
C(1)-C(6)-C(7)	119.94(14)
C(8)-C(7)-C(6)	174.34(17)
C(7)-C(8)-C(9)	165.00(16)
C(10)-C(9)-C(14)	117.58(15)
C(10)-C(9)-C(8)	126.84(14)
C(14)-C(9)-C(8)	115.58(14)
C(11)-C(10)-C(9)	121.13(15)
C(10)-C(11)-C(12)	120.90(15)
C(13)-C(12)-C(11)	117.41(15)
C(13)-C(12)-C(15)	116.04(14)
C(11)-C(12)-C(15)	126.52(15)
C(14)-C(13)-C(12)	121.59(15)
C(13)-C(14)-C(9)	121.37(15)
C(16)-C(15)-C(12)	165.68(17)
C(15)-C(16)-C(17)	175.17(18)
C(18)-C(17)-C(22)	116.55(14)
C(18)-C(17)-C(16)	123.46(15)
C(22)-C(17)-C(16)	119.99(15)
C(19)-C(18)-C(17)	122.63(15)
C(18)-C(19)-C(20)	121.38(15)
N(2)-C(20)-C(21)	121.78(14)
N(2)-C(20)-C(19)	121.53(14)
C(21)-C(20)-C(19)	116.66(14)
C(22)-C(21)-C(20)	121.76(15)
C(21)-C(22)-C(17)	121.00(14)
C(21)-C(22)-C(23)	119.90(14)
C(17)-C(22)-C(23)	119.08(14)
C(24)-C(23)-C(22)	176.14(16)
C(23)-C(24)-C(25)	171.57(16)
C(26)-C(25)-C(24)	169.47(16)
C(25)-C(26)-C(27)	168.91(16)
C(28)-C(27)-C(26)	167.89(16)
C(27)-C(28)-C(29)	170.04(16)
C(30)-C(29)-C(28)	171.14(17)
C(29)-C(30)-C(1)	177.23(17)
N(1)-C(31)-C(32)	115.71(13)
C(33)-C(32)-C(31)	112.44(14)
C(32)-C(33)-C(34)	113.00(17)
N(1)-C(35)-C(36)	114.50(13)
C(37)-C(36)-C(35)	113.36(14)
C(36)-C(37)-C(38)	112.80(15)
N(2)-C(39)-C(40)	115.45(13)
C(41)-C(40)-C(39)	112.06(13)
C(42)-C(41)-C(40)	113.21(13)
N(2)-C(43)-C(44)	114.98(13)
C(45)-C(44)-C(43)	112.70(13)
C(44)-C(45)-C(46)	112.63(14)

Table 4. Anisotropic displacement parameters ($\text{\AA}^2 \times 10^3$) for af022. The anisotropic displacement factor exponent takes the form: $-2 \pi^2 [h^2 a^{*2} U_{11} + \dots + 2 h k a^* b^* U_{12}]$

	U11	U22	U33	U23	U13	U12
N(1)	40(1)	52(1)	45(1)	-1(1)	9(1)	-7(1)
N(2)	41(1)	40(1)	48(1)	-6(1)	13(1)	-6(1)
C(1)	42(1)	41(1)	29(1)	5(1)	2(1)	-2(1)
C(2)	46(1)	40(1)	35(1)	2(1)	6(1)	0(1)
C(3)	41(1)	48(1)	30(1)	2(1)	3(1)	-5(1)
C(4)	47(1)	51(1)	39(1)	-3(1)	8(1)	-13(1)
C(5)	57(1)	42(1)	39(1)	-4(1)	8(1)	-8(1)
C(6)	44(1)	45(1)	33(1)	1(1)	5(1)	-2(1)
C(7)	53(1)	39(1)	39(1)	-2(1)	4(1)	-2(1)
C(8)	50(1)	35(1)	41(1)	-2(1)	7(1)	-1(1)
C(9)	46(1)	33(1)	35(1)	-3(1)	3(1)	-1(1)
C(10)	47(1)	32(1)	65(1)	-11(1)	12(1)	-10(1)
C(11)	49(1)	34(1)	65(1)	-13(1)	15(1)	-4(1)
C(12)	45(1)	35(1)	34(1)	-1(1)	1(1)	-6(1)
C(13)	65(1)	30(1)	53(1)	-3(1)	16(1)	-8(1)
C(14)	66(1)	31(1)	56(1)	-6(1)	22(1)	0(1)
C(15)	48(1)	35(1)	44(1)	-4(1)	3(1)	-5(1)
C(16)	48(1)	39(1)	41(1)	-3(1)	2(1)	-4(1)
C(17)	42(1)	39(1)	39(1)	1(1)	3(1)	-7(1)
C(18)	51(1)	37(1)	51(1)	-7(1)	8(1)	-4(1)
C(19)	45(1)	43(1)	53(1)	-6(1)	14(1)	-2(1)
C(20)	40(1)	38(1)	37(1)	0(1)	5(1)	-4(1)
C(21)	45(1)	35(1)	38(1)	-4(1)	7(1)	-5(1)
C(22)	40(1)	41(1)	33(1)	0(1)	5(1)	-2(1)
C(23)	44(1)	38(1)	38(1)	1(1)	3(1)	-8(1)
C(24)	40(1)	35(1)	41(1)	-3(1)	5(1)	-7(1)
C(25)	44(1)	30(1)	41(1)	-4(1)	1(1)	-5(1)
C(26)	42(1)	30(1)	43(1)	-6(1)	3(1)	-3(1)
C(27)	42(1)	32(1)	42(1)	-8(1)	6(1)	0(1)
C(28)	42(1)	34(1)	40(1)	-6(1)	4(1)	3(1)
C(29)	41(1)	37(1)	38(1)	-5(1)	7(1)	1(1)
C(30)	45(1)	42(1)	34(1)	-2(1)	5(1)	4(1)
C(31)	41(1)	60(1)	50(1)	-1(1)	7(1)	-7(1)
C(32)	48(1)	52(1)	52(1)	-2(1)	12(1)	-10(1)
C(33)	62(1)	57(1)	83(2)	-10(1)	22(1)	-15(1)
C(34)	113(2)	71(2)	125(2)	27(2)	35(2)	-24(2)
C(35)	43(1)	46(1)	52(1)	6(1)	13(1)	2(1)
C(36)	48(1)	40(1)	48(1)	0(1)	12(1)	-2(1)
C(37)	60(1)	44(1)	67(1)	-5(1)	21(1)	-7(1)
C(38)	91(2)	60(1)	64(1)	-16(1)	19(1)	-24(1)
C(39)	36(1)	48(1)	45(1)	0(1)	8(1)	-3(1)
C(40)	44(1)	41(1)	45(1)	-2(1)	8(1)	-1(1)
C(41)	53(1)	40(1)	49(1)	1(1)	13(1)	3(1)
C(42)	66(1)	47(1)	50(1)	0(1)	17(1)	1(1)
C(43)	43(1)	42(1)	42(1)	0(1)	7(1)	-9(1)
C(44)	45(1)	46(1)	40(1)	-2(1)	7(1)	-5(1)
C(45)	52(1)	47(1)	48(1)	0(1)	7(1)	-1(1)
C(46)	60(1)	59(1)	65(1)	8(1)	10(1)	5(1)

Table 5. Hydrogen coordinates ($\times 10^4$) and isotropic displacement parameters ($\text{\AA}^2 \times 10^3$) for af022.

	x	y	z	U(eq)
H(2A)	8812	1669	-621	49
H(4A)	10557	3992	-387	54
H(5A)	8644	4416	0	55
H(10A)	3618	4839	826	57
H(11A)	1506	4589	1159	58
H(13A)	1727	2138	767	58
H(14A)	3829	2384	448	60
H(18A)	-3258	3127	1736	56
H(19A)	-5179	2324	1880	56
H(21A)	-3577	345	1157	47
H(31A)	13113	2760	-870	60
H(31B)	12478	3424	-499	60
H(32A)	11848	3383	-1659	60
H(32B)	11065	4007	-1306	60
H(33A)	14100	4031	-1288	79
H(33B)	13251	4687	-981	79
H(34A)	13807	5268	-1794	152
H(34B)	12110	5241	-1817	152
H(34C)	12868	4557	-2137	152
H(35A)	10703	1275	-864	56
H(35B)	11995	1582	-1148	56
H(36A)	9032	1874	-1582	54
H(36B)	10327	2176	-1867	54
H(37A)	9645	459	-1714	67
H(37B)	10944	760	-1998	67
H(38A)	8978	378	-2666	106
H(38B)	9282	1354	-2717	106
H(38C)	7985	1046	-2434	106
H(39A)	-7881	824	1694	52
H(39B)	-7117	1716	1726	52
H(40A)	-6649	488	2574	52
H(40B)	-5813	1360	2606	52
H(41A)	-7928	2103	2622	56
H(41B)	-8868	1273	2505	56
H(42A)	-8636	1629	3428	80
H(42B)	-6928	1591	3493	80
H(42C)	-7853	755	3376	80
H(43A)	-5584	-220	1107	51
H(43B)	-6882	-323	1432	51
H(44A)	-3931	-472	1928	52
H(44B)	-5251	-608	2238	52
H(45A)	-4675	-1660	1376	59
H(45B)	-5977	-1800	1696	59
H(46A)	-4066	-2717	2029	92
H(46B)	-4333	-2093	2499	92
H(46C)	-3023	-1937	2186	92

Table 6. Torsion angles [deg] for af022.

C(6)-C(1)-C(2)-C(3)	0.0(2)
C(30)-C(1)-C(2)-C(3)	-179.29(14)
C(35)-N(1)-C(3)-C(2)	13.5(2)
C(31)-N(1)-C(3)-C(2)	-179.34(14)
C(35)-N(1)-C(3)-C(4)	-167.08(14)
C(31)-N(1)-C(3)-C(4)	0.0(2)
C(1)-C(2)-C(3)-N(1)	179.98(14)
C(1)-C(2)-C(3)-C(4)	0.6(2)
N(1)-C(3)-C(4)-C(5)	-179.81(14)
C(2)-C(3)-C(4)-C(5)	-0.4(2)
C(3)-C(4)-C(5)-C(6)	-0.4(3)
C(4)-C(5)-C(6)-C(1)	1.0(2)
C(4)-C(5)-C(6)-C(7)	179.48(15)
C(2)-C(1)-C(6)-C(5)	-0.8(2)
C(30)-C(1)-C(6)-C(5)	178.53(14)
C(2)-C(1)-C(6)-C(7)	-179.35(14)
C(30)-C(1)-C(6)-C(7)	0.0(2)
C(5)-C(6)-C(7)-C(8)	-167.4(17)
C(1)-C(6)-C(7)-C(8)	11.0(18)
C(6)-C(7)-C(8)-C(9)	-4(2)
C(7)-C(8)-C(9)-C(10)	180(95)
C(7)-C(8)-C(9)-C(14)	-1.2(7)
C(14)-C(9)-C(10)-C(11)	0.2(2)
C(8)-C(9)-C(10)-C(11)	179.15(16)
C(9)-C(10)-C(11)-C(12)	-0.1(3)
C(10)-C(11)-C(12)-C(13)	-0.3(2)
C(10)-C(11)-C(12)-C(15)	-178.38(16)
C(11)-C(12)-C(13)-C(14)	0.7(2)
C(15)-C(12)-C(13)-C(14)	179.01(15)
C(12)-C(13)-C(14)-C(9)	-0.7(3)
C(10)-C(9)-C(14)-C(13)	0.3(2)
C(8)-C(9)-C(14)-C(13)	-178.84(15)
C(13)-C(12)-C(15)-C(16)	-8.3(8)
C(11)-C(12)-C(15)-C(16)	169.8(6)
C(12)-C(15)-C(16)-C(17)	-4(3)
C(15)-C(16)-C(17)-C(18)	-173(2)
C(15)-C(16)-C(17)-C(22)	8(2)
C(22)-C(17)-C(18)-C(19)	0.0(2)
C(16)-C(17)-C(18)-C(19)	-179.78(15)
C(17)-C(18)-C(19)-C(20)	-1.2(3)
C(43)-N(2)-C(20)-C(21)	10.4(2)
C(39)-N(2)-C(20)-C(21)	-179.49(14)
C(43)-N(2)-C(20)-C(19)	-171.72(15)
C(39)-N(2)-C(20)-C(19)	-1.6(2)
C(18)-C(19)-C(20)-N(2)	-176.30(15)
C(18)-C(19)-C(20)-C(21)	1.7(2)
N(2)-C(20)-C(21)-C(22)	177.01(14)
C(19)-C(20)-C(21)-C(22)	-1.0(2)
C(20)-C(21)-C(22)-C(17)	-0.2(2)
C(20)-C(21)-C(22)-C(23)	-178.73(14)
C(18)-C(17)-C(22)-C(21)	0.7(2)
C(16)-C(17)-C(22)-C(21)	-179.50(14)
C(18)-C(17)-C(22)-C(23)	179.22(14)
C(16)-C(17)-C(22)-C(23)	-1.0(2)
C(21)-C(22)-C(23)-C(24)	173(2)
C(17)-C(22)-C(23)-C(24)	-5(3)

C(22)-C(23)-C(24)-C(25)	3(3)
C(23)-C(24)-C(25)-C(26)	4.0(19)
C(24)-C(25)-C(26)-C(27)	-2.9(17)
C(25)-C(26)-C(27)-C(28)	5.3(15)
C(26)-C(27)-C(28)-C(29)	-2.3(16)
C(27)-C(28)-C(29)-C(30)	0.6(19)
C(28)-C(29)-C(30)-C(1)	-9(4)
C(2)-C(1)-C(30)-C(29)	-176(100)
C(6)-C(1)-C(30)-C(29)	5(4)
C(3)-N(1)-C(31)-C(32)	-80.33(19)
C(35)-N(1)-C(31)-C(32)	87.21(18)
N(1)-C(31)-C(32)-C(33)	174.54(15)
C(31)-C(32)-C(33)-C(34)	175.28(17)
C(3)-N(1)-C(35)-C(36)	71.32(19)
C(31)-N(1)-C(35)-C(36)	-96.24(16)
N(1)-C(35)-C(36)-C(37)	-179.63(13)
C(35)-C(36)-C(37)-C(38)	-179.86(14)
C(20)-N(2)-C(39)-C(40)	-83.69(18)
C(43)-N(2)-C(39)-C(40)	86.69(17)
N(2)-C(39)-C(40)-C(41)	177.28(13)
C(39)-C(40)-C(41)-C(42)	171.83(14)
C(20)-N(2)-C(43)-C(44)	72.68(18)
C(39)-N(2)-C(43)-C(44)	-97.79(16)
N(2)-C(43)-C(44)-C(45)	-177.63(13)
C(43)-C(44)-C(45)-C(46)	178.99(14)

Symmetry transformations used to generate equivalent atoms:

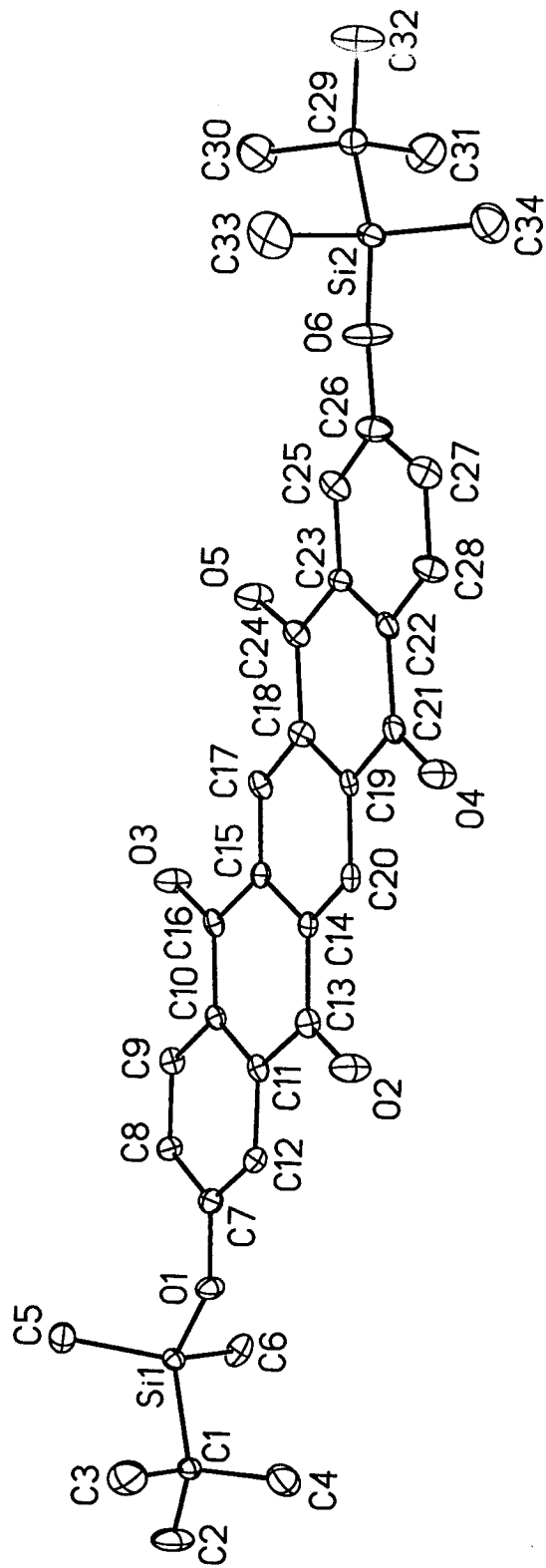


Table 1. Crystal data and structure refinement for af2010b.

Identification code	af2010b
Empirical formula	C ₃₄ H ₃₈ O ₆ Si ₂
Formula weight	598.82
Temperature	203(2) K
Wavelength	0.71073 Å
Crystal system, space group	Monoclinic, C2/c
Unit cell dimensions	a = 41.360(8) Å alpha = 90 deg. b = 7.8221(16) Å beta = 111.15(3) deg. c = 21.349(4) Å gamma = 90 deg.
Volume	6441(2) Å ³
Z, Calculated density	8, 1.235 Mg/m ³
Absorption coefficient	0.153 mm ⁻¹
F(000)	2544
Crystal size	0.30 x 0.30 x 0.06 mm
Theta range for data collection	1.06 to 29.19 deg.
Limiting indices	-55<=h<=50, 0<=k<=10, 0<=l<=28
Reflections collected / unique	7577 / 7577 [R(int) = 0.0583]
Completeness to theta = 29.19	86.9 %
Absorption correction	Semi-empirical from equivalents
Max. and min. transmission	0.9909 and 0.9556
Refinement method	Full-matrix least-squares on F ²
Data / restraints / parameters	7577 / 0 / 379
Goodness-of-fit on F ²	1.037
Final R indices [I>2sigma(I)]	R1 = 0.0755, wR2 = 0.3152
R indices (all data)	R1 = 0.0830, wR2 = 0.3276
Largest diff. peak and hole	0.498 and -0.502 e.Å ⁻³

Table 2. Atomic coordinates ($\times 10^4$) and equivalent isotropic displacement parameters ($\text{\AA}^2 \times 10^3$) for ar2010b. U(eq) is defined as one third of the trace of the orthogonalized U_{ij} tensor.

	x	y	z	U(eq)
Si(1)	988(1)	3412(1)	4547(1)	22(1)
Si(2)	4078(1)	5596(1)	13066(1)	26(1)
O(1)	1153(1)	3908(4)	5370(1)	33(1)
O(2)	1580(1)	5099(5)	7847(2)	47(1)
O(3)	2663(1)	1861(5)	7511(1)	39(1)
O(4)	2299(1)	6053(5)	10254(1)	43(1)
O(5)	3380(1)	2672(5)	9952(2)	44(1)
O(6)	3846(1)	4541(5)	12360(2)	49(1)
C(1)	579(1)	4784(5)	4218(2)	25(1)
C(2)	357(1)	4285(8)	3486(2)	55(1)
C(3)	682(2)	6674(6)	4251(3)	56(1)
C(4)	351(1)	4510(8)	4644(3)	53(1)
C(5)	1305(1)	3942(6)	4140(2)	38(1)
C(6)	883(1)	1089(6)	4473(3)	40(1)
C(7)	1459(1)	3536(5)	5892(2)	26(1)
C(8)	1734(1)	2630(5)	5810(2)	28(1)
C(9)	2038(1)	2297(4)	6362(2)	23(1)
C(10)	2073(1)	2846(4)	7010(2)	22(1)
C(11)	1793(1)	3749(4)	7090(2)	23(1)
C(12)	1491(1)	4097(4)	6533(2)	22(1)
C(13)	1820(1)	4354(5)	7766(2)	25(1)
C(14)	2154(1)	4031(4)	8350(2)	22(1)
C(15)	2437(1)	3161(4)	8265(2)	20(1)
C(16)	2407(1)	2540(5)	7587(2)	24(1)
C(17)	2747(1)	2911(5)	8818(2)	25(1)
C(18)	2790(1)	3586(4)	9454(2)	23(1)
C(19)	2506(1)	4475(4)	9533(2)	22(1)
C(20)	2192(1)	4682(4)	8981(2)	22(1)
C(21)	2546(1)	5268(5)	10195(2)	26(1)
C(22)	2885(1)	5079(5)	10764(2)	24(1)
C(23)	3166(1)	4179(4)	10689(2)	23(1)
C(24)	3133(1)	3381(5)	10035(2)	26(1)
C(25)	3481(1)	4008(5)	11229(2)	30(1)
C(26)	3526(1)	4768(5)	11848(2)	34(1)
C(27)	3248(1)	5663(5)	11926(2)	34(1)
C(28)	2935(1)	5798(5)	11392(2)	32(1)
C(29)	4481(1)	4217(5)	13412(2)	30(1)
C(30)	4681(1)	4220(9)	12920(3)	57(1)
C(31)	4378(1)	2366(7)	13505(3)	55(1)
C(32)	4732(2)	4891(9)	14091(3)	61(2)
C(33)	4185(2)	7751(7)	12844(4)	65(2)
C(34)	3835(2)	5741(8)	13642(3)	53(1)

Table 3. Bond lengths [Å] and angles [deg] for af2010b.

Si(1)-O(1)	1.684(3)
Si(1)-C(6)	1.862(5)
Si(1)-C(5)	1.864(4)
Si(1)-C(1)	1.909(4)
Si(2)-O(6)	1.682(3)
Si(2)-C(33)	1.847(5)
Si(2)-C(34)	1.851(5)
Si(2)-C(29)	1.897(4)
O(1)-C(7)	1.382(5)
O(2)-C(13)	1.217(5)
O(3)-C(16)	1.246(4)
O(4)-C(21)	1.236(5)
O(5)-C(24)	1.229(5)
O(6)-C(26)	1.391(5)
C(1)-C(3)	1.533(6)
C(1)-C(4)	1.543(6)
C(1)-C(2)	1.551(6)
C(7)-C(12)	1.397(5)
C(7)-C(8)	1.405(5)
C(8)-C(9)	1.404(5)
C(9)-C(10)	1.406(5)
C(10)-C(11)	1.416(5)
C(10)-C(16)	1.503(5)
C(11)-C(12)	1.407(5)
C(11)-C(13)	1.485(5)
C(13)-C(14)	1.512(5)
C(14)-C(20)	1.393(5)
C(14)-C(15)	1.420(5)
C(15)-C(17)	1.410(5)
C(15)-C(16)	1.488(4)
C(17)-C(18)	1.407(5)
C(18)-C(19)	1.426(5)
C(18)-C(24)	1.519(5)
C(19)-C(20)	1.413(5)
C(19)-C(21)	1.496(5)
C(21)-C(22)	1.497(5)
C(22)-C(28)	1.400(5)
C(22)-C(23)	1.414(5)
C(23)-C(25)	1.402(5)
C(23)-C(24)	1.489(5)
C(25)-C(26)	1.399(6)
C(26)-C(27)	1.408(6)
C(27)-C(28)	1.386(6)
C(29)-C(32)	1.540(6)
C(29)-C(31)	1.541(7)
C(29)-C(30)	1.557(6)
O(1)-Si(1)-C(6)	107.9(2)
O(1)-Si(1)-C(5)	110.35(18)
C(6)-Si(1)-C(5)	111.1(2)
O(1)-Si(1)-C(1)	103.04(15)
C(6)-Si(1)-C(1)	111.63(18)
C(5)-Si(1)-C(1)	112.47(19)
O(6)-Si(2)-C(33)	109.3(3)
O(6)-Si(2)-C(34)	110.8(2)
C(33)-Si(2)-C(34)	110.6(3)

O(6)-Si(2)-C(29)	101.90(17)
C(33)-Si(2)-C(29)	111.2(2)
C(34)-Si(2)-C(29)	112.8(2)
C(7)-O(1)-Si(1)	134.5(3)
C(26)-O(6)-Si(2)	135.6(3)
C(3)-C(1)-C(4)	109.0(4)
C(3)-C(1)-C(2)	110.0(4)
C(4)-C(1)-C(2)	107.1(4)
C(3)-C(1)-Si(1)	109.3(3)
C(4)-C(1)-Si(1)	110.7(3)
C(2)-C(1)-Si(1)	110.7(3)
O(1)-C(7)-C(12)	117.4(3)
O(1)-C(7)-C(8)	123.5(3)
C(12)-C(7)-C(8)	119.1(3)
C(9)-C(8)-C(7)	120.6(3)
C(8)-C(9)-C(10)	120.9(3)
C(9)-C(10)-C(11)	118.2(3)
C(9)-C(10)-C(16)	119.7(3)
C(11)-C(10)-C(16)	122.0(3)
C(12)-C(11)-C(10)	120.7(3)
C(12)-C(11)-C(13)	119.4(3)
C(10)-C(11)-C(13)	119.9(3)
C(7)-C(12)-C(11)	120.5(3)
O(2)-C(13)-C(11)	120.9(3)
O(2)-C(13)-C(14)	120.9(3)
C(11)-C(13)-C(14)	118.2(3)
C(20)-C(14)-C(15)	119.2(3)
C(20)-C(14)-C(13)	119.1(3)
C(15)-C(14)-C(13)	121.6(3)
C(17)-C(15)-C(14)	120.1(3)
C(17)-C(15)-C(16)	120.0(3)
C(14)-C(15)-C(16)	119.9(3)
O(3)-C(16)-C(15)	119.3(3)
O(3)-C(16)-C(10)	122.3(3)
C(15)-C(16)-C(10)	118.3(3)
C(18)-C(17)-C(15)	121.0(3)
C(17)-C(18)-C(19)	118.4(3)
C(17)-C(18)-C(24)	120.2(3)
C(19)-C(18)-C(24)	121.4(3)
C(20)-C(19)-C(18)	120.2(3)
C(20)-C(19)-C(21)	119.7(3)
C(18)-C(19)-C(21)	120.0(3)
C(14)-C(20)-C(19)	121.0(3)
O(4)-C(21)-C(19)	119.3(3)
O(4)-C(21)-C(22)	122.2(3)
C(19)-C(21)-C(22)	118.4(3)
C(28)-C(22)-C(23)	117.8(3)
C(28)-C(22)-C(21)	120.5(3)
C(23)-C(22)-C(21)	121.7(3)
C(25)-C(23)-C(22)	120.8(3)
C(25)-C(23)-C(24)	118.3(3)
C(22)-C(23)-C(24)	120.9(3)
O(5)-C(24)-C(23)	121.6(3)
O(5)-C(24)-C(18)	120.6(3)
C(23)-C(24)-C(18)	117.6(3)
C(26)-C(25)-C(23)	120.2(4)
O(6)-C(26)-C(25)	116.9(4)
O(6)-C(26)-C(27)	123.9(4)
C(25)-C(26)-C(27)	119.2(4)
C(28)-C(27)-C(26)	120.1(4)

C(27)-C(28)-C(22)	121.8(4)
C(32)-C(29)-C(31)	108.9(4)
C(32)-C(29)-C(30)	107.0(4)
C(31)-C(29)-C(30)	109.0(4)
C(32)-C(29)-Si(2)	111.8(3)
C(31)-C(29)-Si(2)	110.0(3)
C(30)-C(29)-Si(2)	110.1(3)

Symmetry transformations used to generate equivalent atoms:

Table 4. Anisotropic displacement parameters ($\text{Å}^2 \times 10^3$) for af2010b. The anisotropic displacement factor exponent takes the form: $-2 \pi^2 [h^2 a^{*2} U_{11} + \dots + 2 h k a^* b^* U_{12}]$

	U11	U22	U33	U23	U13	U12
Si (1)	25 (1)	24 (1)	17 (1)	-2 (1)	7 (1)	-1 (1)
Si (2)	28 (1)	29 (1)	19 (1)	1 (1)	5 (1)	0 (1)
O (1)	25 (1)	52 (2)	22 (1)	-4 (1)	6 (1)	6 (1)
O (2)	36 (2)	80 (2)	24 (1)	-11 (2)	8 (1)	21 (2)
O (3)	30 (1)	58 (2)	27 (1)	-11 (1)	8 (1)	18 (1)
O (4)	33 (2)	73 (2)	23 (1)	-8 (1)	11 (1)	16 (2)
O (5)	31 (2)	66 (2)	33 (2)	-9 (2)	10 (1)	20 (2)
O (6)	35 (2)	61 (2)	32 (2)	-21 (2)	-11 (1)	15 (2)
C (1)	24 (2)	28 (2)	21 (2)	0 (1)	6 (1)	-1 (1)
C (2)	39 (3)	80 (4)	30 (2)	-3 (2)	-5 (2)	16 (2)
C (3)	53 (3)	31 (2)	78 (4)	7 (2)	17 (3)	10 (2)
C (4)	44 (3)	72 (4)	50 (3)	19 (3)	26 (2)	22 (2)
C (5)	37 (2)	41 (2)	37 (2)	1 (2)	16 (2)	-5 (2)
C (6)	33 (2)	33 (2)	59 (3)	-9 (2)	22 (2)	-4 (2)
C (7)	27 (2)	26 (2)	26 (2)	-2 (1)	8 (1)	-5 (1)
C (8)	27 (2)	37 (2)	19 (2)	-7 (1)	9 (1)	2 (2)
C (9)	27 (2)	20 (2)	27 (2)	-7 (1)	14 (1)	5 (1)
C (10)	24 (2)	20 (2)	21 (2)	0 (1)	9 (1)	-1 (1)
C (11)	30 (2)	19 (2)	21 (2)	-3 (1)	12 (1)	-2 (1)
C (12)	20 (2)	23 (2)	25 (2)	-5 (1)	11 (1)	3 (1)
C (13)	27 (2)	27 (2)	24 (2)	-2 (1)	13 (1)	5 (1)
C (14)	21 (2)	23 (2)	22 (2)	2 (1)	10 (1)	0 (1)
C (15)	24 (2)	20 (2)	21 (2)	0 (1)	13 (1)	0 (1)
C (16)	32 (2)	24 (2)	20 (2)	1 (1)	14 (1)	3 (1)
C (17)	30 (2)	24 (2)	22 (2)	4 (1)	12 (1)	6 (1)
C (18)	26 (2)	21 (2)	22 (2)	-1 (1)	8 (1)	2 (1)
C (19)	28 (2)	22 (2)	20 (2)	4 (1)	14 (1)	2 (1)
C (20)	24 (2)	22 (2)	22 (2)	0 (1)	12 (1)	-1 (1)
C (21)	26 (2)	35 (2)	19 (2)	2 (1)	10 (1)	3 (1)
C (22)	27 (2)	26 (2)	17 (2)	1 (1)	6 (1)	-6 (1)
C (23)	26 (2)	19 (2)	21 (2)	1 (1)	5 (1)	-2 (1)
C (24)	32 (2)	26 (2)	21 (2)	1 (1)	10 (1)	5 (1)
C (25)	33 (2)	27 (2)	25 (2)	0 (1)	7 (2)	3 (2)
C (26)	33 (2)	32 (2)	28 (2)	-6 (2)	1 (2)	0 (2)
C (27)	45 (2)	34 (2)	24 (2)	-11 (2)	12 (2)	5 (2)
C (28)	35 (2)	35 (2)	23 (2)	-5 (2)	7 (2)	6 (2)
C (29)	28 (2)	34 (2)	25 (2)	-1 (2)	6 (2)	-2 (2)
C (30)	45 (3)	77 (4)	55 (3)	7 (3)	25 (2)	18 (3)
C (31)	41 (3)	44 (3)	74 (4)	14 (3)	14 (3)	9 (2)
C (32)	50 (3)	70 (4)	38 (3)	-11 (3)	-13 (2)	5 (3)
C (33)	74 (4)	37 (3)	84 (4)	34 (3)	30 (3)	18 (3)
C (34)	64 (3)	61 (3)	39 (3)	-2 (2)	25 (2)	2 (3)

Table 5. Hydrogen coordinates ($\times 10^4$) and isotropic displacement parameters ($\text{\AA}^2 \times 10^3$) for ar2010b.

	x	y	z	U(eq)
H(2A)	151	4992	3328	82
H(2B)	291	3092	3470	82
H(2C)	491	4459	3200	82
H(3A)	475	7374	4084	84
H(3B)	822	6860	3976	84
H(3C)	815	6984	4712	84
H(4A)	145	5215	4469	79
H(4B)	481	4826	5106	79
H(4C)	284	3317	4624	79
H(5A)	1508	3216	4323	56
H(5B)	1374	5130	4225	56
H(5C)	1199	3754	3659	56
H(6A)	1096	431	4644	60
H(6B)	759	802	4005	60
H(6C)	739	824	4732	60
H(8A)	1714	2244	5380	33
H(9A)	2221	1700	6298	28
H(12A)	1309	4711	6593	26
H(17A)	2929	2284	8762	29
H(20A)	2007	5267	9039	26
H(25A)	3663	3380	11175	36
H(27A)	3274	6170	12341	41
H(28A)	2750	6388	11454	38
H(30A)	4887	3514	13101	86
H(30B)	4749	5381	12863	86
H(30C)	4533	3768	12488	86
H(31A)	4586	1669	13682	82
H(31B)	4229	1911	13075	82
H(31C)	4256	2352	13816	82
H(32A)	4934	4157	14252	91
H(32B)	4616	4894	14415	91
H(32D)	4803	6045	14035	91
H(33A)	3975	8429	12669	97
H(33D)	4290	7656	12506	97
H(33B)	4346	8301	13242	97
H(34D)	3632	6456	13441	79
H(34A)	3982	6237	14065	79
H(34B)	3763	4606	13721	79

Table 6. Torsion angles [deg] for af2010b.

C(6)-Si(1)-O(1)-C(7)	69.8(4)
C(5)-Si(1)-O(1)-C(7)	-51.7(4)
C(1)-Si(1)-O(1)-C(7)	-172.0(4)
C(33)-Si(2)-O(6)-C(26)	-62.5(6)
C(34)-Si(2)-O(6)-C(26)	59.7(6)
C(29)-Si(2)-O(6)-C(26)	179.9(5)
O(1)-Si(1)-C(1)-C(3)	68.0(4)
C(6)-Si(1)-C(1)-C(3)	-176.5(3)
C(5)-Si(1)-C(1)-C(3)	-50.9(4)
O(1)-Si(1)-C(1)-C(4)	-52.2(4)
C(6)-Si(1)-C(1)-C(4)	63.3(4)
C(5)-Si(1)-C(1)-C(4)	-171.0(3)
O(1)-Si(1)-C(1)-C(2)	-170.7(3)
C(6)-Si(1)-C(1)-C(2)	-55.2(4)
C(5)-Si(1)-C(1)-C(2)	70.4(4)
Si(1)-O(1)-C(7)-C(12)	-175.4(3)
Si(1)-O(1)-C(7)-C(8)	4.4(6)
O(1)-C(7)-C(8)-C(9)	179.9(4)
C(12)-C(7)-C(8)-C(9)	-0.3(6)
C(7)-C(8)-C(9)-C(10)	0.6(6)
C(8)-C(9)-C(10)-C(11)	-0.2(5)
C(8)-C(9)-C(10)-C(16)	-177.3(3)
C(9)-C(10)-C(11)-C(12)	-0.5(5)
C(16)-C(10)-C(11)-C(12)	176.5(3)
C(9)-C(10)-C(11)-C(13)	-179.9(3)
C(16)-C(10)-C(11)-C(13)	-2.9(5)
O(1)-C(7)-C(12)-C(11)	179.3(3)
C(8)-C(7)-C(12)-C(11)	-0.5(5)
C(10)-C(11)-C(12)-C(7)	0.9(5)
C(13)-C(11)-C(12)-C(7)	-179.8(3)
C(12)-C(11)-C(13)-O(2)	2.3(6)
C(10)-C(11)-C(13)-O(2)	-178.4(4)
C(12)-C(11)-C(13)-C(14)	-177.3(3)
C(10)-C(11)-C(13)-C(14)	2.0(5)
O(2)-C(13)-C(14)-C(20)	-3.6(6)
C(11)-C(13)-C(14)-C(20)	176.0(3)
O(2)-C(13)-C(14)-C(15)	179.9(4)
C(11)-C(13)-C(14)-C(15)	-0.5(5)
C(20)-C(14)-C(15)-C(17)	2.2(5)
C(13)-C(14)-C(15)-C(17)	178.7(3)
C(20)-C(14)-C(15)-C(16)	-176.7(3)
C(13)-C(14)-C(15)-C(16)	-0.2(5)
C(17)-C(15)-C(16)-O(3)	-2.8(5)
C(14)-C(15)-C(16)-O(3)	176.2(3)
C(17)-C(15)-C(16)-C(10)	-179.5(3)
C(14)-C(15)-C(16)-C(10)	-0.5(5)
C(9)-C(10)-C(16)-O(3)	2.5(6)
C(11)-C(10)-C(16)-O(3)	-174.5(4)
C(9)-C(10)-C(16)-C(15)	179.1(3)
C(11)-C(10)-C(16)-C(15)	2.1(5)
C(14)-C(15)-C(17)-C(18)	-3.2(5)
C(16)-C(15)-C(17)-C(18)	175.7(3)
C(15)-C(17)-C(18)-C(19)	2.5(5)
C(15)-C(17)-C(18)-C(24)	-176.9(3)
C(17)-C(18)-C(19)-C(20)	-0.8(5)
C(24)-C(18)-C(19)-C(20)	178.6(3)

C(17)-C(18)-C(19)-C(21)	-177.7(3)
C(24)-C(18)-C(19)-C(21)	1.6(5)
C(15)-C(14)-C(20)-C(19)	-0.5(5)
C(13)-C(14)-C(20)-C(19)	-177.2(3)
C(18)-C(19)-C(20)-C(14)	-0.2(5)
C(21)-C(19)-C(20)-C(14)	176.8(3)
C(20)-C(19)-C(21)-O(4)	2.1(6)
C(18)-C(19)-C(21)-O(4)	179.1(4)
C(20)-C(19)-C(21)-C(22)	-177.9(3)
C(18)-C(19)-C(21)-C(22)	-0.9(5)
O(4)-C(21)-C(22)-C(28)	0.0(6)
C(19)-C(21)-C(22)-C(28)	-180.0(3)
O(4)-C(21)-C(22)-C(23)	-179.9(4)
C(19)-C(21)-C(22)-C(23)	0.1(5)
C(28)-C(22)-C(23)-C(25)	0.4(5)
C(21)-C(22)-C(23)-C(25)	-179.6(3)
C(28)-C(22)-C(23)-C(24)	-180.0(3)
C(21)-C(22)-C(23)-C(24)	0.0(5)
C(25)-C(23)-C(24)-O(5)	-4.2(6)
C(22)-C(23)-C(24)-O(5)	176.2(4)
C(25)-C(23)-C(24)-C(18)	-179.7(3)
C(22)-C(23)-C(24)-C(18)	0.7(5)
C(17)-C(18)-C(24)-O(5)	2.3(6)
C(19)-C(18)-C(24)-O(5)	-177.0(4)
C(17)-C(18)-C(24)-C(23)	177.8(3)
C(19)-C(18)-C(24)-C(23)	-1.6(5)
C(22)-C(23)-C(25)-C(26)	-1.7(6)
C(24)-C(23)-C(25)-C(26)	178.7(4)
Si(2)-O(6)-C(26)-C(25)	156.1(4)
Si(2)-O(6)-C(26)-C(27)	-25.8(8)
C(23)-C(25)-C(26)-O(6)	180.0(4)
C(23)-C(25)-C(26)-C(27)	1.8(6)
O(6)-C(26)-C(27)-C(28)	-178.6(4)
C(25)-C(26)-C(27)-C(28)	-0.6(7)
C(26)-C(27)-C(28)-C(22)	-0.7(7)
C(23)-C(22)-C(28)-C(27)	0.8(6)
C(21)-C(22)-C(28)-C(27)	-179.2(4)
O(6)-Si(2)-C(29)-C(32)	-177.4(4)
C(33)-Si(2)-C(29)-C(32)	66.3(5)
C(34)-Si(2)-C(29)-C(32)	-58.6(4)
O(6)-Si(2)-C(29)-C(31)	-56.3(4)
C(33)-Si(2)-C(29)-C(31)	-172.6(4)
C(34)-Si(2)-C(29)-C(31)	62.5(4)
O(6)-Si(2)-C(29)-C(30)	63.9(4)
C(33)-Si(2)-C(29)-C(30)	-52.4(4)
C(34)-Si(2)-C(29)-C(30)	-177.3(4)

Symmetry transformations used to generate equivalent atoms: